



Optimization for sustainable utilization of low temperature geothermal systems

Silja Rán Sigurðardóttir

Doctor of Philosophy

December 2013

School of Science and Engineering

Reykjavík University

Ph.D. DISSERTATION

ISBN 978-9935-9147-3-6



Optimization for sustainable utilization of low temperature geothermal systems

by

Silja Rán Sigurðardóttir

Thesis submitted to the School of Science and Engineering
at Reykjavík University in partial fulfillment
of the requirements for the degree of
Doctor of Philosophy

December 2013

Thesis Committee:

Dr. Ágúst Valfells, Supervisor
Docent, Reykjavik University, Iceland

Dr. Hlynur Stefánsson, Co-Supervisor
Docent, Reykjavik University, Iceland

Dr. Halldór Pálsson
Docent, University of Iceland, Iceland

Dr. Guðni Axelsson, Examiner
Adjunct, University of Iceland, Iceland

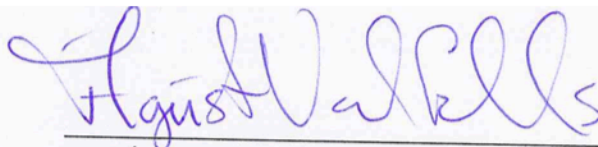
Dr. Lazaros Papagergiou, Examiner
Docent, University College London (UCL), United Kingdom

Copyright
Silja Rán Sigurðardóttir
December 2013

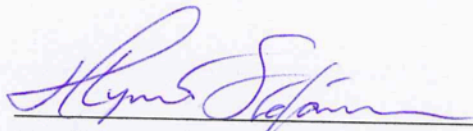
The undersigned hereby certify that they recommend to the School of Science and Engineering at Reykjavík University for acceptance this thesis entitled **Optimization for sustainable utilization of low temperature geothermal systems** submitted by Silja Rán Sigurðardóttir in partial fulfillment of the requirements for the degree of **Doctor of Philosophy**.

20.12.2013

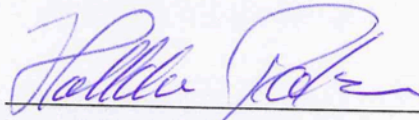
Date



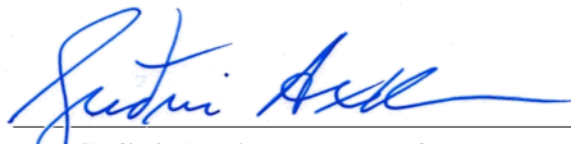
Dr. Ágúst Valfells, Supervisor
Docent, Reykjavik University, Iceland



Dr. Hlynur Stefánsson, Co-Supervisor
Docent, Reykjavik University, Iceland



Dr. Halldór Pálsson
Docent, University of Iceland, Iceland



Dr. Guðni Axelsson, Examiner
Adjunct, University of Iceland, Iceland



Dr. Lazaros Papagergiou, Examiner
Docent, University College London (UCL), United Kingdom

The undersigned hereby grants permission to the Reykjavík University Library to reproduce single copies of this thesis entitled **Optimization for sustainable utilization of low temperature geothermal systems** and to lend or sell such copies for private, scholarly or scientific research purposes only.

The author reserves all other publication and other rights in association with the copyright in the thesis, and except as herein before provided, neither the thesis nor any substantial portion thereof may be printed or otherwise reproduced in any material form whatsoever without the author's prior written permission.

20.12.2013
Date

Silja Rán Sigurðardóttir
Silja Rán Sigurðardóttir
Doctor of Philosophy

Optimization for sustainable utilization of low temperature geothermal systems

Silja Rán Sigurðardóttir

December 2013

Abstract

Low temperature geothermal resources provide hot water that is commonly used for space heating and various applications. A geothermal resource is considered to be a renewable energy source that can be utilized by current and future generations if sustainability considerations are respected. The goal of this work is to determine if utilization of a geothermal reservoir can be optimized under sustainable operation. One way to carry out this kind of optimization is to connect reservoir and operational optimization models directly. The underlying reservoir model used here is a lumped parameter model (LPM). A LPM model can be used to simulate pressure (drawdown) changes in a low temperature reservoir with respect to harvesting levels. One scenario is to maximize the present value of profit where important parameters include production rate, water level (drawdown) and production capacity from which the profit can be calculated. Optimization over a time period subject to underlying developing constraints is often referred to as dynamic optimization. This problem is essentially a mixed integer non-linear dynamic optimization problem, often referred to as mixed integer dynamic optimization (MIDO). Three solution methods for the optimization problem are discussed, tested and compared. The parameters of the LPM are obtained by non-linear least square estimation where the LPM is essentially a simplified approach to characterize a spatially distributed reservoir. Data from four different geothermal fields are calibrated to the LPM, validated with split validation and the best calibrations chosen for the optimization application. Profit is first maximized assuming long-term production based on demand from historical data. Different performance indices for the geothermal utilization are then optimized and various scenarios are considered and compared under annually increased demand.

Ákvarðanataka fyrir sjálfbæra nýtingu lághitajarðvarmakerfa

Silja Rán Sigurðardóttir

Desember 2013

Útdráttur

Lághitajarðvarmasvæði eru auðlindir sem gera það kleift að heitt vatn sé nýtt til húshitunar fyrir heimili eða margskonar atvinnustarfsemi. Jarðvarmi er talin vera endurnýjanleg auðlind sem komandi kynslóðir munu geta nýtt sér að því tilskildu að sjálfbær nýting sé höfð að leiðarljósi. Markmiðið með þessu verkefni er að komast að því hvort hægt sé að besta sjálfbæra nýtingu á slíkri auðlind. Ein leið til að útfæra slíka bestun er að tengja forðafræðilíkan beint við rekstrar-bestunar líkan (e. operational optimization). Slíkt líkan er hægt að nota til að herma þrýstingsbreytingar (breytingar í niðurdrætti) í lágvarma jarðhitageymi (e. low temperature reservoir) með tilliti til framleiðslugetu. Taka má fyrir tilfelli þar sem hagnaður er bestaður þar sem mikilvægar breytur sem nota má til að reikna hagnað eru meðal annars, framleiðslustig, vatnshæð (niðurdráttur) og framleiðslugeta. Þegar bestað er yfir tíma-bil með undirliggjandi breytilegri skorðu er oft talað um hreyfina bestun (e. dynamic optimization). Þetta vandamál er í eðli sínu blendin ólínuleg hreyfin bestun (e. mixed integer non-linear dynamic optimization) oft kallað blendin hreyfin bestun (e. mixed integer dynamic optimization). Þrjár lausnaraðferðir eru ræddar, prófaðar og bornar saman. Kennistærðir forðafræðilíkansins eru fengnar með ólínulegri aðferð minnstu kvaðrata, en forðafræðilíkanið sýnir í eðli sínu fram á mikla einföldun á flóknu jarðvarmakerfi þar sem rúmfræðilegir eiginleikar kerfisins eru ekki teknir með inn í myndina. Gögn frá fjórum mismunandi jarðvarmasvæðum eru aðlöguð að forðafræðilíkaniinu. Þessi aðlögun er staðfest og bestu niðurstöðurnar notaðar í bestuninni. Hagnaður er fyrst hámarkaður fyrir langvarandi vinnslu og m.v. að söguleg eftirspurn haldist óbreytt. Að lokum er mismunandi markföllum beitt til að besta nýtingu jarðvarmakerfa og margs konar tilvik eru skoðuð miðað við að eftirspurn sem byggð er á sögulegum gögnum aukist á árs grundvelli.

To my parents

Acknowledgements

I would like to thank Orkuveita Reykjavíkur (Reykjavik Energy) for their funding and data and Landvirkjun and Orkusjodur (The National Energy Authority) for funding. My university, Reykjavik University, School of Science and Engineering I thank for general support and funding. And to my professors, Ágúst Valfells, Halldór Pálsson and Hlynur Stefánsson thank you for your ideas, constructive criticism and mental support.

Publications

- 1 Sigurdardottir, S. R., Valfells, A., Palsson, H., and Stefansson, H. (2010). Optimizing Revenue of a Geothermal System with respect to operation and expansion. In *Proceedings of the World Geothermal Congress 2010*, pages 1-7, Bali, Indonesia. See Appendix A
- 2 Sigurdardottir, S. R., Valfells, A., Palsson, H., and Stefansson, H. (2012). Mixed integer optimization model for harvesting of geothermal reservoir. *Geothermics (in review)*, pages 1 - 21. See Appendix B
- 3 Sigurdardottir, S. R., Valfells, A., Palsson, H., and Stefansson, H. (2013). Applicability and applications of a mixed integer optimization method for sustainable production, based on a lumped parameter model of a geothermal reservoir. *In preparation*.

Contents

List of Figures	xiii
List of Tables	xix
List of Abbreviations	xxiii
Nomenclature	xxv
Notation for objective functions	xxvii
1 Introduction	1
1.1 Geothermal energy and sustainability	1
1.2 Geothermal reservoir modeling	4
1.3 Optimization	5
1.4 Objective and Contribution	10
1.5 Structure of the thesis	11
2 Modeling approach	13
2.1 Lumped parameter model (LPM)	13
2.1.1 Integration of the lumped parameter model	15
2.2 Optimization model	18
2.2.1 Objective function	18
2.2.2 Constraint 1: Mass balance equations on matrix form	19
2.2.3 Constraint 2: Demand	20
2.2.4 Constraint 3: Sustainability	20
2.2.5 Constraint 4: Production Capacity	21
2.2.6 The optimization problem	23
3 Solution approach	25
3.1 Conversion to MINLP	25

3.1.1	Feasibility and optimality	26
3.1.2	Convexity	28
3.1.3	Modeling languages for MINLP	31
3.2	Relaxation to MILP	31
3.2.1	Branch & bound with cutting planes	31
3.2.2	A piecewise linear approximation	35
3.2.3	Lower bound constraint for the piecewise linear approximation . .	36
3.2.4	Updating algorithm for piecewise linear approximation	38
3.2.5	Piecewise under-and over-estimators	41
3.2.6	Updating algorithm for under-and over-estimators	44
3.3	Relaxation to NLP	45
3.3.1	Sequential quadratic programming (SQP)	45
4	Results	51
4.1	Parameter estimation and validation of the LPM	51
4.1.1	Field data	51
4.1.2	Parameter estimation and validation	55
4.2	Testing of algorithms for the optimization model	62
4.2.1	Piecewise linear approximation	63
4.2.2	Piecewise under- and over-estimators	76
4.2.3	Relaxation to NLP	80
4.3	Optimization of long term utilization of a geothermal field under un- changed periodic demand	82
4.3.1	Necessary parameters for the optimization	84
4.3.2	Laugarnes field	85
4.3.3	Sensitivity analysis for Laugarnes field	89
4.3.4	Reykir field	91
4.3.5	Sensitivity analysis for Reykir field	95
4.4	Optimization of long term utilization under annually increased demand . .	96
4.4.1	Laugarnes field	100
4.4.2	Reykir field	108
5	Conclusion	115
5.1	Discussion	115
5.2	Perspectives and future work	119
A	Paper 1	129
B	Paper 2	137

List of Figures

2.1	N-Tank LPM system. The system can be closed ($\sigma_N = 0$) or open	14
2.2	Graphical comparison of three different numerical methods to integrate a bivariate function. The Euler method, the backward Euler method and the modified Euler method. h_i represent drawdown at time t_i	17
3.1	Graphical display of a univariate function that has both global and local maxima.	28
3.2	Graphical display of a univariate convex, concave and linear functions for comparison.	28
3.3	The branch-and-bound tree. The blue nodes are fathomed, they are either non-feasible solutions or optimal relaxation solutions, with an objective value smaller than that of the current optimum (for maximization) in the tree. The red node is the optimal solution	32
3.4	Cutting planes example. Undesirable fractional solutions are removed from the feasible set.	34
3.5	Cutting planes example. After undesirable solutions have been removed .	34
3.6	Graphical display of a univariate piecewise linear approximation for six time steps.	35
3.7	<i>If $F(x) = x^2$ is approximated around $x_0 = 1$ with first degree Taylor approximation, the linear function becomes $F(x) \approx 2x - 1$ and the comparable constraint to equation 3.18 becomes: $G(x) \geq 1/2$. The constraint prevents the decision variable from traveling unreasonably far (down) from the nonlinear function.</i>	37
3.8	The figure on the left displays a univariate case for a concave over-estimator. The figure on the right displays a secant line that can serve as an over-estimator for a the convex univariate function $g(x)$	42
3.9	Under-and over-estimators (envelopes) for univariate functions. The piecewise case is shown on the right.	43

4.1	Location of geothermal fields in Reykjavik. From: Gunnlaugsson et al. [2000]	52
4.2	Location of production wells and reference wells in Laugarnes field. Reference wells are marked with a red circle. From Ivarsson [2011]	53
4.3	Location of production wells and reference wells in Reykir and Reykjahlid fields. Reference wells are marked with a red circle. Reykjahlid field is the right side and Reykir field on the left side. From Ivarsson [2011]	54
4.4	Location of production wells and the reference well in Ellidaar field. Reference well is marked with a red circle. From Ivarsson [2011]	55
4.5	Fit for Laugarnes and Reykir. The figure above displays graphically the fit for Laugarnes field presented in table 4.3 for a three - tank open model. The figure below displays graphically the fit for Reykir field presented in table 4.2 for two - tank open model. The vertical axis shows drawdown from average meters above sea level for each geothermal field respectively.	58
4.6	Fit for Ellidaar and Reykjahlid. The figure above displays graphically the fit for Ellidar field presented in table 4.2 for a two - tank open model. The figure below displays graphically the fit for Reykjahlid presented in table 4.3 for three - tank open model. The vertical axis shows drawdown from average meters above sea level for each geothermal field respectively.	60
4.7	A fit for Reykir and Reykjahlid combined as one reservoir. The vertical axis shows drawdown from average meters above sea level for each geothermal field respectively.	62
4.8	Graphical results from a simple linear demand function. $m_{e,i} = \bar{m}_e + m_I t_i$ where $m_I = 25/12$. Demand is assumed to be linear and increase 25 kg/s a year.	65
4.9	Graphical results from a simple linear demand function, example 4.2. Demand is on the upper figure and drawdown on the lower figure. The linear demand function is: $m_{e,i} = \bar{m}_e + m_I t_i$ where $m_I = 25/12$. Demand is assumed to be linear and increase 100 kg/s a year.	66
4.10	Example 4.3. Graphical results from adding constraint 5 (equation 3.18) to the model. The upper bound for the decision variables \dot{m}_i is a simple linear demand function. $m_{e,i} = \bar{m}_e + m_I t_i$ where $m_I = 100/12$. Demand is assumed to be linear and increase 100 kg/s a year.	68
4.11	Constraint 5 decreases the error between linear and non-linear substantially and gives a more realistic solution and is active from the point where production can no longer follow demand, i.e., $\dot{m}_i < m_{e,i}$	69

4.12	Example 4.4. Graphical results for the updating development of the decision variable \dot{m}_i and the reference point $m_{z,i}$. The updating algorithm replaces the reference point for iteration $k + 1$ with the solution from iteration k	70
4.13	Example 4.5. Graphical results for the updating development of the decision variable \dot{m}_i and the reference point $m_{z,i}$. The updating algorithm replaces the reference points for iteration $k + 1$ with a mix from the solution from iteration k and the reference point from iteration k in such way that if the reference point is below the solution it moves up for the next iteration and if it is above the solution it moves down for the next iteration, see algorithm 2.	72
4.14	Example 4.5. Graphical results from a simple linear demand function using updating algorithm 2.	73
4.15	Example 4.5. The non-linear part of the objective function (non-linear and linearized) and the left side of constraint 5. The figure below displays iteration 3 where constraint 5 is still active and the figure above displays the last iteration, iteration 12 where constraint 5 is no longer active. . . .	74
4.16	Example 4.5. The figure above displays profit (with and without interest rate) as a function of 30 iterations, development of present value profit calculated with the MILP relaxation and than calculated non-linearly afterward. The figure below displays the same calculation but assumes no interest rate. The solution does not change after around 9 iterations. . . .	75
4.17	Graphical results for the updating development of the decision variable \dot{m}_i and the upper-bound \dot{m}_i^{over} . The updating algorithm replaces the upper-bound for iteration $k + 1$ with a mix from the solution from iteration k and the upper-bound from iteration k in such way that if the upper-bound is below the solution it moves up for the next iteration and if it is above the solution it moves down for the next iteration, see algorithm 2, see also section 3.2.6	77
4.18	Graphical results from a simple linear demand function using piecewise under-and over-estimators and updating algorithm see section 3.2.6	78
4.19	The figure above displays profit (with and without interest rate) as a function of 30 iterations, development of present value profit calculated with the MILP relaxation and than calculated non-linearly afterward. The figure below displays the same calculation but assumes no interest rate. The solution does not change after 4 iterations.	79
4.20	Graphical result where the NLP solution is displayed as an upper bound for the MILP relaxations. Both for the present value that is optimized and assuming no interest rate.	81

4.21	The demand is historical production repeated periodically. Six times for Laugarnes field a) and four times for Reykir field b). Resolution of data is in months.	83
4.22	Wholesale price as a proportion of retail price, Rarik und Landsvirkjun, from [Statistics Iceland, 2012].	85
4.23	Scenario 1. Production and drawdown. Resolution is in months. MA stands for moving average a year. Figure 4.23a displays production and demand for the next 155.5 years. Figure 4.23b displays the development of drawdown in two of the three tanks (this is a three tank model, see description of the LPM model in chapter 2.1).	88
4.24	Scenario 1. Figure 4.24a graphical display of the cost components. Figure 4.24b displays development of Present Value (PV) of profit for 155.5 years, resolution in years.	89
4.25	Scenario 1. Sensitivity analysis. Figure 4.25a displays proportional change in profit considering 10 % increase/decrease in the parameters from the Lumped Parameter Model (LPM). Figure 4.25b displays proportional change in Profit considering 10 % increase/decrease in the economical parameters. Please note the different scales on the two figures above.	90
4.26	Scenario 2. Production and drawdown. Figure 4.26a displays production and demand for the next 138 years. Demand is periodic and based on historical production data, repeated four times. Production can not exceed demand. In this scenario the production follows the demand exactly. Figure 4.26b displays the development of drawdown in the two tanks (this is a two tank model see chapter 2.1).	93
4.27	Scenario 2. Figure 4.27a graphical display of the cost components. Figure 4.27b displays development of Present Value (PV) of profit for 155.5 years, resolution in years.	94
4.28	Scenario 2. Sensitivity analysis. Proportional change in profit considering 10 % increase/decrease in the economical parameters.	95
4.29	The demand is historical production repeated periodically with a yearly trend of 2%. Resolution of data is in months.	99
4.30	Scenario 3. Drawdown and production for Laugarnes. Profit Maximized (PV). Figure 4.30a displays the maximum drawdown, average yearly drawdown, and drawdown in month resolution. Figure 4.30b displays average production a year, average demand a year and frequency of adding a pump. 102	

4.31	Scenario 4. Drawdown and production for Laugarnes. Profit Maximized (assuming no interest rate). Figure 4.31a displays the maximum drawdown, average yearly drawdown, and drawdown in month resolution. Figure 4.31b displays average production a year, average demand a year and frequency of adding a pump.	103
4.32	Scenario 5. Drawdown and production for Laugarnes. Deviation minimized. Figure 4.32a displays the maximum drawdown, average yearly drawdown, and drawdown in month resolution. Figure 4.32b displays average production a year, average demand a year and frequency of adding a pump.	104
4.33	Scenario 6. Drawdown and cash flow of profit without an interest rate for Laugarnes. Deviation was minimized (no sustainability constraint). Figure 4.33a displays the maximum drawdown, average yearly drawdown, and drawdown in month resolution. Figure 4.33b displays the cash flow of the profit. Without a sustainability limit the cash flow start to become negative in about 130 years of production.	105
4.34	Scenario 7. Drawdown and production for Laugarnes. Deviation minimized ($y(i) \leq 5$, only 5 pumps can be added in each month). Figure 4.34a displays the maximum drawdown, average yearly drawdown, and drawdown in month resolution. Figure 4.34b displays average production a year, average demand a year and frequency of adding a pump.	107
4.35	Scenario 8. Drawdown and production for Reykir. Present value of profit maximized. The result is very similar result for scenario 9 and 10. Figure 4.35a displays the maximum drawdown, average yearly drawdown, and drawdown in month resolution. Figure 4.35b displays average production a year, average demand a year and frequency of adding a pump.	109
4.36	Scenario 11. Drawdown and production for Reykir. Present value of profit maximized (no sustainability constraint). Figure 4.36a displays the maximum drawdown, average yearly drawdown, and drawdown in month resolution. Figure 4.36b displays average production a year, average demand a year and frequency of adding a pump.	110
4.37	Scenario 12. Drawdown and production for Reykir. Profit maximized (no sustainability constraint). Figure 4.35a displays the maximum drawdown, average yearly drawdown, and drawdown in month resolution. Figure 4.35b displays average production a year, average demand a year and frequency of adding a pump.	111

- 4.38 **Scenario 13.** Drawdown and cash flow of non-present value for Reykir field. Deviation minimized (no sustainability constraint). Figure 4.38a displays the maximum drawdown, average yearly drawdown, and drawdown in month resolution. Figure 4.38b displays the cash flow of the non present value. 112
- 4.39 **Scenario 14.** Drawdown and production for Reykir. Deviation minimized (constraint added: $y_i \leq 5$, only 5 pumps can be added in each month). Figure 4.34a displays the maximum drawdown, average yearly drawdown, and drawdown in month resolution. Figure 4.34b displays average production a year, average demand a year and frequency of adding a pump. 113

List of Tables

4.1	Some of the main properties of the geothermal fields utilized for Reykjavik such as average temperature, number of production wells, average production in GJ and kg/s and proportion of production from each field in 2010. From Ivarsson [2011]	52
4.2	Results from fit for two-tank open model for the four geothermal fields. The first of two columns for each field represents results for the parameter fit performed by MATLAB [MATLAB, 2012]. The second column represents the quality metrics of the fit. Bold values represent fitted parameters chosen for the optimization.	57
4.3	Results from fit for two-tank open model for the four geothermal fields. The first of two columns for each field represents results for the parameter fit performed by MATLAB [MATLAB, 2012]. The second column represents the quality metrics of the fit. Bold values represent fitted parameters chosen for the optimization.	59
4.4	Results from Reykir and Reykjahlid as one field Combined production is calibrated to one reference well MG-1. The first of two columns for each field represents results for the parameter fit performed by MATLAB [MATLAB, 2012]. The second column represents the quality metrics of the fit.	61
4.5	Results from optimization with demand function: $m_{e,i} = \bar{m}_e + m_I t_i$, $m_I = 25/12$. Optimized for $t_n = 311$ months. Starting time $t_1 = 1$	64
4.6	Results from optimization with demand function: $m_e(i) = \bar{m}_e + m_I t_i$, $m_I = 100/12$. Optimized for $t_n = 311$ months and starting time is $t_1 = 1$	64
4.7	Results from optimization with demand function: $m_{e,i} = \bar{m}_e + m_I t_i$, $m_I = 100/12$. Optimized for $t_n = 311$ months. Starting time $t_1 = 1$	67

4.8	Results from optimization with demand function: $m_e(i) = \bar{m}_e + m_I t_i$, $m_I = 100/12$ adding constraint represented by equation 3.18 and an updating process where $m_{z,i+1}^{(k+1)} = \dot{m}_i^{(k)}$ and $h_{z,i+1}^{(k+1)} = h_{1,i}^{(k)}$, algorithm 1. Optimized for $t_n = 311$ months. Starting time $t_1 = 1$	67
4.9	Results from optimization with demand function: $m_{e,i} = \bar{m}_e + m_I t_i$, where $m_I = 100/12$ using algorithm 2 and constraint 5, equation 3.18. Optimized for $t_n = 311$ months with starting time $t_1 = 1$	71
4.10	Results from optimization with demand function: $m_{e,i} = \bar{m}_e + m_I t_i$, $m_I = 100/12$. For MILP relaxation, $\mathcal{J}_2(h_{1,i}, \dot{m}_i, i) = h_{1,i} \dot{m}_i$ is replaced by z_i and an updating process is used, see section 3.2.6). Optimized for $t_n = 311$ months and starting time $t_1 = 1$	76
4.11	Results from optimization with demand function: $m_{e,i} = \bar{m}_e + m_I t_i$, $m_I = 25/12$. Optimized for $t_n = 311$ months. Starting time $t_1 = 1$	80
4.12	Results from NLP optimization where the integer variable is relaxed to a real value with demand function: $m_{e,i} = \bar{m}_e + m_I t_i$, $m_I = 100/12$	80
4.13	Other parameters for the optimization model.	84
4.14	Parameters for Scenario 1.	86
4.15	Results for Scenario 1.	86
4.16	Parameters for Scenario 2.	91
4.17	Results for Scenario 2.	92
4.18	Summary of the 14 operation scenarios compared in this work. Scenarios 1 and 2 have to do with Laugarnes and Reykir fields, not assuming annually increases demand. Scenario 3-7 have to do with Laugarnes under annually increased demand and different objective functions and/or constraints and scenarios 8-14 have to do with Reykir field under annually increased demand and different objective functions and/or constraints. . .	96
4.19	Numerical results from optimization. The objective functions compared are present value of profit, profit (with $r = 0$) and sum of deviation between demand and production (equation 4.5). Shortfall is calculated by equation 4.8. Maximum drawdown is maximal value of $h_{1,i}$ calculated after the optimization has been performed. The table also displays timing and frequency of adding pumps, number of iteration for the optimization and the error (see equation 3.19) between the linear and non-linear objective and or constraint. Objectives and added/removed constraint are in bold script in the tables for each scenario.	100

4.20 Numerical results from optimization. The objective functions compared are present value of profit, profit (with $r = 0$) and sum of deviation between demand and production (equation 4.5). Shortfall is calculated by equation 4.8. Maximum drawdown is maximal value of $h_{1,i}$ calculated after the optimization has been performed. The table also displays timing and frequency of adding pumps, number of iteration for the optimization and the error (see equation 3.19) between the linear and non-linear objective and or constraint. Objectives and added/removed constraint are in bold script in the tables for each scenario. 108

List of Abbreviations

DO	Dynamic optimization
DP	Dynamic programming
HJB	Hamilton-Jacobi-Bellman
LP	Linear programming
LPM	Lumped parameter model
MIDO	Mixed-integer dynamic optimization
MILP	Mixed-integer linear programming
MILPr1	Relaxation 1: MILP relaxation with piecewise linear approximation
MILPr2	Relaxation 2: MILP relaxation with under- and over-estimators
MINLP	Mixed-integer non-linear programming
NLP	Non-linear programming
NLPr2	Relaxation 3: NLP relaxation
PV	Present value
SQP	Sequential quadratic programming

Nomenclature

Sets

\mathcal{I}	$\{1 \dots n\}$ Time steps
\mathcal{E}	$\{1 \dots N\}$ Number of tanks in the LPM model

Indices

i	Discrete time index
j	Index for number of tanks in the LPM model

Decision Variables

\dot{m}_i	Extraction from tank 1 at time i , [kg/s]
y_i	Number of pumps added to the system at time i

State Variables

t_i	Discrete time, $t_1 \leq t_i \leq t_n, \forall i \in \mathcal{I}$, [s]
$h_{j,i}$	Drawdown at time i in tank j , $\forall j \in \mathcal{E}$ and $i \in \mathcal{I}$, [m]

Parameters

σ_{jk}	The conductivity between tanks j and k , [$\text{m} \cdot \text{s}$]
σ_N	The conductivity between tank N and the external environment of the system, [$\text{m} \cdot \text{s}$]

S Conductivity matrix [$N \times N$]

H_0	The external drawdown, [m]
$h_{j,1}$	Initial condition. Drawdown in tank j at time $i = 1 \forall j \in \mathcal{E}$, [m]
h_1^{max}	Maximum drawdown of tank 1, sustainability constraint, [m]
$h_{e,i}$	Historical value of drawdown, at time i , [m]
$\dot{m}_{e,i}$	Historical value of demand at time i , [kg/s]
$h_{z,i}$	Drawdown reference point for the piecewise linear approximation at time step i , [m]
$\dot{m}_{z,i}$	Production reference point for the piecewise linear approximation at time step i , [kg/s]
κ_j	Storage coefficient of tank j , $\forall j \in \mathcal{E}$, [$\text{m} \cdot \text{s}^2$]

K Storage coefficient matrix [$N \times N$]

g	Gravitational acceleration [m/s^2]
Δt	Time step, $\Delta t = t_{i+1} - t_i$, [s]
ρ	Density of water at 25°C, [kg/m^3]
C_{Elect}	Price of electricity, [\$/J]
C_{Water}	Price of water, [\$/m ³]
C_{Pump}	Price of installing a pump, [\$/]
$P_{\text{Power},i}$	Production capacity, pumping power needed at time step i , [W]

Notation for the optimization methods compared

\mathcal{J}	Objective function. Profit with no interest rate assumed. This notation is also used for mathematical explanations.
\mathcal{J}^{PV}	Objective function. Present value of profit optimized.
$\mathcal{J}_{MILPr1}^{PV}$	Objective function. The present value of profit for the MILP relaxation with a piecewise linear approximation, r1.
\mathcal{J}_{MILPr1}	Objective function. Profit calculated with no interest rate assumed.
$\mathcal{J}_{MINLPPr1}^{PV}$	Objective function. The present value of the profit calculated non-linearly with the values from the relaxation, after the optimization has been performed.
$\mathcal{J}_{MINLPPr1}$	Objective function. Profit calculated non-linearly with the values from r1, after the optimization has been performed. No interest rate assumed.
$\mathcal{J}_{MILPr2}^{PV}$	Objective function. Profit for the MILP relaxation with under-and over-estimators, r2.
\mathcal{J}_{MILPr2}	Objective function. Profit calculated with no interest rate assumed, r2.
$\mathcal{J}_{MINLPPr2}^{PV}$	Objective function. Present value of the profit calculated non-linearly with the values from the relaxation, after the optimization has been performed.
$\mathcal{J}_{MINLPPr2}$	Objective function. The profit calculated non-linearly with the values from the relaxation, after the optimization has been performed. No interest rate assumed.
$\mathcal{J}_{NLPPr3}^{PV}$	Objective function. Present value of profit for the NLP relaxation, r3.
\mathcal{J}_{NLPPr3}	Objective function. The profit for the NLP relaxation, r3.
\mathcal{J}^{DEV}	Objective function. Deviation between production and demand minimized.
$\mathcal{J}_{2,Error}^{PV}$	Error of the relaxation by comparing \mathcal{J}_2 (with an interest rate) approximated and then calculated non-linearly after the optimization has been performed.
$\mathcal{J}_{2,Error}$	Error of the relaxation by comparing \mathcal{J}_2 (without interest rate) approximated and then calculated non-linearly after the optimization has been performed.

Chapter 1

Introduction

1.1 Geothermal energy and sustainability

Geothermal energy can be harnessed by extracting heat from the Earth's crust. It is a promising source for heat and power as it is considered to be a *renewable* resource that may be utilized in a *sustainable* manner. Geothermal energy is now widely utilized all around the world, either directly or for power generation. Using renewable energy sources is one way of reducing dependency on fossil fuels. Renewable energy technologies with sustainability considerations have been evaluated by several authors [[Hepbasli, 2008](#); [Lund, 2007](#); [Evans et al., 2008](#); [Varun et al., 2009](#); [Axelsson, 2010](#)].

Geothermal systems can be classified according to their temperature and the presence of fluid. Systems with temperature less than 150 °C are usually referred to as low temperature or low enthalpy systems. They are typically hydrothermal permeable systems that have geothermal fluid naturally present and thus ideal for direct usage. High temperature systems with temperature ranging from 150 °C to 300+ °C, are usually used for conversion to power. Such systems are quite different as they usually contain fluid in two phases and phase changes are more likely to occur. Direct use of geothermal energy is considered to be the oldest and most common form of renewable energy utilization and has alone almost doubled in the past 10 years [[Lund et al., 2011](#)]. Power generation from geothermal energy sources is expected to increase rapidly as well, around 73% in the next 5 years [[Bertani, 2010](#)]. Worldwide potential of geothermal energy utilization is considerable as well and can provide a partial contribution to the sustainable energy use in the world [[Axelsson, 2010](#)]. To meet increased demand, governments and businesses (in countries where geothermal energy is available) need to decide whether or not to es-

establish a geothermal energy utilization scheme, as well as to design operational strategies for those systems to meet demand in a profitable way without compromising the future potential of the resource. Although most geothermal systems are considered renewable, the economic horizon of large-scale investments such as power plants may be greater than the characteristic time for regeneration of the reservoir for a given system. It is thus important to take into account the effects of *long-term* utilization on such fields and an operation strategy that aims for sustainable production. For a profitable utilization of a geothermal resource, it is very important to gather general knowledge of the relative field, by e.g. drilling exploratory wells and gather production history. Thorough exploration is however costly and it is unlikely that uncertainty can be eliminated completely. The size and dynamic characteristics of geothermal reservoirs are thus in some cases poorly understood when capital investments begin.

The term sustainability has become somewhat fashionable in some areas, such as politics and the broadcast media. It is thus important to understand what it means in the geothermal context and to make a clear distinction between renewability and sustainability. Renewability is a property of a resource where the energy extracted from the system is always replaced by additional energy. This replacement of energy is required to take place at a similar time scale as the extraction. Fossil fuels can thus be considered renewable on a geological time scale, but are considered finite energy sources on a human time scale [Stefansson, 2000]. Sustainability on the other hand refers to the endurance capacity of the exploitation where production levels can be maintained over a long period of time [Rybach and Mongillo, 2006]. A renewable system can thus be exploited in a sustainable or a non-sustainable manner.

Low temperature geothermal systems are most commonly used for space heating and provision of hot water and in some cases generation of electrical power [Xin et al., 2012]. In particular, the vast geothermal resources in Iceland have been utilized to a considerable extent, mainly for space heating. A low temperature geothermal field is harnessed by drilling a number of wells in to the field. This fluid is used as a heat source, and once heat has been extracted from the fluid it may or may not be re-injected into the field. The production from the field is determined simply by the flow rate and temperature of the extracted fluid. Historical experience indicates that geothermal fields respond to production by declining pressure (or *drawdown*¹) and sometimes declining temperature [Axelsson, 1991; de Paly et al., 2012]. This could imply that limiting production might become a

¹ In this work drawdown represents the distance from average height to the surface of the water in the wells (water level)

necessity after an extended period of operation. From a financial point of view, due to the time value of money, excessive production can be beneficial since the annual revenue in the early years has the greatest effect upon the present value of the operation. [Lovekin \[2000\]](#) concluded that a particular aggressive exploitation scenario resulted in a discounted return of investment and present worth almost three times higher than a conservative use of the resource, despite higher costs of make-up wells at later stages in the operation. A good example could be the 300 MW Hellisheidi power plant in Iceland, but that remains to be seen. It was built up in three big units in 3 years, which could suggest an excessive production from the beginning. The main drawback of excessive production is that in the long-term sense, it can lead to resource deterioration or even depletion. It was for example shown in [\[Eugster and Rybach, 2000\]](#) that the time required for thermal recovery in a specific geothermal system was roughly equal to production time. The increased use of geothermal resources has raised questions regarding their sustainable production and how the resource is harnessed in an optimal manner. Currently it is unclear how to design optimal operation strategies of power plants or district heating utilities that satisfy the customer and ensure both profitable and sustainable power production.

There are many ways to evaluate sustainability. In [Axelsson \[2010\]](#) sustainability is evaluated from the operational experience of a geothermal reservoir. [Axelsson \[2010\]](#) considers *three* main sustainable production modes for a long term utilization (more than 100 years) of a geothermal system: Constant production below an evaluated sustainability limit, step-wise increase in production until the sustainability limit has been assessed, excessive cycle production with long breaks and excessive production for 30 to 50 years followed by a reduced production for 150 to 170 years. [Duan et al. \[2011\]](#) discuss a criteria with five main categories of sustainability: resource, technological, environmental, economical and social attributes where sustainability is evaluated by a fuzzy synthetic evaluation, by ranking the categories but excluding social and economic attributes. In this work, and for a more tangible insight of the term, sustainability will be mostly considered in terms of the exergy of the fluid and utilization efficiency. With that methodology it is possible to simply calculate the maximum drawdown for a giving system and use it as a sustainability constraint in an optimization model. For further reading on exergy and sustainability see [\[Hepbasli, 2008; Lund, 2007; Dincer, 2002\]](#).

1.2 Geothermal reservoir modeling

In designing an operational strategy of utilizing geothermal energy it is of considerable interest to be able to predict the dynamic response of the geothermal reservoir from the production. By doing so it may be possible to manage production in such a way that revenue or profit is maximized while ensuring long-term production capability. A plan for capital investments such as purchasing and installing borehole pumps can also be constructed. To do so it is highly useful to construct a representative model of the underlying reservoir showing the responds to fluid being pumped from it.

Several methods exist for reservoir modeling in geothermal systems. Common ones are e.g. volumetric methods, detailed mathematical modeling and lumped parameter modeling (LPM). Volumetric methods involve conceptual modeling and are based on estimation of the total heat stored in a volume of rock but do not take into account the dynamic response of the system [Axelsson, 2008]. Detailed numerical models involve high resolution in three dimensions and are eminently suitable for a number of tasks such as selecting borehole locations etc. Such detailed modeling depend on various parameters and data. Lack of such data makes it difficult to construct detailed numerical models. The computational cost of these models can as well become prohibitive when they are to be used for optimization applications.

Lumped parameter modeling (LPM) approach has been applied by several authors [Grant, 1983; Pruess et al., 1986; Gudmundsson and Olsen, 1987; Axelsson, 1989; Martinovic, 1990; Satman et al., 2005] and represents the dynamics of the system without information about detailed spatial variation. The lumped parameter models are practical in predicting the production capacity of geothermal fields if fast computation is needed and are not dependent on various parameters like detailed numerical models. A representative lumped model is very likely to serve as a useful tool in the decision making process with regards to the exploitation rate, investment cost and sustainability considerations. The main concern of this work is to look at how to exploit a resource in a sustainable manner in light of reservoir dynamics and increased market demand. In order to do this it is necessary to include both the dynamics of the reservoir and the markets.

The Reykjavik metropolitan area utilizes six geothermal systems. Four of them are liquid-phase low temperature geothermal systems; Laugarnes field, Ellidaar field, Reykir field and Reykjahlid field. The other two, Nesjavellir and Hellisheidi are high temperature geothermal systems that have been exploited for a short period of time compared to the

other four. The focus here is only on the four liquid-phase low temperature geothermal systems, where geothermal fluid is naturally present and no phase change occurs. In the LPM the systems are assumed to be isothermal [Axelsson, 1989] and re-injection does not occur. Data records for production and water level from those four fields will be examined and calibrated to the LPM for a potential use where an operational optimization model is connected to the LPM. In order to estimate how reliable such calibration is, they are validated by a split sample validation [Picard and Berk, 1990]. That result is used to simulate the behaviour of the geothermal fields. The simulation serves as an underlying constantly developing constraint in the optimization model which is the topic of next section.

1.3 Optimization

Optimization algorithms have served as suitable tools for solving complex mathematical problems in several fields of technology. Those problems include complex design, decision analysis and optimal control. Optimization methods have been increasingly applied in the renewable energy sector in recent years [Banos et al., 2010]. Optimization often deals with *decision analysis* of problems where a certain objective function or performance index is either maximized or minimized. The objective function holds one or more unknown variables, usually referred to as *decision variables* as well as it usually needs to satisfy a set of *constraints*². An objective function can be optimized for one instant time only (*static optimization*) or over a certain time period (*dynamic optimization*). It can also be seen as solving one-period problem versus solving a multi-period problem. In a dynamic optimization, decisions today depend upon decisions yesterday etc.

In this work, the objective function is both a function of time and an underlying system of differential equations. This is thus a dynamic optimization problem. For a more intuitive understanding of the operational model, imagine a firm holder of a district heating utility. He strives for both profitable business and satisfied customers as well as to utilize the resource in a sustainable way for future generations. How can he do that? As explained in section 1.2, the resource under consideration in this work is a low-temperature geothermal field with a certain number of wells. In order to get to the water, it usually needs to be pumped from the wells. The number of pumps needed depends on their power capacity and the drawdown. The dynamics of the system, i.e. how drawdown responds to production can be evaluated with the LPM. Demand for energy is assumed to be known. Decision variables in the optimization therefore include production and number of pumps

² Not all optimization problems are constrained, cf. unconstrained optimization

needed. Other decisions include the time point at which pumps should be bought and installed and when a defined sustainability limit is reached. The drawdown is a function of production and is thus a *state variable* in the model. Possible performance indices include maximization of profit or minimization of demand that can *not* be met. Constraints include a sustainability limit and pumping capacity (it is very unlikely to be profitable to buy an infinite number of pumps). The lumped parameter model is (in this work) applied in such a way that one field is considered as one reservoir and spatial variations of the system are ignored. This means for example that for a certain period of time, it can be optimized exactly how many pumps are needed for the whole field and exactly when they are needed, but not where they should be located. The pumps are represented by a time dependent integer and the functions representing pump capacity and profit are non-linear. This is thus inherently a mixed integer non-linear optimization of a process that can be described by an underlying system of differential equations, the LPM.

In a general form this sort of problem can be written as:

$$\begin{aligned}
& \underset{\mathbf{x}, \mathbf{u}, \mathbf{y}}{\text{maximize}} && \mathcal{J}(\mathbf{u}, \mathbf{x}, \mathbf{y}, t_n) := \int_{t_0}^{t_n} l(t, \mathbf{x}(t), \mathbf{u}(t), \mathbf{y}(t)) \beta^t dt, \\
& \text{subject to} && \\
& && \dot{\mathbf{x}}(t) = \mathbf{f}(t, \mathbf{x}(t), \mathbf{u}(t)), \quad x(t_0) = x_0 \quad u(t_0) = u_0 \\
& && \mathbf{g}(t, \mathbf{x}(t), \mathbf{u}(t), \mathbf{y}(t)) \leq 0 \\
& && \mathbf{u}^L(t) \leq \mathbf{u}(t) \leq \mathbf{u}^U(t) \\
& && \mathbf{x}^L(t) \leq \mathbf{x}(t) \leq \mathbf{x}^U(t)
\end{aligned} \tag{1.1}$$

The goal is to find the control trajectory $\mathbf{u} \in \mathbb{R}$, where $[t_0, t_n]$ is the time interval of interest in order to maximize the cost function or performance index $l : [t_0, t_n] \in \mathbb{R}$. Now, $\mathbf{x} : [t_0, t_n] \in \mathbb{R}$ is a state vector and \mathbf{f} is a vector set of equality constraints. $\mathbf{y} : [t_0, t_n] \in \mathbb{Z}^+$ is an integer decision vector, $\mathbf{g} : [t_0, t_n] \in \mathbb{R}$ is a vector of inequality constraints, x_0 and u_0 are the initial conditions and \mathbf{u}^L and \mathbf{u}^U represent lower and upper bound of the control trajectory and \mathbf{x}^L and \mathbf{x}^U of the state variable. β is a discount factor $0 \leq \beta \leq 1$.

There are several names for such problems in the literature, but they are usually referred to as *mixed-integer dynamic optimization (MIDO)* or *mixed-integer optimal control (MIOC)*. These sorts of problems (MIDO or MIOC) can be seen as members of the class of mixed-integer optimization problems just like *mixed-integer linear programming*

(MILP) and *mixed-integer nonlinear programming* (MINLP). Another point of view is to see MIDO and MIOC as a special kind of dynamic optimization or optimal control problems [Sager, 2006].

The terms optimal control, dynamic optimization and trajectory optimization refer to a problem where it is desired to determine the inputs to a dynamical system that optimizes a specified objective function while satisfying any constraints on the motion of the system. These terms are often interchanged in the literature. If the inputs to the system are static parameters and the desired result is to find the value of these parameters and the trajectory vector that optimizes a given objective function, the term dynamic optimization or trajectory optimization is often used. The term optimal control is often used for an optimization where the input to the system are control functions [Rao, 2009]. Other publications imply that optimal control is a subclass of dynamic optimization. The term dynamic optimization might however also refer to parameter estimation or is easily confused with dynamic programming. With that in mind and since the input to the system here are not functions but static parameters, the problem here will be referred to as dynamic optimization.

It is very important to state at this point that this sort of problems are in general extremely challenging to solve. No general algorithms exist that yield acceptable results for all problem instances [Sager, 2012]. Many different approaches have been proposed over the years to solve such problems as they relate to many different mathematical disciplines. The so-called *indirect methods* and *direct methods* are often compared in the literature in this relation [Betts, 2001; Diehl, 2011; Binder et al., 2001]. Binder et al. [2001] discusses three general approaches to solve dynamic optimization problems:

Firstly, solution of the Hamilton-Jacobi-Bellman (HJB) equation and *Dynamic programming* (DP) in the discrete setting. Dynamic programming suffers from the Bellman's "curse of dimensionality" as computational complexity of the DP algorithm increases exponentially with dimensionality of the state. This makes DP an impractical method in large-scale applications. It was however not thoroughly investigated whether DP could be successfully applied to this problem.

Secondly, indirect methods, i.e. *calculus of variations* which is an extension of calculus to infinite dimensional space that was developed into *the maximum principle*. The maximum principle is often considered as a dynamic generalization of the method of Lagrange multiplier [Chow, 1997]. The indirect methods iterate on necessary optimality conditions to find a solution, so the method finds the optimal "indirectly". Indirect

methods involve differentiation that is not possible with an integer function and appear to be too mathematically expensive for such a problem like the one considered here. It is however not excluded that a relaxation to NLP with an indirect method would give a promising result which is attempted in this work.

Thirdly, direct methods. This work will focus more on direct methods since they have been considered more promising in the literature for the past two decades, especially in dealing with real live large scale dynamic optimization problems [Sager, 2012]. Other approaches will not be discussed here in detail, for further reading see e.g., [Bryson, 1999; Bellman, 1957; Dadebo and McAuley, 1995; Luus, 2000].

With direct methods, non-linear dynamic optimization problem can be transcribed into a NLP problem with discretization, or in this work a MINLP of the form:

$$\begin{aligned}
 & \underset{z,y}{\text{maximize}} && l(z,y), \\
 & \text{subject to} && \\
 & && f(z,y) = 0, \\
 & && g(z,y) \leq 0, \\
 & && z \in \mathcal{Z}, \\
 & && y \in \mathcal{Y}
 \end{aligned} \tag{1.2}$$

where $\mathcal{Z} \subset \mathbb{R}^{n_z}$ and $\mathcal{Y} \subset \mathbb{Z}_+^{n_y}$ are the sets of real numbers and positive integer variables respectively. n_z is the number of continuous variables and n_y the number of integer variable. The functions $l : \mathbb{R}^{n_z+n_y} \rightarrow \mathbb{R}$, $g : \mathbb{R}^{n_z+n_y} \rightarrow \mathbb{R}^m$ and $f : \mathbb{R}^{n_z+n_y} \rightarrow \mathbb{R}^m$ are usually required to be twice continuously differentiable functions. The differential equations from the optimization problem represented by equation 1.1 can now be seen as the equality constraints of the MINLP problem and the decision variable z represents the control and state variables. Minimization (instead of maximization) can readily be included along with upper and lower bound of the decision variables like in a dynamic optimization problem.

One of the most important advantages of direct methods compared to indirect methods is that they can easily treat inequality constraints, like the inequality path constraints, g in the optimization problem represented by equation 1.2 here above. When a non-linear dynamic optimization problem is converted into NLP, the optimization can be treated with well developed NLP methods [Diehl et al., 2005].

Direct methods are based on a finite dimensional parameterization of the control trajectory, but differ in the way the state trajectory is handled (\mathbf{x} in equation 1.1). Discretization is usually constructed via shooting, multiple shooting, or collocation [von Stryk, 1993; Bock and Plitt, 1984]. In this work direct collocation will be applied, i.e. the differential equation is discretized by a numerical procedure, defining a grid of n points that cover the time interval $[t_0, t_n]$, $t_0 = t_1 < \dots < t_n = t_n$.

Mixed-integer nonlinear program (MINLP) optimization problems (like equation 1.2 above) combine the combinatorial difficulty of optimizing over discrete variable sets with the challenges of handling nonlinear functions. It is thus not surprising that MINLPs are in general NP-hard (not solvable in polynomial time). It has even been shown that very special subclasses of MINLP are NP-hard. One particular subclass of the problem represented by equation 1.2 is a static, pure integer optimization problem that consist of a convex quadratic function and linear constraints. Such problems and therefore the general class of MINLPs have been proven to be NP-hard [Garey and Johnson, 1979; Sager, 2006].

It is also very useful to make a distinction between the so called *convex*³ and *non-convex* MINLPs. If the functions, $l \in \mathbb{R}$, $f \in \mathbb{R}^m$ and $g \in \mathbb{R}^m$ are all convex, the MINLP is called convex; otherwise non-convex. Convex and non-convex MINLP are both NP-hard in general, but it is much easier to solve convex ones in theory and practice.

Direct methods are also about adapting algorithms originally developed for MINLPs to optimization problems embedding underlying dynamic systems. That includes relaxing the problem to a form that is solvable in polynomial time. Most MINLP are solved by applying a form of a so called *tree-search*. The tree methods include for example nonlinear branch-and-bound [Gupta and Ravindran, 1985] and branch-and-bound with cutting planes [Stubbs and Mehrotra, 1999] methods. Methods applied along with the tree-search to account for the NP-hardness of the MINLP include; relaxation to MILP with a linearization, under-and over-estimators or outer approximation, convexification, relaxation of the integer to NLP, extended cutting plane etc, see [Grossman, 2002] for a good overview.

Here, the problem is first solved by relaxing it to MILP where non-linear functions

³ For a maximization it is theoretically *concave* instead of *convex*. But the literature usually talks in terms of minimization and thus *convex* and *non-convex* optimization.

are approximated with Taylor approximation. The MILP is solved with an optimization algorithm using branch-and-bound with cutting planes. In certain cases an updating algorithm is needed for a good linear approximation. The problem is also solved by defining under-and over-estimators of the non-linear functions which is another kind of relaxation to MILP. Finally the problem is solved by relaxing it to NLP. The three relaxation methods are compared and discussed. One relaxation method is then chosen to carry out an optimization for different operational scenarios.

1.4 Objective and Contribution

This thesis is an interdisciplinary work of *operations research* and *geothermal reservoir modeling*. Operational research or optimization (introduced in the section 1.3) is in itself interdisciplinary mathematical science that focuses on the effective use of a specific technology, such as geothermal energy.

The main objective of this thesis is to develop an efficient optimization algorithm that can be used to find an optimal production scheme for utilizing a geothermal resource in a sustainable way. Sustainability implies long term utilization in terms of production capacity and development of water level in a reservoir. In this way, decision support is provided in terms of looking at the "big picture" in utilizing a geothermal resource.

Important factors that need to be accounted for are:

- A geothermal system needs to be described mathematically and simulated with an acceptable model.
- An optimization model with the capacity to describe the possible operational scenarios needs to be established. This optimization model needs to be solvable within an acceptable time frame. If a relaxation is required it needs to be significant.
- The two factors above must be connected together allowing the construction of a sustainable optimal production scheme for a geothermal reservoir. Different optimization scenarios in terms of different objective functions and constraints can then be compared.

Another concern of this work, and perhaps more philosophical one relates to different objective functions (cf. the last factor here above). I.e., what is an optimal or the correct

objective function? Is the present value of profit the only legitimate objective function? Are there other objectives in the system that if optimized would give value to the operation? It is e.g. very important to meet demand. A demand/production objective function can be used to minimize the deviation between production and demand. Another point of view is to consider whether the interest rate (present value of money) is necessary in terms of sustainability considerations. The main idea of sustainability is to value next generations and their needs as much as the current generation. Using an interest rate and maximizing profit skews the results substantially in the favor of the current generations. It is thus interesting to maximize profit without using an interest rate.

The main contribution of this work is that a methodology has been developed and tested to optimize the production scheme for a geothermal resource. This model can be used with any sufficient data set for a low temperature geothermal reservoir and give information on what would be a good production scheme for the long term utilization. This methodology can be applied to short term utilization as well, but the main objective is not to generate exact monthly overview but rather to have a good long term overview.

1.5 Structure of the thesis

The remainder of the thesis is organized as follows:

- *Chapter 2* explains the modelling approach. First the LPM, it's structure and how it can be integrated. The constraints of the optimization model are outlined along with the optimization model itself.
- *Chapter 3* goes deeper into theory related to optimization and outlines theoretically solution methods for the optimization problem.
- *Chapter 4* presents the results. First a parameter fit for the LPM is conducted where different types of LPM models are compared and data for four geothermal fields are tested. Secondly the optimization methods introduced in chapter 3 are tested. Finally an optimization method is chosen to apply for a long term utilization for two geothermal fields, chosen from two of the best parameter fits.
- *Chapters ?? and ??* summarize the results and suggests open problems and possible further research.

Chapter 2

Modeling approach

This chapter explains the modeling approach, the lumped parameter model (LPM) and how it is numerically integrated. The optimization model is explained by accounting for the objective function and each constraint respectively. Through that explanation it should be clear how the optimization model is constructed and how it is directly connected to a reservoir model, i.e. the LPM.

2.1 Lumped parameter model (LPM)

The reservoir modeling in this study is based on a lumped parameter description of a liquid phase hydrothermal reservoir. As in [Satman et al. \[2005\]](#) and [Axelsson \[1989\]](#) a geothermal system consisting of generally three parts is considered. The first part can be visualized as the central part of the reservoir, the second as the outer part and the third as the recharge source. This kind of system can also be considered as a series of connected storage tanks (capacitors) that represent the neighborhood of a geothermal well (see figure 2.1). These storage tanks are connected together so that fluid can flow between them. Fluid can also flow from the smallest tank to the surface, representing the production. The states of these tanks are generally represented by pressure head and the pressure difference between tanks along with connection conductances that determine the actual flow between them. Drawdown will be used to describe the states here instead of pressure.

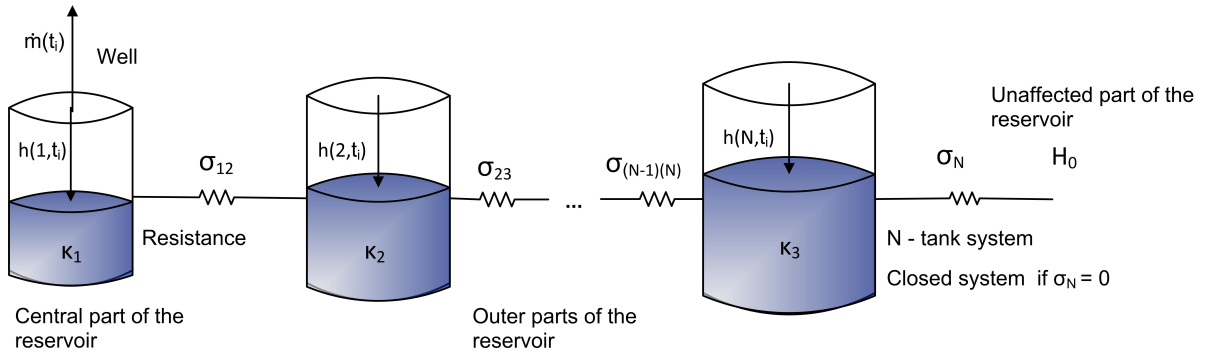


Figure 2.1: N-Tank LPM system. The system can be closed ($\sigma_N = 0$) or open

The tanks have storage coefficients¹ κ and drawdown (pressure) $h_{t_i,j}$, $\forall j \in \mathcal{E} := \{1 \dots N\}$ at a discrete time step $t_i = i$, $\forall i \in \mathcal{I} := \{1 \dots n\}$.

The tanks are connected by upto $N(N-1)/2$ resistors where σ_{jk} connects tank j to tank k . The network is open if the last tank N is connected through a resistor σ_N to an external tank with a fixed drawdown H_0 , which allows fluid to flow either in or out of the system. The network is closed when $\sigma_N = 0$. The mass flow from the system at time step i is represented by \dot{m}_i . The initial state of the system at time $i = 1$ is assumed to be equal to a fixed drawdown (pressure) and a fixed mass flow.

The flow between the tanks is related to the difference in drawdown in connected tanks. For $N = 3$, this relation can be written as three coupled differential equations, one for each storage tank. This results in

$$\kappa_1 \frac{dh_1}{dt} = \sigma_{12}(h_2 - h_1) + \frac{\dot{m}}{\rho g} \quad (2.1)$$

$$\kappa_2 \frac{dh_2}{dt} = \sigma_{12}(h_1 - h_2) + \sigma_{23}(h_3 - h_2) \quad (2.2)$$

$$\kappa_3 \frac{dh_3}{dt} = \sigma_{23}(h_2 - h_3) + \sigma_3(h_0 - h_3) \quad (2.3)$$

For an N dimensional system the basic system equation matrix form can be written as:

$$\mathbf{K} \frac{\partial}{\partial t} \mathbf{h} = \mathbf{S} \mathbf{h} + \mathbf{u} \quad (2.4)$$

¹ Storage coefficients indicate free-surface storage

where

$$\mathbf{K} = \begin{bmatrix} \kappa_1 & 0 & \dots & 0 \\ 0 & \ddots & \ddots & \vdots \\ \vdots & \ddots & \kappa_{N-1} & 0 \\ 0 & \dots & 0 & \kappa_N \end{bmatrix} \quad \mathbf{h} = \begin{bmatrix} h_1 \\ \vdots \\ h_N \end{bmatrix} \quad \mathbf{u} = \begin{bmatrix} \dot{m}/\rho g \\ 0 \\ \vdots \\ 0 \\ \sigma_N H_0 \end{bmatrix}$$

$$\mathbf{S} = \begin{bmatrix} -\sigma_{12} & \sigma_{12} & 0 & \dots & 0 \\ \sigma_{12} & -(\sigma_{12} + \sigma_{23}) & \sigma_{23} & \ddots & \vdots \\ 0 & \ddots & \ddots & \ddots & 0 \\ \vdots & \ddots & \ddots & \ddots & \sigma_{(N-1)N} \\ 0 & \dots & 0 & \sigma_{(N-1)N} & -(\sigma_{(N-1)N} + \sigma_N) \end{bmatrix}$$

There are various ways to integrate the system above, either analytically in continuous time or with numerical methods in discrete time. As explained in 1.3 the optimization model will be solved by converting the inherently non-linear mixed integer dynamic optimization model to MINLP with discretization. In this work, direct collocation will be applied which means the system above (the state variables) are discretized as well as the decision variables. The system is thus integrated numerically which is the topic of next section.

2.1.1 Integration of the lumped parameter model

The lumped parameter model system of differential equations is solved by numerical integration. A solution needs to be approximated for the following system:

$$\mathbf{K} \frac{\partial}{\partial t} \mathbf{h} = \mathbf{S} \mathbf{h} + \mathbf{u}, \text{ where } \mathbf{h}_{i=1} = \mathbf{h}_1 \quad (2.5)$$

Three different methods will be considered.

The forward Euler method

The Euler method can solve ordinary differential equations numerically for a given initial value. The derivative of \mathbf{h} can be approximated as:

$$\frac{\partial}{\partial t}\mathbf{h} \approx \frac{\mathbf{h}_{i+1} - \mathbf{h}_i}{\Delta t} \quad (2.6)$$

where Δt is the size of the discrete time step, $\Delta t = t_{i+1} - t_i$. Combining equations 2.5 and 2.6 and solving for \mathbf{h}_{i+1} gives:

$$\mathbf{h}_{i+1} = \mathbf{h}_i + (\mathbf{K})^{-1}\Delta t(\mathbf{S}\mathbf{h}_i + \mathbf{u}_i) \quad (2.7)$$

Methods for numerical integration are often classified into *implicit* and *explicit* methods. The forward Euler method is an explicit method as the future time step \mathbf{h}_{i+1} is defined in terms of past time step only, i.e. \mathbf{h}_i and \mathbf{u}_i . Explicit methods are usually easier to implement but can have stability issues if the time step is not sufficiently small, i.e. they have a bounded stability domain.

The backward Euler method

Implicit methods can be used to replace explicit methods in case of strictly bounded stability domain. The backward Euler method is an implicit method. If \mathbf{h}_i denotes the future time step at time step i and \mathbf{h}_{i-1} denotes the current state the derivative of \mathbf{h} can also be found as:

$$\frac{\partial}{\partial t}\mathbf{h} \approx \frac{\mathbf{h}_i - \mathbf{h}_{i-1}}{\Delta t} \quad (2.8)$$

Combining equations 2.5 and 2.8 and solving for \mathbf{h}_{i+1} gives:

$$\mathbf{h}_{i+1} = (\mathbf{K} - \Delta t\mathbf{S})^{-1}(\mathbf{K}\mathbf{h}_i + \Delta t\mathbf{u}_{i+1}) \quad (2.9)$$

The modified Euler method

A relatively simple, implicit and accurate method to integrate the lumped equations is a central finite difference approximation of the time derivative, often referred to as *Tustin's method* or *the modified Euler method*. Here, the function is considered at both the be-

ginning and at the end of each time step, taking the average of the two. This is also an implicit method that requires a value of \mathbf{u}_{i+1} , or a future time step. Here the numerical approximation of equation 2.5 becomes:

$$\mathbf{K} \frac{\mathbf{h}_i - \mathbf{h}_{i-1}}{\Delta t} = \mathbf{S} \frac{\mathbf{h}_i + \mathbf{h}_{i-1}}{2} + \frac{\mathbf{u}_i + \mathbf{u}_{i-1}}{2} \quad (2.10)$$

Solving for \mathbf{h}_i and writing in terms of \mathbf{h}_{i+1} gives

$$\mathbf{h}_{i+1} = \left(\mathbf{K} - \frac{\Delta t}{2} \mathbf{S} \right)^{-1} \left(\left(\mathbf{K} + \frac{\Delta t}{2} \mathbf{S} \right) \mathbf{h}_i + \frac{\Delta t}{2} (\mathbf{u}_{i+1} + \mathbf{u}_i) \right) \quad (2.11)$$

In this work, the time step Δt is based on the resolution of the measured data which is in months, i.e. a relatively big time step. The modified Euler method is chosen since it is not bounded by stability domain and proves to be more accurate than the backward Euler method (see figure 2.2).

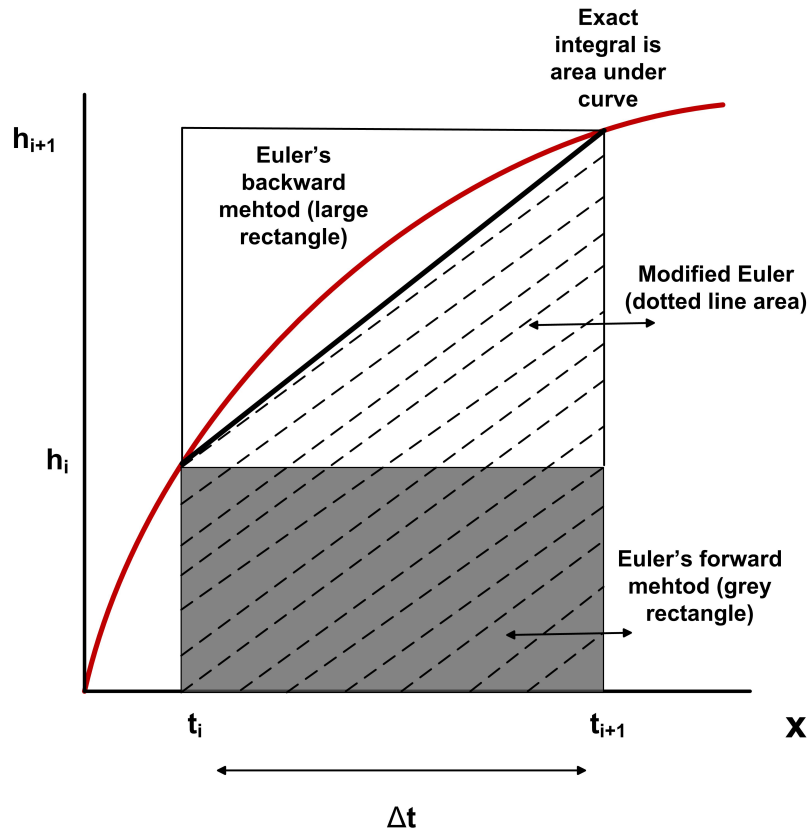


Figure 2.2: Graphical comparison of three different numerical methods to integrate a bivariate function. The Euler method, the backward Euler method and the modified Euler method. h_i represent drawdown at time t_i

2.2 Optimization model

The objective here is to maximize or minimize an objective function over a period of time by determining the decision and state variables² of the dynamic system explained in last section. In this section the objective function will be the present value of *profit*. Other performance indices will be discussed in results. The lumped parameter model is a dynamic N -dimensional system, depending on the number of tanks. The decision variable is the mass flow/production \dot{m}_i and the state variables the drawdown in each of the tanks $h_{i,j}$ at a discrete time step i , $\forall i \in \mathcal{I}$. An integer decision variable (vector) y_i , that is not a part of the underlying dynamic system, is added to the model to decide in which time steps production capacity should be increased (a new pump should be installed).

2.2.1 Objective function

The *present value* of profit is calculated as the difference between income from selling the water, production cost and cost by installing an additional pump times a *discount factor* based on an interest rate.

The discount factor is defined as β and represents the factor by which a future cash flow must be multiplied in each time step, in order to obtain the present value:

$$\beta^i = \frac{1}{(1+r)^i} \quad (2.12)$$

Discrete time steps i and an annually-compounded fixed interest rate r are assumed here. The present value of income is thus calculated as:

$$\text{PV}_{\text{Income}} = \sum_{i=1}^n \frac{\Delta t \cdot \dot{m}_i \cdot C_{\text{Water}}}{\rho(1+r)^i}, \quad \dot{m}_i \in \mathbb{R}_+ \quad \forall i \in \mathcal{I} \quad (2.13)$$

The water for district heating is assumed to be sold at a fixed price per cubic meter C_{Water} , Δt represents the size of time step and the parameters ρ (here above) and g (in equation 2.14) represent the density of the water and the gravitational acceleration.

² Can also be referred to as control and state trajectories

The present value of the production cost is calculated as:

$$PV_{\text{Production}} = \sum_{i=1}^n \frac{\Delta t \cdot C_{\text{Electric}} \cdot g \cdot \dot{m}_i \cdot h_{1,i}}{(1+r)^i}, \quad \dot{m}_i, h_{1,i} \in \mathbb{R}_+ \quad \forall i \in \mathcal{I} \quad (2.14)$$

The electricity needed to pump the water from the well is assumed to be bought at fixed price C_{Electric} , [\$/J]. This equation contains a product of a decision variable and a state variable and is thus non-linear. One way to solve the optimization problem is to deal with this equation specially. That will be covered in chapter 3.

New pumps are installed at a price C_{Pump} where y is a decision vector representing how many pumps are installed at time i . The present value of installing an additional pump is calculated as:

$$PV_{\text{Pump}} = \sum_{i=1}^n \frac{y_i \cdot C_{\text{Pump}}}{(1+r)^i}, \quad y_i \in \mathbb{Z}_+ \quad \forall i \in \mathcal{I} \quad (2.15)$$

The profit is finally calculated as:

$$PV_{\text{Profit}} = PV_{\text{Income}} - PV_{\text{Production}} - PV_{\text{Pump}} \quad (2.16)$$

2.2.2 Constraint 1: Mass balance equations on matrix form

Drawdown is a function of demand. Constraint 1 contains this relationship with a discrete approximation of the Lumped Parameter Model. See also section 2.1.1.

$$\mathbf{h}_{i+1} = \left(\mathbf{K} - \frac{\Delta t}{2} \mathbf{S} \right)^{-1} \left(\left(\mathbf{K} + \frac{\Delta t}{2} \mathbf{S} \right) \mathbf{h}_i + \frac{\Delta t}{2} (\mathbf{u}_{i+1} + \mathbf{u}_i) \right), \quad \forall i \in \mathcal{I} \quad (2.17)$$

where

$$\mathbf{u} = \begin{bmatrix} \dot{m}/\rho g \\ 0 \\ \vdots \\ 0 \\ \sigma_N H_0 \end{bmatrix}, \quad \forall i \in \mathcal{I} \quad (2.18)$$

2.2.3 Constraint 2: Demand

The demand constraint states that production \dot{m}_i can not exceed demand $\dot{m}_{e,i}$. The demand can theoretically be any function of time.

$$\dot{m}_i \leq \dot{m}_{e,i}, \quad \forall i \in \mathcal{I} \quad (2.19)$$

2.2.4 Constraint 3: Sustainability

For each geothermal system, and for each mode of production, there is certain power required to extract the water from the well, P_{Well} and certain exergy contained in the water X_{Water}

$$P_{\text{Well}} = \dot{m}gh \quad (2.20)$$

$$X_{\text{Water}} = \dot{m}e_x \quad (2.21)$$

Exergy is a measure of how much work can be done by a system during ideal process that brings the system into equilibrium with its surroundings. For the geothermal liquid under consideration this is taken to be the work that could be done via Carnot cycle between an incompressible liquid and a heat sink at a given temperature as the liquid cools down. Thus the specific exergy of the fluid is approximated as:

$$e_x = c \left((T_h - T_0) - T_0 \ln \frac{T_h}{T_0} \right) \quad (2.22)$$

where c is the heat capacity of water in $\text{J} \cdot \text{kg}^{-1}\text{K}^{-1}$, T_h is the temperature of the fluid and T_0 is the temperature of the heat sink in Kelvin. The equation above is derived using the assumption that c is a constant in the temperature range T_0 to T_h , which is valid for an incompressible fluid at a small temperature range, such as considered in this work.

One possible sustainability criterion is to require that the energy needed to pump a given amount of water from the well must be less or equal to a given fraction of the exergy of that water:

$$P_{\text{Well}} \leq \delta X_{\text{Water}} \quad (2.23)$$

where δ is the exergy efficiency of a typical power production system at the well fluid temperature. For $\delta = 1$ the system is irreversible under Carnot efficiency. The efficiency

of a space heating system such as the one in this work is of course considerably lower. The cost of the investment should also be taken into account for the sustainability limit. In this case efficiency is assumed to be 10% of the Carnot efficiency which means that there is at least 10 times more exergy available in the geothermal fluid than can be utilized for power production under reversible condition.

Maximum drawdown can now be determined by the following equation:

$$h_1^{\max} = \frac{e_x \delta}{g} \quad (2.24)$$

The drawdown in the reservoir (tank 1, figure 2.1) is not allowed to exceed a certain maximum drawdown due to the sustainability criterion defined in equation 2.23.

$$h_{1,i} \leq h_1^{\max}, \quad \forall i \in \mathcal{I} \quad (2.25)$$

2.2.5 Constraint 4: Production Capacity

As described in the section above and by equation (2.20) there is a certain power required to extract the water from the well. The power needed for pumping at time i , $P_{\text{Power},i}$ is calculated as:

$$P_{\text{Power},i} = g \cdot h_{1,i} \cdot \dot{m}_i \leq P_{\text{Pump}} \cdot \sum_{m=1}^i y_m \quad \forall i \in \mathcal{I}, \quad \text{and} \quad m \leq i \leq n \quad (2.26)$$

where P_{Pump} represents the power rating of one pump and y_i is an integer representing how many pumps need to be installed at time i .

There are various options for choosing a pump for a reservoir and each case needs to be carefully considered, e.g. in regards of chemical properties, pressure of the water, etc. In other words, each reservoir needs to be examined individually. Those considerations are outside the scope of this work. It will be assumed that the power rating of each pump is 250 kW [Gunnarsson, 2012].

Since $h_{1,i}$ and \dot{m}_i from equation 2.26 are both unknown decision/state variables this is a nonlinear constraint. This can be dealt with in exactly the same way as for production

part of the objective function.

Now y_i represents the number of pumps installed at time i , where y is a vector of non-negative integers. One pump is assumed to be present in the beginning so y at time $i = 1$ is always at least 1.

$$\begin{aligned} P_{\text{Power},i} &= g \cdot h_{1,i} \cdot \dot{m}_i \\ &\leq 250 \cdot 10^3 \sum_{m=1}^i y_m \end{aligned} \tag{2.27}$$

Here it is important to point out that this is a simplified version of the reality. One well can usually not produce more than 50 kg/s.

2.2.6 The optimization problem

The optimization model now becomes:

$$\begin{aligned}
 & \underset{h_{j,i}, m_i, y_i}{\text{maximize}} && \text{PV}_{\text{Profit}} = \text{PV}_{\text{Income}} - \text{PV}_{\text{Production}} - \text{PV}_{\text{Pump}}, \\
 & \text{subject to} && \\
 & h_{j,i+1} = \left(\mathbf{K} - \frac{\Delta t}{2} \mathbf{S} \right)^{-1} \left(\left(\mathbf{K} + \frac{\Delta t}{2} \mathbf{S} \right) h_{j,i} + \frac{\Delta t}{2} (\mathbf{u}_{i+1} + \mathbf{u}_i) \right) \\
 & \text{P}_{\text{Power},i} \leq 250 \cdot 10^3 \sum_{m=1}^i y_m && (2.28) \\
 & 0 \leq \dot{m}_i \leq \dot{m}_{e,i} && \text{Upper-and lower bounds} \\
 & 0 \leq h_{1,i} \leq h_1^{\text{max}} \\
 & y_i \geq 0 \\
 & h_{j,1} = \mathbf{h}_0, \quad \dot{m}_1 = m_0 \quad y_1 \geq 1 && \text{Initial values} \\
 & \text{where } y_i \in \mathbb{Z}_+, \text{ and } h_{j,i}, \dot{m}_i \in \mathbb{R} \quad \forall i \in \mathcal{I} \text{ and } \forall j \in \mathcal{E}
 \end{aligned}$$

As seen in the optimization model here above, the state variable $h_{1,i}$ is restricted to be greater than zero. Practically in geothermal fields this is not entirely true, since wells can experience *overpressure*, but if $h_{1,i}$ is a negative number it skews the production part of the objective function, equation 2.14. Therefore, the pump actually behaves like a turbine, which means that instead of paying for production, extra money is "earned" for each time step that $h_{1,i}$ is less than zero which is not a realistic scenario. $h_{2,i}$ and $h_{3,1}$ can however be less than zero since they do not effect the objective function directly. This could be sorted out by including only positive values of $h_{1,i}$ in the production function (equation 2.14). This is however not straightforward since $h_{1,i}$ is a state variable in the optimization model, but could possible be solved with a an extra integer mechanism. Since overpressure did not occur in the smallest tank represented by $h_{1,i}$ for the data in this work, this was not investigated further here.

This sort of optimization model can be seen as a mixed-integer dynamic optimization model (MIDO) that can be converted into mixed-integer non-linear optimization (MINLP) model. That model is then solved by relaxing it to mixed-integer linear programming (MILP) by a linear approximation or under-and over-estimators or by relaxing it to a non-linear programming (NLP). Explaining those solution applications is the subject of Chapter 3.

Chapter 3

Solution approach

This chapter suggests three solution methods to solve a MIDO problem like the one represented by equation 2.28 in last section. The model will first be contextualized with the more general form of MIDO and MINLP, i.e. the optimization problems represented by equations 1.1 and 1.2 in chapter 1. If the optimization model can be seen as a MINLP, it can also be relaxed to either MILP or NLP. Feasibility, optimality and convexity will be briefly addressed. Then, two different ways of relaxing the MINLP to MILP will be explained along with further mathematical arrangements needed for an acceptable solution. Finally the model will be relaxed to NLP and discussed what such solution means in context with MILP relaxation.

3.1 Conversion to MINLP

As discussed in section 1.3 the optimization problem will be solved by looking at it as MINLP. For a simplified overview of the optimization problem (equation 2.28), introduced in last chapter, a function \mathcal{J} is defined as the objective function:

$$\mathcal{J}^{\text{PV}}(\dot{m}_i, h_{j,i}, y_i, n) = \mathcal{J}_1 + \mathcal{J}_2 + \mathcal{J}_3 := \text{PV}_{\text{Profit}}, \quad (3.1)$$

where $\mathcal{J}_1^{\text{PV}} = \text{PV}_{\text{Income}}$, $\mathcal{J}_2^{\text{PV}} = \text{PV}_{\text{Production}}$ and $\mathcal{J}_3^{\text{PV}} = \text{PV}_{\text{Pump}}$ (see equations 2.13 - 2.15 in chapter 2).

If the discount factor to calculate present value is defined as $\beta = 1/(1 + r)$, where r is a constant, and U and L represent upper and lower bound, then the optimization

problem can be written as:

$$\begin{aligned}
 & \underset{\dot{m}_i, h_{j,i}, y_i}{\text{maximize}} && \mathcal{J}^{\text{PV}}(\dot{m}_i, h_{j,i}, y_i, n) = \sum_{i=1}^n (C_1 \cdot \dot{m}_i - C_2 \cdot \dot{m}_i h_{1,i} - C_3 \cdot y_i) \beta^i, \\
 & \text{subject to} && \\
 & && \mathbf{f}(\dot{m}_i, h_{j,i}, h_{j,i+1}) = 0 \\
 & && \mathbf{g}(\dot{m}_i, h_{1,i}, y_i) \leq 0 \\
 & && \dot{m}_i^L \leq \dot{m}_i \leq \dot{m}_i^U \\
 & && h_{j,i}^L \leq h_{j,i} \leq h_{j,i}^U \\
 & && y_i^L \leq y_i \leq y_i^U
 \end{aligned} \tag{3.2}$$

where $\dot{m}_i \in \mathbb{R}$, $h_{j,i} \in \mathbb{R}$ and $y_i \in \mathbb{Z}_+$, $\forall i \in \mathcal{I}$ and $j \in \mathcal{E}$. The functions $\mathbf{f} \in \mathbb{R}^{N \times n}$ and $\mathbf{g} \in \mathbb{R}^{m \times n}$ represent the equality and inequality constraints respectively where N represents the dimension of the dynamic system and m the number of inequality constraints. C_1 , C_2 and C_3 are constants (bigger than zero) where $C_1 = \frac{\Delta t}{\rho} C_{\text{Water}}$, $C_2 = \Delta t \cdot C_{\text{Electric}} \cdot g$ and $C_3 = C_{\text{Pump}}$ (see equations 2.13 - 2.15).

If $z := (m, h) \in \mathbb{R}^{N \times n}$, the optimization problem (equation 3.2) her above is almost identical to the optimization problem represented by equation 1.2, and can thus be solved as MINLP.

In the next sections the objective function will be referred to as \mathcal{J} instead of \mathcal{J}^{PV} . The ^{PV} notation simply means the present value. It is important to distinguish between present value of the profit and the value of the profit with an interest rate of $r = 0$, especially when linear relaxation has been conducted.

3.1.1 Feasibility and optimality

A proper way of solving an optimization problem involves consideration of *feasibility* and *optimality*. All points \dot{m}_i , $h_{j,i}$ and y_i that satisfy both the constraints \mathbf{f} and \mathbf{g} in problem 3.2 are said to be feasible.

Definition 3.1. (Feasibility)

A set \mathcal{F} of all points fulfilling these constraints can be defined as

$$\mathcal{F} := \{\dot{m}_i \in \mathbb{R}, h_{j,i} \in \mathbb{R}, y_i \in \mathbb{Z}_+ : \mathbf{f}(m_i, h_{j,i}, y_i) = 0, \mathbf{g}(m_i, h_{j,i}, y_i) \leq 0, \forall i \in \mathcal{I}, j \in \mathcal{E}\} \quad (3.3)$$

and is referred to as the feasible set. If the feasible set \mathcal{F} is empty, the problem has no solution and is said to be infeasible.

Solving an optimization problem thus implies finding among the feasible set, a point or set of points which maximizes (or minimizes) the objective function \mathcal{J} . Those particular points are denoted by $(\dot{m}'_i, h'_{j,i}, y'_i)$, $\forall i \in \mathcal{I}, j \in \mathcal{E}$, and are known as the *optimal solution* and the value of the objective function \mathcal{J} at this point is the *optimal value*. When a function is maximized the optimal value is referred to as *maximum* and *minimum* when a function is minimized.

Now a global maximum¹ $(\dot{m}'_i, h'_{j,i}, y'_i)$ for the optimization problem represented by equation 3.2 is a point in the feasible set which produces the maximum value for the objective function over \mathcal{F} . I.e. $(\dot{m}'_i, h'_{j,i}, y'_i)$ satisfies;

$$\begin{aligned} \mathcal{J}(\dot{m}'_i, h'_{j,i}, y'_i) &\geq \mathcal{J}(\dot{m}_i, h_{j,i}, y_i) \\ \forall \dot{m}_i, h_{j,i}, y_i &\in \mathcal{F} \\ \forall i \in \mathcal{I}, j \in \mathcal{E} \end{aligned} \quad (3.4)$$

In general it can be mathematically expensive to obtain the global maximum since this implies exploring the whole feasible space. Another type of maximum, called local maximum can also be considered, see figure 3.1 for a graphical display of global and local optimum for a univariate function. A local maximum is a feasible point $(\dot{m}^*_i, h^*_{j,i}, y^*_i)$ for which there exists a neighborhood $\mathcal{N}(\dot{m}^*_i, h^*_{j,i}, y^*_i)$ around $(\dot{m}^*_i, h^*_{j,i}, y^*_i)$, such that:

$$\begin{aligned} \mathcal{J}(\dot{m}^*_i, h^*_{j,i}, y^*_i) &\geq \mathcal{J}(\dot{m}_i, h_{j,i}, y_i) \\ \forall \dot{m}_i, h_{j,i}, y_i &\in \mathcal{F} \cap \mathcal{N}(\dot{m}^*_i, h^*_{j,i}, y^*_i) \\ \forall i \in \mathcal{I}, j \in \mathcal{E} \end{aligned} \quad (3.5)$$

¹ Maximization will be considered here. The relationship between minimization and maximization is the following: $\max \mathcal{J}(x) = -\min(-\mathcal{J}(x))$.

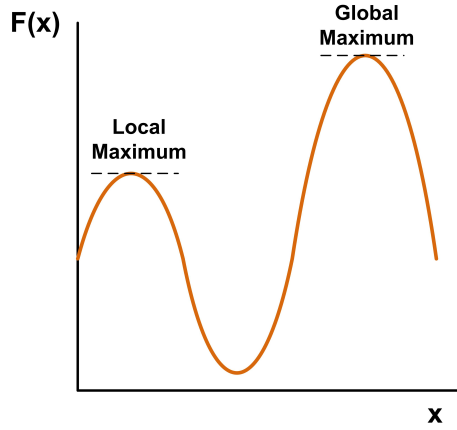


Figure 3.1: Graphical display of a univariate function that has both global and local maxima.

3.1.2 Convexity

Many researchers have focused on a special case of problems like equation 3.2, i.e. when \mathcal{J} and g are convex and f is affine. Then the optimization problem is said to be *convex*.

Definition 3.2. If $\mathbf{v} := (\mathbf{m}, \mathbf{h}, \mathbf{y})$. The function $\mathcal{J}(\mathbf{v})$ is said to be convex if the following inequality hold for any two points \mathbf{v}_1 and \mathbf{v}_2 :

$$\mathcal{J}(\alpha \mathbf{v}_1 + (1 - \alpha) \mathbf{v}_2) \leq \alpha \mathcal{J}(\mathbf{v}_1) + (1 - \alpha) \mathcal{J}(\mathbf{v}_2) \quad \forall \alpha \in [0, 1]$$

The function $\mathcal{J}(\mathbf{v})$ is concave if $-\mathcal{J}(\mathbf{v})$ is convex (see figure 3.2), i.e.:

$$\mathcal{J}(\alpha \mathbf{v}_1 + (1 - \alpha) \mathbf{v}_2) \geq \alpha \mathcal{J}(\mathbf{v}_1) + (1 - \alpha) \mathcal{J}(\mathbf{v}_2) \quad \forall \alpha \in [0, 1]$$

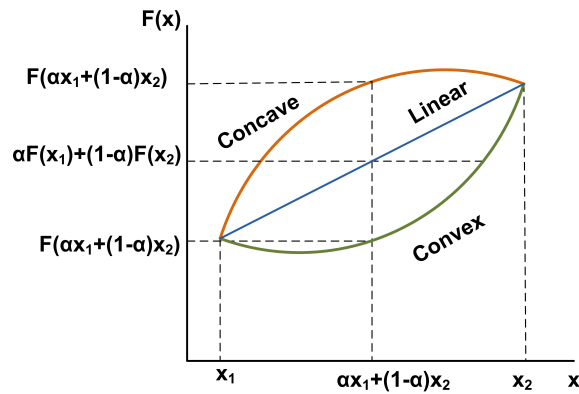


Figure 3.2: Graphical display of a univariate convex, concave and linear functions for comparison.

For a convex optimization problem, it holds that:

Theorem 3.1. *Let \mathbf{v}^* be a local optimal of a convex/concave problem. Then \mathbf{v}^* is also a global optimal.*

Proof. [Nash and Sofer, 1996] □

A discrete problem is said to be convex/concave if it's continuous relaxation is convex/concave. As for the problem in this work and most of engineering optimization problems, this is not the case. Neither the objective function \mathcal{J} nor the inequality constraint g are strictly convex/concave. This will now be shown.

Theorem 3.2. *Supposing $\mathcal{J}(\mathbf{v})$ has continuous second-order partial derivatives. Then \mathcal{J} is said to be convex if the Hessian matrix, $H_{\mathcal{J}}$ is positive semidefinite and concave if it is negative semidefinite.*

Proof. [Bazaraa et al., 2013] □

Definition 3.3. *If \mathcal{J} is twice differentiable at $\mathbf{v} = (\hat{\mathbf{m}}, \mathbf{h}, \mathbf{y})$, then the Hessian matrix of \mathcal{J} is given by*

$$H_{\mathcal{J}} = \begin{bmatrix} \frac{\delta^2 \mathcal{J}}{\delta \hat{\mathbf{m}}^2} & \frac{\delta^2 \mathcal{J}}{\delta \hat{\mathbf{m}} h} & \frac{\delta^2 \mathcal{J}}{\delta \hat{\mathbf{m}} y} \\ \frac{\delta^2 \mathcal{J}}{\delta h \hat{\mathbf{m}}} & \frac{\delta^2 \mathcal{J}}{\delta h^2} & \frac{\delta^2 \mathcal{J}}{\delta h y} \\ \frac{\delta^2 \mathcal{J}}{\delta y \hat{\mathbf{m}}} & \frac{\delta^2 \mathcal{J}}{\delta y h} & \frac{\delta^2 \mathcal{J}}{\delta y^2} \end{bmatrix} \quad (3.6)$$

Matrix $H_{\mathcal{J}}$ is positive semidefinite if all its eigenvalues are nonnegative. Matrix $H_{\mathcal{J}}$ is negative semidefinite if all its eigenvalues are non-positive and matrix H is indefinite (non-convex/non-concave) if it has at least one positive eigenvalue and at least one negative eigenvalue.

To show that the optimization problem represented by equation 3.2 is non-convex, the Hessian of \mathcal{J} is calculated:

$$H_{\mathcal{J}} = \begin{bmatrix} 0 & -C_2 & 0 \\ -C_2 & 0 & 0 \\ 0 & 0 & 0 \end{bmatrix} \quad (3.7)$$

Now the eigenvalues of the Hessian are $\lambda_1 = 0$, $\lambda_2 = C_2$ and $\lambda_3 = -C_2$ which means that matrix H is indefinite and thus that \mathcal{J} is non-convex.

The production capacity constraint, constraint 4, equation 2.26 is also non-linear, since it is a multiple of the decision variable \dot{m}_i and the state variable $h_{1,i}$. Even though such bilinear functions² are non-convex (non-concave), they are known for being *quasi-concave* [Greenberg and Pierskalla, 1970] for \dot{m}_i and $h_{j,i} \in \mathbb{R}_+$, $\forall i \in \mathcal{I}$ and $j \in \mathcal{E}$.

Many non-convex/concave problems are known to be very hard to solve. It has been shown that if the objective function is quasi-convex (quasi-concave), the optimization problem is more likely to be solved efficiently, though slower than convex optimization problems. That means that the algorithm might still be very computationally expensive [Kiwiel, 2001].

The objective function \mathcal{J} is a separable function [Burer and Letchford, 2012], a sum of two linear functions and a quasi-concave bilinear function (see equation 3.2). That and the fact that it is very likely to be easier to solve a quasi-convex optimization problem than a non-convex one, brings out the question whether the objective function here is quasi-convex. Any convex function is also quasi-convex, but the sum of quasi-convex functions is not necessarily quasi-convex. It can however be shown that \mathcal{J} is *quasi-convex* for big values of $h_{1,i}$, but unfortunately those values are not in the feasible set \mathcal{F} . The objective function is thus neither convex nor quasi-convex. This is thus a non-convex optimization.

This means that a global optimal solution for MINLP (and even NLP) can *not* be guaranteed with heuristic algorithms. Bussieck and Vigerske [2012] give a good overview of MINLP solvers that all guarantee global optimal solutions, but for convex MINLP only. There do however exist methods for non-convex MINLP that have proved to work very well in practice [Bussieck and Vigerske, 2012]. The reality is however that it is very hard to find global optimal solution for non-convex problems and proving the optimality is even harder. One of the problems of actually finding a global optimal is that, in theory, any relaxation whether it is to MILP or NLP can cut off the feasible space. Hence, for these kind of problems it is even challenging finding a local optimum. This work will thus attempt to find local optimum for the optimization problem represented by equation 3.2 and refer to *that* as the optimal solution. The local optimal can however be a global optimal, but it is not guaranteed.

² A function of two variables is bilinear if it is linear with respect to each of its variables.

3.1.3 Modeling languages for MINLP

The most popular modeling languages for MINLP include AIMMS [Bisschop and Entriken, 1993], AMPL [Fourer et al., 1993], GAMS [Brooke et al., 1993], MOSEL [Colombani and Heipcke, 2002] and TOMLAB [Holmstrom, 1999]. The systems mentioned here, except TOMLAB that is built on top of MATLAB [MATLAB, 2012], are domain-specific languages. A syntax for specifying optimization problems is defined and parsed by the respective system to provide information to the solver through a back-end [Belotti et al., 2012].

The modeling language applied in this work is MATLAB via the TOMLAB Optimization Environment [Holmstrom, 1999] using the GUROBI [Gurobi, 2012] solver for the MILP relaxation and the SNOPT [Gill et al., 2005] for the NLP relaxation. The key method of the GUROBI solver utilizes the *Branch & bound method* with *cutting planes* for solving MILP. The SNOPT solver utilizes the *Sequential quadratic programming (SQP)* algorithm. Those methods will be briefly accounted for in sections 3.2 and 3.3 respectively. Both the GUROBI solver and the SNOPT solver have other properties not mentioned above. Those will not be accounted for in this work.

3.2 Relaxation to MILP

In this section the optimization model represented by equation 3.2 in section 3.1 will be relaxed in such a way that it holds linear functions only. The objective function and constraint 4, equation 2.26, need thus to be reformulated. There is more than one way to do that and two different approaches will be introduced. A piecewise linear approximation and a piecewise upper-and-lower bound method. An updating algorithm is necessary for both methods for an increasing demand function, where the optimization model is solved in each iteration step. The GUROBI solver [Gurobi, 2012] is used to employ the *Branch-and-bound method with cutting planes* to solve the MILP relaxation.

3.2.1 Branch & bound with cutting planes

Branch-and-bound with cutting planes, often referred to as *branch-and-cut* is an algorithm usually applied to solve MILP problems. It is essentially a *branch & bound* algorithm that relaxes the MILP to *linear programming (LP)*. It applies tree search to ac-

When a point is reached where the search tree has fathomed nodes only, the original MILP has been solved. In other words, once an optimal solution has been obtained (at any point in the tree), the objective value for that solution (assuming maximization) is a valid lower bound for the optimal solution of the original MILP. Then it is known that a value lower than that value will not be accepted as an optimum. There exist also a valid upper bound at any time during the tree search, often referred to as the best bound. That bound is the maximum of all objected values of all the current fathomed nodes. The difference between this lower and upper bound is known as *gap*. Optimality is reached when the gap is zero.

Cutting planes

The branch-and-bound introduced above was presented with binary variables only, fixed on each node of the search tree. This restriction can be seen in terms of inequality constraints added respectively to the LP relaxation:

$$y_i \geq 0 \quad (3.8)$$

or

$$y_i \leq 1 \quad (3.9)$$

where $0 \leq y_i \leq 1$. For the general integer programs where $y_i \in \mathbb{Z}$ those inequality equations become:

$$y_i \geq \lfloor y_i \rfloor \quad (3.10)$$

or

$$y_i \leq \lceil y_i \rceil \quad (3.11)$$

where $\lfloor y_i \rfloor$ means rounding down and $\lceil y_i \rceil$ means rounding up to the next integer value. Such inequalities thus *cut off* a part of the feasible set of the problem relaxation. The concept of cutting planes can be extended to more general inequalities that are globally valid. The main idea of cutting planes is that they tighten the formulation by cutting of particular relaxation solutions, see figure 3.4. The optimal solution of the LP lies on a vertex of the feasible region. The algorithm aims at adding more and more cuts until the feasible set of the LP is imposed to almost only integer solutions (figure 3.5). This is done during the solution process and unlike branching this is done without simultaneously creating additional sub-problems.

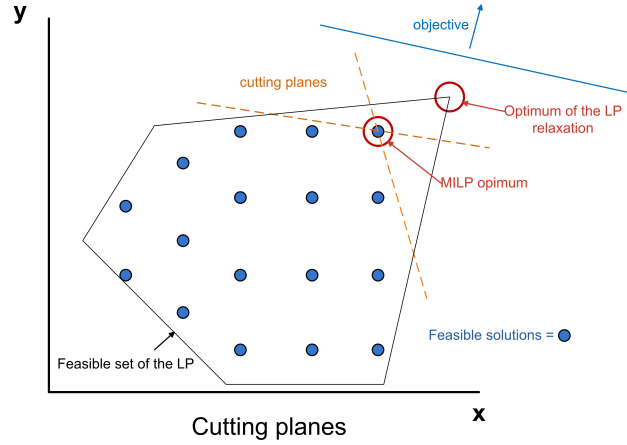


Figure 3.4: Cutting planes example. Undesirable fractional solutions are removed from the feasible set.

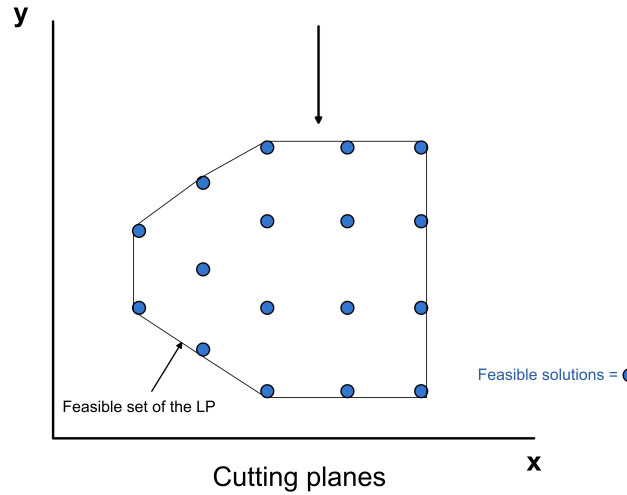


Figure 3.5: Cutting planes example. After undesirable solutions have been removed

Branch-and-bound with cutting planes is a very well developed method for solving MILP. Theoretically it should be possible to transform the method to the non-linear case, i.e. simply relax the MINLP to a NLP and solve a NLP-branch-and-bound with cutting planes. This is an ongoing work in the literature, see [Belotti et al., 2012; Bussieck and Vigerske, 2012] for an overview. The *SBB* solver does e.g. ensure global optimal solutions for convex MINLP [GAMS, 2002]. Such methods were however not considered in this work since the NLP sub-problems are likely to have a considerably longer solution time.

3.2.2 A piecewise linear approximation

Non-linear objective function

The objective function is a nonlinear equation since it holds a product of the variables \dot{m}_i and $h_{1,i}$, see equation 2.14 or the objective function \mathcal{J} in equation 3.2. The non-linear part of the objective function, \mathcal{J} is approximated with a 2-dimensional Taylor approximation. For any non-linear 2-dimensional function $f(x, y)$, $x, y \in \mathbb{R}$, the Taylor approximation is:

$$f(x, y) \approx f(x_0, y_0) + f_x(x_0, y_0)(x - x_0) + f_y(x_0, y_0)(y - y_0) \quad (3.12)$$

where x_0 and y_0 are the reference points that the function is linearly approximated around. The Taylor approximation for \mathcal{J}_2 becomes

$$\mathcal{J}_2(\dot{m}, h_{1,i}) = C_2 \dot{m}_i \cdot h_{1,i} \approx C_2(h_{z,i} \cdot \dot{m}_{z,i} + h_{z,i}(\dot{m}_i - \dot{m}_{z,i}) + \dot{m}_{z,i}(h_{1,i} - h_{z,i})) := \mathcal{J}_{2,\text{MILPr1}} \quad (3.13)$$

where $h_{z,i}$ and $\dot{m}_{z,i}$ represent the reference points for the linear approximation at time step i . I.e. the reference points change with each time step. This is thus a piecewise linear approximation, see figure 3.6 for a graphical display of a univariate function $F(x)$.

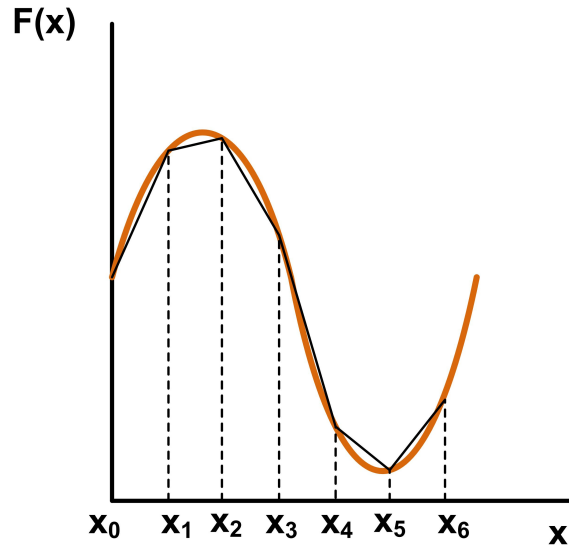


Figure 3.6: Graphical display of a univariate piecewise linear approximation for six time steps.

Equation 3.13 now replaces $\mathcal{J}_2 = \dot{m}_i \cdot h_{1,i}$ in the objective function. The objective function from equation 3.2 now becomes:

$$\mathcal{J}(\dot{m}_i, h_{z,i}, y_i, n) \approx \mathcal{J}_{\text{MILPr1}}^{\text{PV}}$$

where

$$\mathcal{J}_{\text{MILPr1}}^{\text{PV}} := \sum_{i=1}^n (C_1 \cdot \dot{m}_i - C_2 (\cdot h_{z,i} \cdot \dot{m}_{z,i} + h_{z,i} (\dot{m}_i - \dot{m}_{z,i}) + \dot{m}_{z,i} (h_{1,i} - h_{z,i})) - C_3 \cdot y_i) \beta^i \quad (3.14)$$

If no interest rate is included $\beta = 1$ and equation 3.14 is denoted with $\mathcal{J}_{\text{MILPr1}}$.

Non-linear constraint

In Constraint 4, equation 2.26 is also non-linear, and is approximated in the same way as the objective function. Constraint 4 thus becomes:

$$P_{\text{Power},i} \approx g \cdot (\cdot h_{z,i} \cdot \dot{m}_{z,i} + h_{z,i} (\dot{m}_i - \dot{m}_{z,i}) + \dot{m}_{z,i} (h_{1,i} - h_{z,i})) \quad (3.15)$$

$$\leq P_{\text{Pump}} \cdot \sum_{m=1}^i y_m \quad (3.16)$$

$$\forall i \in \mathcal{I} \quad \text{and} \quad m \leq i \leq n \quad (3.17)$$

3.2.3 Lower bound constraint for the piecewise linear approximation

The first problem that arises in running the MILP relaxation with the piecewise linear approximation (equations 3.14 and 3.15) is the tendency of the model to push the decision variable \dot{m}_i (and the state variable $h_{1,i}$) to unrealistic values, such that $\dot{m}_i \ll \dot{m}_{z,i}$ and $h(1,i) \ll h_{z,i}$.

This only happens under substantially increased annual demand and long term utilization where demand can no longer be met. In other words, when the upper-bound of constraint 2, equation 2.19 become *inactive*, since the production \dot{m}_i is substantially smaller than the demand $m_{e,i}$.

Very small values of \dot{m}_i and $h_{1,i}$ result in a very small value of the production function (the linear approximation of equation 2.14, equation 3.14), even down to values smaller than zero, which results in a higher value of the objective function, or higher value of the *linear approximation of the objective function*. As a result the error between linear and

nonlinear production becomes unacceptable and the optimal solution is simply incorrect since production can not be less than zero.

To prevent this from happening, i.e. to stop the objective function from pushing the decision variables to unreasonable values, a constraint is included on how far production and drawdown may deviate from the fixed points of the linearization, see equation 3.18.

Constraint 5

$$h_{z,i} \cdot \dot{m}_{z,i} + h_{z,i}(\dot{m}_i - \dot{m}_{z,i}) + \dot{m}_{z,i}(h_{1,i} - h_{z,i}) \geq \frac{h_{z,i} \cdot \dot{m}_{z,i}}{2} \quad (3.18)$$

The constraint ensures that the linearization of $\dot{m}_i h_{1,i}$ has to be greater than a certain proportion of the multiple of the reference points, see equation 3.18. This is best explained graphically. Figure 3.7 displays how such a constraint would affect the Taylor approximation for a simple univariate function like $F(x) = x^2$ around $x_0 = 1$ for one time step. The linear function becomes $F(x) \approx 2x - 1$ and the comparable constraint to equation 3.18 becomes: $G(x) \geq 1/2$. The constraint prevents the decision variable from traveling unreasonably far (down) from the nonlinear function. This can be looked at as lower bound of the linear approximation. The upper bounds, i.e. constraint 2 (equation 2.19) prevent the decision variable from traveling too far from the nonlinear function in the other direction. This constraint thus serves as a necessary narrower lower bound

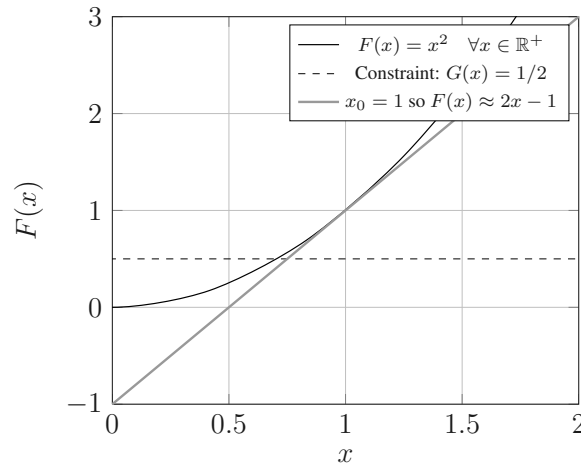


Figure 3.7: If $F(x) = x^2$ is approximated around $x_0 = 1$ with first degree Taylor approximation, the linear function becomes $F(x) \approx 2x - 1$ and the comparable constraint to equation 3.18 becomes: $G(x) \geq 1/2$. The constraint prevents the decision variable from traveling unreasonably far (down) from the nonlinear function.

to prevent the decision variable to take unreasonable values. Now, dividing the multiple of the reference points by 3 in equation 3.18 (cf. $G(X) \geq 1/3$) would result in a lower

bound less narrow, and thus higher error between linear and nonlinear production in the optimization. Using the multiple itself (cf. $G(X) \geq 1$) would result in a very narrow lower bound, and thus smaller error, but it actually resulted in an unfeasible solution.

Here it is necessary to keep in mind that constraints like this one reduce the feasible set and can thus in theory exclude a potential local optimal solution of the problem. Since this constraint works as a lower bound and this is a maximization problem it is however very unlikely to be the case. Another very important point is that the purpose of this constraint is not to find the correct solution, but to steer the solution in the right direction. A solution with constraint 5 (equation 3.18) active is not the correct solution as constraint 5 is not a part of the problem itself. It is thus necessary to apply an iterative optimization process at this point where the reference points and thus constraint 5 are updated in each iteration. How constraint 5 effects the optimization itself is numerically tested and discussed in the result chapter.

3.2.4 Updating algorithm for piecewise linear approximation

As discussed in last section an updating algorithm with k iterations is needed in order to obtain a good linear approximation. An algorithm that considers a linear approximation of the objective function and moves towards an optimal solution with an updating process is often called *Frank Wolfe algorithm* [Frank and Wolfe, 1956; Jaggi, 2013]. It has also been referred to as the *conditional gradient method* and is in principle a classical first order direction method.

Firstly it needs to be explained where the reference points that will be updated come from. Now $m_{e,i}$ represents the demand and \dot{m}_i is a decision variable and represents possible production. Constraint 2 states that production can not exceed demand and serves thus as the upper value \dot{m}_i^U of the decision variable \dot{m}_i . That upper value relates directly to the state variable in the objective function $h_{1,i}$ since h_i is a function of \dot{m}_i . The initial values for the reference points that relate to production ($m_{z,i}^{(k=1)}$) are chosen first and the reference points relating to drawdown ($h_{z,i}^{(k=1)}$) are thus calculated according to $m_{z,i}^1$ using equation 2.11. Theoretically, any demand function can be chosen such that $m_{e,i} := m_{z,i}^{(k=1)}$ or $m_{e,i} := \delta m_{z,i}^{(k=1)}$ where $\delta \in [0, 1]$ and is chosen such that $m_{z,i}^{(k=1)} \in \mathcal{F}$, where \mathcal{F} is the feasible set of the optimization problem. The demand function can be calculated from average demand with e.g. a yearly or monthly trend. Historical data trends can also be repeated periodically (like in this work) or the demand can be simulated stochastically.

In developing an updating algorithm for the piecewise linear approximation, the reference points ($m_{z,i}$ and $h_{z,i}$) were first replaced with the optimal solution in each iteration k until an acceptable *stopping criteria* is reached.

Before continuing it is necessary to introduce the stopping criteria used. For an updating process, the optimization is updated until the error between the linear and non-linear part of the objective function (the production, function \mathcal{J}) is acceptable.

This error is calculated by comparing the percentage difference between non-linear and linear production from the optimal output for the decision and state variable:

$$\mathcal{J}_{2,Error} := \frac{100|\mathcal{J}_{2,MILPr1} - \mathcal{J}_{2,MINLPr1}|}{\mathcal{J}_{2,MINLPr1}} \leq \epsilon \quad (3.19)$$

$\mathcal{J}_{2,MINLPr1}$ represent the non-linear function that can be calculated from the decision and state variables after the optimization has been performed. Interest rate is not included in calculating the error as a stopping criteria for the updating algorithm. This is due to the fact that an interest rate can reduce the accuracy of such calculation substantially, since it has great effect in the end of the time period and very small effect in the beginning of the time period being optimized. $\mathcal{J}_{2,Error}^{PV}$ that calculates the error between the present value of linear and non-linear production is however calculated in section 4.2 for comparison purposes.

In the first algorithm (algorithm 1) pursued, the piecewise linear approximation introduced in section 3.2.2 is applied on the non-linear part of the objective function and two constraint, constraint 4 and constraint 5 (equations 2.27 and 3.18). The reference points are updated by replacing them by the new solution in each iteration (see red framed in algorithm 1).

Algorithm 1**A Frank Wolfe type updating algorithm 1**

Initial values for the reference points $\dot{m}_{z,i}^{(k=1)}$ and $h_{z,i}^{(k=1)}$, $\forall i \in \mathcal{I}$ are chosen such that $\dot{m}_{z,i}^{(k=1)} := \delta \dot{m}_{e,i}$ and since \mathbf{h}_i is a function of \dot{m}_i (see equation 2.11), $h_{z,i}^{(k=1)}$ is calculated from $\dot{m}_{z,i}^{(k=1)}$. δ is chosen $0 \leq \delta \leq 1$ such that $h_{z,i}^{(k=1)}(\dot{m}_{z,i}^{(k=1)}) \in \mathcal{F}$ where \mathcal{F} is the feasible set. $\dot{m}_{z,i}^{(k=1)}$ is in other words scaled down so that when $h_{z,i}^{(k=1)}$ is calculated, it never reaches the sustainability constraint, see equation 2.24.

```

k := 1 {Starting Point}
limit :=  $\mathcal{J}_{2,\text{Error}}(k) \leq \epsilon$  {Equation 3.19}
while (NOT limit) and  $k \leq k_{max}$  do
    Define demand function for  $m_{i,e}$ 
     $\dot{m}_{z,i}^{(k=1)} := \delta \dot{m}_{i,e}$  such that  $h_{z,i}^{(k=1)}(\dot{m}_{z,i}^{(k=1)}) \in \mathcal{F}$ 
    Solve Optimization Problem: {Problem 3.2}
     $\mathcal{J}_{\text{MILPr1}}^{\text{PV},*}(\dot{m}_i^*, \mathbf{h}_i^*, y_i^*) = \arg \max_{\mathcal{F}} \mathcal{J}_{\text{MILPr1}}^{\text{PV}}(\dot{m}_i, \mathbf{h}_i, y_i)$ 
    Calculate:  $\text{limit} := \mathcal{J}_{2,\text{Error}}(k)$ 
    if limit == TRUE then
        Break;
        => A solution has been found.
    else
        if  $k == k_{max}$  then
            Break;
            => A sufficient solution has not been found.
        end if
        else
            Define optimal solution as solution k;
             $\dot{m}_i^* := \dot{m}_i^{(k)}$ 
             $h_{1,i}^* := h_{1,i}^{(k)}$ 
            Update reference points such that:
            

$\dot{m}_{z,i}^{(k+1)} = \dot{m}_i^{(k)}$

 {Replace the the next reference point with the current solution}
            

$h_{z,i}^{(k+1)} = h_{1,i}^{(k)}$

 $\forall i \in \mathcal{I}$ 
             $k := k + 1$  {Next iterate}
        end if
        Calculate:  $\text{limit} := \mathcal{J}_{2,\text{Error}}(k)$ 
    end while
end while

```

Algorithm 1 certainly improves the solution but does not converge very well, see section 4.2 example 4.4.

Now, in an attempt for a better solution, the reference points are now replaced by a weighted mean of the solution at k and the reference point at k (instead of the solution only), such that $\dot{m}_{z,i}^{(k+1)} = (1 - \alpha)\dot{m}_{z,i}^{(k)} + \alpha\dot{m}_i^{(k)}$, where $\alpha \in [0.1]$. In this way the reference points and the solution are directed towards each other and the solution converges to an optimal with a sufficiently small error. How fast it converges is however dependent on the size of α . A value of α less than 0.5 usually gives good results. I.e. the algorithm converges more slowly for smaller α but is more likely to find an accurate solution. Defining $\alpha = 2/(2 + k)$ [Jaggi, 2013] gave a very good result for the optimization model in this work. In that way α decreases in every iteration, which means e.g. that the first update is

closer to $\dot{m}_i^{(k)}$ than $\dot{m}_{z,i}^{(k)}$ until the update is almost only dependent on the last value of the reference point. That prevents the reference points from oscillating around the solution and thus slowing the convergence process as happens in algorithm 1.

Algorithm 2
A Frank Wolfe type updating algorithm 2

Initial values for the reference points are chosen like in algorithm 1. Now it is updated in such a way that the new value for the reference point updated at $k + 1$ is a mix of the optimal solution and reference point at iteration k , such that $\dot{m}_{z,i}^{(k+1)} = (1 - \alpha)\dot{m}_{z,i}^{(k)} + \alpha\dot{m}_i^{(k)}$.

```

 $k := 1$  {Starting Point}
 $limit := \mathcal{J}_{2, \text{Error}}(k) \leq \epsilon$  {Equation 3.19}
while (NOT  $limit$ ) and  $k \leq k_{max}$  do
    Define demand function for  $m_{i,e}$ 
     $m_{z,i}^{(k=1)} := \delta m_{i,e}$  such that  $h_{z,i}^{(k=1)}(\dot{m}_{z,i}^{(k=1)}) \in \mathcal{F}^4$ 
    Solve Optimization Problem: {Problem 3.2}
     $\mathcal{J}_{\text{MILPr1}}^{\text{PV},*}(\dot{m}_i^*, \mathbf{h}_i^*, y_i^*) = \arg \max_{\mathcal{F}} \mathcal{J}_{\text{MILPr1}}^{\text{PV}}(\dot{m}_i, \mathbf{h}_i, y_i)$ 
    Calculate:  $found := \mathcal{J}_{2, \text{Error}}(k)$ 
    if  $limit == \text{TRUE}$  then
        Break;
        => A solution has been found.
    else
        if  $k == k_{max}$  then
            Break;
            => A sufficient solution has not been found.
        end if
    else
        Define optimal solution as solution  $k$ ;
         $\dot{m}_i^* := \dot{m}_i^{(k)}$ 
         $h_{1,i}^* := h_{1,i}^{(k)}$ 
         $\alpha := \text{Step length}, \alpha := 2/(2 + k)$  { $\alpha$  is  $0 \leq \alpha \leq 1$ }
        Update reference points such that:
        

$\dot{m}_{z,i}^{(k+1)} = (1 - \alpha)\dot{m}_{z,i}^{(k)} + \alpha\dot{m}_i^{(k)}$

 {Replace the the next reference point with the current solution}
        

$h_{z,i}^{(k+1)} = (1 - \alpha)h_{z,i}^{(k)} + \alpha h_{1,i}^{(k)}$

 $\forall i \in \mathcal{I}$ 
         $k := k + 1$  {Next iterate}
    end if
    Calculate:  $limit = \mathcal{J}_{2, \text{Error}}(k)$ 
end while

```

3.2.5 Piecewise under-and over-estimators

As mentioned before there is more than one way of relaxing the MINLP to a form that can be solved in an acceptable time frame. One way is to replace each non-concave function⁵ $\mathcal{J}(\dot{m}_i, h_{j,i}, y_i)$ or $\mathbf{g}(\dot{m}_i, h_{j,i}, y_i)$ from equation 3.2 with a concave over-estimating function $\hat{\mathcal{J}}(\dot{m}_i, h_{j,i}, y_i)$ or $\hat{\mathbf{g}}(\dot{m}_i, h_{j,i}, y_i)$ such that $\hat{\mathcal{J}}(\dot{m}_i, h_{j,i}, y_i) \geq \mathcal{J}(\dot{m}_i, h_{j,i}, y_i)$ and

⁵ Convex for a minimization.

$\hat{\mathbf{g}}(\dot{m}_i, h_{j,i}, y_i) \geq \mathbf{g}(\dot{m}_i, h_{j,i}, y_i), \forall i \in \mathcal{I} \text{ and } j \in \mathcal{E}$. See figure 3.8 for a univariate case.

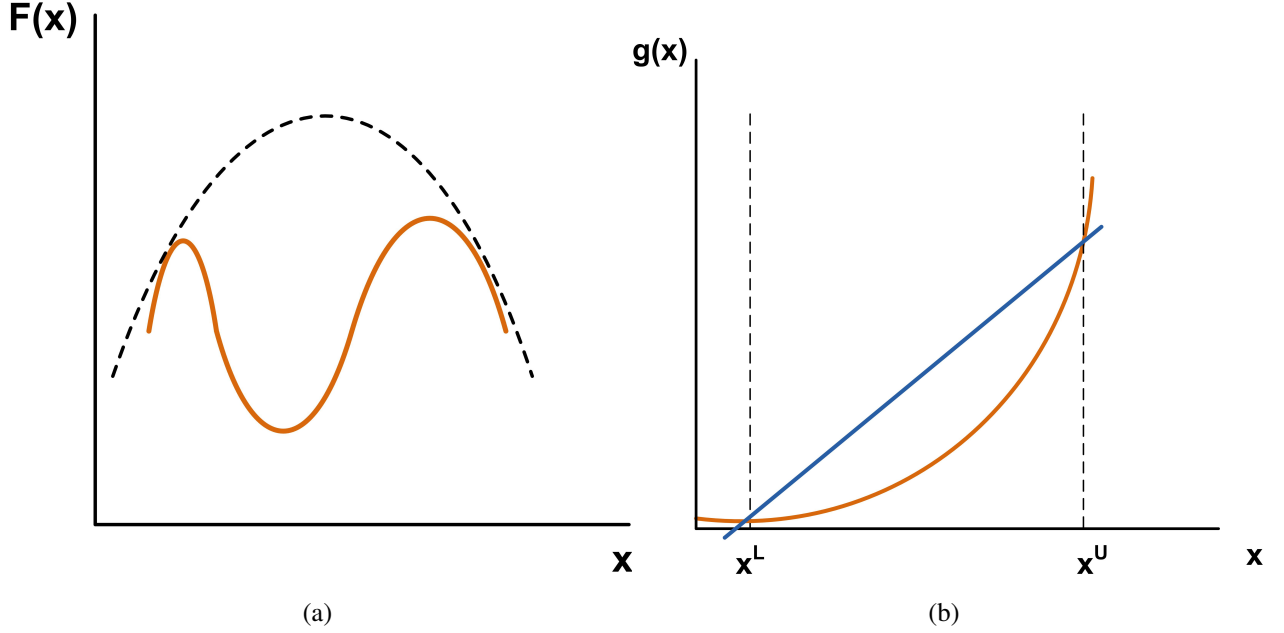


Figure 3.8: The figure on the left displays a univariate case for a concave over-estimator. The figure on the right displays a secant line that can serve as an over-estimator for a the convex univariate function $g(x)$.

For an even more comprehensible example, a univariate convex separable function $g(x)$ (see figure 3.8 on the right) can be over-estimated by a *secant line* which matches the concave function at the upper and lower bound such that [Falk and Soland, 1969; Grossmann and Biegler, 2004]:

$$\hat{g} = g(x^L) + \left(\frac{g(x^U) - g(x^L)}{x^U - x^L} \right) (x - x^L) \quad (3.20)$$

$$x^L \leq x \leq x^U$$

An important class of non-convex/concave optimization problems correspond to non-linear programming problems with bilinear or linear fractional terms as they commonly arise in engineering design problems like this one. The non-linear part here is namely a bilinear term. The bilinear term of the non-linear part of the objective function is the same as the non-linear constraint, a multiple of the state and the decision variable, $\dot{m}_i h_{1,i}$.

In order to add both *under-and over-estimators* a variable $z_i := \dot{m}_i h_{1,i}$ can simply act as a place holder for the non-linear part of $\mathcal{J}(\dot{m}_i, h_{j,i}, y_i)$ or $\mathbf{g}(\dot{m}_i, h_{j,i}, y_i)$. Then a constraint is added which will force z_i to be approximately equal to the non-linear part of the objective function (\mathcal{J}_2) and the non-linear constraint (equation 2.26). Looking at it in

terms of the objective function only, a constraint of the form $\hat{\mathcal{J}}_2(\dot{m}_i, h_{j,i})$ that serves as a concave over-estimator is added to the optimization model, such that $z_i \geq \hat{\mathcal{J}}_2(\dot{m}_i, h_{j,i})$. Another constraint of the form $z_i \leq \overline{\mathcal{J}}_2(\dot{m}_i, h_{j,i})$ is then added where $\overline{\mathcal{J}}_2$ is a convex under-estimating function [Grossmann and Biegler, 2004; Burer and Letchford, 2012]. In order to generate a MILP relaxation of the MINLP problem, one must use *linear* under- and over-estimators. Since the non-linear constraint is a bilinear function and the objective function has a bilinear term this can easily be obtained.

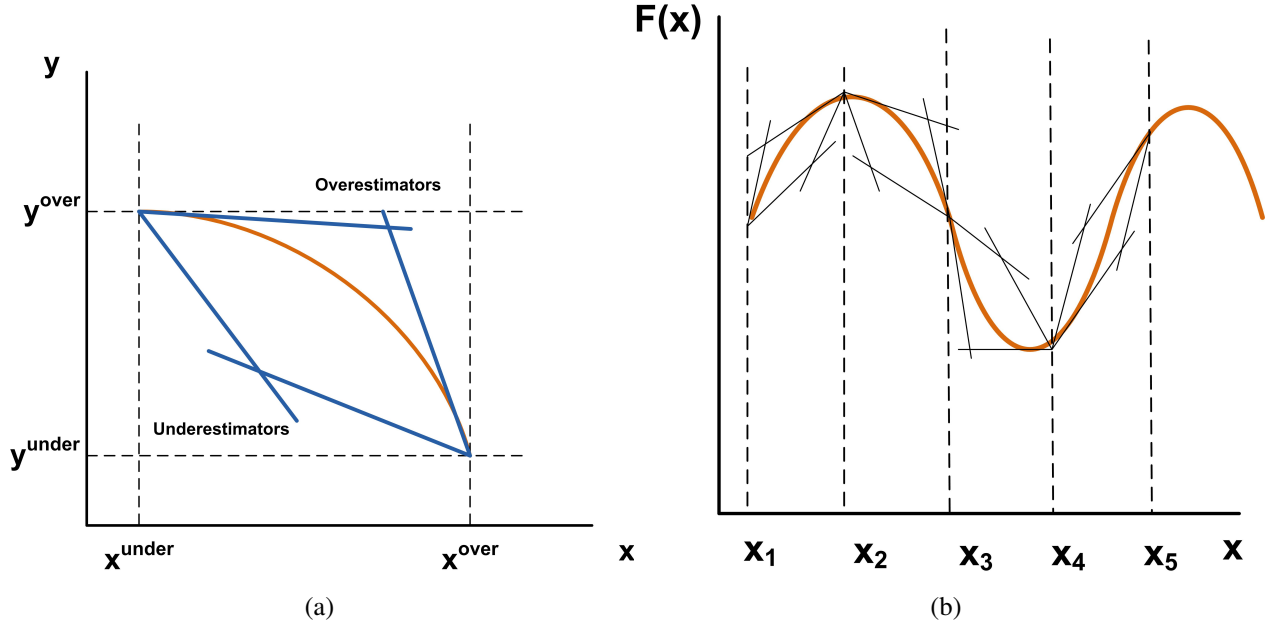


Figure 3.9: Under- and over-estimators (envelopes) for univariate functions. The piecewise case is shown on the right.

Like in Hart et al. [1976], the bivariate function $z_i = \dot{m}_i h_{1,i}$ is considered over the rectangular domain such that $\dot{m}_i^{under} \leq \dot{m}_i \leq \dot{m}_i^{over}$ and $h_{1,i}^{under} \leq h_{1,i} \leq h_{1,i}^{over}$. The under and over estimators change in each time step i for all $i \in \mathcal{I}$ like in the linear approximation in section 3.2.2. See figure 3.9 for a graphical display of a univariate function. Now since z_i denotes the placeholder variable, the valid under- and over-estimators (convex/concave envelopes) are as follows:

$$z_i \geq \dot{m}_i^{under} h_{1,i} + h_{1,i}^{under} \dot{m}_i + \dot{m}_i^{under} h_{1,i}^{under} \quad (3.21)$$

$$z_i \geq \dot{m}_i^{over} h_{1,i} + h_{1,i}^{over} \dot{m}_i + \dot{m}_i^{over} h_{1,i}^{over} \quad (3.22)$$

$$z_i \leq \dot{m}_i^{under} h_{1,i} + h_{1,i}^{over} \dot{m}_i + \dot{m}_i^{under} h_{1,i}^{over} \quad (3.23)$$

$$z_i \leq \dot{m}_i^{over} h_{1,i} + h_{1,i}^{under} \dot{m}_i + \dot{m}_i^{over} h_{1,i}^{under} \quad (3.24)$$

Equations 3.21-3.24 are now added as constraints to the optimization model where the under-estimator are simply zero and the over-estimator for production is $\dot{m}_i^{over} = \delta m_{e,i}$ and $h_{1,i}^{over}$ is calculated from \dot{m}_i^{over} .

The objective function from problem 3.2 now becomes:

$$\mathcal{J}(\dot{m}_i, h_{j,i}, y_i, n) \approx \mathcal{J}_{\text{MILPr2}}^{\text{PV}}$$

where

$$\mathcal{J}_{\text{MILPr2}}^{\text{PV}} := \sum_{i=1}^n (C_1 \cdot \dot{m}_i - C_2 z_i - C_3 \cdot y_i) \beta^i \quad (3.25)$$

If no interest rate is assumed ($\beta = 1$) and equation 3.25 is denoted with $\mathcal{J}_{\text{MILPr2}}$, constraint 4 becomes:

$$P_{\text{Power},i} \approx g \cdot z_i \quad (3.26)$$

$$\leq P_{\text{Pump}} \cdot \sum_{m=1}^i y_m \quad (3.27)$$

$$\forall i \in \mathcal{I} \quad \text{and} \quad m \leq i \leq n \quad (3.28)$$

Constraint 5, defined by equation 3.18 is not needed here since there are already under-estimators present.

3.2.6 Updating algorithm for under-and over-estimators

An updating algorithm with k iterations is also needed for the method with under- and over-estimators. The function optimized in each iteration is equation 3.25, where z_i is constrained by equations 3.21-3.24.

The updating process from algorithm 2 is applied and initial values chosen like in algorithm 1 and 2. Where $\dot{m}_i^{over} := m_{z,i}^{(k)}$ and $h_{1,i}^{over} := h_{z,i}^{(k)}$ and $h_{1,i}^{under}$ and \dot{m}_i^{under} are set equal to zero.

The stopping criteria is based on the error calculated by comparing the percentage difference between z_i and $\dot{m}_i h_{1,i}$ from the optimal output for the decision and state variable:

$$\mathcal{J}_{2,\text{Error}} := \frac{100|\mathcal{J}_{2,\text{MILPr2}} - \mathcal{J}_{2,\text{MINLPr2}}|}{\mathcal{J}_{2,\text{MINLPr2}}} \leq \epsilon \quad (3.29)$$

3.3 Relaxation to NLP

Problem 3.2 is now relaxed to NLP such that $y_i \in \mathbb{R}_+$, $\forall i \in \mathcal{I}$. The solution from relaxing to NLP yields an *upper bound* for the MINLP⁶ since an integer solution gives a poorer or equal solution in optimization. Such solution can however fail to give realistic values for y as it is now in \mathbb{R} and can take very small values that can theoretically be scattered around the feasible set.

The method applied here for solving the NLP is *Sequential Quadratic Programming (SQP)* using the SNOPT solver. The SQP is one of the most successful methods for the numerical solution of constrained non-linear optimization problems and has been proven to give a local optimal solution [Gill et al., 2005]. It is very valuable to have a secure local optimal for the problem even though it is in the form of an upper bound. The SQP will now be briefly explained and a numerical solution can be seen in section 4.2.3.

3.3.1 Sequential quadratic programming (SQP)

The SQP algorithm was first proposed by [Wilson, 1963]. It is essentially a generalization of Newton's method for unconstrained optimization. The objective function is replaced by a quadratic approximation and the constraint are linearized. The SQP methods then solves a sequence of these sub-problems.

For such an optimization, necessary and sufficient optimality conditions need to be stated. In order to do that the concepts of the *Lagrangian*, the *active set* and the *linear independence constraint qualification (LICQ)* need to be introduced. Following definitions and theorems are put forward here for readers not familiar with optimization and can be all be found in standard textbooks on non-linear optimization, e.g. [Nocedal and Wright, 2006; Bertsekas, 2003; Fletcher, 1987].

If the integer variable from the optimization problem represented by equation 3.2 has

⁶ or *lower bound* for minimization

been relaxed from \mathbb{Z} to \mathbb{R} it can be written as

$$\begin{aligned}
 & \underset{\mathbf{v} \in \mathbb{R}}{\text{maximize}} && \mathcal{J}(\mathbf{v}) \\
 & \text{subject to} && \\
 & && \mathbf{f}(\mathbf{v}) = 0 \\
 & && \mathbf{g}(\mathbf{v}) \leq 0 \\
 & && \mathbf{v}^L \leq \mathbf{v} \leq \mathbf{v}^U
 \end{aligned} \tag{3.30}$$

where $\mathbf{v} = (\dot{\mathbf{m}}, \mathbf{h}, \mathbf{y})$, $\forall, \dot{\mathbf{m}} \in \mathbb{R}^{n_{\dot{m}}}$, $\mathbf{y} \in \mathbb{R}^{n_y}$ and $\mathbf{h} \in \mathbb{R}^{n_h}$

Definition 3.4. (Lagrangian) The Lagrangian \mathcal{L} of a constraint non-linear optimization problem represented by equation 3.30 above is defined by

$$\mathcal{L}(\mathbf{v}, \boldsymbol{\lambda}, \boldsymbol{\mu}) = \mathcal{J}(\mathbf{v}) - \boldsymbol{\lambda}^\top \mathbf{f}(\mathbf{v}) + \boldsymbol{\mu}^\top \mathbf{g}(\mathbf{v}) \tag{3.31}$$

where $\boldsymbol{\lambda} \in \mathbb{R}^{n_f}$ and $\boldsymbol{\mu} \in \mathbb{R}^{n_g}$ represent the Lagrangian multipliers of the system. \mathcal{L} is called Lagrangian (function) of problem 3.30.

Definition 3.5. (Active constraint and active set) If $\tilde{\mathbf{v}} \in \mathcal{F}$, it is said to be a feasible point of problem 3.30. The inequality constraint g_i , $i \in \{1 \dots m\}$ is said to be active if $g_i(\tilde{\mathbf{v}}) = 0$. The set of indices of all active constraints can thus be defined as

$$\mathcal{A}(\tilde{\mathbf{v}}) := \{i : g_i(\tilde{\mathbf{v}}) = 0, 1 \leq i \leq m\} \tag{3.32}$$

the active set associated with $\tilde{\mathbf{v}}$. Active constraints are often required to be linearly independent.

Definition 3.6. (Linear dependent constraint qualification)

If the gradient of the constraints $\nabla \mathbf{f}_i(\tilde{\mathbf{v}})$, $i \in \{1 \dots n_f\}$ and $\nabla g_i(\tilde{\mathbf{v}})$, $i \in \mathcal{A}(\tilde{\mathbf{v}})$ at $\tilde{\mathbf{v}}$ are linearly independent, it can be said that the linear independence constraint qualification (LICQ) holds.

The first order necessary condition for optimality are given by the following theorem of Karush, Kuhn and Tucker [Karush, 1939; Kuhn and Tucker, 1951].

Theorem 3.3. (The Karush-Kuhn-Tucker (KKT) conditions)

If \mathbf{v}^* is defined as a local optimal of problem 3.30 and for which LICQ holds. Then there exist Lagrange multipliers $\boldsymbol{\lambda}^* \in \mathbb{R}^{n_f}$ and $\boldsymbol{\mu}^* \in \mathbb{R}^{n_g}$ such that the following conditions

are satisfied:

$$\mathbf{0} = \nabla \mathcal{L}(\mathbf{v}^*, \boldsymbol{\lambda}^*, \boldsymbol{\mu}^*) \quad (3.33a)$$

$$\mathbf{0} = \mathbf{f}(\mathbf{v}^*) \quad (3.33b)$$

$$\mathbf{0} \geq \mathbf{g}(\mathbf{v}^*) \quad (3.33c)$$

$$\mathbf{0} \leq \boldsymbol{\mu}^* \quad (3.33d)$$

$$\mathbf{0} = \boldsymbol{\mu}^{*\top} \mathbf{g}(\mathbf{v}^*) \quad (3.33e)$$

$$\mathbf{0} = \boldsymbol{\mu}^{*\top} \mathbf{g}(\mathbf{v}^*) \quad (3.33f)$$

If condition 3.33a-3.33f hold, $(\mathbf{v}^*, \boldsymbol{\lambda}^*, \boldsymbol{\mu}^*)$ is referred to as *the Karush-Kuhn-Tucker (KKT) point*.

Proof. Fletcher [1987] and Nocedal and Wright [2006] □

The second order necessary condition is given by:

Theorem 3.4. (Second order necessary conditions of optimality)

Let $\mathbf{v}^* \in \mathbb{R}^{n_v}$ be local optimal point of problem 3.30, where LICQ holds in \mathbf{v}^* . Let $\boldsymbol{\lambda} \in \mathbb{R}^{n_f}$ and $\boldsymbol{\mu} \in \mathbb{R}^{n_g}$ be the unique Lagrange multipliers such that the KKT conditions are satisfied. If small variations $\Delta \mathbf{v}$ from the local optimal are considered such that for every vector $\Delta \mathbf{v} \in \mathbb{R}^{n_v}$ with

$$\mathbf{f}_i(\mathbf{v}^* + \Delta \mathbf{v}) - \mathbf{f}_i(\mathbf{v}^*) \approx \nabla \mathbf{f}_i(\mathbf{v}^*) \Delta \mathbf{v} = \mathbf{0}, \quad i \in \{1 \dots n_f\} \quad (3.34a)$$

$$\mathbf{g}_i(\mathbf{v}^* + \Delta \mathbf{v}) - \mathbf{g}_i(\mathbf{v}^*) \approx \nabla \mathbf{g}_i(\mathbf{v}^*) \Delta \mathbf{v} = \mathbf{0}, \quad i \in \mathcal{A}(\mathbf{v}^*) \quad (3.34b)$$

it holds that

$$\Delta \mathbf{v}^\top \nabla^2 \mathcal{L}(\mathbf{v}^*, \boldsymbol{\lambda}^*, \boldsymbol{\mu}^*) \Delta \mathbf{v} \geq \mathbf{0} \quad (3.35)$$

Proof. Fletcher [1987] and Nocedal and Wright [2006] □

The sufficient second order conditions are given by

Theorem 3.5. (Second order sufficient condition of optimality)

Let $\mathbf{v}^* \in \mathbb{R}^{n_v}$ be local optimal point of problem 3.30, where LICQ holds in \mathbf{v}^* . Let $\boldsymbol{\lambda} \in \mathbb{R}^{n_f}$ and $\boldsymbol{\mu} \in \mathbb{R}^{n_g}$ be the unique Lagrange multipliers such that the KKT conditions are satisfied. If small variations $\Delta \mathbf{v}$ from the local optimal are considered such that for

every vector $\Delta \mathbf{v} \in \mathbb{R}^{n_v}$ with

$$\nabla \mathbf{f}_i(\mathbf{v}^*) \Delta \mathbf{v} = \mathbf{0}, \quad i \in \{1 \dots n_f\} \quad (3.36a)$$

$$\nabla \mathbf{g}_i(\mathbf{v}^*) \Delta \mathbf{v} = \mathbf{0}, \quad i \in \mathcal{A}(\mathbf{v}^*) \quad \text{and} \quad \mu_i > 0 \quad (3.36b)$$

$$\nabla \mathbf{g}_i(\mathbf{v}^*) \Delta \mathbf{v} \geq \mathbf{0}, \quad i \in \mathcal{A}(\mathbf{v}^*) \quad \text{and} \quad \mu_i = 0 \quad (3.36c)$$

it holds that

$$\Delta \mathbf{v}^\top \nabla^2 \mathcal{L}(\mathbf{v}^*, \boldsymbol{\lambda}^*, \boldsymbol{\mu}^*) \Delta \mathbf{v} > 0 \quad (3.37)$$

Proof. Nocedal and Wright [2006] □

Algorithm 3 is a general form of a SQP algorithm. $H_{\mathcal{J}}^{(k)}$ is the Hessian of the Lagrangian $H_{\mathcal{J}}^{(k)} := \nabla^2 \mathcal{L}(\mathbf{v}^k, \boldsymbol{\lambda}^{(k)}, \boldsymbol{\mu}^{(k)})$. It can be the exact Hessian or a numerical approximation. The stopping criteria is either a KKT condition inside a certain tolerance or a small increment of the Lagrangian in the search direction such that $\|\nabla \mathcal{L} \Delta \mathbf{v}\| \leq \epsilon$.

Algorithm 3
A basic SQP algorithm

$k := 1$ {Starting Point}
 Guess the values for the initial iteration, $\mathbf{v}^{(k=1)}$ and the Lagrangian multipliers $\boldsymbol{\lambda}^{(k=1)}$ and $\boldsymbol{\mu}^{(k=1)}$
 $found := \text{Stopping criteria}$ {KKT condition inside a certain tolerance or $\|\nabla \mathcal{L} \Delta \mathbf{v}\| \leq \epsilon$ }
while (NOT $found$) and $k \leq k_{max}$ **do**
 Evaluate $\mathcal{J}(\mathbf{v}^{(k)})$, $\mathbf{f}(\boldsymbol{\lambda}^{(k)})$ and $\mathbf{g}(\boldsymbol{\mu}^{(k)})$
 Evaluate $\nabla \mathcal{J}(\mathbf{v}^{(k)})$, $\nabla \mathbf{f}(\boldsymbol{\lambda}^{(k)})$ and $\nabla \mathbf{g}(\boldsymbol{\mu}^{(k)})$
 Evaluate $H_{\mathcal{J}}^{(k)}$
 Compute $\Delta \mathbf{v}$ and the Lagrange multipliers $\tilde{\boldsymbol{\lambda}}$ and $\tilde{\boldsymbol{\mu}}$ by a solution of the quadratic program

$$\begin{aligned}
 &\underset{\Delta \mathbf{v} \in \mathbb{R}}{\text{maximize}} && \nabla \mathcal{J}(\mathbf{v}^{(k)})^\top \Delta \mathbf{v} + \frac{1}{2} \Delta \mathbf{v}^\top H_{\mathcal{J}}^{(k)} \Delta \mathbf{v} \\
 &\text{subject to} &&
 \end{aligned}
 \tag{3.38}$$

$$\begin{aligned}
 \mathbf{f}(\mathbf{v}^{(k)}) + \nabla \mathbf{f}(\mathbf{v}^{(k)})^\top \Delta \mathbf{v} &= \mathbf{0} \\
 \mathbf{g}(\mathbf{v}^{(k)}) + \nabla \mathbf{g}(\mathbf{v}^{(k)})^\top \Delta \mathbf{v} &\leq \mathbf{0}
 \end{aligned}$$

Determine the step length $\alpha^{(k)}$
 Perform the following updating steps with a step length $\alpha^{(k)}$

$$\mathbf{v}^{(k+1)} = \mathbf{v}^{(k)} + \alpha^{(k)} \Delta \mathbf{v} \tag{3.39a}$$

$$\boldsymbol{\lambda}^{(k+1)} = \boldsymbol{\lambda}^{(k)} + \alpha^{(k)} (\tilde{\boldsymbol{\lambda}} - \boldsymbol{\lambda}^{(k)}) \tag{3.39b}$$

$$\boldsymbol{\mu}^{(k+1)} = \boldsymbol{\mu}^{(k)} + \alpha^{(k)} (\tilde{\boldsymbol{\mu}} - \boldsymbol{\mu}^{(k)}) \tag{3.39c}$$

Calculate $found$
if $found == \text{TRUE}$ **then**
 Break;
 \Rightarrow A solution has been found.
else
 if $k == k_{max}$ **then**
 Break;
 \Rightarrow A sufficient solution has not been found.
 end if
 else
 $k := k + 1$ {Next iterate}
 end if
end while

Chapter 4

Results

This chapter accounts for the results of this research. That includes the parameter fit for the LPM by comparing four different geothermal fields in the Reykjavik area and choosing the best parameter fit to use in an optimization; numerical testing for the optimization methods and algorithms explained in chapter 3; and optimization of long term utilization with and without annual increase in demand.

4.1 Parameter estimation and validation of the LPM

In this section four geothermal fields will first be briefly introduced in terms of production history, number of wells and location. The data was made available by [\[Ivarsson, 2011\]](#) and [\[Reykjavik Energy, 2011\]](#). Four fields will be fitted to different kinds of lumped parameter models. The results of the data fit are validated and compared.

4.1.1 Field data

The Laugarnes and Ellidaar geothermal fields lie within the city limit of Reykjavik and Reykir and Reykjahlid lie around 20 km northeast of the city. Reykir and Reykjahlid are only separated by a hill and are often refereed to as one field divided into the two sub-areas Reykir and Reykjahlid. Figure 4.1 shows the location of the geothermal fields utilized for district heating in Reykjavik [\[Gunnlaugsson et al., 2000\]](#). Table 4.1 shows a comparison of a few properties of those fields such as temperature and average production.

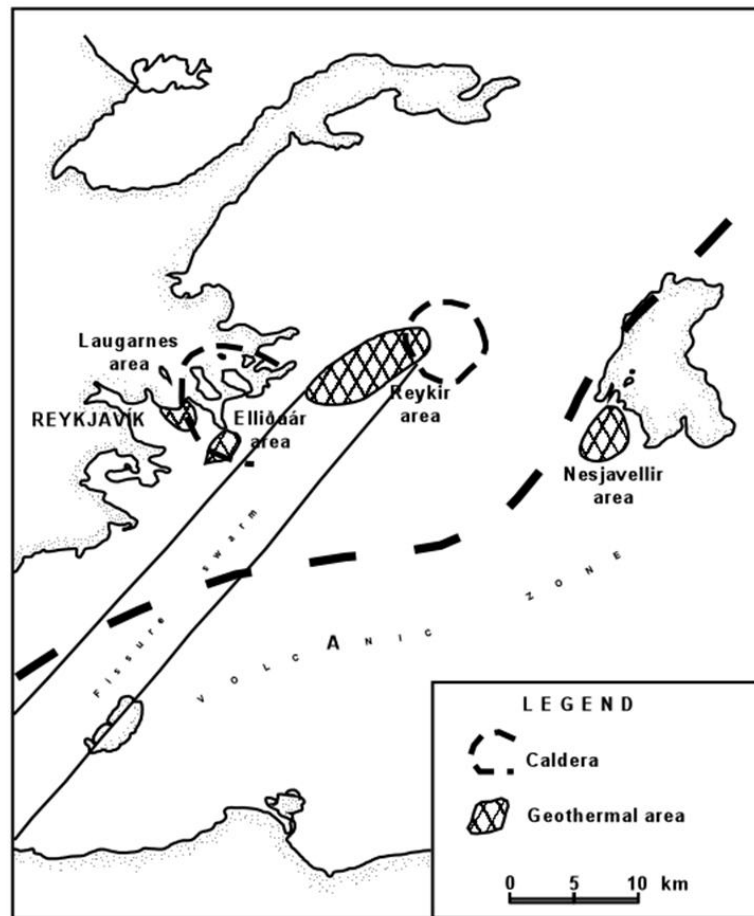


Figure 4.1: Location of geothermal fields in Reykjavik. From: [Gunnlaugsson et al. \[2000\]](#).

Geothermal field	Average temperature (°C)	Number of production wells in 2010	Average elevation above sea level (m)	Average production 2010 (GJ)	Average production 2010 (kg/s)	Proportion of production for Reykjavik (%) in 2010
Laugarnes Field	127.7	10	22.8	4.34	129	6.9
Ellidar Field	86.7	8	36.7	1.99	61.0	3.2
Reykir Field	81.7	22	64.3	11.2	344	17.8
Reykjahlid Field	93.0	12	64.3	13.4	410	21.3

Table 4.1: Some of the main properties of the geothermal fields utilized for Reykjavik such as average temperature, number of production wells, average production in GJ and kg/s and proportion of production from each field in 2010. From [Ivarsson \[2011\]](#).

Laugarnes field

The Laugarnes field production data has been recorded from 1962 with monthly time resolution. Now there are 10 production wells used in the field (figure 4.2), two of which started production a bit later or around 1980. The production has decreased slightly since Nesjavellir started production in 1990. Two reference wells (reference wells are usually selected to collect data on water level and temperature and don't serve as production wells) are in the field, RV-7 and RV-34 with data for pressure (drawdown) recorded since 1967 and 1985 respectively. Combined production from those ten production wells was calibrated to the model using the data from reference well RV-34. Figure 4.2 shows the location of the wells in Laugarnes where the reference wells are marked with a red circle. When choosing between two reference wells it would in general be more appropriate to choose the one with data recorded for a longer period of time. The quality metrics for calibrating to RV-7 did however give a poorer result. The initial state for the drawdown is assumed to be the average meters above sea level (a.m.s.l) in those eleven wells. In [Sigurðardóttir et al. \[2012\]](#) the a.m.s.l benchmark was considered from RV-34 only.

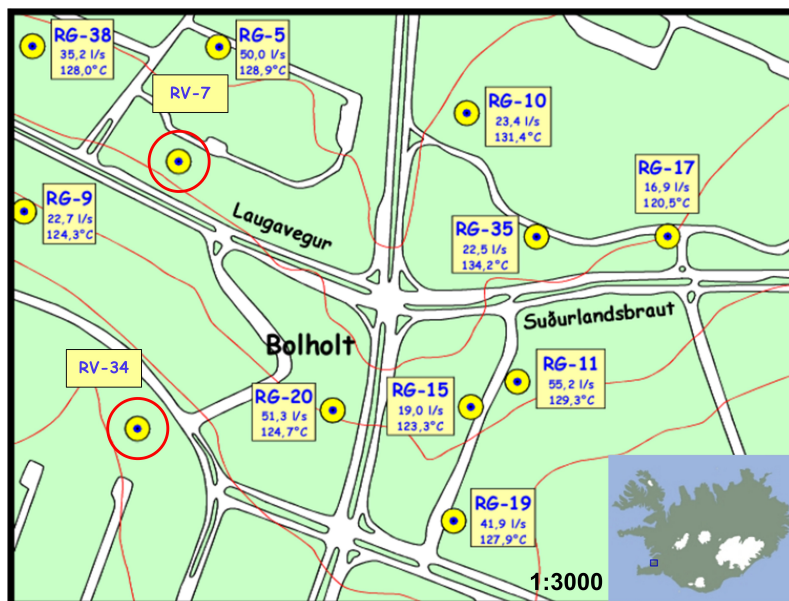


Figure 4.2: Location of production wells and reference wells in Laugarnes field. Reference wells are marked with a red circle. From [Ivarsson \[2011\]](#).

Reykir field

Reykir field operates 22 wells (left side on figure 4.3) with recorded data starting from 1971 - 1976 with monthly resolution. The combined production was fitted to the model in terms of reference well MG-1 with data from 1976 to 2010 and a.m.s.l was used as

a benchmark for drawdown for the 23 wells. There are two reference wells in Reykir field, SR-1 and MG-1. There exist a longer period of recorded data for MG-1 as well as the quality metrics for calibrating SR-1 to the production data gave a slightly poorer result.

Reykjahlid field

Reykjahlid field operates 12 wells (right side on figure 4.3) with recorded data starting from 1974 - 1979. All records have a monthly resolution. The combined production was fitted to the model in terms of the only reference well in the area, MG-28, with recorded data for water level from 1985.

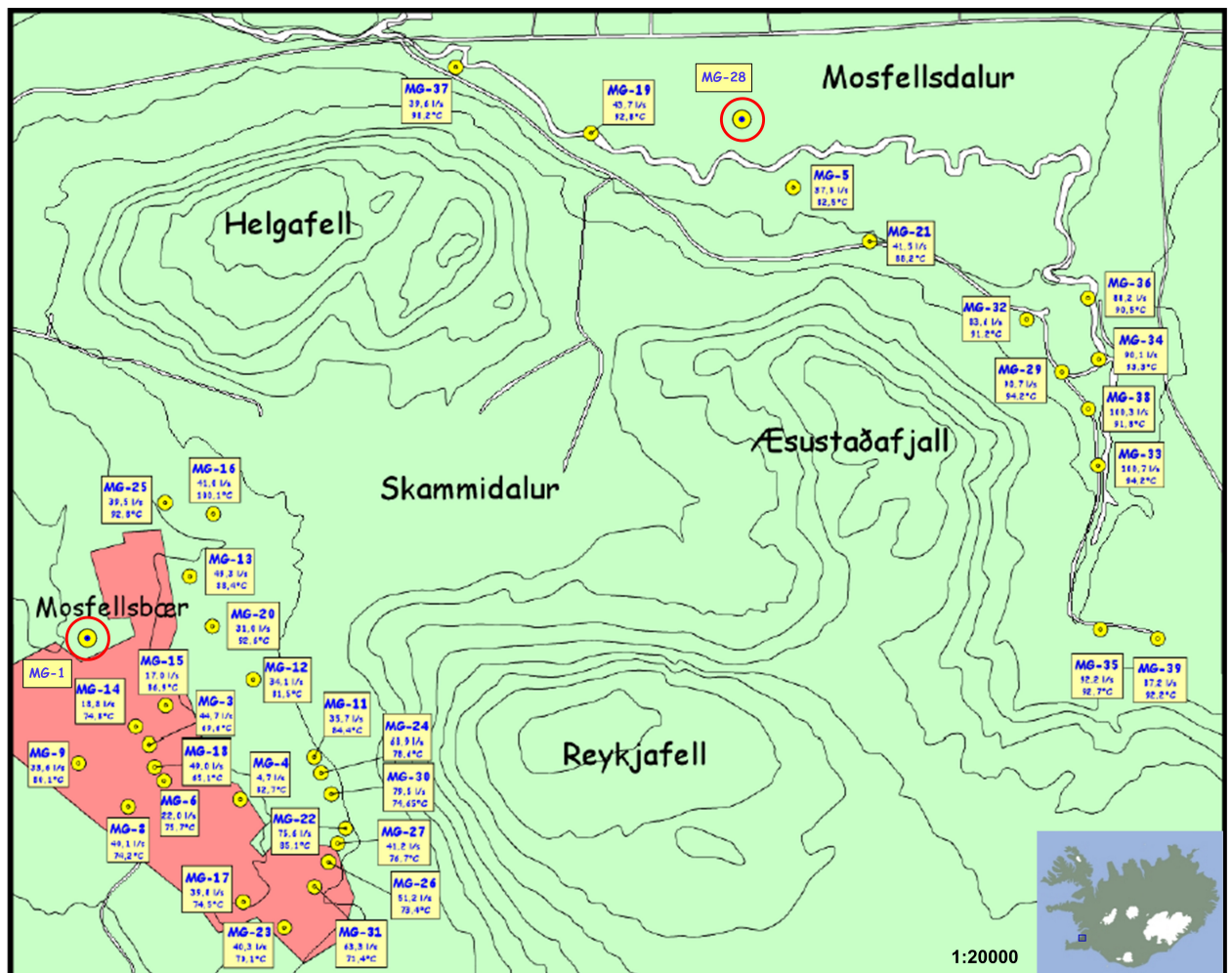


Figure 4.3: Location of production wells and reference wells in Reykir and Reykjahlid fields. Reference wells are marked with a red circle. Reykjahlid field is the right side and Reykir field on the left side. From Ivarsson [2011].

Reykir and Reykjahlid as one field

Gunnlaugsson et al. [2000] describes Reykir as one field and Reykir and Reykjahlid as sub-areas as they lie close together (see figure 4.3) and the data suggest that their water levels are correlated. The Laugarnes and Ellidaar fields also lie close together. Their data do however not suggest any correlation between them and Gunnlaugsson et al. [2000] suggest they must be separated by hydrological barriers since chemistry, isotopic compositions and temperature of the water differ between these areas. Reference well MG-1 was chosen as it has longer period of water level data and gave a better result than the other reference wells.

Ellidaar field

Eight wells are operated in the Ellidaar field (figure 4.4) with recorded data starting from 1969 - 1985. All records have monthly resolution. The combined production was fitted to the only reference well in the area, RV-27 with recorded data for water level from 1969.

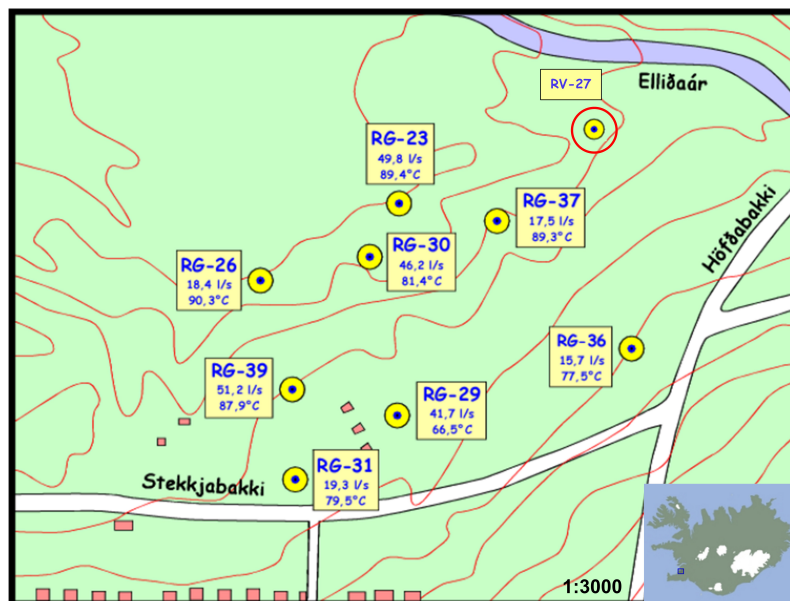


Figure 4.4: Location of production wells and the reference well in Ellidaar field. Reference well is marked with a red circle. From Ivarsson [2011].

4.1.2 Parameter estimation and validation

A lumped parameter model (LPM) was fitted to each of five data sets respectively, Laugarnes, Reykir, Reykjahlid, Ellidaar and Reykir-Reykjahlid (as one field). The model

parameters are estimated by minimizing the sum squares of the difference between predicted drawdown and measured data, such that:

$$\min \frac{1}{2} \|\mathbf{h}_e - \mathbf{h}(\mathbf{h}_{i,1}, \mathbf{K}, \mathbf{S}, t)\|_2^2 = \min \frac{1}{2} \sum_i (h_{e,i} - \mathbf{h}(\mathbf{h}_{i,1}, \mathbf{K}, \mathbf{S}, t_i))^2 \quad (4.1)$$

where $h_{e,i}$ is a measured observation at time step i and $\mathbf{h}(\mathbf{h}_{i,1}, \mathbf{K}, \mathbf{S}, t_i)$ is the predicted drawdown at the same time step. This returns the vectors of the values for the initial drawdown in each tank, \mathbf{h} the storage coefficients, κ and the conductance values σ which are the characteristic parameters for the particular geothermal system in question. This is solved by using a least squares minimizer in MATLAB [MATLAB, 2012] that uses an interior-reflective Newton Method for large scale problems.

In modeling pressure response (change in drawdown) for Laugarnes field, 207 of 311 data points were fitted to the lumped parameter model (LPM), or two third of the data. The fit was validated using the rest of the data. This was done for a single-tank model, closed and open, two-tank model, closed and open and three-tank model closed and open. The LPM model was explained in section 2.1 in terms of N-tanks. For Laugarnes a two-tank open model and three tank-open model gave the best result which are shown in figure 4.5a (three-tank open model) and in tables 4.2 and 4.3.

For Reykir 277 of 415 data points were fitted to the model and the fit validated for the rest of the data. As for Laugarnes the data was calibrated to six different lumped parameter models. Two-tank open model and three tank-open model gave the best result and can be viewed in figure 4.5b (two-tank open model) and tables 4.2 and 4.3.

For Reykjhlid, 207 of 310 data point were fitted to the model and the fit validated with the rest of the data. Result for two-tank open model and three tank-open model can be viewed in table 4.2 and 4.3 as they gave the best result of the six different lumped parameter models, see results in figure 4.6b (three-tank open model) and tables 4.2 and 4.3.

For Ellidaar, 329 of 494 data points were fitted to the model and the fit validated for the rest of the data. Result for two-tank open model and three tank-open model can be viewed in figure 4.6a (two-tank open model) and tables 4.2 and 4.3.

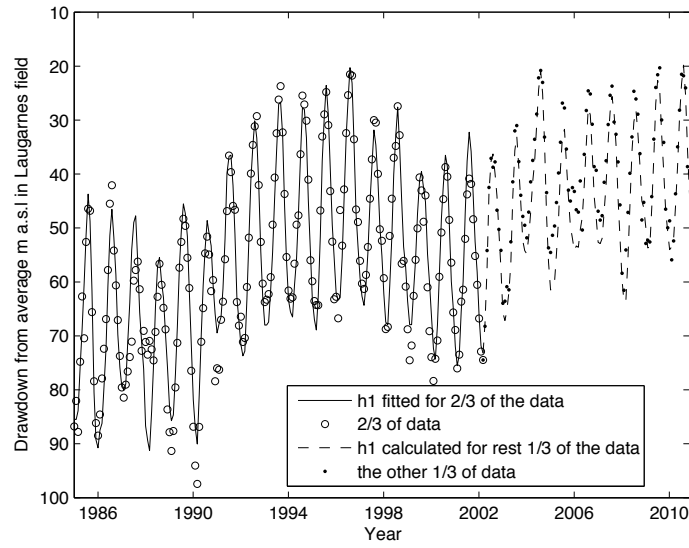
The result for the calibration by combining the production for Reykir and Reykjahlid for two tank open model and three tank closed model can be viewed in table 4.4 and figure 4.7.

Each of the tables display the results for the parameters for the initial state, storage coefficients, κ and resistors, σ in the first half, and the quality metrics of the fit in the second half. The quality metrics include: the root mean square (RMS) error, R^2 , which measures how successful the fit is explaining the variation of the data, the maximum error and the average error between historical and predicted data. The initial state represents the drawdown at time $i = 1$ in the tanks $h_{j,1} \dots h_{N,1}$. The number of parameters depend on the size of the LPM model, i.e. number of tanks.

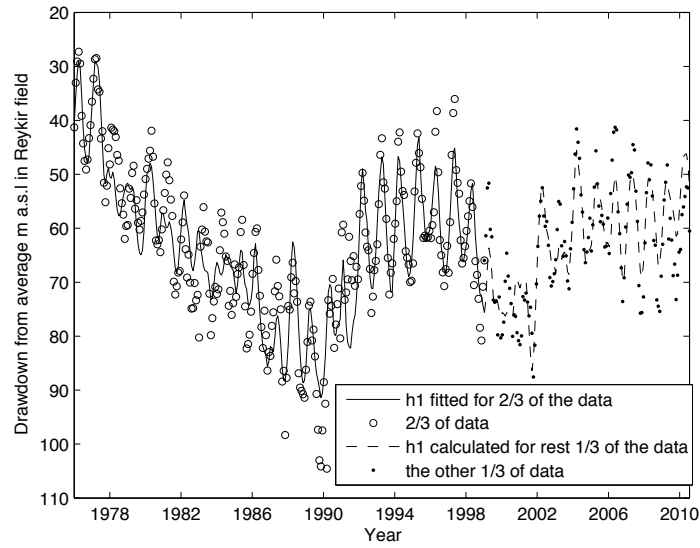
Two - tank open									
Parameters	Laugarnes		Reykir		Reykjahlid		Ellidaar		Units
	2/3 of data	Validation	2/3 of data	Validation	2/3 of data	Validation	2/3 of data	Validation	
κ_1	61.58	-	7851	-	59656	-	398.7	-	$\text{m} \cdot \text{s}^2$
κ_2	1776	-	$3.45 \cdot 10^6$	-	$6.10 \cdot 10^5$	-	$3.29 \cdot 10^7$	-	$\text{m} \cdot \text{s}^2$
σ_{12}	0.026	-	0.00094	-	0.026	-	0.00018	-	$\text{m} \cdot \text{s}$
σ_{23}	0.0024	-	0.030	-	0.0024	-	0.021	-	$\text{m} \cdot \text{s}$
$h_{1,i=1}$	88.80	-	40.66	-	87.22	-	0.25	-	m
$h_{2,i=1}$	86.94	-	-20.62	-	87.30	-	-11.91	-	m
H_0	-17.76	-	20.04	-	52.67	-	-50.00	-	m
RMS	5.33	8.37	5.69	5.61	13.34	12.32	11.96	5.96	m
R^2	89.38	48.99	84.53	70.37	9.94	less than zero	76.37	less than zero	%
Max Error	20.32	15.42	27.11	14.86	36.88	27.57	42.70	23.17	m
Ave. Error	4.00	7.71	4.32	4.39	10.55	10.22	9.03	4.66	m

Table 4.2: Results from fit for two-tank open model for the four geothermal fields. The first of two columns for each field represents results for the parameter fit performed by MATLAB [MATLAB, 2012]. The second column represents the quality metrics of the fit. Bold values represent fitted parameters chosen for the optimization.

As well as evaluating future response of the reservoir the storage coefficients (κ) from the LPM can be used to evaluate it's size. Two types of storage mechanisms can be considered. First, the storage coefficients are controlled by liquid-formation compressibility from which the volume (m^3) can be calculated from the porosity and compressibility of the water and the rock. Secondly the storage coefficient can be used to calculate the surface area of the modeled portion of the reservoir. Spatial constraints of the LPM need to be considered carefully though, as volume values for the reservoir calculated from κ might be unrealistic. Surface area values should be comparable with e.g., values from conceptual modeling. This is explained in more detail in [Garcia et al., 2011; Axelsson, 1989]. Looking at the data for κ and σ in tables 4.2 and 4.3 it is for example quite noticeable from κ_1 that the central part of Reykir field is substantially bigger than the central part of Laugarnes field. The σ_{12} for Laugarnes is however substantially bigger than σ_{12} for Reykir which suggest that water from outer parts of Laugarnes field flows more easily to the central part of the reservoir than for Reykir



(a) Laugarnes field. Results from calibrating data to a three - tank open LPM model.



(b) Reykir field. Results from calibrating data to a two - tank open LPM model.

Figure 4.5: Fit for Laugarnes and Reykir. The figure above displays graphically the fit for Laugarnes field presented in table 4.3 for a three - tank open model. The figure below displays graphically the fit for Reykir field presented in table 4.2 for two - tank open model. The vertical axis shows drawdown from average meters above sea level for each geothermal field respectively.

The data was fitted to the LPM model with a one-tank closed model and the LPM was then expanded to a three-tank open model or until an acceptable accuracy of the fit was obtained. This methodology was also used in [Axelsson and Arason \[1992\]](#). The LPM is expanded step by step in order to find an interval for a good guess for the initial state and the parameters by starting with few parameters and increasing them. It is important

to point out here that randomly choosing initial values and working with only one type of LPM is also an option here. The author wanted however to get a feeling for different sizes of LPM and their response to the data.

When the data was calibrated to one-tank model it gave higher RMS value than the results here display, that is the deviation between the model and measured water level was greater. The RMS value decreases as the complexity of the lumped parameter model increases and the two-tank and three-tank models yield very similar result, the result in [Satman et al. \[2005\]](#) was similar.

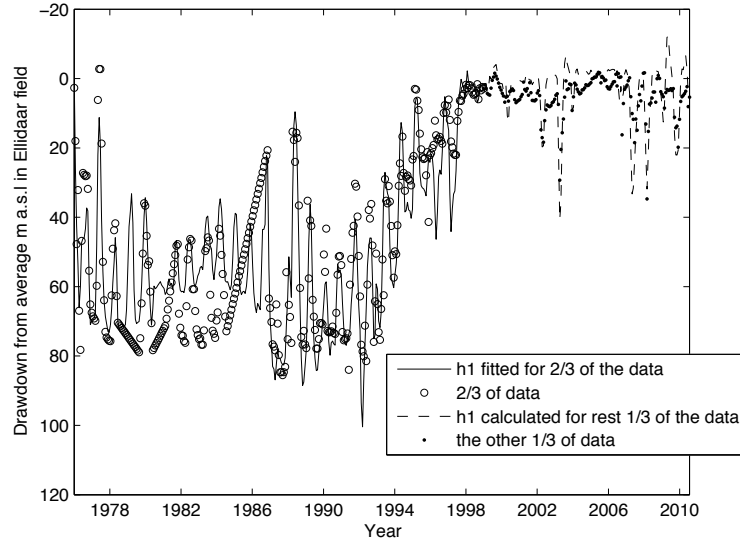
Three - tank open									
Parameters	Laugarnes		Reykir		Reykjahlid		Ellidaar		Units
	2/3 of data	Validation	2/3 of data	Validation	2/3 of data	Validation	2/3 of data	Validation	
κ_1	64.9	-	7688	-	102.2	-	394.6	-	$\text{m} \cdot \text{s}^2$
κ_2	1663	-	$3.44 \cdot 10^6$	-	24860	-	$3.88 \cdot 10^5$	-	$\text{m} \cdot \text{s}^2$
κ_3	$43.7 \cdot 10^6$	-	$4.90 \cdot 10^7$	-	$2.10 \cdot 10^5$	-	$1.92 \cdot 10^8$	-	$\text{m} \cdot \text{s}^2$
σ_{12}	0.059	-	0.00094	-	0.027	-	0.00018	-	$\text{m} \cdot \text{s}$
σ_{23}	0.00026	-	0.026	-	0.0019	-	0.029	-	$\text{m} \cdot \text{s}$
σ_3	0.063	-	0.0014	-	0.00079	-	0.032	-	$\text{m} \cdot \text{s}$
$h_{i=1,1}$	85.41	-	40.65	-	85.54	-	0.74	-	m
$h_{i=1,2}$	84.38	-	-20.40	-	83.07	-	-13.68	-	m
$h_{i=1,3}$	-0.55	-	24.25	-	59.33	-	-12.67	-	m
H_0	-2.33	-	-150.0	-	-22.46	-	-149.8	-	m
RMS	4.90	4.50	5.69	6.04	12.02	8.55	11.76	24.14	m
R^2	91.06	85.26	84.56	65.71	26.88	23.32	78.54	less than zero	%
Max Error	20.30	11.01	27.23	14.01	30.34	20.41	40.90	42.46	m
Ave. Error	3.58	3.72	4.31	4.83	9.70	7.11	8.55	23.14	m

Table 4.3: Results from fit for two-tank open model for the four geothermal fields. The first of two columns for each field represents results for the parameter fit performed by MATLAB [\[MATLAB, 2012\]](#). The second column represents the quality metrics of the fit. Bold values represent fitted parameters chosen for the optimization.

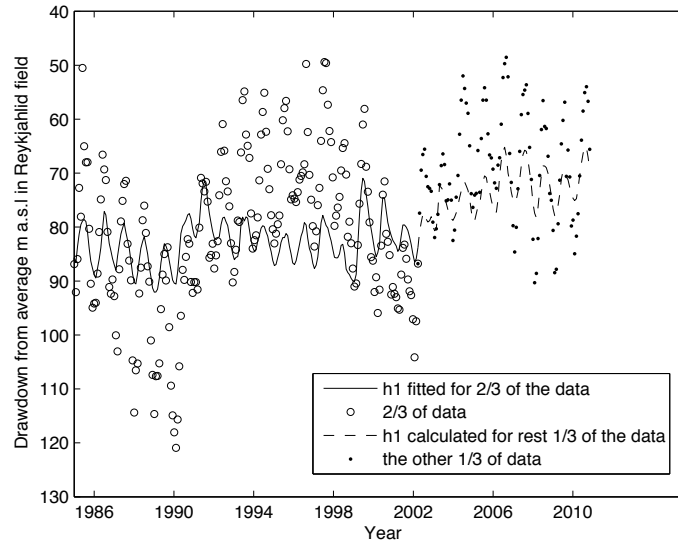
It is very important not to overestimate the LPM, i.e. how many tanks are needed. A two-tank model can be better than a three-tank model. The best results were for a two-tank open model and a three-tank open model except for Reykir and Reykjahlid when modeled as one field, a three-tank closed model clearly gave a better result than three-tank open model.

Validating the data fits helps choose between two-and three-tank model. As for Laugarnes the three - tank model is a straightforward choice. For the two-tank modeling the RMS increases from 5.33 to 8.37 as it is validated and the R^2 decreases from 89.38% to 48% (table 4.2), as for three-tank model the RMS decreases and the R^2 decreases slightly (table 4.3). For Reykir, both fits with validation are quite good although the fit for two-tank model is slightly better.

Reykjahlid and Ellidaar fields do not give an acceptable fit as the validations result



(a) Ellidaar field. Results from calibrating data to a two - tank open LPM model.



(b) Reykjahlid field. Results from calibrating data to a three - tank open LPM model.

Figure 4.6: Fit for Ellidaar and Reykjahlid. The figure above displays graphically the fit for Ellidar field presented in table 4.2 for a two - tank open model. The figure below displays graphically the fit for Reykjahlid presented in table 4.3 for three - tank open model. The vertical axis shows drawdown from average meters above sea level for each geothermal field respectively.

in an unacceptable value of R^2 . The production in Ellidaar field decreased substantially after 1995 (see development of drawdown in figure 4.6a) and it is therefore difficult to validate such data set. In Reykjahlid, where the quality of data seems to be satisfactory, the high RMS and the low R^2 could only be explained by the spatial constraints of the LPM model. This emphasizes the importance of validating the fit for such modeling and restates that the LPM needs be used carefully in evaluating future response of a geother-

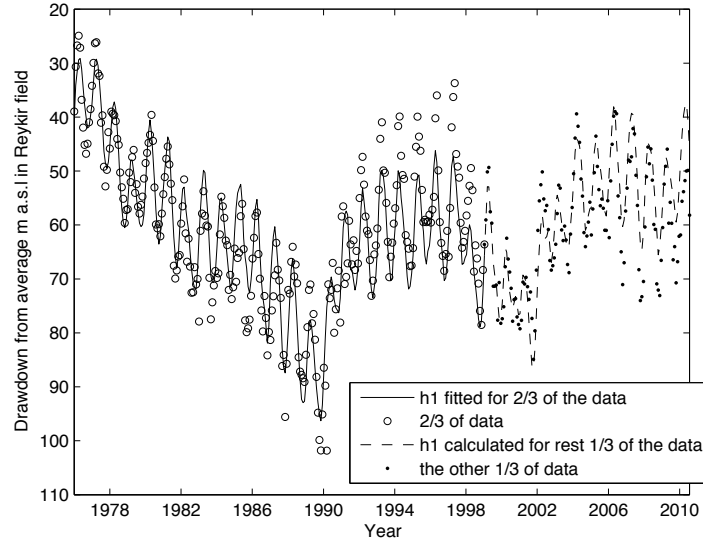
mal system as such systems are comprehensively more complicated than the LPM model assumes.

Reykir + Reykjahlid					
Parameters	Two - tank open		Three - tank closed		Units
	2/3 of data	Validation	2/3 of data	Validation	
κ_1	7514	-	7734	-	$\text{m} \cdot \text{s}^2$
κ_2	18072	-	16334	-	$\text{m} \cdot \text{s}^2$
κ_3	-	-	$3.14 \cdot 10^7$	-	$\text{m} \cdot \text{s}^2$
σ_{12}	0.0052	-	0.0051	-	$\text{m} \cdot \text{s}$
σ_{23}	0.0012	-	0.0012	-	$\text{m} \cdot \text{s}$
σ_3	-	-	-	-	$\text{m} \cdot \text{s}$
$h_{1,i=1}$	40.32	-	40.70	-	m
$h_{2,i=1}$	25.81	-	26.13	-	m
$h_{3,i=1}$	-	-	-34.08	-	m
h_0	-34.69	-	-	-	m
RMS	5.53	5.78	5.69	5.18	m
R^2	85.41	68.65	84.29	74.70	%
Max Error	26.60	14.10	27.28	12.51	m
Ave. Error	4.32	4.66	4.44	4.14	m

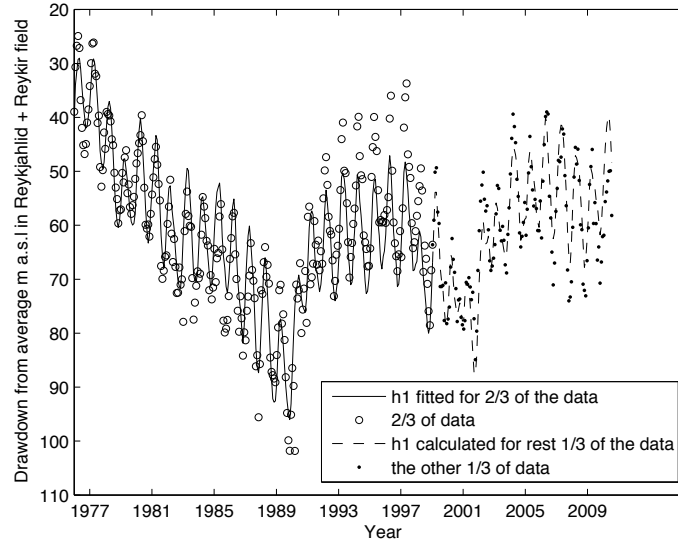
Table 4.4: Results from Reykir and Reykjahlid as one field Combined production is calibrated to one reverence well MG-1. The first of two columns for each field represents results for the parameter fit performed by MATLAB [MATLAB, 2012]. The second column represents the quality metrics of the fit.

As for Reykir and Reykjahlid both of the fits are considered acceptable although three - tank closed model gave a slightly better result. Interestingly it could imply that Reykir geothermal field alone can be considered as a two-tank open system, but when it is modeled with Reykjahlid the whole system can be considered a closed three-tank system.

The fit for a three-tank open model for Laugarnes, a two-tank open model and three-tank open model for Reykir and two-tank open model and three-tank closed model for Reykir and Reykjahlid are all considered to be suitable fits to use as representative models. Only Laugarnes and Reykir field are however chosen as a suitable examples for the optimization which follows, the three-tank open model for Laugarnes is used since it has the smallest RMS value and the highest R^2 value, and a two-tank model for Reykir, since it is a suitable fit and it saves some computational cost in the optimization. It is relative to ask at this point why a closed LPM wasn't chosen for the optimization. Since the only significant result for calibrating the data to a closed model gave a rather large value for κ_3 (see table 4.4 here above) it is not very likely to give a very different result from a three - tank open model and was therefore not chosen for the optimization. It is however very interesting to perform an optimization with a closed LPM where the last tank has a smaller value.



(a) Reykir plus Reykjahlid. Two - Tank open



(b) Reykir plus Reykjahlid Three - Tank closed

Figure 4.7: A fit for Reykir and Reykjahlid combined as one reservoir. The vertical axis shows drawdown from average meters above sea level for each geothermal field respectively.

4.2 Testing of algorithms for the optimization model

In this section three different solution methods introduced for solving the problem represented by equation 3.2 in chapter 3 will be tested. The objective function \mathcal{J} represents profit and will be maximized. Two different MILP relaxations will be applied. The

objective function will be approximated with a piecewise linear Taylor series and piecewise under-and over-estimators will be applied. Finally the optimization problem will be solved with a NLP relaxation.

The demand function or the upper-bound of the decision variable, $\dot{m}_i^U = \dot{m}_{e,i} \forall i \in \mathcal{I}$ (see section 2.2.3) is a very important parameter in the model. \dot{m} will follow \dot{m}_e exactly until other constraints of the model are active. For that reason, \dot{m}_e implicitly affects the behavior of the state variable $h_{1,i}$ since it is a function \dot{m} . Other state variables $h_{2,i}$ and $h_{3,i}$ (for a 3-tank model) are not affected as much by \dot{m} (implicitly \dot{m}_e) since their dynamical response is not as strong¹.

In testing the algorithms for the above mentioned methods, $\dot{m}_{e,i}$ is represented by a simple linear function. However, the behavior of $\dot{m}_{e,i}$ in practice is very dynamic as shown in sections 4.3 and 4.4.

The results include the optimized present value of profit compared to the profit calculated with no interest rate after the optimization has been performed. Comparing linear and non-linear present value of the profit can skew the error evaluation substantially since values at the end of the time period are greatly affected by interest rate compared to values in the beginning of the time period. The error is evaluated from the non-linear part of the function only, or the part that represents production, \mathcal{J}_2 , see equations 3.1 and 3.2. This was also explained in section 3.2.4.

4.2.1 Piecewise linear approximation

To obtain a good first degree Taylor approximation (see section 3.2.2) proper values of the reference points are essential. The closer they are to the optimal solution the better. Initial values for the reference points for production $\dot{m}_{z,i}$ are set as the expected demand or the upper bound of the decision variable \dot{m}_i^U . The reference points for the drawdown are calculated from expected demand. With small disruption in demand, or when the control trajectory can follow the upper bound rather accurately, no updating algorithm is needed.

¹ This depends on the parameter fit of the LPM model, the dynamical response (change in drawdown) to production of the state variable is dependent upon how big the tanks are and how fast the fluid can flow between them.

Example 4.1. Consider the following demand function:

$$m_e(i) = \bar{m}_e + m_I t_i \quad (4.2)$$

where \bar{m}_e is the average available historical demand and m_I is the monthly increase in demand. With a 25 kg/s increase in demand per year ($m_I = 25/12$) the model can be optimized successfully without the lower bound constraint shown in section 3.2.3 and an updating algorithm, see numerical results in table 4.5

$\mathcal{J}_{2,\text{Error}}^{\text{PV}}$	$\mathcal{J}_{2,\text{Error}}$	$\mathcal{J}_{\text{MILPr1}}^{\text{PV}}$	$\mathcal{J}_{\text{MINLP}}^{\text{PV}}$	$\mathcal{J}_{\text{MILPr1}}$	$\mathcal{J}_{\text{MINLP}}$
0.00031 %	0.0021 %	32,942,116 \$	32,942,013 \$	69,723,560 \$	69,723,151 \$

Table 4.5: Results from optimization with demand function: $m_{e,i} = \bar{m}_e + m_I t_i$, $m_I = 25/12$. Optimized for $t_n = 311$ months. Starting time $t_1 = 1$.

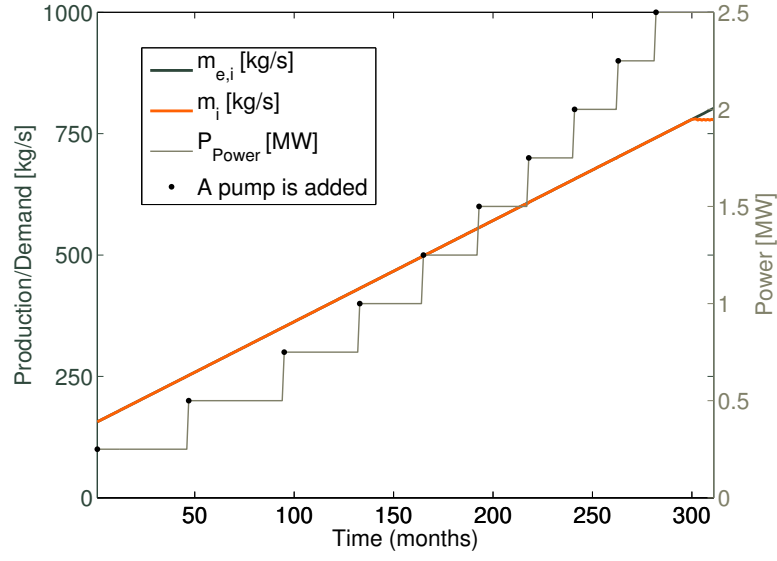
As seen in figure 4.8, production can not meet demand at the very end of the period (cf. constraint 2, see section 2.2.3). This is not due to the sustainability constraint introduced in section 2.2.4, but it is highly dependent on the temperature of the system. In this example, the sustainability constraint limit is located at a depth of 751 m. The reason that production can not meet demand after 300 months in this case has more to do with the economic factors of the model since it is very likely that it doesn't pay off to pump deeper. Those consideration will be further accounted for in sections 4.3 and 4.4.

Example 4.2. An example that has the same demand function is now considered where $m_I = 4m_I = 100/12$. With such a big disruption in demand, it is more likely that the sustainability limit is reached, which means that production can not follow demand. It is desirable to see how that would affect the optimization for a longer period of time. That sort of behavior will very likely reduce the accuracy of the linearization since the decision variable can no longer follow the upper bounds nor the reference points (which are the upper bound here) for bigger part of the time period. For further reference see sections 3.2.3 and 3.2.4 where the linearization is explained.

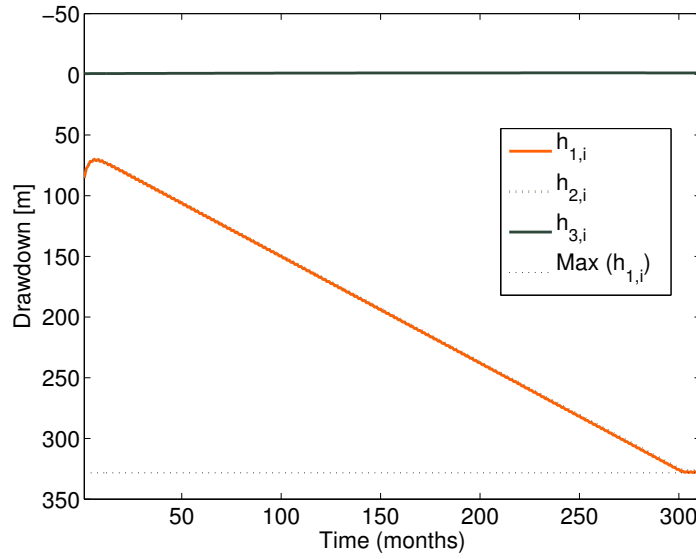
$\mathcal{J}_{2,\text{Error}}^{\text{PV}}$	$\mathcal{J}_{2,\text{Error}}$	$\mathcal{J}_{\text{MILPr1}}^{\text{PV}}$	$\mathcal{J}_{\text{MINLP}}^{\text{PV}}$	$\mathcal{J}_{\text{MILPr1}}$	$\mathcal{J}_{\text{MINLP}}$
67.5 %	981 %	78,357,586 \$	25,442,062 \$	184,450,350 \$	36,437,802 \$

Table 4.6: Results from optimization with demand function: $m_e(i) = \bar{m}_e + m_I t_i$, $m_I = 100/12$. Optimized for $t_n = 311$ months and starting time is $t_1 = 1$.

There are two important things to notice in table 4.6. First of all, the error between linear and non-linear production ($\mathcal{J}_{2,\text{Error}}^{\text{PV}}$ and $\mathcal{J}_{2,\text{Error}}$) is absolutely unacceptable. Secondly



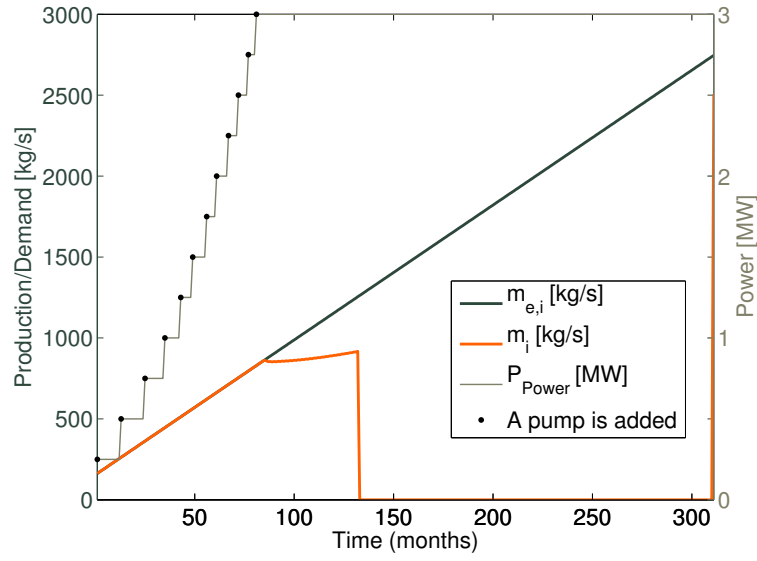
(a) Demand



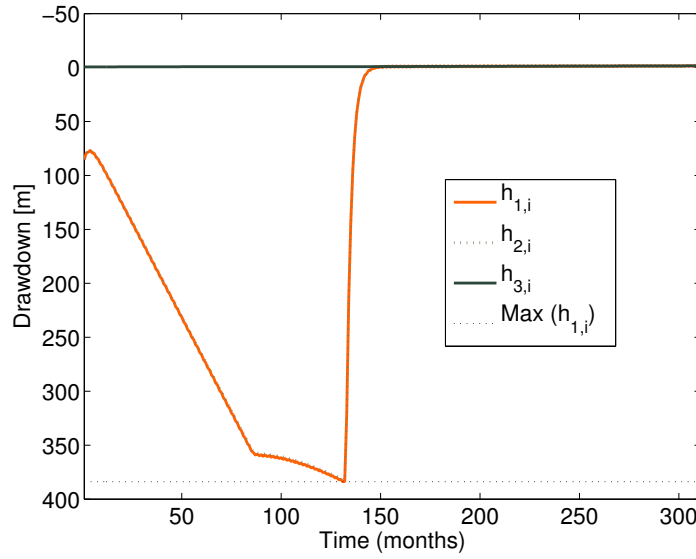
(b) Drawdown

Figure 4.8: Graphical results from a simple linear demand function. $m_{e,i} = \bar{m}_e + m_I t_i$ where $m_I = 25/12$. Demand is assumed to be linear and increase 25 kg/s a year.

there is a big difference between the error calculated from present value of the production ($\mathcal{J}_{2,\text{Error}}^{\text{PV}}$) and the error from production assuming no interest rate $\mathcal{J}_{2,\text{Error}}$. It is thus necessary to calculate the error between linear and non-linear production assuming no interest rate. $\mathcal{J}_{2,\text{Error}}$ is thus considered as the main benchmark in evaluating the error between linear and non-linear.



(a) Demand



(b) Drawdown

Figure 4.9: Graphical results from a simple linear demand function, example 4.2. Demand is on the upper figure and drawdown on the lower figure. The linear demand function is: $\dot{m}_{e,i} = \bar{m}_e + m_I t_i$ where $m_I = 25/12$. Demand is assumed to be linear and increase 100 kg/s a year.

Constraint 5

Figure 4.9 shows when the decision variable can not follow the upper bounds anymore, the optimization pushes the decision variables $\dot{m}_i \ll \dot{m}_{z,i}$ and thus the state variables ($h_{1,i} \ll h_{z,i}$) to a very small value. This was more thoroughly explained in section 3.2.3.

Example 4.3. The same function as in 4.2 is now optimized with the constraint 5 added to the model (equation 3.18).

$\mathcal{J}_{\text{Error}}^{\text{PV}}$	$\mathcal{J}_{\text{Error}}$	$\mathcal{J}_{\text{MILPr1}}^{\text{PV}}$	$\mathcal{J}_{\text{MINLP}}^{\text{PV}}$	$\mathcal{J}_{\text{MILPr1}}$	$\mathcal{J}_{\text{MINLP}}$
5.71%	8.08%	52,480,518 \$	49,486,439 \$	106,916,778 \$	98,775,490 \$

Table 4.7: Results from optimization with demand function: $m_{e,i} = \bar{m}_e + m_I t_i$, $m_I = 100/12$. Optimized for $t_n = 311$ months. Starting time $t_1 = 1$.

Looking at table 4.7 it is obvious that adding constraint 5 to the model decreases the error between linear and non-linear. The non-linear profit ($\mathcal{J}_{\text{MINLP}}$ calculated afterwards) increases, which means that it also is a better solution. The error is however still quite large when compared to the best case in this work. Figure 4.10 displays the result for production and drawdown for this example and figure 4.11 displays the non-linear part of the objective function ($\dot{m}_i h_{1,i}$) versus the linearized part versus constraint 5 (see equation 3.18). The upper figure shows the result from optimizing without constraint 5 and the lower figure with constraint 5. As figure 4.11 shows, constraint 5 is active as soon as production can not meet demand ($\dot{m}_i < m_{e,i}$)

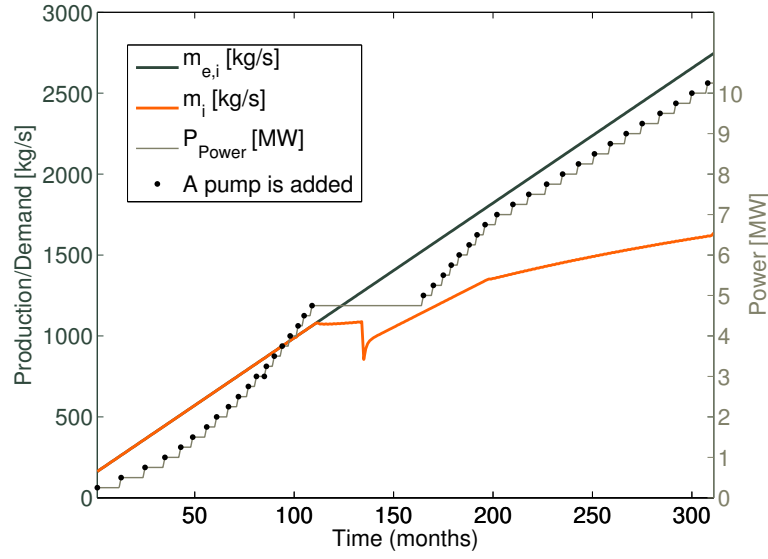
Updating algorithm

Since the error from last example is still quite large a simple updating process was tested. The reference points were simply replaced by the solution found by the MILP relaxation procedure. Then the optimization was performed again to see if that kind of an updating algorithm converges to an error value that can be considered acceptable.

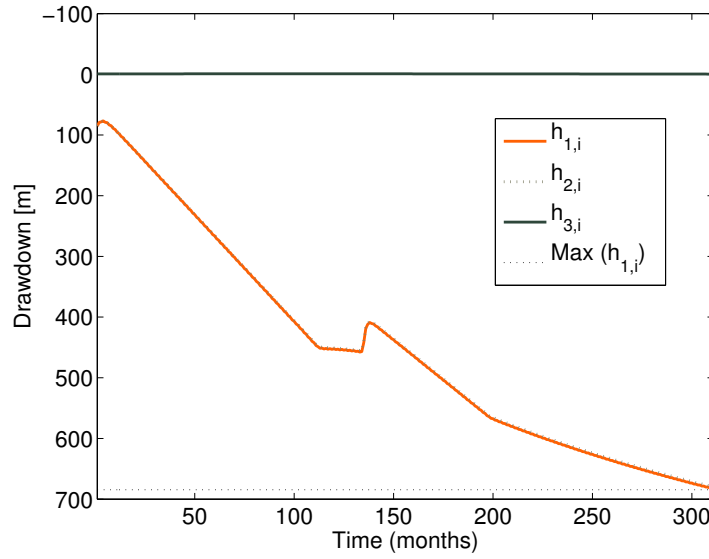
Example 4.4. Optimization conducted using algorithm 1 from section 3.2.4.

Iteration	$\mathcal{J}_{2,\text{Error}}^{\text{PV}}$	$\mathcal{J}_{2,\text{Error}}$	$\mathcal{J}_{\text{MILPr1}}^{\text{PV}}$	$\mathcal{J}_{\text{MINLP}}^{\text{PV}}$	$\mathcal{J}_{\text{MILPr1}}$	$\mathcal{J}_{\text{MINLP}}$
1	6.05 %	8.08 %	52,480,518 \$	49,486,439 \$	106,916,778 \$	98,775,490 \$
2	2.89 %	5.94 %	52,170,437 \$	50,706,760 \$	106,949,712 \$	102,586,632 \$
3	10.45 %	9.80 %	51,954,979 \$	47,037,247 \$	106,673,261 \$	93,169,082 \$
4	5.46 %	8.74 %	53,339,924 \$	50,575,969 \$	109,741,893 \$	102,310,287 \$
5	2.13 %	4.87 %	51,355,826 \$	50,283,227 \$	104,241,385 \$	101,145,816 \$
6	15.5 %	14.59 %	53,961,973 \$	46,727,177 \$	112,866,705 \$	92,079,219 \$
7	5.65 %	8.81 %	53,370,046 \$	50,516,034 \$	109,809,863 \$	102,088,752 \$
8	2.28 %	5.32 %	51,524,201 \$	50,374,156 \$	104,771,071 \$	101,398,625 \$

Table 4.8: Results from optimization with demand function: $m_e(i) = \bar{m}_e + m_I t_i$, $m_I = 100/12$ adding constraint represented by equation 3.18 and an updating process where $m_{z,i+1}^{(k+1)} = \dot{m}_i^{(k)}$ and $h_{z,i+1}^{(k+1)} = h_{1,i}^{(k)}$, algorithm 1. Optimized for $t_n = 311$ months. Starting time $t_1 = 1$.



(a) Demand

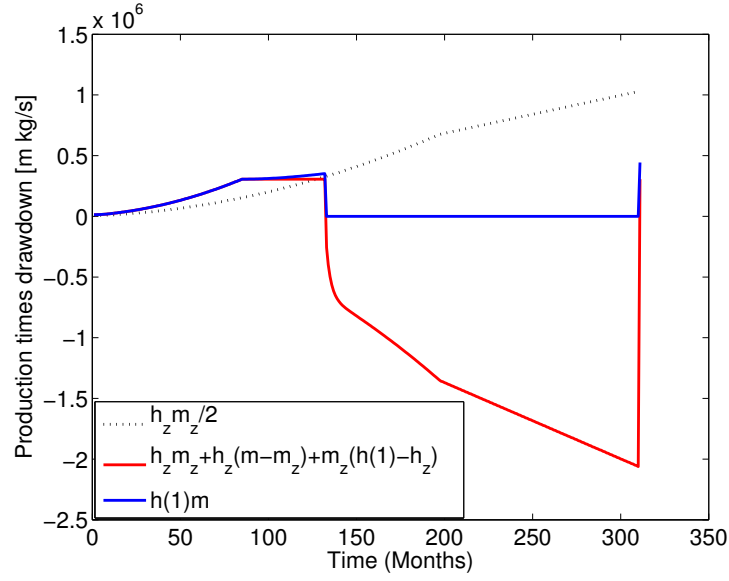


(b) Drawdown

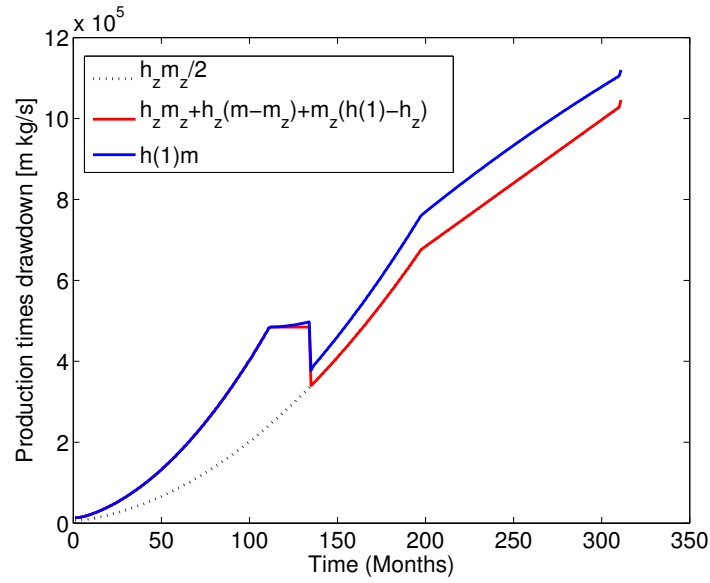
Figure 4.10: Example 4.3. Graphical results from adding constraint 5 (equation 3.18) to the model. The upper bound for the decision variables \dot{m}_i is a simple linear demand function. $m_{e,i} = \bar{m}_e + m_I t_i$ where $m_I = 100/12$. Demand is assumed to be linear and increase 100 kg/s a year.

After 8 iterations as seen in table 4.8 the error is still rather large (though smaller than in previous example) and the algorithm does not show a convergent behavior. Figure 4.12 displays graphically the development of updating process using algorithm 1.

The solution of the optimization \dot{m}_i^k seems to oscillate around the reference point $m_{z,i+1}^k = m_{1,i}^k$ but never gets close enough for smaller error. It is clear that an updating algorithm helps, but an updating process needs to be applied that can direct the so-



(a) Without constraint 5, example 4.2



(b) With constraint 5, example 4.3

Figure 4.11: Constraint 5 decreases the error between linear and non-linear substantially and gives a more realistic solution and is active from the point where production can no longer follow demand, i.e., $\dot{m}_i < m_{e,i}$

lution in the right direction. That is exactly what algorithm 2 introduced in section 3.2.4 does.

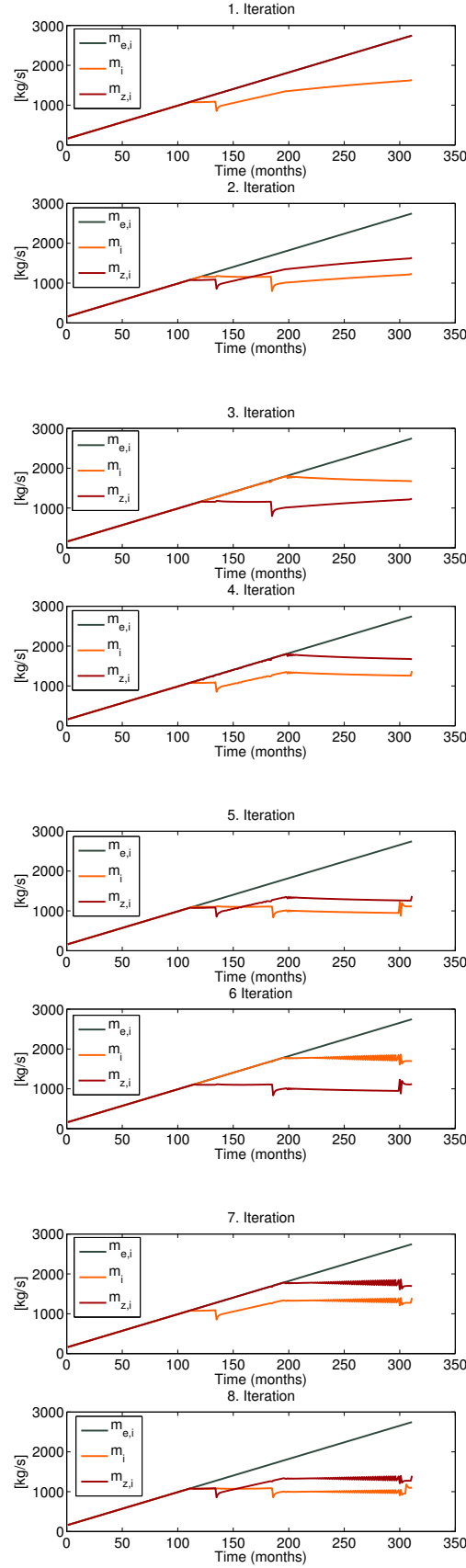


Figure 4.12: Example 4.4. Graphical results for the updating development of the decision variable \dot{m}_i and the reference point $m_{z,i}$. The updating algorithm replaces the reference point for iteration $k + 1$ with the solution from iteration k .

Example 4.5. *Reference points are updated with algorithm 2 represented in section 3.2.4.*

Iteration	$\mathcal{J}_{2,\text{Error}}^{\text{PV}}$	$\mathcal{J}_{2,\text{Error}}$	$\mathcal{J}_{\text{MILPr1}}^{\text{PV}}$	$\mathcal{J}_{\text{MINLP}}^{\text{PV}}$	$\mathcal{J}_{\text{MILPr1}}$	$\mathcal{J}_{\text{MINLP}}$
1	6.06 %	8.11 %	52,543,956 \$	49,542,512 \$	106,990,970 \$	98,835,993 \$
2	2.50 %	5.49 %	51,973,183 \$	50,705,504 \$	106,312,057 \$	102,420,934 \$
3	1.82 %	4.50 %	51,374,145 \$	50,454,887 \$	104,376,538 \$	101,558,820 \$
4	1.72 %	2.39 %	51,119,506 \$	50,257,446 \$	103,803,288 \$	101,592,375 \$
\vdots	\vdots	\vdots	\vdots	\vdots	\vdots	\vdots
9	0.29 %	0.39 %	50,977,496 \$	50,828,605 \$	103,344,631 \$	103,001,247 \$
10	0.19 %	0.37 %	50,968,736 \$	50,872,574 \$	103,053,819 \$	102,788,095 \$
11	0.09 %	0.13 %	50,958,140 \$	50,910,325 \$	103,234,420 \$	103,130,078 \$
12	0.05 %	0.10 %	50,953,862 \$	50,927,085 \$	103,075,184 \$	103,001,550 \$

Table 4.9: Results from optimization with demand function: $m_{e,i} = \bar{m}_e + m_I t_i$, where $m_I = 100/12$ using algorithm 2 and constraint 5, equation 3.18. Optimized for $t_n = 311$ months with starting time $t_1 = 1$.

The stopping criteria for this example was $\mathcal{J}_{2,\text{Error}} \leq 0.1\%$. As seen in table 4.9 the algorithm converges to that value in 12 iterations. Figure 4.13 displays graphically iterations 1-4 and 9-12. As seen in the figure \dot{m}_i^k and $m_{z,i+1}^k = m_{1,i}^k$ gradually get closer until they have almost the same value.

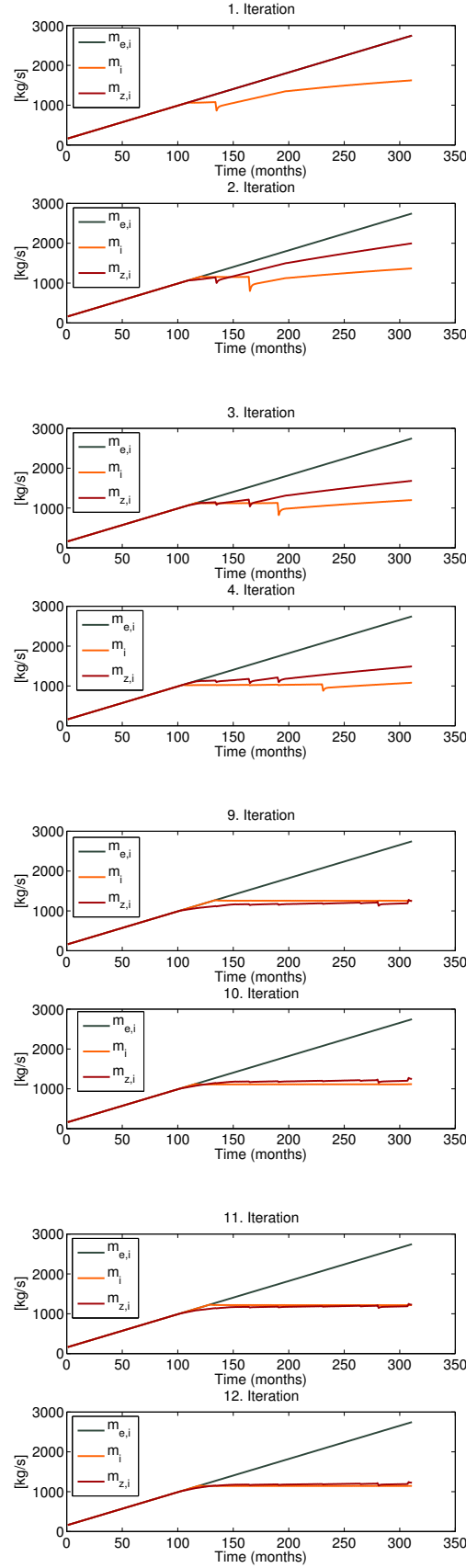
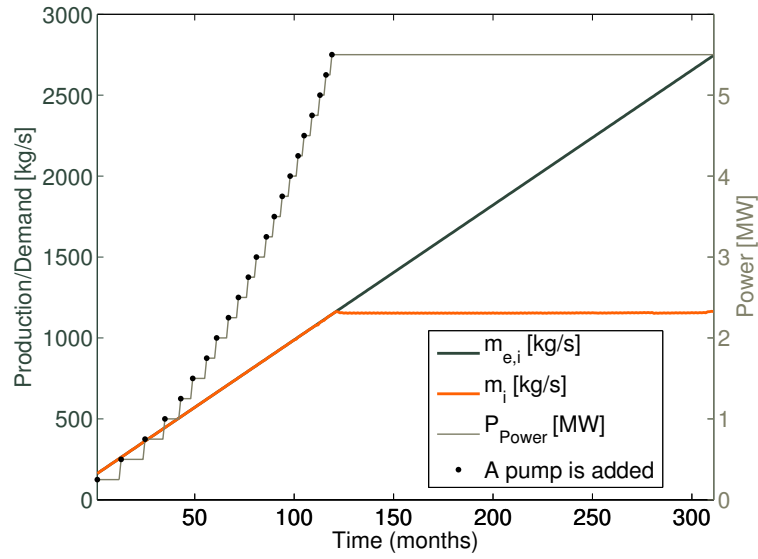
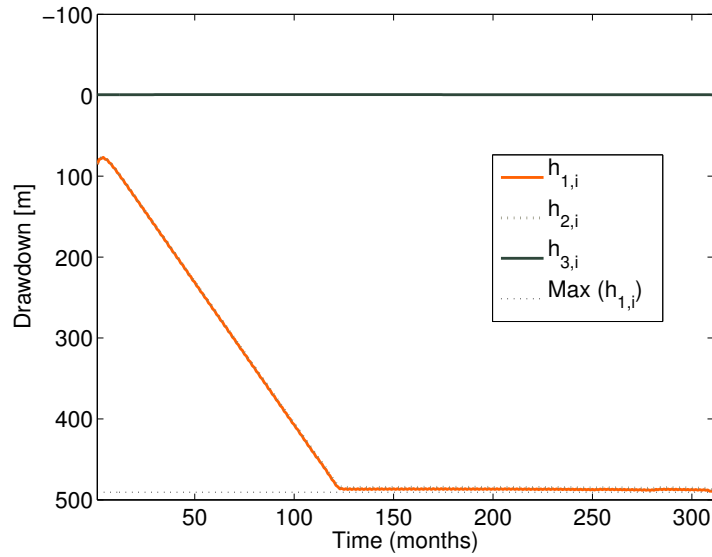


Figure 4.13: Example 4.5. Graphical results for the updating development of the decision variable \dot{m}_i and the reference point $\dot{m}_{z,i}$. The updating algorithm replaces the reference points for iteration $k + 1$ with a mix from the solution from iteration k and the reference point from iteration k in such way that if the reference point is below the solution it moves up for the next iteration and if it is above the solution it moves down for the next iteration, see algorithm 2.



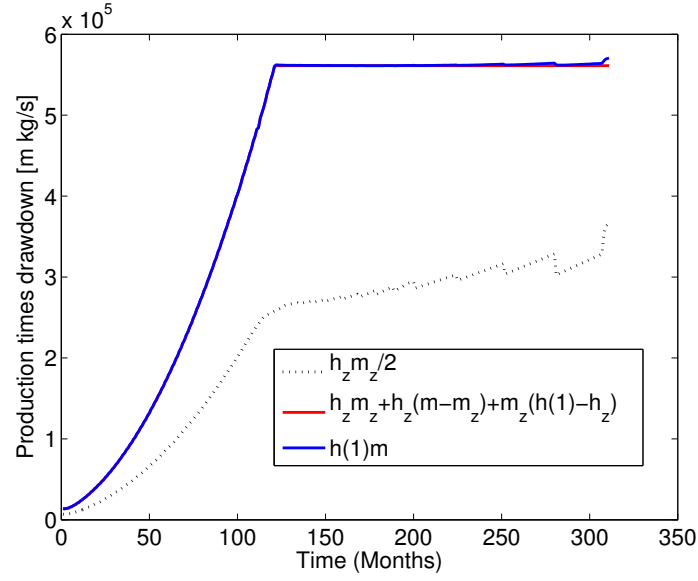
(a)



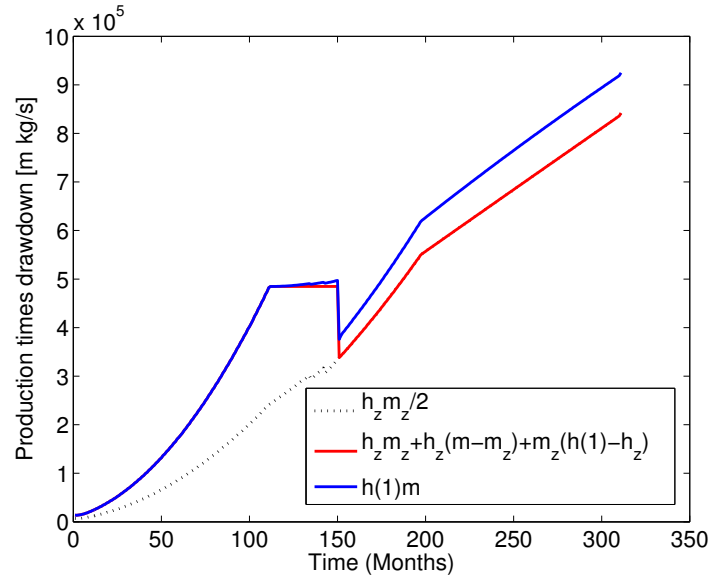
(b)

Figure 4.14: Example 4.5. Graphical results from a simple linear demand function using updating algorithm 2.

Figure 4.14 displays the result for production and drawdown for this example and figure 4.15 displays the non-linear part of the model versus the linearized part versus constraint 5. The upper figure displays iteration 12 and the lower figure iteration 3. Constraint 5 is still active at iteration 3, but no longer at the last iteration. It is very important that constraint 5 is not active for the final solution as it cuts off the feasible set. Constraint 5 thus serves its purpose which is only to steer the solution in the right direction.



(a) Iteration 12



(b) Iteration 3

Figure 4.15: Example 4.5. The non-linear part of the objective function (non-linear and linearized) and the left side of constraint 5. The figure below displays iteration 3 where constraint 5 is still active and the figure above displays the last iteration, iteration 12 where constraint 5 is no longer active.

Since this is a sufficient solution it needs to be considered whether it is really an optimal solution to the problem. One way is to relax the stopping criteria to an even smaller value and see whether the solution changes. Figure 4.16 displays 30 iterations for the objective function, comparing the objective function linearized and calculated non-linearly

afterwards and the development of the error, both with and without interest rate². As seen in the figures the difference between linear and non-linear stops to change as they become equal in around 9 iterations. From this information it is considered that a stopping criteria of 1% error seems to be enough, especially when it is being optimized for a longer period of time as conducted in sections 4.3 and 4.4.

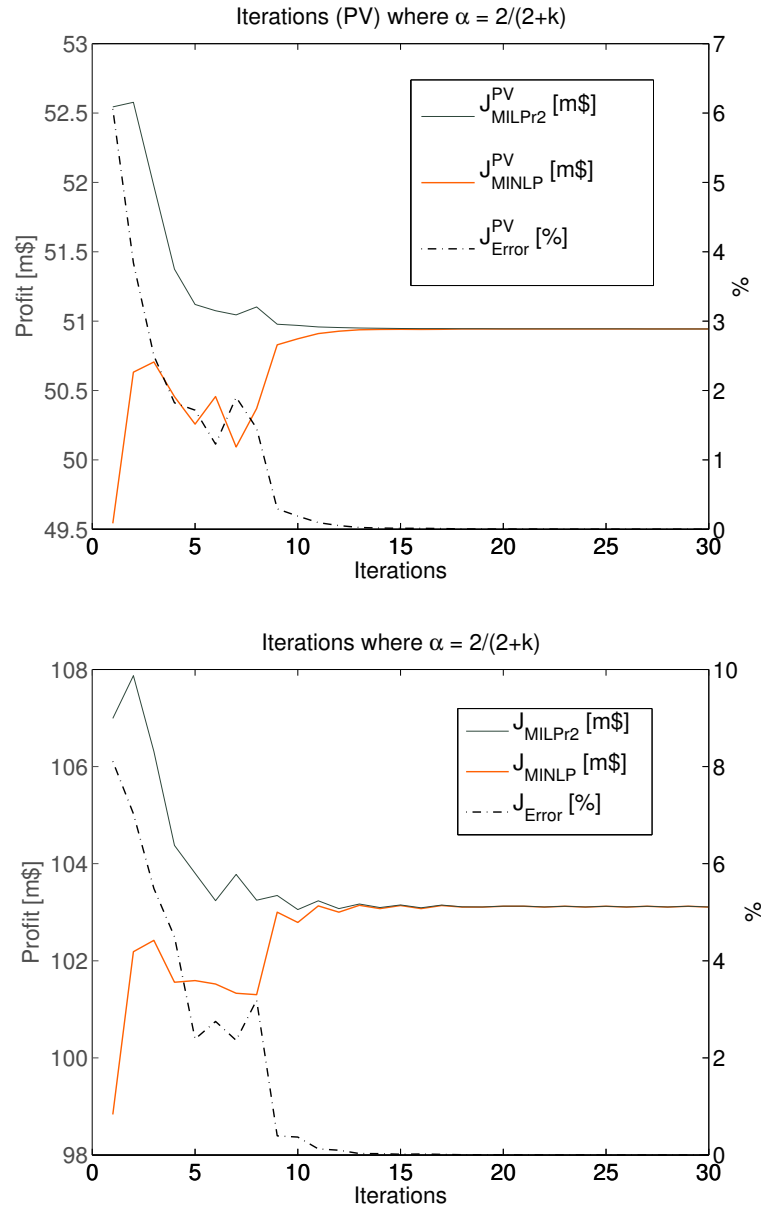


Figure 4.16: Example 4.5. The figure above displays profit (with and without interest rate) as a function of 30 iterations, development of present value profit calculated with the MILP relaxation and then calculated non-linearly afterward. The figure below displays the same calculation but assumes no interest rate. The solution does not change after around 9 iterations.

² The objective function is the present value of profit, the profit is calculated without interest rate for comparison purpose only

4.2.2 Piecewise under- and over-estimators

It has been shown above that solving a MILP relaxation of the problem is not easy. Another way to solve such problems is to use the methodology described in section 3.2.5. The non-linear (and non-convex) part of the objective function $\mathcal{J}_2(h_{1,i}, \dot{m}_i, i) = h_{1,i}\dot{m}_i, \forall i \in \mathcal{I}$ is replaced with a linear variable $z_i, \forall i \in \mathcal{I}$ that has convex and concave under-and over-estimators. Like in example 4.5, an updating process is also needed here where the under and over estimators are updated according to algorithm 2, see also section 3.2.6.

Example 4.6. *Piecewise under- and over-estimators with an updating process where $m_{e,i} = \bar{m}_e + m_I t_i, m_I = 100/12$.*

Iteration	$\mathcal{J}_{2,\text{Error}}^{\text{PV}}$	$\mathcal{J}_{2,\text{Error}}$	$\mathcal{J}_{\text{MILPr2}}^{\text{PV}}$	$\mathcal{J}_{\text{MINLP}}^{\text{PV}}$	$\mathcal{J}_{\text{MILPr2}}$	$\mathcal{J}_{\text{MINLP}}$
1	27.31%	248.45%	62,129,352.29 \$	48,802,720.89 \$	135,257,324.41 \$	98,261,841.99 \$
2	6.70%	29.31%	51,356,835.39 \$	48,134,067.63 \$	105,236,763.74 \$	94,806,749.63 \$
3	0.05%	0.13%	49,841,374.12 \$	49,815,051.81 \$	100,258,531.38\$	100,184,420.29 \$
4	0.02 %	0.051%	49,819,547.04 \$	49,809,124.21 \$	100,195,794.98\$	100,166,241.61 \$

Table 4.10: Results from optimization with demand function: $m_{e,i} = \bar{m}_e + m_I t_i, m_I = 100/12$. For MILP relaxation, $\mathcal{J}_2(h_{1,i}, \dot{m}_i, i) = h_{1,i}\dot{m}_i$ is replaced by z_i and an updating process is used, see section 3.2.6). Optimized for $t_n = 311$ months and starting time $t_1 = 1$.

As seen in table 4.10 the algorithm here converges considerable faster than in example 4.5. The stopping criteria is $\mathcal{J}_{2,\text{Error}} < 0.1\%$. The value of the objective function does however return a 3% smaller optimal than in example 4.5. This suggests this is either not a local optimal or it could be another local optimal. Figure 4.17 displays the iteration for \dot{m}_i graphically and figure 4.18 displays the results for production and drawdown.

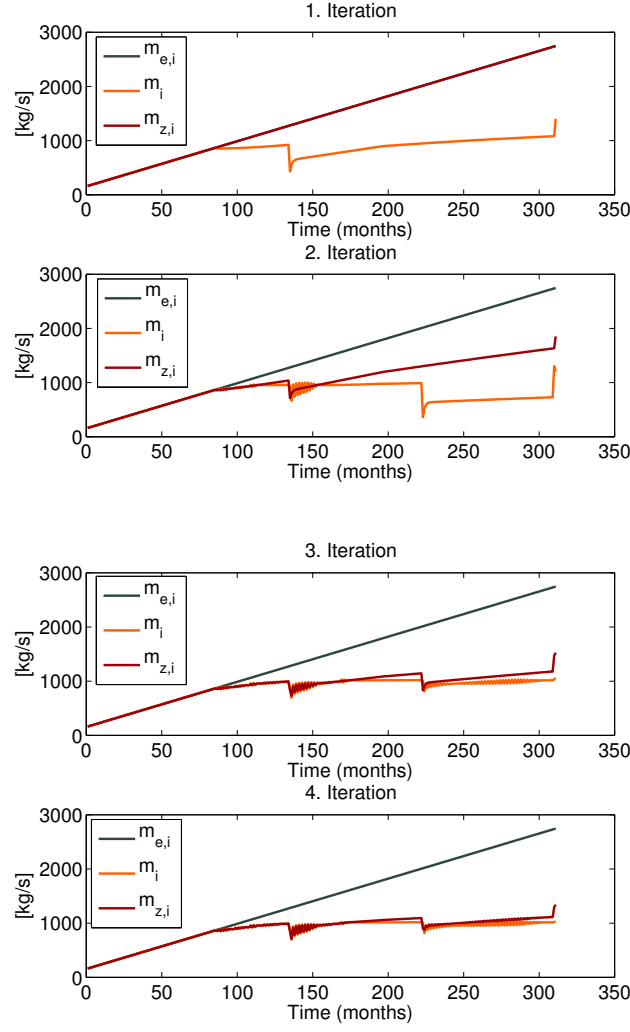
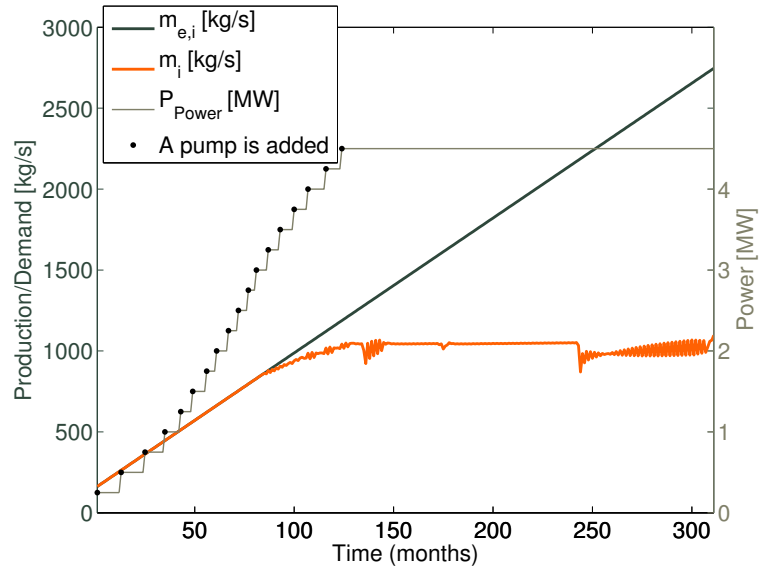
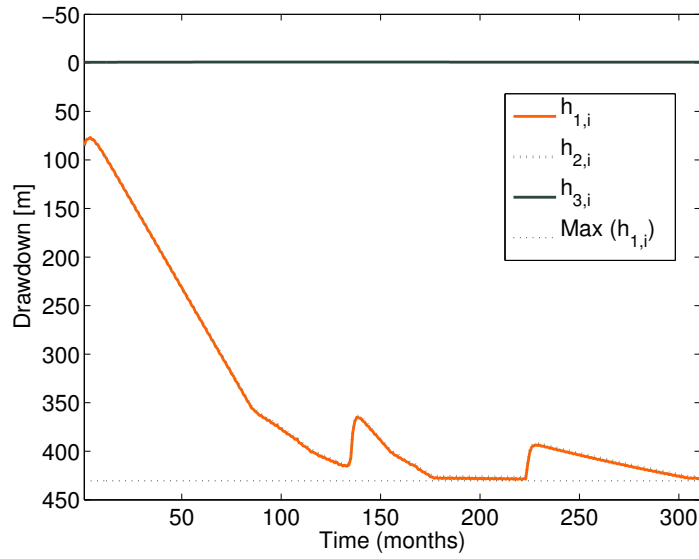


Figure 4.17: Graphical results for the updating development of the decision variable \dot{m}_i and the upper-bound \dot{m}_i^{over} . The updating algorithm replaces the upper-bound for iteration $k + 1$ with a mix from the solution from iteration k and the upper-bound from iteration k in such way that if the upper-bound is below the solution it moves up for the next iteration and if it is above the solution it moves down for the next iteration, see algorithm 2, see also section 3.2.6



(a)



(b)

Figure 4.18: Graphical results from a simple linear demand function using piecewise under-and over-estimators and updating algorithm see section 3.2.6

If the stopping criteria is relaxed to very small value the solutions does not change after the 4. iteration. See figure 4.19.

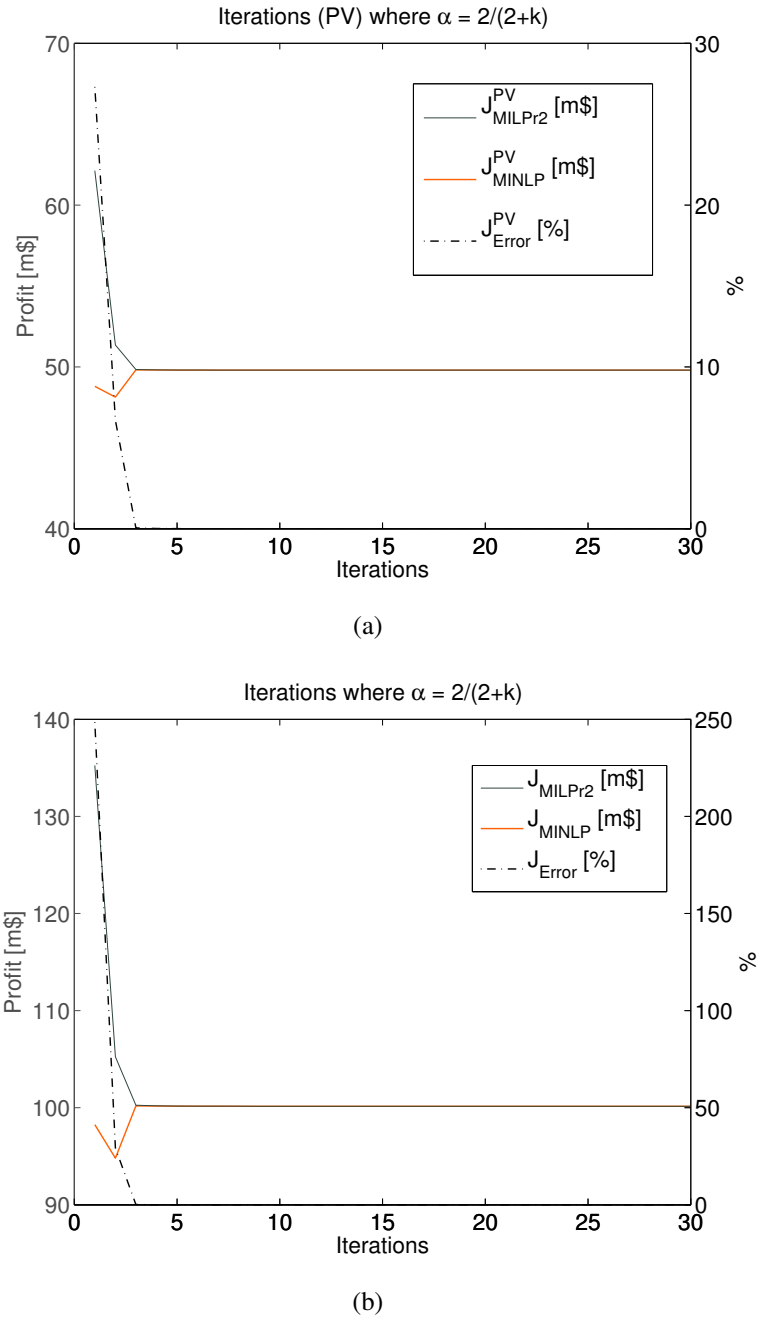


Figure 4.19: The figure above displays profit (with and without interest rate) as a function of 30 iterations, development of present value profit calculated with the MILP relaxation and then calculated non-linearly afterward. The figure below displays the same calculation but assumes no interest rate. The solution does not change after 4 iterations.

Since there is approximately 3% error between the objective value, applying linear piecewise approximation versus applying under-and over-estimators it is interesting to see if that is also the case with a slightly different demand function. E.g. like the one in example 4.1 that has a smaller increase in demand.

Example 4.7. The optimization is now performed with $m_{e,i} = \bar{m}_e + m_I t_i$ where $m_I = 25/12$.

$\mathcal{J}_{2,\text{Error}}^{\text{PV}}$	$\mathcal{J}_{2,\text{Error}}$	$\mathcal{J}_{\text{MILPr2}}^{\text{PV}}$	$\mathcal{J}_{\text{MINLP}}^{\text{PV}}$	$\mathcal{J}_{\text{MILPr1}}$	$\mathcal{J}_{\text{MINLP}}$
0.00031 %	0.0021 %	32,941,756 \$	32,941,653 \$	69,724,598\$	69,724,189 \$

Table 4.11: Results from optimization with demand function: $m_{e,i} = \bar{m}_e + m_I t_i$, $m_I = 25/12$. Optimized for $t_n = 311$ months. Starting time $t_1 = 1$.

Only one iteration is needed for an acceptable error. As can be seen in table 4.11 the solution identical to the solution from example 4.1. This suggests that both methods work very well if Constraint 2 from section 2.2.3 stays active for the most of the time period. If the demand function is however substantially increasing the relaxation with a piecewise linear function gives a better result.

4.2.3 Relaxation to NLP

The same problem is now solved with a NLP relaxation. That means that y is no longer an integer but a real number. It is known that $\mathcal{J}_{\text{MINLP}} \leq \mathcal{J}_{\text{NLP}}$, i.e. the same non-linear problem always gives an higher optimal solution if the integer is relaxed to a real number. The solution here is thus an upper-bound for the MILP relaxations.

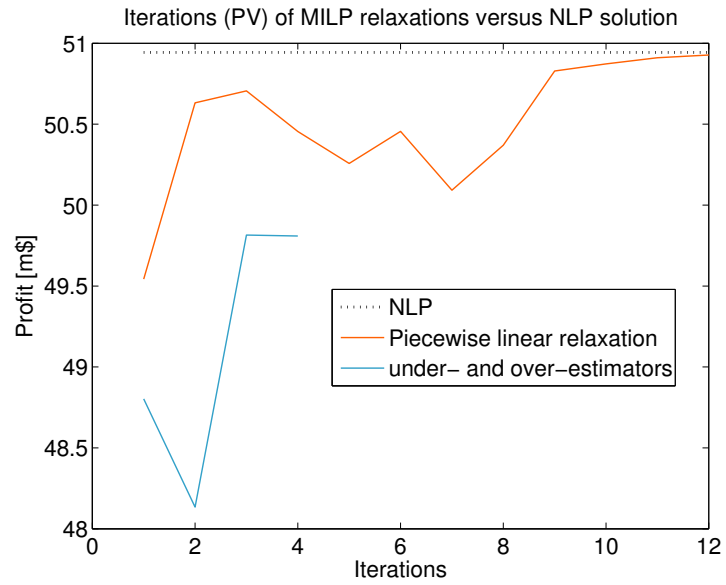
Example 4.8. The same demand function is used where $m_{e,i} = \bar{m}_e + m_I t_i$, $m_I = 100/12$. Table 4.12 displays the present value of the profit and the profit without interest rate.

$\mathcal{J}_{\text{NLPPr3}}^{\text{PV}}$	$\mathcal{J}_{\text{NLPPr3}}$
50,943,249\$	103,115,496\$

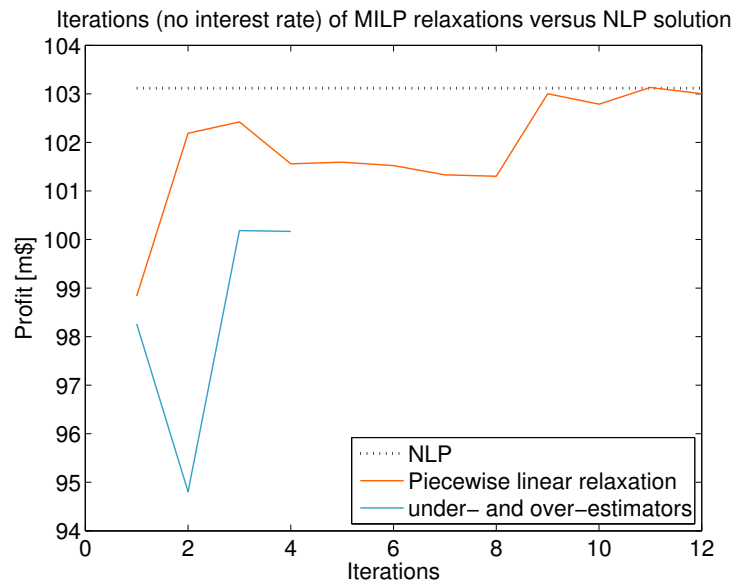
Table 4.12: Results from NLP optimization where the integer variable is relaxed to a real value with demand function: $m_{e,i} = \bar{m}_e + m_I t_i$, $m_I = 100/12$.

As can be seen in table 4.12 the optimal solution is almost identical to the solution for the MILP relaxation with a piecewise linear approximation (table 4.9, the difference is around 0.1%, see example 4.5. The solution from example 4.6 (table 4.10) is not as good or around 3% below the optimal here.

Figure 4.20 displays the NLP relaxation as an upper-bound to the MILP relaxations from example 4.5 and 4.6. This suggest very strongly that piecewise linear approximation does indeed give a local optimal solution to this problem.



(a)



(b)

Figure 4.20: Graphical result where the NLP solution is displayed as an upper bound for the MILP relaxations. Both for the present value that is optimized and assuming no interest rate.

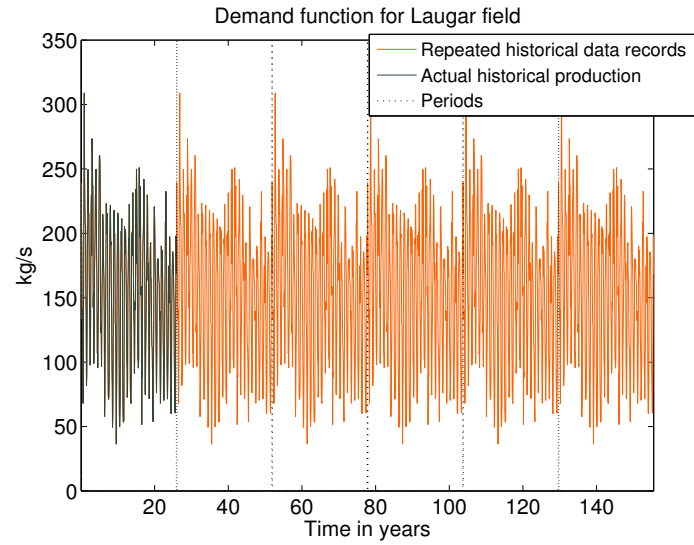
Now in considering what is a suitable method, the NLP relaxation yields the solution relatively faster than the piecewise linear approximation, but can not give a realistic timing and number of pumps. The NLP relaxation adds pumps to the system as value of y_i less than 0.5 at time step i , which means flooring and ceiling function can not be used to guess appropriate number and timing of pumps. The NLP relaxation can however be very useful if one only wants to know how many pumps are needed for certain time period without

worrying about when they should be added. This relaxation also worked for a period of 1800 months (around 150 years). But optimizing, e.g. 300 years of utilization did not give a result in 24 hours. The piecewise linear approximation is chosen to solve the problem using a more realistic demand function. That is the subject of the next two sections.

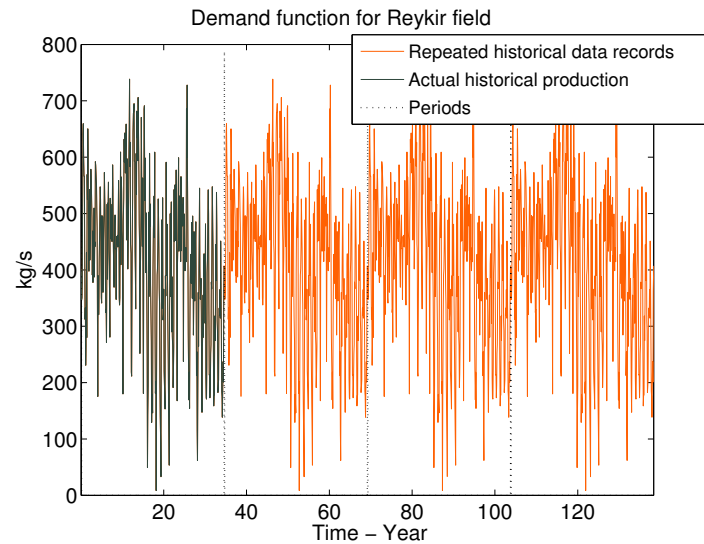
4.3 Optimization of long term utilization of a geothermal field under unchanged periodic demand

In this section the profit for long term utilization for Laugarnes field and Reykir field will be optimized using optimization model 2.28. The piecewise linear approximation, MILPr1, introduced in section 3.2.2 and numerically tested in section 4.2.1 will be applied here to account for the non-linearity in the model. The parameters from section 4.1.2 are used in the optimization for the underlying reservoir. The data resolution of the optimization is in months but often displayed graphically as an moving average in years for a better overview.

The demand function here, $m_{e,i}$, is simply repeated data records from each of the fields respectively. For Laugarnes field the known data record is repeated six times for 155 years of production and for Reykir field it is repeated four times for 138 years of production, see figure 4.21. No yearly trend will be considered.



(a)



(b)

Figure 4.21: The demand is historical production repeated periodically. Six times for Laugarnes field a) and four times for Reykir field b). Resolution of data is in months.

The scenario in this section, i.e. where profit is maximized and the demand is repeated historical records will be referred to as *Scenario 1* for Laugarnes field and *Scenario 2* for Reykir field. Other scenarios will appear in next section.

There are however other necessary parameters that need to be considered such as price of water and electricity and how much it costs to add a pump to the system. They will be introduced in the first subsection. Then an optimization and sensitivity analysis will be performed for the two fields respectively.

4.3.1 Necessary parameters for the optimization

Parameters for the optimization model are shown in table 4.13.

Parameter	Value	Units
$\dot{m}_{i=1}$	239	kg/s
C_{Water}	0.8695	\$/m ³
C_{Electric}	0.0805/3.6 · 10 ⁶	\$/J
C_{Pump}	150,000	\$
r	5.5 %	yearly rate

Table 4.13: Other parameters for the optimization model.

The initial demand, $\dot{m}_{i=1}$ is the first significant value from the Laugarnes field data. The values for C_{Water} , and C_{Electric} , are taken from price listings from Reykjavik Energy [Reykjavik Energy, 2011]. The quoted retail price for electricity is used unchanged in the modeling since in the scenario of selling hot water for district heating, one would have to pay full retail price for electricity like any other customer. In selling the water however it is very likely that a district heating firm buys the water at relatively low (wholesale) price and sells it to the customer for a higher (retail) price.

Statistic Iceland [Statistics Iceland, 2012] provides numbers for retail price versus wholesale price for electricity from 1980 to 2004, for the following companies: Rarik (both wholesale price and retail price), Landsvirkjun (wholesale price) and Orkuveita Reykjavíkur (retail price).

Assuming that the ratio between retail and wholesale price is somewhat similar for water, those numbers can be used to get an idea of what the appropriate water price might be. Those proportions range between 16% and 50% with an average around 40%, see figure 4.22.

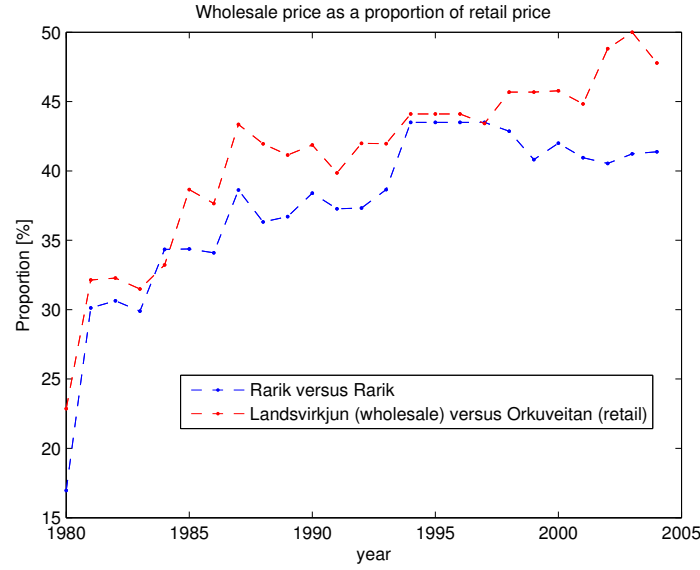


Figure 4.22: Wholesale price as a proportion of retail price, Rarik und Landsvirkjun, from [Statistics Iceland, 2012].

In addition, transportation and distribution of the water needs to be considered. Statistic Iceland [Statistics Iceland, 2012] also keeps track of information from 1983 - 2006 regarding production and primary energy versus losses in transport and distribution. Assuming that something similar applies to transporting and distribution of water plus operational cost, it is assumed here that the wholesale water price is not more than 25% of the retail price (C_{Water}), see table 4.13.

The value for C_{Pump} is the cost for adding a new pump. Those prices are of course dependent upon properties of the pumps, e.g, how much power they can handle and in what sort of condition they operate. Here, the price for one pump is assumed to be \$150,000 [Gunnarsson, 2012].

The interest rate is taken from a listing presented by the Central Bank of Iceland in November 2011. Interest rate here is considered to be a yearly based constant.

4.3.2 Laugarnes field

As mentioned before, demand for hot water from the Laugarnes field is generated by repeating the period for historical production data, six times for a period of 155 year (see figure 4.21a and 4.23a). The initial values for the reference points are the historical values representing demand, $m_{e,i}$, and the reference points for drawdown are calculated from the

demand with the LPM model. The optimization is executed for a period of 155.5 years.

The parameters used here can be viewed in table 4.14 and numerical results in table 4.15. For this scenario, production was able to follow demand quite accurately for the whole period, that resulted in a good linearization in the first iteration so the updating algorithm (Algorithm 2) was not needed here.

Parameters	Scenario 1: Values	Units
C_{Water}	$0.25 \cdot 0.8695$	$\$/\text{m}^3$
C_{Pump}	150,000	\$
C_{Elect}	$0.0805/3600000$	$\$/\text{J}$
r	5.5%	
Efficiency δ	10%, (Maximum drawdown is 751 m)	
Exergy, e_x	73,612 ($T_0 = 288\text{K}$, $T_i = 400.7\text{K}$)	J/kg
Number of years, n	155.5 years or 1866 months	
Trend in demand	0%	

Table 4.14: Parameters for Scenario 1.

Figure 4.23a displays the demand, $\dot{m}_{e,i}$, for the next 155.5 years and the optimized production \dot{m}_i . One pump is added in the beginning. According to the optimization result it doesn't pay off to add another pump. For that reason production follows demand exactly except in six different months where the production is 97 – 99% of the demand because of insufficient pumping capacity. This implies that production is in general not limited by financial or physical constraint for this scenario. The resolution of the data is on a monthly basis and for a better overview of the data, the demand and production are also represented as a *moving average* with a resolution in years, figure 4.23a.

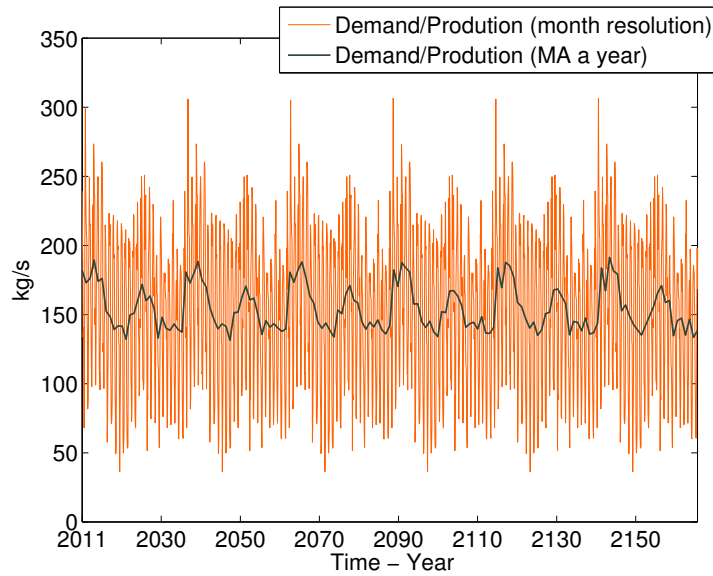
Results	Scenario 1	Units
Profit , PV_{Profit}	20,113,517	\$
Income , PV_{Income}	21,683,862	\$
Production , $PV_{\text{Production-linear}}$	2,017,029	\$
Production , $PV_{\text{Production-nonlinear}}$	2,017,029	\$
Pump Cost , PV_{Pump}	149,332	\$
Number of pumps , y	1	
Pump added	In month 1	
Maxium Drawdown	98.2 m	
Iterations	1	
Error, Equation 3.19	0.0000472 %	%

Table 4.15: Results for Scenario 1.

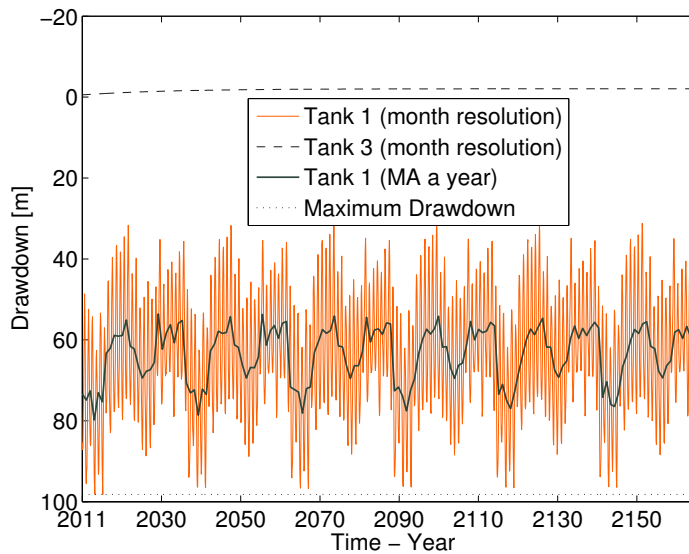
Figure 4.23b displays the development of drawdown in the tanks. Tank 1 ($h_{1,i}$) and tank 2 ($h_{2,i}$) fluctuate identically, and thus it is unnecessary to show tank 2 graphically

in figure 4.23b. It is however necessary to model the reservoir in terms of three tanks to obtain a good fit to the data. The drawdown fluctuates between approximately 35 m drawdown and 100 m drawdown and the trend in the drawdown is seemingly slightly upwards (less drawdown with time). For this period of data examined, there is a slight decline in the historical production data. That can be explained by the fact that after 1990 a new heat source, Nesjavellir, started production which resulted in reduced demand from Laugarnes area. Adding other geothermal sources is however beyond the scope here. The main concerns are decisions regarding production and installation of pumps, and the timing of these decisions in the next 100 to 200 years for a profitable and sustainable production.

Assuming demand for the next 155 year (like in this scenario) the system will remain in equilibrium and operation remains profitable and sustainable. One pump is installed in the beginning, the maximum drawdown is 98.2 m, see table 4.15 and figure 4.23b. Production plus pump cost account for only 8% of the profit, see figure 4.24a.



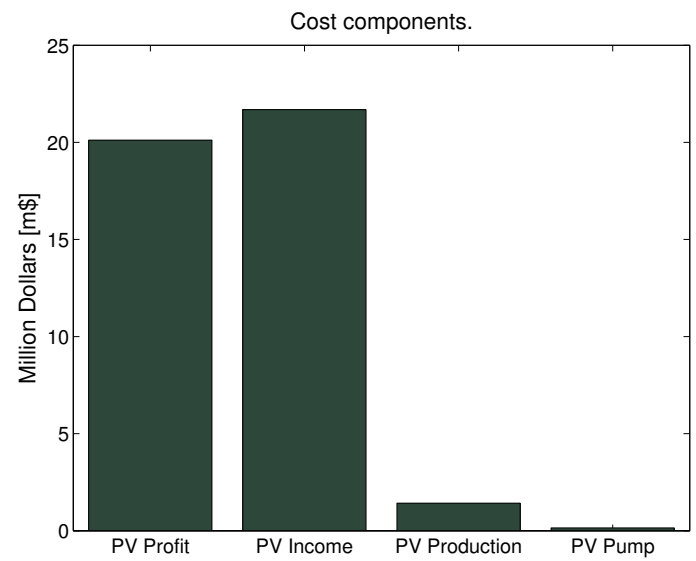
(a)



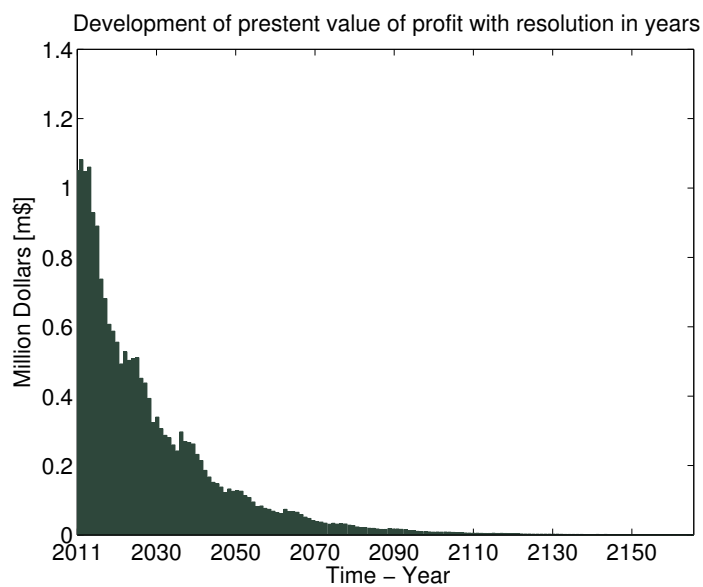
(b)

Figure 4.23: **Scenario 1.** Production and drawdown. Resolution is in months. MA stands for moving average a year. Figure 4.23a displays production and demand for the next 155.5 years. Figure 4.23b displays the development of drawdown in two of the three tanks (this is a three tank model, see description of the LPM model in chapter 2.1).

The present value is substantially greater for the first 40 to 60 years (see figure 4.24b) where it then becomes almost zero in approximately 110 years. In terms optimizing the present value of profit, it might be practical to optimize a shorter period of time. The objective of this work is however to look at long term utilization. This will be considered in next section.



(a)



(b)

Figure 4.24: **Scenario 1.** Figure 4.24a graphical display of the cost components. Figure 4.24b displays development of Present Value (PV) of profit for 155.5 years, resolution in years.

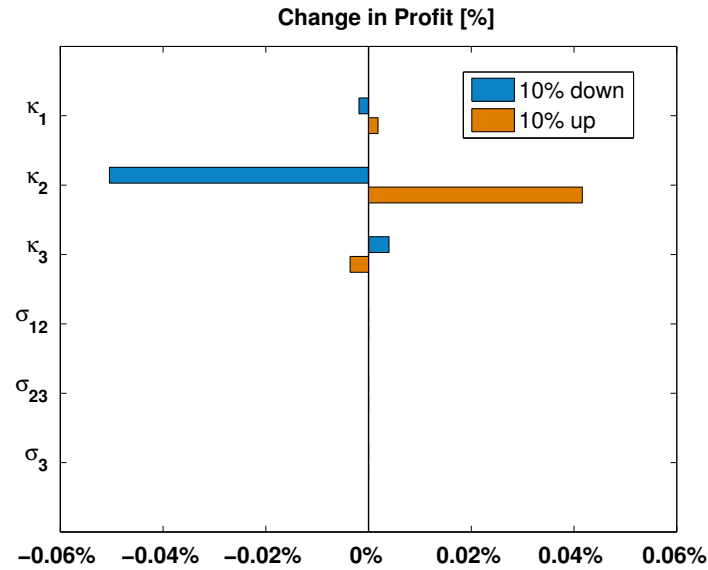
4.3.3 Sensitivity analysis for Laugarnes field

It is of interest to see how much a small change in the parameters discussed in chapter 4.1 affect the profit.

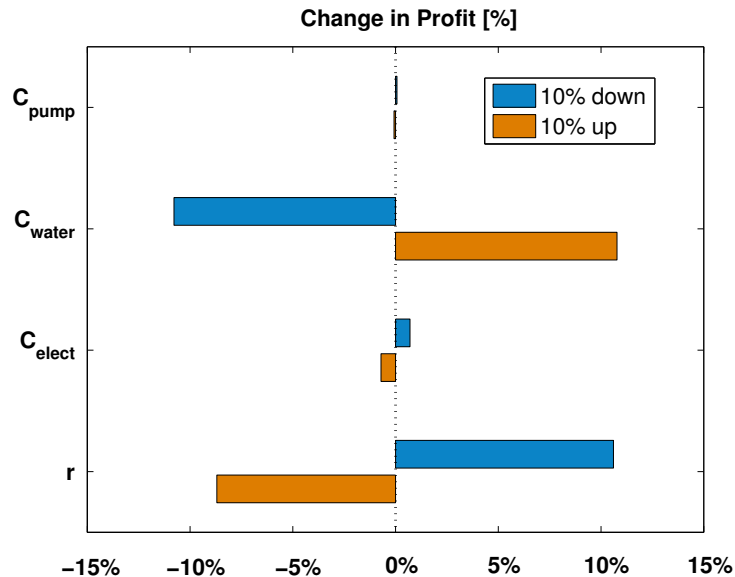
Figure 4.25 shows the sensitivity of the profit with regards to variation of the lumped

model parameters κ , σ (see table 4.3 for the three-tank open model for Laugarnes) and the economical parameters from table 4.13. The values of the parameters are varied by 10% and the result from the optimization of each variation (the present value of profit) compared.

A 10% change in the LPM parameters affects the profit by less than 1%. That could



(a)



(b)

Figure 4.25: **Scenario 1.** Sensitivity analysis. Figure 4.25a displays proportional change in profit considering 10 % increase/decrease in the parameters from the Lumped Parameter Model (LPM). Figure 4.25b displays proportional change in Profit considering 10 % increase/decrease in the economical parameters. Please note the different scales on the two figures above.

suggest that the data fit does not need to be extremely accurate, or like according to [Satman et al. \[2005\]](#), a 3-tank open model is not suitable here since the confidence interval range of the parameters is too high. That could indicate that working with a different type of lumped parameter model, e.g. a model with only 2-tanks as in [Satman et al. \[2005\]](#) is more suitable. It does however not change the fact that the best match to the data was obtained for a 3-tank open model.

The profit is most sensitive to the price received for water and interest rate. Those parameters are considered to be constants here, which they are of course not in reality. Those results indicate the need to model this problem with stochastic interest rate and price.

4.3.4 Reykir field

Demand for hot water in Reykir field was generated by repeating the period for historical production data, four times for a period of 138 year (see figure 4.21b and 4.26a). The initial values for the reference points are the demand, and the reference points for drawdown are calculated from the demand with the LPM model. The optimization is executed for 138 years.

Parameters	Scenario 2: Values	Units
C_{Water}	$0.25 \cdot 0.8695$	$\$/\text{m}^3$
C_{Pump}	150,000	\$
C_{Elect}	$0.0805/3600000$	$\$/\text{J}$
r	5.5%	
Efficiency δ	10%, (Maximum drawdown is 286 m)	
Exergy, e_x	28,069 ($T_0 = 288\text{K}$, $T_i = 354.7\text{K}$)	J/kg
Number of years, n	138 years or 1660 months	
Trend in demand	0%	

Table 4.16: Parameters for Scenario 2.

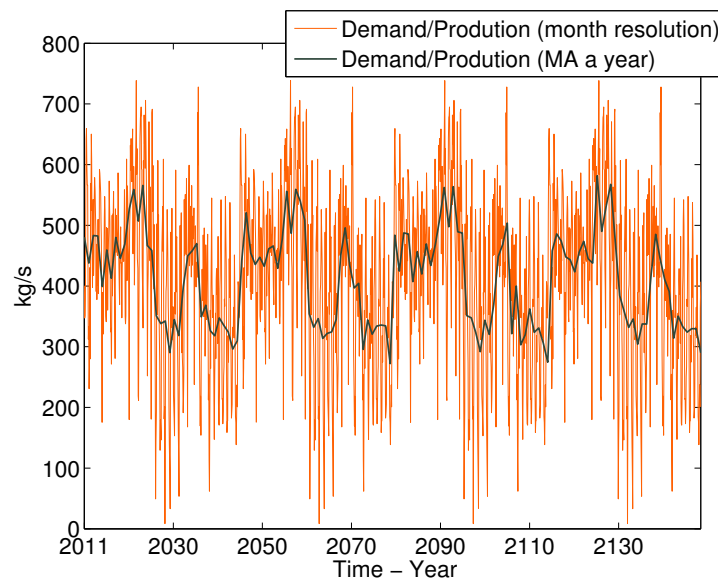
The parameters used here can be viewed in table 4.16 and numerical results in table 4.17. Like for Laugarnes field, the production was able to follow demand very accurately for the whole period, that results in a very good linearization in the first iteration so the updating algorithm (Algorithm 2) was also not needed here.

Figure 4.26a displays the demand, $\dot{m}_{e,i}$, for the next 138 years and optimized production \dot{m}_i . Three pumps are needed, two added in the first year and one in year 10. Production follows demand exactly for the whole period and for that reason is the error between linear and non-linear zero. Reykir field produces a substantially bigger amount of water than Laugarnes field. It is thus not surprising that more pumps are added in Reykir field.

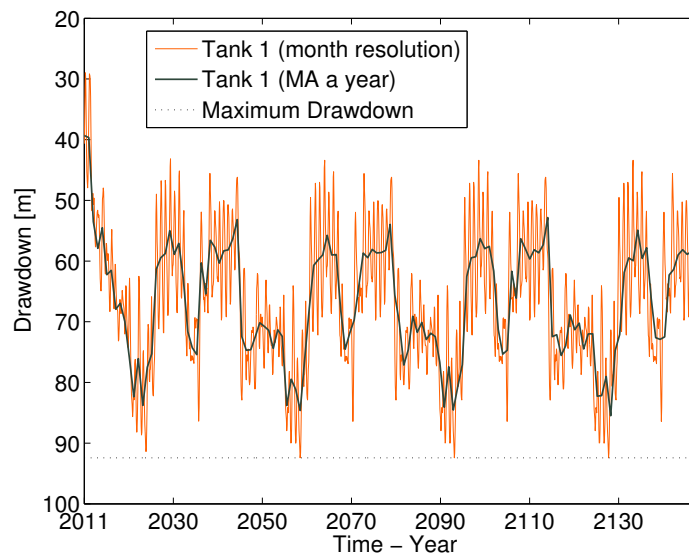
Results	Scenario 2	Units
Profit , PV_{Profit}	53,287,276	\$
Income , PV_{Income}	57,287,228	\$
Production , $PV_{\text{Production-linear}}$	3,621,250	\$
Production , $PV_{\text{Production-nonlinear}}$	3,621,250	\$
Pump Cost , PV_{Pump}	378,702	\$
Number of pumps , y	1	
Pump added	In month 1, 7 and 130 (year 10)	
Maxium Drawdown	92.2 m	
Iterations	1	
Error, Equation 3.19	0 %	%

Table 4.17: Results for Scenario 2.

Like for Scenaro 1, for a better overview of the data, the demand and production are also represented as a moving average with a resolution in years, figure 4.26a.



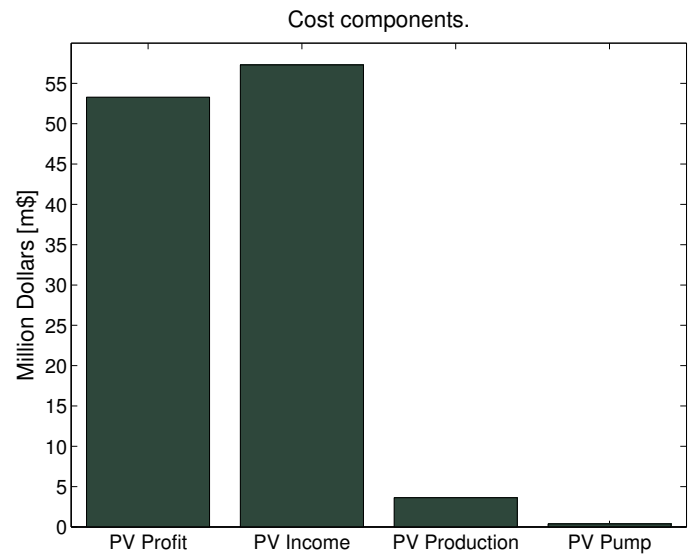
(a)



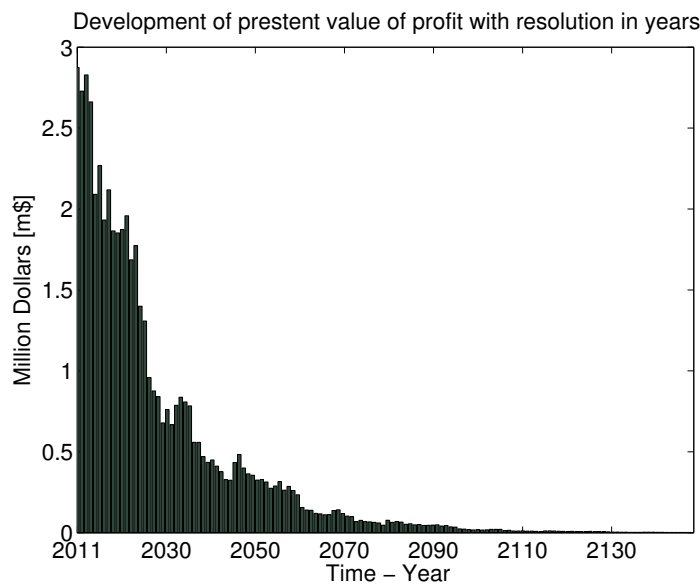
(b)

Figure 4.26: **Scenario 2.** Production and drawdown. Figure 4.26a displays production and demand for the next 138 years. Demand is periodic and based on historical production data, repeated four times. Production can not exceed demand. In this scenario the production follows the demand exactly. Figure 4.26b displays the development of drawdown in the two tanks (this is a two tank model see chapter 2.1).

The maximum drawdown is 92.4 m, see table 4.17 and figure 4.26b. Production plus pump cost are around 7.5% of the profit (figure 4.27a) which is slightly less than for Laugarnes field.



(a)



(b)

Figure 4.27: **Scenario 2.** Figure 4.27a graphical display of the cost components. Figure 4.27b displays development of Present Value (PV) of profit for 155.5 years, resolution in years.

Here the drawdown fluctuates between approximately 45 m drawdown and down to around 90 m drawdown and the trend in the drawdown is actually very slightly downwards. It can be seen from the fact that the maximum drawdown occurs around year 117 for Reykir field but in year 5 for Laugarnes field. For a longer period of production this does not effect the drawdown in Reykir field all that much. An optimization was also conducted for 280 years of production (with the same demand scheme) for Reykir field and the maximum drawdown moved from 92.2 m to 94.2 m. It can thus be assumed that

with this sort of demand scheme, the system will remain in equilibrium (for an open LPM model) and operation remains profitable and sustainable.

Like for Laugarnes field the present value is substantially greater for the first 40 to 60 years (see figure 4.27b) where it then becomes almost zero in approximately 110 years. So when the profit value of profit is maximized it is important to take this behavior into account. It might be practical to choose a shorter period of time or simple another objective function which is the subject of next section 4.4. First a sensitivity analysis will be conducted for Scenario 2.

4.3.5 Sensitivity analysis for Reykir field

Small change in the LPM parameters did not effect the profit for Scenario 2 at all. This does not support that a 2-tank model is more suitable than a three-tank model. This rather supports the idea that the parameter fit might not need to be very accurate.

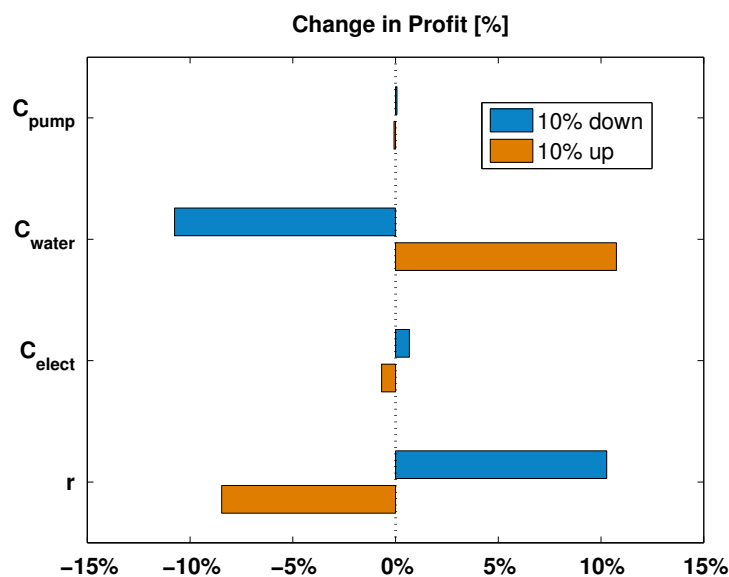


Figure 4.28: **Scenario 2.** Sensitivity analysis. Proportional change in profit considering 10 % increase/decrease in the economical parameters.

Like for Laugar field the profit is most sensitive to the price received for water and interest rate, which indicates that stochastic methods might be appropriate where price for water and interest rate are stochastic parameters. Such modeling is out the scope but is already being considered as future work.

4.4 Optimization of long term utilization under annually increased demand

In this section three harvesting strategies will be examined for the two fields Laugarnes and Reykir. Here, the optimization will be performed by considering an *annual increase in demand*. As in the last section, the piecewise linear approximation (sections 3.2.2 and 4.2.1) will be applied and the parameters from section 4.1.2 are used for the underlying reservoir. For further understanding of the behavior of the model and improvement suggestion for the harvesting strategies, three different objective functions and in some cases slightly different constraints will be considered and altogether *14 scenarios* are compared, see summary in table 4.18.

Scenarios

Field	Scenario	Objective	Constraint added to model	Constraint removed from model
Laugarnes	Scenario 1	$\max PV_{\text{Profit}}$		
Reykir	Scenario 2	$\max PV_{\text{Profit}}$		
Laugarnes	Scenario 3	$\max PV_{\text{Profit}}$		
	Scenario 4	$\max \text{Profit} _{r=0}$		
	Scenario 5	$\min \sum_{i=1}^n (\dot{m}_{e,i} - \dot{m}_i)$	$\text{Profit} \geq 0$	
	Scenario 6	$\min \sum_{i=1}^n (\dot{m}_{e,i} - \dot{m}_i)$	$\text{Profit} \geq 0$	$h_{1,t} \leq h_1^{\max}$
	Scenario 7	$\min \sum_{i=1}^n (\dot{m}_{e,i} - \dot{m}_i)$	$\text{Profit} \geq 0$ $y_i \leq 5$	
Reykir	Scenario 8	$\max PV_{\text{Profit}}$		
	Scenario 9	$\max \text{Profit} _{r=0}$		
	Scenario 10	$\min \sum_{i=1}^n (\dot{m}_{e,i} - \dot{m}_i)$	$\text{Profit} \geq 0$	
	Scenario 11	$\max PV_{\text{Profit}}$		$h_{1,t} \leq h_1^{\max}$
	Scenario 12	$\max \text{Profit} _{r=0}$		$h_{1,t} \leq h_1^{\max}$
	Scenario 13	$\min \sum_{i=1}^n (\dot{m}_{e,i} - \dot{m}_i)$	$\text{Profit} \geq 0$	$h_{1,t} \leq h_1^{\max}$
	Scenario 14	$\min \sum_{i=1}^n (\dot{m}_{e,i} - \dot{m}_i)$	$\text{Profit} \geq 0$ $y_i \leq 5$	

Table 4.18: Summary of the 14 operation scenarios compared in this work. Scenarios 1 and 2 have to do with Laugarnes and Reykir fields, not assuming annually increases demand. Scenario 3-7 have to do with Laugarnes under annually increased demand and different objective functions and/or constraints and scenarios 8-14 have to do with Reykir field under annually increased demand and different objective functions and/or constraints.

Scenarios 1 and 2 were thoroughly introduced in last section. In *scenarios 3* (Laugarnes) and *8* (Reykir) the present value of profit is maximized exactly according to equation 2.28 in chapter 2. The only thing that differs from scenarios 1 and 2 is the demand as annual increase is assumed here.

The objective function for Scenario 1,2,3 and 8 is:

$$PV_{\text{Profit}} = \mathcal{J}_{\text{MILPr1}}^{\text{PV}} \quad (4.3)$$

The present value of profit has been introduced as *the objective function* in this work. The result is however biased in terms of when financial decisions are taken as they are more important today than 30 years from now, see e.g. figures 4.24 and 4.24. It is thus interesting to exclude the interest rate factor and maximize the profit without an interest rate. It is interesting to see if optimizing without an interest rate is more beneficial for the customer for long term production.

In *scenarios 4* (Laugarnes) and *9* (Reykir) profit is maximized again, according to equation 2.28 but the interest rate is set to zero ($r = 0$).

The objective function for scenario 4 and 9 is:

$$\text{Profit}|_{r=0} = \mathcal{J}_{\text{MILPr1}} \quad (4.4)$$

The third objective function focuses on the consumers point of view only. It is unacceptable for the consumer when demand for energy can not be fulfilled. It is however not always economical to meet demand and focusing on meeting substantially increased demand can increase the risk of unsustainable production and financial loss.

The objective proposed *minimizes* the sum of deviation between demand and production and adds the constraint that profit can not go below zero. Thus, in *scenarios 5* (Laugarnes) and *10* (Reykir) the sum of the deviation between demand and production is minimized (resolution is in months).

The objective function is thus:

$$\mathcal{J}^{DEV} = \sum_{i=1}^n (\dot{m}_{e,i} - \dot{m}_i) \quad (4.5)$$

Constraint added:

$$\text{Profit}|_{r=0} \geq 0 \quad (4.6)$$

In *scenarios 10* and *11*, that both account for Reykir field, the present value of profit and the profit with $r = 0$ are maximized respectively by taking out the sustainability constraint, constraint 3 (equation 2.25).

In *scenarios 6* (Laugarnes) and *12* (Reykir) the sum of deviation (equation 4.5) between demand and production is minimized without a sustainability constraint.

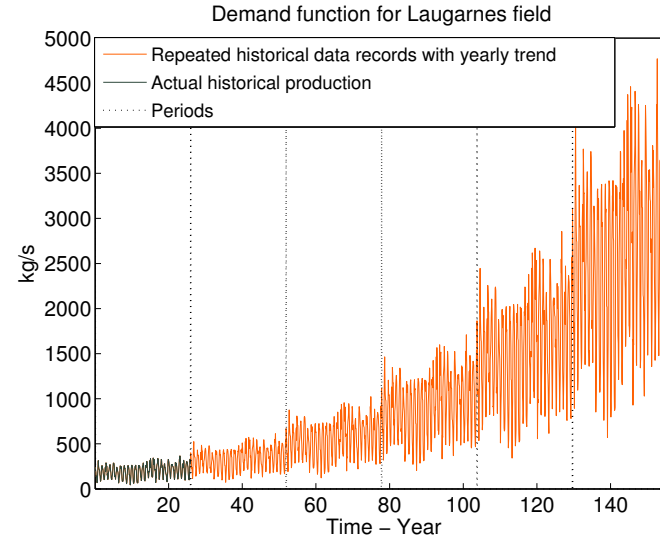
In *scenarios 7* (Laugarnes) and *14* (Reykir) the sum of deviation is minimized again. Now a constraint is added to restrict how fast production capacity can be increased. I.e., a maximum of 5 pumps are allowed to be added in one month.

Constraint added:

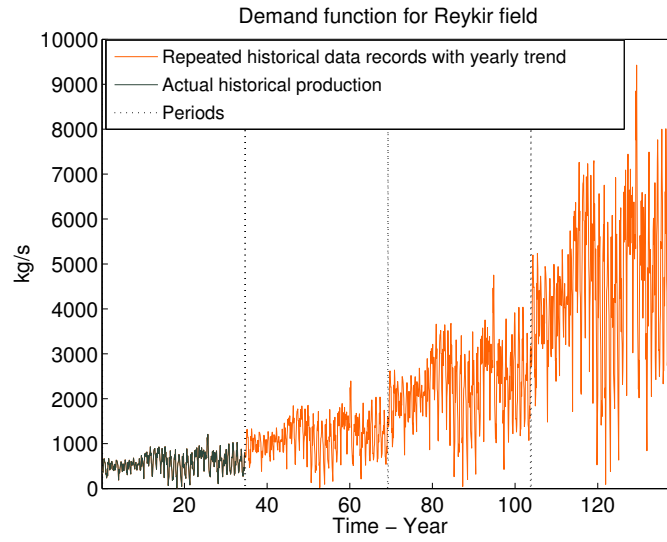
$$y_i \leq 5 \quad (4.7)$$

Demand function

According to the National Energy Authority of Iceland [[National Energy Authority of Iceland, 2012](#)] annual demand from low temperature fluid increased 1.78% per year from 1990 - 2010. All of the scenarios here are assumed to have an operational disruption accounting for 2% annual increase in demand as they are optimized over considerable long time periods. The demand is generated by repeating the historical data (and adding a yearly trend) six times for Laugarnes (155 years) and four times for Reykir (138 years) like in last section, see figure 4.29. In reality such an increase in production will very likely require a higher numbers of new wells, although it is no way of knowing what the technology in 100 years can bring.



(a)



(b)

Figure 4.29: The demand is historical production repeated periodically with a yearly trend of 2%. Resolution of data is in months.

Results from scenarios

Results from the scenarios can be viewed in tables 4.19 and 4.20. The tables display the main conclusions from the optimization for comparison. The objective functions compared include: present value of profit, PV_{Profit} (equation 2.16), *profit* (equation 2.16 with $r = 0$) and the *sum of deviation between demand and production* (equation 4.5). *Shortfall in production* is calculated to get a better overview of how well the demand can be fulfilled. Shortfall in production is one minus the sum of production divided by sum of

demand

$$\text{Shortfall in production} = 1 - \frac{\sum_{i=1}^n m_i}{\sum_{i=1}^n m_{e,i}} \quad (4.8)$$

Regarding the sustainability consideration the *maximum drawdown* and the *sustainability constraint* are compared. Maximum drawdown is simply maximal value of $h_{1,i}$ calculated after the optimization has been performed. This is to account for cases where either sustainability is not reached or the sustainability constraint has been removed from the model. The sustainability constraint was introduced in section 2.2.4.

The tables also display the *timing and frequency of adding pumps*, number of *iteration* for the optimization and the *error* (equation 3.19) between the non-linear part of the model and the linear approximation to account for the performance of the algorithm used for the optimization. Objectives and added/removed constraint are in bold script in the tables for each scenario. Graphical display of the results can be viewed in figures 4.30 to 4.39.

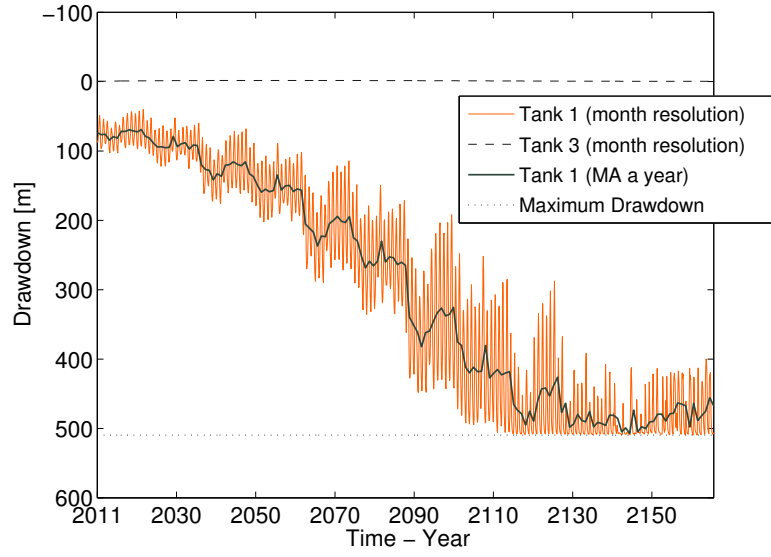
4.4.1 Laugarnes field

Laugarnes						
	(Scenario 1)	Scenario 3 Max PV _{Profit}	Scenario 4 Max Profit _{r=0}	Scenario 5 Min Deviation	Scenario 6 Min Deviation without sustainability constraint	Scenario 7 Min Deviation with max 5 pumps in one month
PV _{Profit}	(20.11 m\$)	28.92 m\$	24.26 m\$	8.61 m\$	0.63 m\$	28.37 m\$
Profit _{r=0}	(164.63 m\$)	510.6 m\$	512.36 m \$	471.4 m\$	298.4 m\$	478 m\$
Sum of deviation	(24 kg/s)	592363 kg/s	499177 kg/s	295839 kg/s	0	295828 kg/s
Shortfall in production	(0.00008)	0.31	0.27	0.15	0	0.15
Maximum drawdown	(98.2 m)	510 m	617 m	751 m	1658 m	751 m
Sustainability constraint	(751 m)	751 m	751 m	751 m	-	751 m
Number of Pumps	(1)	24	34	145	292	111
Frequency of pumps added	(1)	16 times	2 times	2 times	3 times	23 times
Max no. of pumps in one month	(1)	3	33	144	199	5
Iterations	(1)	6	10	5	1	4
Error	(0.00005%)	0.38 %	1.22 %	0.45 %	0	0.82 %

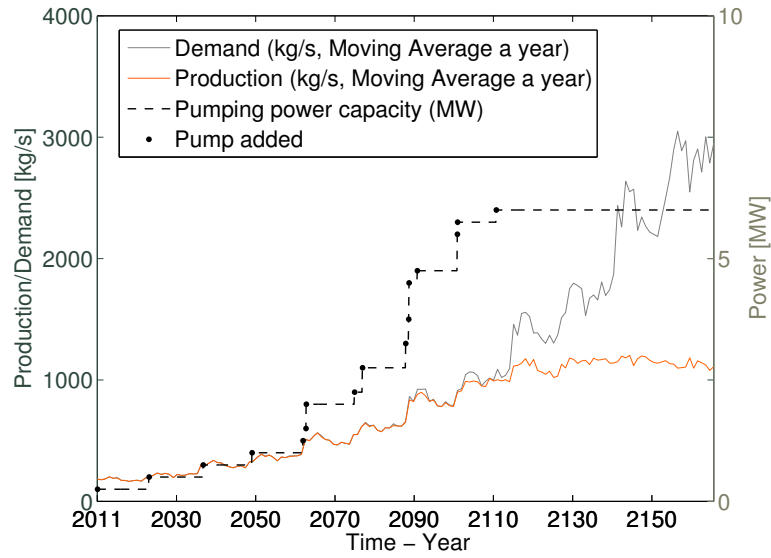
Table 4.19: Numerical results from optimization. The objective functions compared are present value of profit, profit (with $r = 0$) and sum of deviation between demand and production (equation 4.5). Shortfall is calculated by equation 4.8. Maximum drawdown is maximal value of $h_{1,i}$ calculated after the optimization has been performed. The table also displays timing and frequency of adding pumps, number of iteration for the optimization and the error (see equation 3.19) between the linear and non-linear objective and or constraint. Objectives and added/removed constraint are in bold script in the tables for each scenario.

For Laugarnes field 6 scenarios were compared. The approximation algorithm (algorithm 2) is considered to have an acceptable performance for all of the scenarios, 1 to 10 iterations and an error between 0 and 1.22%. Scenario 1 was covered in section 4.3 but

is presented parenthesis in table 4.19 for comparison purposes. Figure 4.30 display the results from scenario 3 where there is an *economically implicit sustainability constraint* (maximum drawdown) in the system that lies above the sustainability constraint itself ($h_1^{max}=751$ m) as it is apparently not optimal to pump deeper than 510 m for this scenario (see figure 4.30a). This also means that after around 100 years of production demand can not be met anymore, see 4.30b. The model is originally calculated in month resolution, but results are displayed in yearly (moving average) resolution as well.



(a) Drawdown

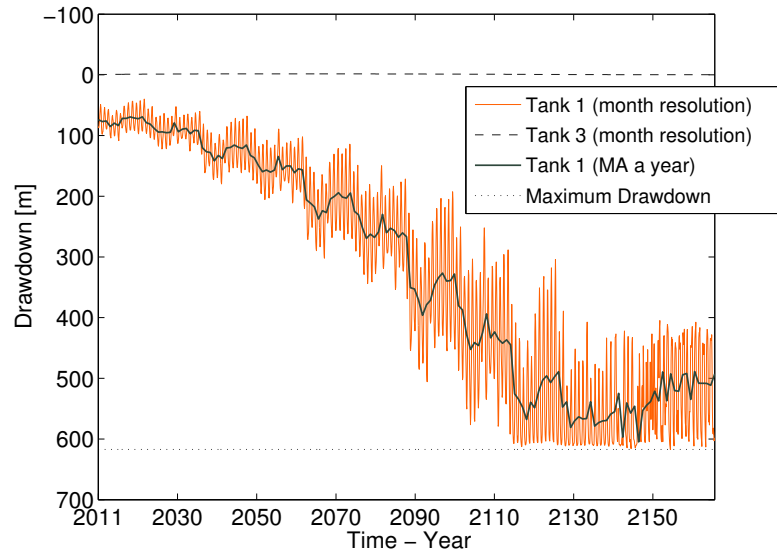


(b) Production/demand

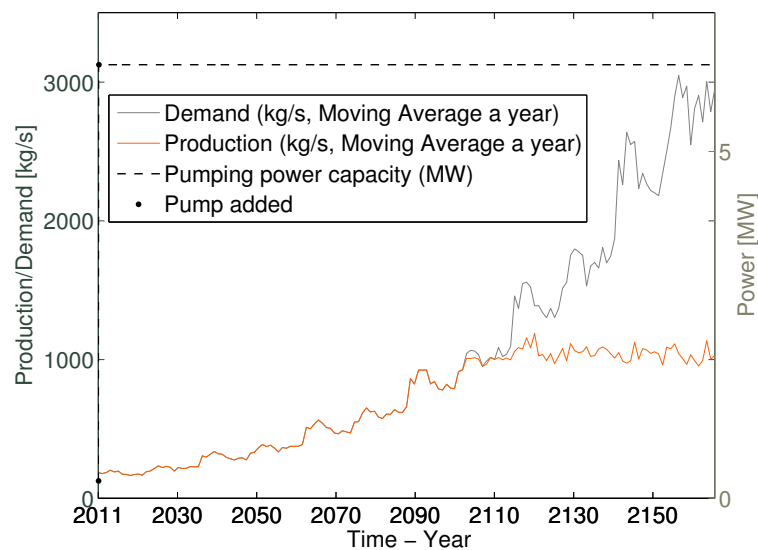
Figure 4.30: **Scenario 3.** Drawdown and production for Laugarnes. Profit Maximized (PV). Figure 4.30a displays the maximum drawdown, average yearly drawdown, and drawdown in month resolution. Figure 4.30b displays average production a year, average demand a year and frequency of adding a pump.

Scenario 4 where the profit (assuming no interest rate) was maximized implies that demand can be fulfilled slightly better than in Scenario 3 as the sum of deviation is smaller and the maximum drawdown bigger. The solution is unrealistic in terms of when the pumps are added. All the 33 pumps are installed in the first year. This occurs since an interest rate is not included in the objective function so it does not matter when the pumps are installed (just that they are installed). Here maximum drawdown is at 617 m

that is also above the calculated sustainability limit. See results for scenario 4 in figure 4.31.



(a) Drawdown



(b) Production/demand

Figure 4.31: **Scenario 4.** Drawdown and production for Laugarnes. Profit Maximized (assuming no interest rate). Figure 4.31a displays the maximum drawdown, average yearly drawdown, and drawdown in month resolution. Figure 4.31b displays average production a year, average demand a year and frequency of adding a pump.

Scenario 5 minimizes the sum of deviation between demand and production. Demand is fulfilled longer and the sustainability constraint for Laugarnes is active at the end of the period, see figure 4.32a. The operation returns profit, even though it was not maximized.

It is noticeable (table 4.19) that the difference (scenario 3 and 4 versus scenario 5) between the present value of profit is bigger than the difference between the profit without an interest rate.

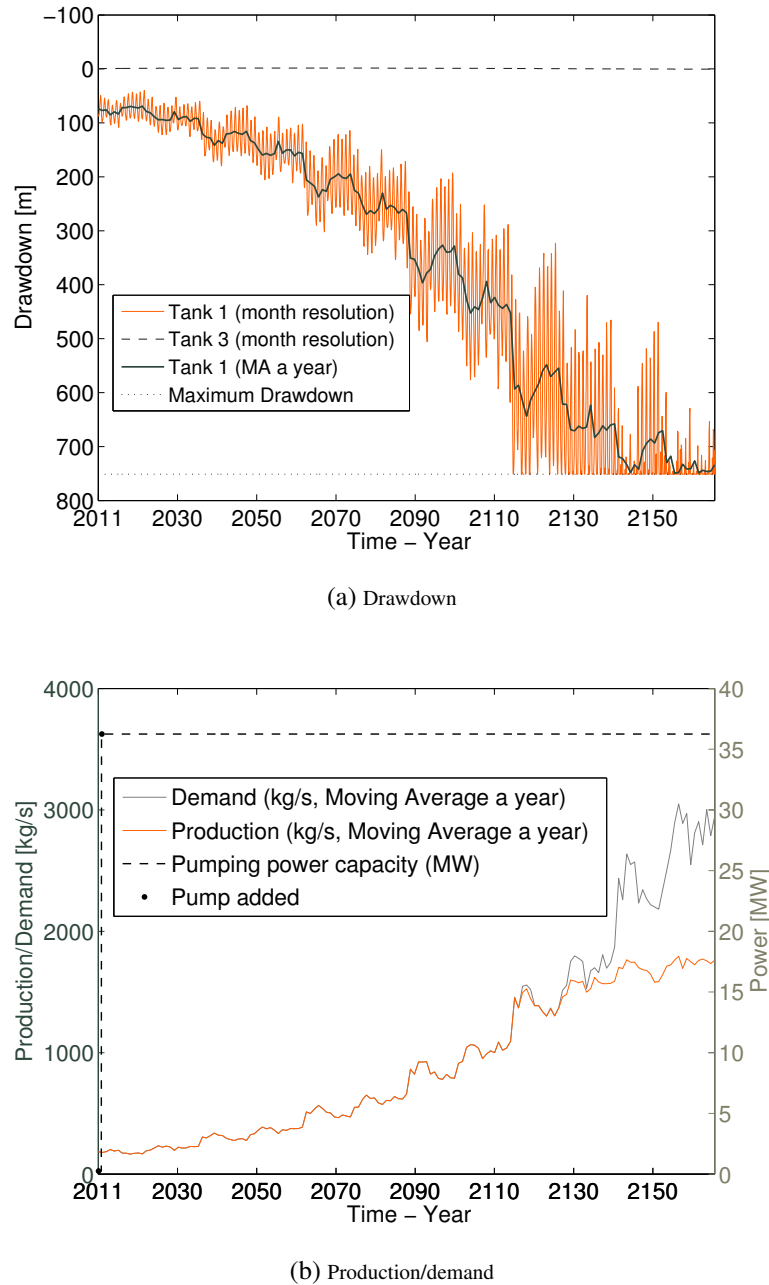
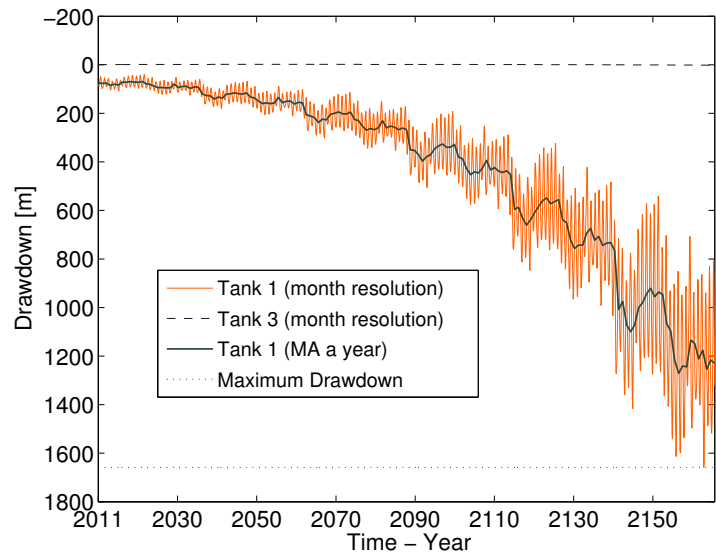


Figure 4.32: **Scenario 5.** Drawdown and production for Laugarnes. Deviation minimized.

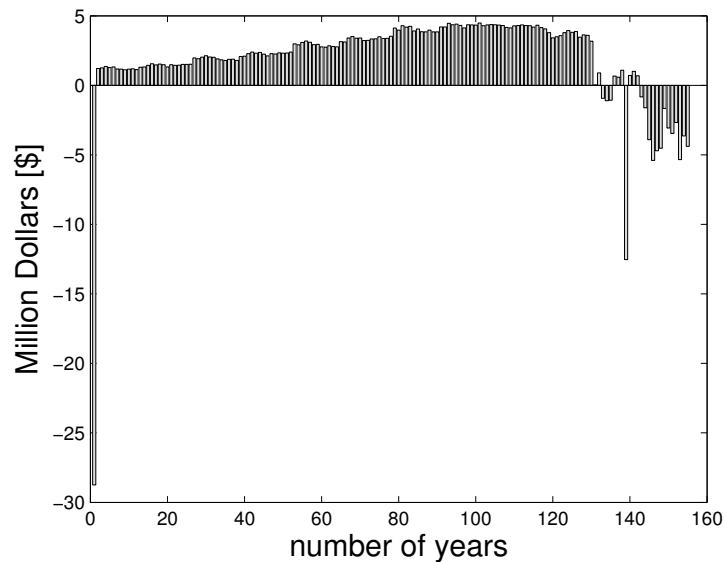
Figure 4.32a displays the maximum drawdown, average yearly drawdown, and drawdown in month resolution. Figure 4.32b displays average production a year, average demand a year and frequency of adding a pump.

For scenario 6, the sum of deviation is minimized but without a sustainability constraint to see whether there is a point where the profit goes to zero. In this case the demand is

fulfilled completely, but at the cost that drawdown goes down to 1658 m and the profit has increased but is not zero. The cash flow of the profit (with no interest rate) for this scenario is displayed in figure 4.33b and shows that after approximately 130 years the profit will start to become negative. If a longer time period were to be optimized, production would need to be slowed down eventually to sustain a profitable production.



(a) Drawdown

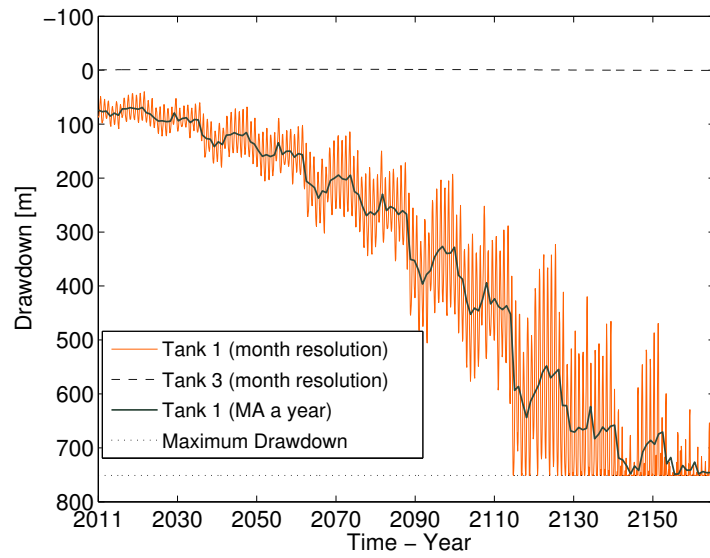


(b) Cash flow of profit assuming no interest rate

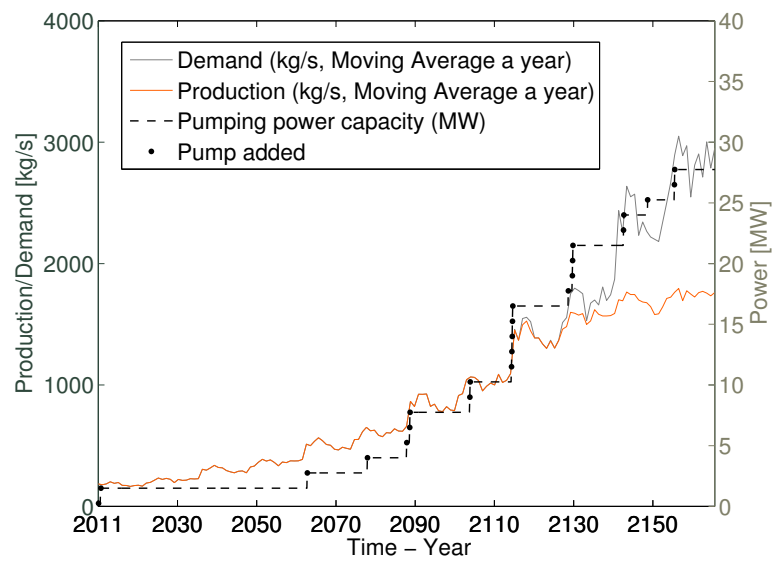
Figure 4.33: **Scenario 6.** Drawdown and cash flow of profit without an interest rate for Laugarnes. Deviation was minimized (no sustainability constraint).

Figure 4.33a displays the maximum drawdown, average yearly drawdown, and drawdown in month resolution. Figure 4.33b displays the cash flow of the profit. Without a sustainability limit the cash flow start to become negative in about 130 years of production.

Scenario 7 attempts to mix scenarios 3 and 5 together as scenario 3 has a more acceptable present value and scenario 3 more acceptable shortage of production. The deviation is minimized but the number of pumps that can be added in one time step is constrained to 5 ($y_i \leq 5$). In scenario 3, the maximum number of new pumps in one time step is 3. This scenario could be considered as sustainable production from the consumer's point of view, with a step-wise increase in production capacity. By doing this the present value of the profit becomes almost the same as when it was maximized where the demand is fulfilled for a considerably longer period of time, see and compare figures 4.34b and 4.30b.



(a) Drawdown



(b) Production/demand

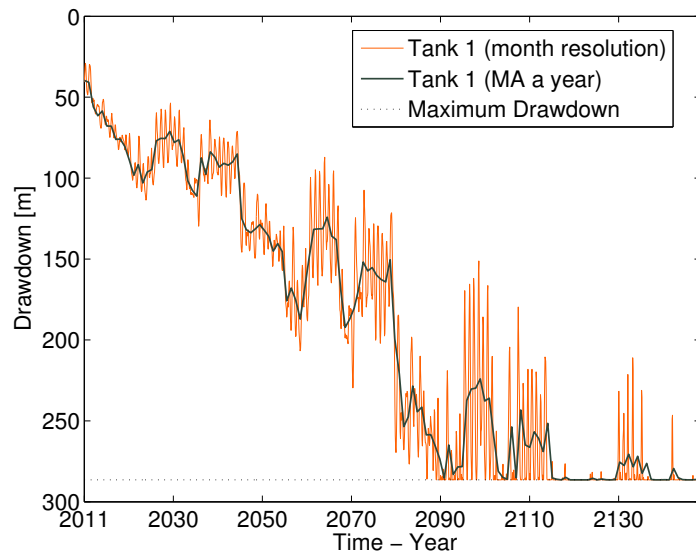
Figure 4.34: **Scenario 7.** Drawdown and production for Laugarnes. Deviation minimized ($y(i) \leq 5$, only 5 pumps can be added in each month). Figure 4.34a displays the maximum drawdown, average yearly drawdown, and drawdown in month resolution. Figure 4.34b displays average production a year, average demand a year and frequency of adding a pump.

4.4.2 Reykir field

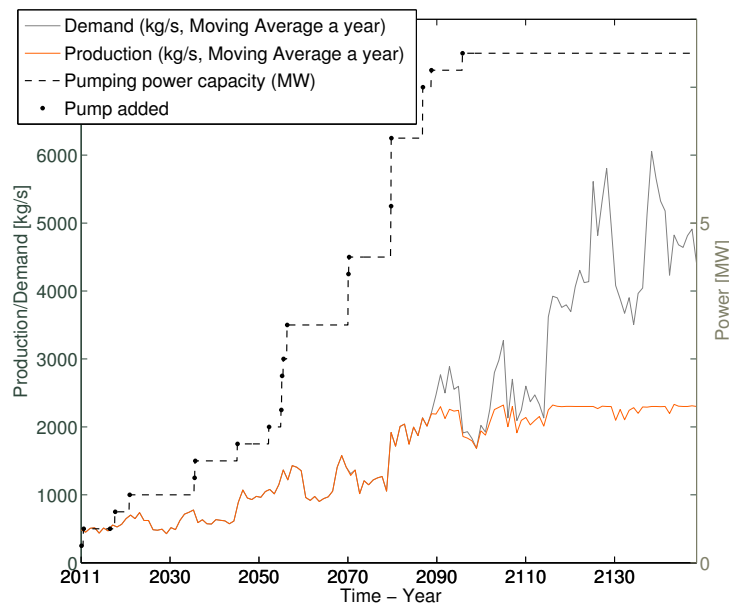
	Reykir							
	(Scenario 2)	Scenario 8 Max PV_{Profit}	Scenario 9 Max Profit $_{ r=0}$	Scenario 10 Min Deviation	Scenario 11 Min PV_{Profit} without sustainability constraint	Scenario 12 Max Profit without sustainability constraint	Scenario 13 Min Deviation without sustainability constraint	Scenario 14 Min Deviation with max 5 pumps in one month
PV_{Profit}	(53.29 m\$)	77.31 m\$	73.14 m\$	64.97 m\$	77.41 m\$	63.07 m\$	31.67 m\$	76.98 m\$
Profit $_{ r=0}$	(374.31 m\$)	1137.7 m\$	1137.9 m\$	1127.7 m\$	1250.2 m\$	1258.6 m\$	1208.2 m\$	1132.8 m\$
Sum of deviation	(0)	1003012 kg/s	1000920 kg/s	999102 kg/s	247457 kg/s	259978 kg/s	0 kg/s	999102 kg/s
Shortfall in production	0	0.28	0.29	0.28	0.07	0.07	0	0.28
Maximum drawdown	(92.2 m)	286 m	286 m	286 m	527 m	556 m	876 m	286 m
Sustainability constraint	(286 m)	286 m	286 m	286 m	-	-	-	286 m
Number of Pumps	3	30	30	106	91	102	324	72
Frequency of pumps added	3 times	20 times	2 times	4 times	34 times	2 times	3 times	16 times
Max no. of pumps in one month	1	4	32	80	23	101	309	117
Iterations	1	4	4	4	3	3	1	5
Error	0 %	0.54 %	0.55 %	0.56 %	0.67 %	0.98 %	0%	0.55%

Table 4.20: Numerical results from optimization. The objective functions compared are present value of profit, profit (with $r = 0$) and sum of deviation between demand and production (equation 4.5). Shortfall is calculated by equation 4.8. Maximum drawdown is maximal value of $h_{1,i}$ calculated after the optimization has been performed. The table also displays timing and frequency of adding pumps, number of iteration for the optimization and the error (see equation 3.19) between the linear and non-linear objective and or constraint. Objectives and added/removed constraint are in bold script in the tables for each scenario.

For Reykir field 8 scenarios were compared. The approximation algorithm has an acceptable performance for all of the scenarios, 1 to 4 iterations and an error between 0 and 0.98%. For scenarios 8 to 10 the sustainability constraint becomes active after about 80 years of production, that also results in a similar number for shortage in production. The graphical results are thus very similar and only displayed for Scenario 8, see figure 4.35.



(a) Drawdown

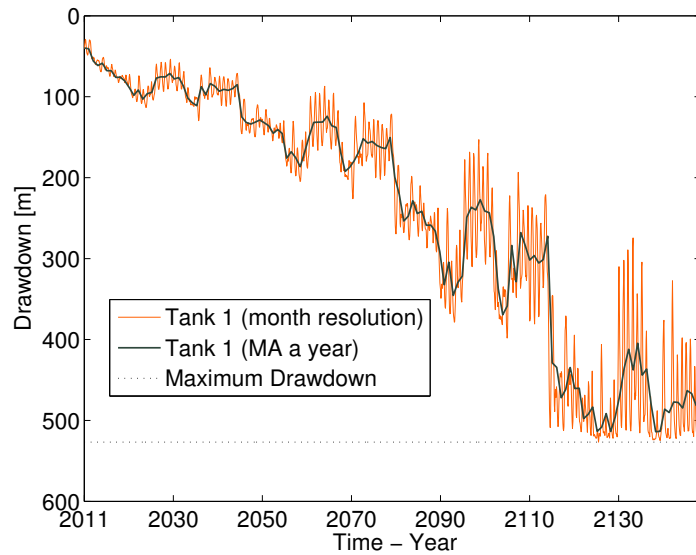


(b) Production/demand

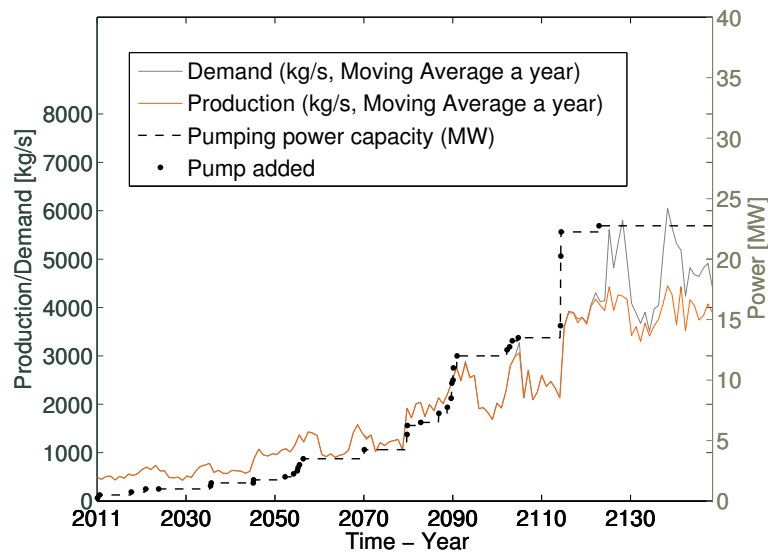
Figure 4.35: **Scenario 8.** Drawdown and production for Reykir. Present value of profit maximized. The result is very similar for scenario 9 and 10. Figure 4.35a displays the maximum drawdown, average yearly drawdown, and drawdown in month resolution. Figure 4.35b displays average production a year, average demand a year and frequency of adding a pump.

To find out if the Reykir field also has what can be called an *economical implicit sustainability* constraint scenarios 8, 9 and 10 are repeated without a sustainability constraint. In maximizing the present value of profit without a sustainability constraint (Scenario 11) there is an economically implicit sustainability constraint (maximum drawdown) at 527 m

(figure 4.36a), which is essentially consistent with the result in Scenario 3 for Laugarnes field. The sum of deviation is substantially smaller which is obvious since the sustainability is ignored. What is interesting though is that from a profit point of view it doesn't matter if maximum drawdown is at 286 m or 527 m.



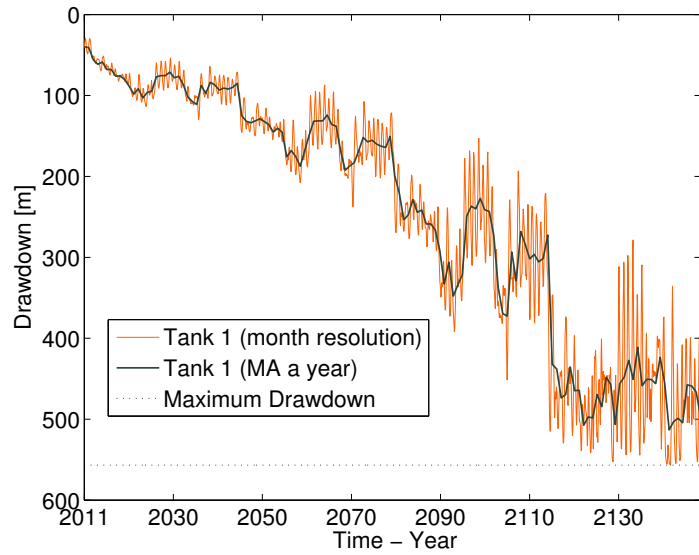
(a) Drawdown



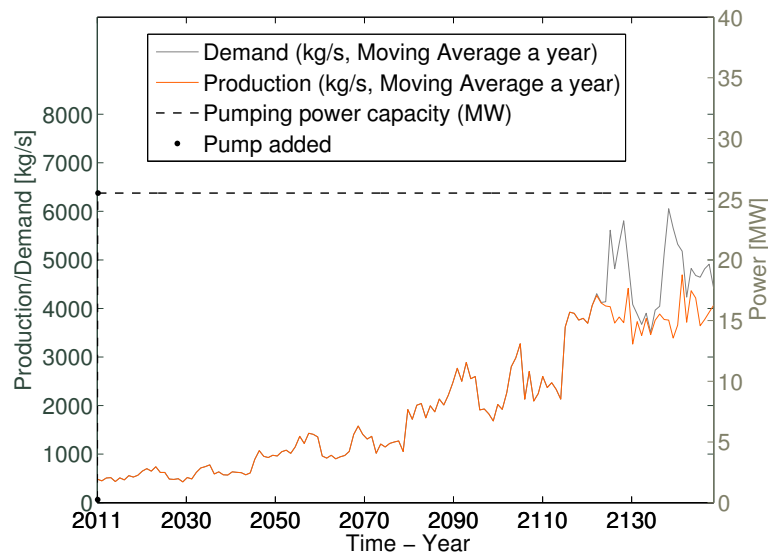
(b) Production/demand

Figure 4.36: **Scenario 11.** Drawdown and production for Reykir. Present value of profit maximized (no sustainability constraint). Figure 4.36a displays the maximum drawdown, average yearly drawdown, and drawdown in month resolution. Figure 4.36b displays average production a year, average demand a year and frequency of adding a pump.

Scenario 12 maximizes non present value of profit without sustainability constraint. Like in scenario 4 the maximum drawdown lies deeper, but for this case the sum of deviation is still slightly bigger. Pumps are all added in the first year.



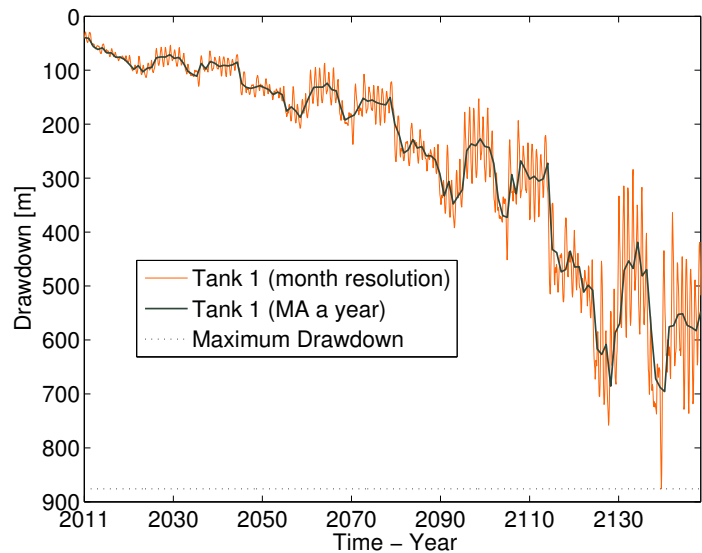
(a) Drawdown



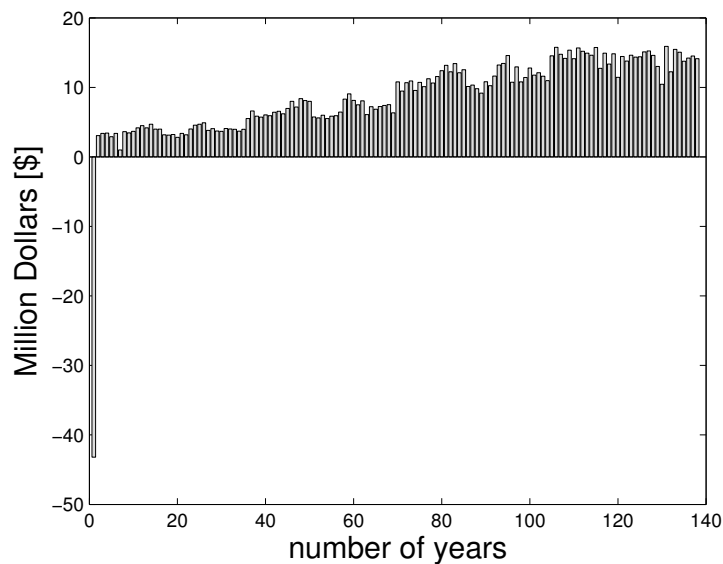
(b) Production/demand

Figure 4.37: **Scenario 12.** Drawdown and production for Reykir. Profit maximized (no sustainability constraint). Figure 4.35a displays the maximum drawdown, average yearly drawdown, and drawdown in month resolution. Figure 4.35b displays average production a year, average demand a year and frequency of adding a pump.

Scenario 13 minimizes the sum of deviation without a sustainability constraint. Like for scenario 6 for Laugarnes field the demand is completely fulfilled. The maximum drawdown is 876 m versus 1658 m for Laugarnes field, see figure 4.38.



(a) Drawdown

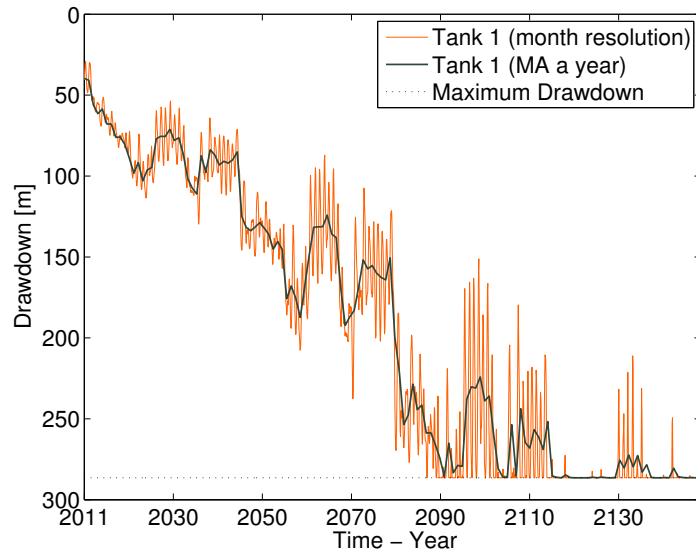


(b) Cash flow of non-present value

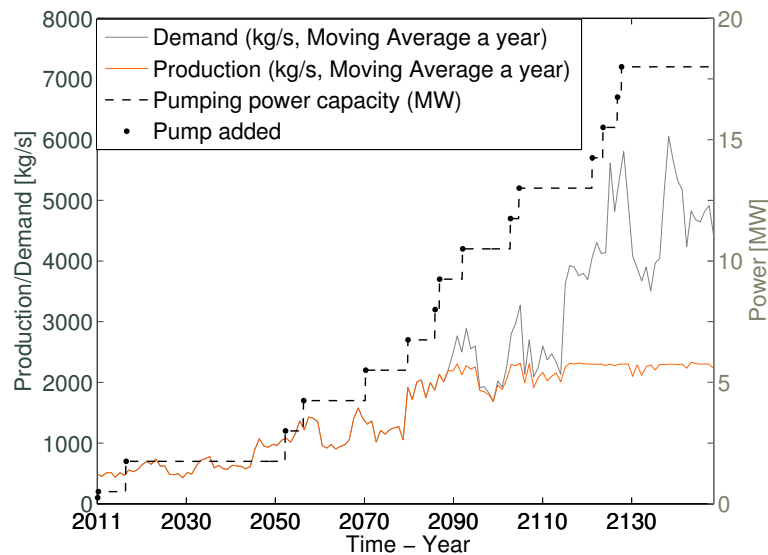
Figure 4.38: **Scenario 13.** Drawdown and cash flow of non-present value for Reykir field. Deviation minimized (no sustainability constraint). Figure 4.38a displays the maximum drawdown, average yearly drawdown, and drawdown in month resolution. Figure 4.38b displays the cash flow of the non present value.

As in scenario 7, the sum of deviation is minimized in scenario 14, and a constraint added to ensure that no more than 5 pumps can be added in one time step. This is con-

sistent with the result in scenario 7. As the profit is almost as high as if it were maximized. The difference is greater in comparison of those scenarios for Laugarnes field, since the the production is severely constrained by the sustainability constraint, see figure 4.39a.



(a) Drawdown



(b) Production/demand

Figure 4.39: **Scenario 14.** Drawdown and production for Reykir. Deviation minimized (constraint added: $y_i \leq 5$, only 5 pumps can be added in each month). Figure 4.34a displays the maximum drawdown, average yearly drawdown, and drawdown in month resolution. Figure 4.34b displays average production a year, average demand a year and frequency of adding a pump.

Chapter 5

Conclusion

5.1 Discussion

Optimization methods

In the attempt to solve a non-convex MINLP problem, three optimization methods were essentially compared. Two linear relaxations (MILPs) and one relaxation from an integer to a real number (NLP relaxation). The MILP relaxation for the piecewise under- and over-estimators gave a poorer optimal than the piecewise linear approximation. It has not been mathematically proved (as far as the author knows) that those methods give a local optimal for problems in a relaxed form of non-convex MINLPs. The relaxation to NLP is therefore very important. It applies the SQP algorithm to solve non-convex NLP and has been proved to give a local optimal. The solution of the NLP relaxation is therefore an upper bound for the local optimal. The solution from the linear approximation matches the solution from the NLP relaxation so it must be a local optimal. The reason why the under- and over- estimator method did not give a better solution is unknown. The under- and over-estimator method was however conducted at the end of this work as a comparison to the other MILP relaxation and thus not thoroughly investigated whether a better solution could be obtained. Selection of the upper bound and lower bound could have been more sophisticated as the algorithm for updating the bounds. The upper bound are chosen from data and the lower bound zero. The updating process behaves in such manner that it updates the upper bound only. It would be interesting to vary the lower bound to see if a better solution or a direction to a better solution can be found.

Parameter estimation

In estimating the reliability of using lumped parameter modeling (LPM) for predicting changes in a low-temperature reservoir it is very important to have a satisfactory data set as well as it is important to validate such calibration. Due to the simplicity of the LPM, it can not always simulate a reservoir. This has now been done, and as seen from the results in section 4.1 a sufficient validated fit can not always be acquired.

The data fit for Ellidaar and Reykjahlid could for example not be validated and thus not be optimized in the manner described in this thesis. On the other hand, it could be argued that the fit for Ellidaar field was actually rather good, the data was simply unfortunate for the validation applied in this work since the production decreased substantially for the period validated.

The reason the fit for Reykir and Reykjahlid as one field was not chosen for the optimization is that even though it was a closed model (which would give an interesting comparison) the last tank (κ_3 , see table 4.4) was so big that the it would have taken a longer period of time and more increase in production, in other words, a more unrealistic scenario to see the difference between the three tank open and closed system. It was thus considered more appropriate to choose Reykir with a two tank open model and hope for a slightly smaller calculation time in the optimization, which then turned out to be negligible.

The sensitivity analysis showed that the accuracy of the LPM parameters is maybe not that important if the present value of profit is optimized as 10% change did not effect the profit much. It could be interesting to see how other parameters change, e.g., how the maximum drawdown changes in terms of change in the LPM parameters by applying sensitivity analysis for annual increase in demand and without the sustainability constraint and also by minimizing the deviation.

Optimization of long term utilization

The benefit from applying optimization instead of calculating drawdown directly from production is that it gives the opportunity to consider different operational scenarios and identify results that otherwise would be overlooked, for example the economically implied sustainability constraint.

Two geothermal fields were chosen for the optimization and different objectives and constraint functions compared. The piecewise linear approximation returns acceptable solutions for all of the scenarios. This suggests that the approximation algorithm is a good solution method for such problems.

In comparing the results from the optimization for Reykir field and Laugarnes field it is immediately noticeable that the sustainability constraint for Reykir lies at 286 m versus 751 m for Laugarnes field. The average temperature at Reykir field is lower than at Laugarnes field (table 4.1) resulting in a shallower sustainability constraint as it is temperature dependent, see also section 2.2.4. For this reason Scenarios 9, 10 and 11 show a very similar result. Whether it is maximizing profit or minimizing deviation between demand and production the production is severely constrained by the shallow sustainability constraint. Scenario 11, 12 and 13 are thus essentially more comparable with scenarios 3, 4, 5.

The main difference between optimizing present value of profit and profit with no interest rate lies in which time steps the pumps are added. The optimal for profit with no interest rate is rather unrealistic as all of the pumps are bought in the first year. From the other end it is of course theoretically financially beneficial for a future energy firm holder if all of the pumps have already been bought.

The economically implied sustainability constraint lies in the range from 510 m to 617 m (see tables 4.19 and 4.20) for both of the fields when the profit is optimized. This is mostly due to the fixed prices used in the model, C_{water} and C_{Elect} , see values in nomenclature. In [Sigurdardottir et al. \[2012\]](#) it was showed that the economically implied sustainability constraint lies deeper for a lower value of C_{water} .

In minimizing deviation between demand and production it is noticeable in all cases (with or without sustainability constraint) that the difference between present value of profit (compared to when profit is maximized) is bigger than the difference between profit without interest rate. That is due to the fact that the price doesn't matter in this scenario, as long as it stays above zero. All the pumps are added in the first year creating poorer present value and a rather unrealistic result.

When minimizing deviation without a sustainability constraint the maximum draw-down for Laugarnes becomes almost double the maximum drawdown for Reykir. That can easily be explained by the fact that the central part of the reservoir, κ_1 from the fit in

section 4.1.2, is substantially bigger for Reykir than for Laugarnes. Minimized deviation without sustainability constraint for Reykir does not suggest a negative cash flow in the end of the period as was the case with Laugarnes, see figures 4.33b and 4.38b, hence the different sizes of the reservoirs. The Laugarnes reservoir empties faster but should recover faster as well do to a relatively high resistor value σ_{12} , see table 4.3.

By adding a constraint that ensures that only 5 pumps can be added in one time step as deviation is minimized the most promising solution is obtained. In this way the needs of the customer and the firm holder today are met since those scenarios (scenarios 5 and 12) have the highest present value of profit and the lowest (sustainable) production shortage at the same time. This suggests that step-wise increased production capacity is the best strategy.

Reservoir and operational optimization models connected directly

The LPM is a quite effective, but a simplified approach to simulate a geothermal reservoir. For such a long term production it would have been practical to assume cooling effect and re-injection. Re-injection is relatively simple to integrate, for example by adding an extra inflow tank to the system. Cooling effect could be modeled by a non-isothermal LPM [Onur et al., 2008].

Connection the LPM to an operational optimization model is important since it can give information otherwise not obtained and multiple different operational scenarios can be tested. This model is however a very simplified version of the reality since various cost are neglected (e.g. drilling, maintenance and transportation). It is also debatable whether it is realistic to maximize profit for such a long term utilization since the present value of profit eventually converges to zero, and whether it is practical in reality to have a draw-down over 300 m in the wells. If profit would not have been maximized this economically implied sustainability constraint would not have appeared. It is also impossible to know what technology will bring in terms of realistic drawdown after more than 100 year. Using a fixed increase in demand is also unrealistic since it is not a fixed number and it is rather unlikely that it will keep increasing so much for more than the next 100 years. The number used (2% increase a year) is however an average of the increase in demand in the last 20 years in Iceland, and it is a known fact that industries will be depending more and more on geothermal energy in the future.

5.2 Perspectives and future work

The optimization of utilizing a geothermal reservoir in a sustainable manner where reservoir and operational optimization models are connected directly, is as far as the author knows a relatively unexplored field. This is essentially a mixed integer non-linear dynamic optimization problem that is converted into a mixed-integer non-linear optimization (MINLP) problem.

In order to solve an MINLP within an acceptable time frame a relaxation of the problem is needed. Three methods were introduced tested and compared. The one proposed here is an iteration algorithm for a piecewise linear approximation. A successful, relatively fast iteration algorithm for this case has been developed and the problem successfully solved.

The algorithm has been generalized by applying it to more than one data set (e.g. Laugarnes field and Reykir field) and comparing various operational scenarios. The optimization results show consistency between the data sets. For a long term sustainable utilization, the best strategy seems to be to *minimize the deviation between expected demand and production capacity by adding pumps and/or wells and increase production capacity in relatively small steps*.

The model was most sensitive to change in interest rate and price of water. Price of electricity also plays a role, and in reality those parameters are not constants, but rather time dependent variables that follow a certain trend and have a stochastic behavior. Such considerations could also be included in the modeling.

Since for this model, it is relatively easy to implement various scenarios, it can in practice be used to fit the specific needs of anyone who wants to implement it, e.g. energy companies and/or contractors. For such a practical usage it would also be important to apply adaptive optimization where the parameter estimation and the optimization is always updated as new data arises.

It would also be interesting to apply this model on more geothermal fields (using e.g. closed LPM models) and even optimizing a network of geothermal fields with subsystems. E.g., modeling Reykjavik as a network of the geothermal fields considered in this work.

Other future studies could include using statistical data for the interest rate, price of water and electricity since they are essentially stochastic variables. It would be interesting to try to solve the problem with Monte Carlo simulations or other stochastic optimization methods. Another variation already briefly discussed is not to consider installing a pump but rather a well with a pump and consider maintenance costs. Adding a well would cost more but increase the total production capacity more.

Finally it would be interesting to apply such modeling on high-temperature systems. The optimization is very likely to be applicable but the lumped parameter model is strictly developed for single phase conditions. It would thus be interesting to integrate this sort of optimization application to a another geological model that could simulate the behavior of a high-temperature reservoir.

Bibliography

- Axelsson, G. (1989). Simulation of pressure response data from geothermal reservoirs by lumped parameter models. In *Proceedings of the Fourteenth Workshop on Geothermal Reservoir Engineering*, pages 257–263, Stanford University, Stanford, California.
- Axelsson, G. (1991). Reservoir engineering studies of small low-temperature hydrothermal systems in Iceland. In *Proceedings of the Sixteenth Workshop on Geothermal Reservoir Engineering*, pages 143–149, Stanford University, Stanford, California.
- Axelsson, G. (2008). Production capacity of geothermal systems. In *Proceedings of the Workshop for Decision Makers in the Direct Heating Use of Geothermal Resources in Asia*, Tianjin, China.
- Axelsson, G. (2010). Sustainable geothermal utilization. Case histories; definitions; research issues and modelling. *Geothermics*, 39:283 – 291.
- Axelsson, G. and Arason, T. (1992). Lumpfit - Automated simulation of pressure change in hydrological reservoirs. Report, National Energy Authority of Iceland, Reykjavik, Iceland.
- Banos, R., Manzano-Aguilario, F., Montoya, F. G., Gil, C., Alcayde, A., and Gomez, J. (2010). Optimization methods applied to renewable and sustainable energy: A review. *Renewable and Sustainable Energy Reviews*, 15:1753–1766.
- Bazaraa, M. S., Sherali, H. D., and Shetty, C. M. (2013). *Nonlinear Programming: Theory and Algorithms*. John Wiley and Sons.
- Bellman, R. (1957). *Dynamic Programming*. Princeton University Press, Princeton.
- Belotti, P., Kirches, C., Leyffer, S., Linderoth, J., Luedtke, J., and Mahajan, A. (2012). Mixed-Integer Nonlinear Optimization. Preprint ANL/MCS-P3060-1112, Mathematics and Computer Science Division, ARGONNE NATIONAL LABORATORY, 700 South Cass Avenue Argonne, Illinois 60439.

- Bertani, R. (2010). Geothermal power generation in the world 2005 - 2010 update report. In *Proceedings of the World Geothermal Congress 2010*, pages 1–3, Bali, Indonesia.
- Bertsekas, D. (2003). *Nonlinear Programming*. Athena Scientific, Belmont, MA.
- Betts, J. T. (2001). *Practical Methods for Optimal Control and Estimation Using Nonlinear Programming. SECOND EDITION*. Society for Industrial and Applied Mathematics (SIAM), Philadelphia.
- Binder, T., Blank, L., Bock, H., Bulirsch, R., Dahmen, W., Diehl, M., Kronseder, T., Marquardt, W., Schlöder, J., and Stryk, O. (2001). Introduction to model based optimization of chemical processes on moving horizons. In Grötschel, M., Krumke, S., and Rambau, J., editors, *Online Optimization of Large Scale Systems: State of the Art*, pages 295–340. Springer.
- Bisschop, J. and Entriken, R. (1993). *AIMMS The Modeling System. Paragon Decision Technology*. Paragon Decision Technology.
- Bock, H. G. and Plitt, K. J. (1984). A Multiple Shooting algorithm for direct solution of optimal control problems. In *Proceedings of the 9th IFAC World Congress*, pages 242–247, Budapest. Pergamon Press.
- Brooke, A., Kendrick, D., Meeraus, A., and Raman, R. (1993). *GAMS, A User's Guide*. GAMS Development Corporation.
- Bryson, A. E. (1999). *Dynamic Optimization*. Addison Wesley Longman, Menlo Park, CA.
- Burer, S. and Letchford, A. N. (2012). Non-convex mixed-integer nonlinear programming: A survey. *Surveys in Operational Research and Management Science*, 17:97–106.
- Bussieck, M. R. and Vigerske, S. (2012). Minlp solver software. *GAMS Development Corp. and Humboldt-Universität*, pages 1–17.
- Chow, G. C. (1997). *Dynamic Economics: Optimization by the Lagrange Method*. Oxford University Press, USA.
- Colombani, Y. and Heipcke, S. (2002). Mosel: An extensible environment for modeling and programming solutions. In Jussien, N. and Laburthe, F., editors, *Proceedings of the Fourth International Workshop on Integration of AI and OR Techniques in Constraint Programming for Combinatorial Optimisation Problems (CP-AI-OR'-02)*, pages 277–290.

- Dadebo, S. A. and McAuley, K. B. (1995). Dynamic optimization of constrained chemical engineering problems using dynamic programming. *Computers and Chemical Engineering*, Volume 19:513 – 525.
- Dakin, R. J. (1965). A tree-search algorithm for mixed integer programming problems. *The computer journal*, 8:250–255.
- de Paly, M., Heicht-Mendez, J., Beck, M., Blum, P., Zell, A., and Bayer, P. (2012). Optimization of energy extraction for closed shallow geothermal systems using linear programming. *Geothermics*, 43:57–65.
- Diehl, M. (2011). *Numerical Optimal Control*. K.U. Leuven Kasteelpark Arenberg 10 3001 Leuven, Belgium.
- Diehl, M., Bock, H. G., Diedam, H., and Wieber, P.-B. (2005). Fast Direct Multiple Shooting Algorithms for Optimal Robot Control. In *Fast Motions in Biomechanics and Robotics*, Heidelberg, Allemagne.
- Dincer, I. (2002). The role of exergy in energy policy making. *Energy Policy*, 30:137–149.
- Duan, Z., Pang, Z., and Wang, X. (2011). Sustainability evaluation of limestone geothermal reservoir with extended production histories in beijing and tianjin, china. *Renewable and Sustainable Energy Reviews*, 40:125–135.
- Eugster, W. and Rybach, L. (2000). Sustainable production from borehole heat exchanger systems. In *Proceedings of the World Geothermal Congress 2000*, pages 825–830, Kyushu, Tohoku, Japan.
- Evans, A., Strezov, V., and Evans, T. J. (2008). Assessment of sustainability indicators for renewable energy technologies. *Renewable and Sustainable Energy Reviews*, 13:1082–1088.
- Falk, J. E. and Soland, R. M. (1969). An algorithm for separable nonconvex programming problems. *Management Science*, 15:550–569.
- Fletcher, R. (1987). *Practical Methods of Optimization*. Wiley, Chichester, 2nd edition.
- Fourer, R., Gay, D. M., and Kernighan, B. W. (1993). *AMPL: A Modeling Language for Mathematical Programming*. The Scientific Press.
- Frank, M. and Wolfe, P. (1956). An algorithm for quadratic programming. *Naval Res. Logis.*, 3:95–110.
- GAMS (2002). *GAMS/SBB Solver Manual*. GAMS Development Corporation, Washington, DC.

- Garcia, J. G., Axelsson, G., Gunnarsson, G., and Gunnlaugsson, E. (2011). Reservoir assessment of the Olfus-Bakki low-temperature geothermal area, SW Iceland. In *Proceedings of Thirty - Sixth Workshop on Geothermal Reservoir Engineering*, pages 1–13, Stanford University, California.
- Garey, M. R. and Johnson, D. S. (1979). *Computers and intractability: A guide to the theory of NP-Completeness*. W.H. Freeman, New York.
- Gill, P. E., Murray, W., and Saunders, M. A. (2005). SNOPT: An SQP Algorithm for Large-Scale Constrained Optimization. *Society for Industrial and Applied Mathematics*, 47(1):99–131.
- Grant, M. A. (1983). Geothermal reservoir modeling. *Geothermics*, 12:251–263.
- Greenberg, H. J. and Pierskalla, W. (1970). A review of quasi-convex functions. *Operations Research*, 19:1553–1570.
- Grossman, I. E. (2002). Review of Nonlinear Mixed-Integer and Disjunctive Programming Techniques. Report, Department of Chemical Engineering, Carnegie Mellon University, Pittsburgh, PA 15213, USA.
- Grossmann, I. E. and Biegler, L. T. (2004). Part ii. future perspective on optimization. *Computers and Chemical Engineering*, 18:1193–1218.
- Gudmundsson, J. S. and Olsen, G. (1987). Water Influx modeling of Svartsengi geothermal field, Iceland. *SPE Reservoir Eng.*, 2:77–84.
- Gunnarsson, A. (2012). Private communication, February 27, 2012. Senior Project Manager for Geothermal at Landsvirkjun Power Company in Iceland.
- Gunnlaugsson, E., Gislason, G., Ivarsson, G., and Kjarran, S. P. (2000). Low temperature geothermal fields utilized for district heating in Reykjavik, Iceland. In *Proceedings of the World Geothermal Congress 2000*, pages 1–5, Kyushu–Tohoku, Japan.
- Gupta, O. K. and Ravindran, A. (1985). Branch and bound experiments in convex non-linear integer programming. *Management Science*, 31(12):1533–1546.
- Gurobi (2012). *Gurobi Optimizer Reference Manual, Version 5.0*. Gurobi Optimization, Inc.
- Hart, W. E., Watson, J. P., and Woodruff, D. L. (1976). Computability of global solutions to factorable nonconvex programs part i - convex underestimating problems. *Mathematical Programming*, 10:147–175.

- Hepbasli, A. (2008). A key review on exergetic analysis and assessment of renewable energy resources for a sustainable future. *Renewable and Sustainable Energy Reviews*, 12:593–661.
- Holmstrom, K. (1999). The tomlab optimization environment in matlab. *Advanced Modeling and Optimization*, 1:47–69.
- Ivarsson, G. (2011). Heating Utility in Reykjavik - Water Production 2010. Internal report, Reykjavik Energy, Reykjavik, Iceland.
- Jaggi, M. (2013). Revisiting Frank-Wolfe: Projection-Free Sparse Convex Optimization. In *Proceedings of the 30th International Conference on Machine Learning*, volume 28, Atlanta, Georgia, USA.
- Karush, W. (1939). Minima of functions of several variables with inequalities asside conditions. Master's thesis, Department of Mathematics, University of Chicago.
- Kiwiel, K. C. (2001). Convergence and efficiency of subgradient methods for quasiconvex minimization. *Mathematical Programming*, 90:1–25.
- Kuhn, H. and Tucker, A. (1951). Nonlinear programming. In Neyman, J., editor, *Proceedings of the Second Berkeley Symposium on Mathematical Statistics and Probability*, Berkeley. University of California Press.
- Land, A. H. and Doig, A. G. (1960). An automatic method of solving discrete programming problems. *Econometrica*, 28:497–520.
- Lovekin, J. (2000). The economics of sustainable geothermal development. In *Proceedings of the World Geothermal Congress 2000*, pages 843–848, Kyushu, Tohoku, Japan.
- Lund, H. (2007). Renewable energy strategies for sustainable development. *Energy*, 32:912–919.
- Lund, J. W., Freeston, D. H., and Boyd, T. L. (2011). Direct utilization of geothermal energy 2010 worldwide review. *Geothermics*, 40:159–180.
- Luus, R. (2000). *Iterative Dynamic Programming*. Chapman and Hall, Boca Raton, FL.
- Martinovic, M. (1990). Lumped and distributed parameter models of the Mosfellssveit geothermal field, SW-Iceland. Report 9, National Energy Authority of Iceland, Grensasvegur 9, Iceland.
- MATLAB (2012). *version 7.14.0 (R2012a)*. The MathWorks Inc., Natick, Massachusetts.
- Nash, S. G. and Sofer, A. (1996). *Linear and Nonlinear Programming*. McGraw-Hill International Editions.

- National Energy Authority of Iceland (2012). Geothermal use in Iceland. [Online; accessed January 2012].
- Nocedal, J. and Wright, S. (2006). *Numerical Optimization*. Springer Verlag, Berlin Heidelberg New York, 2nd edition.
- Onur, M., Sarak, H., Tureyen, O. I., Cinar, M., and Satman, A. (2008). A new non-isothermal lumped-parameter model for low temperature, liquid dominated geothermal reservoirs and its applications. In *Proceedings of the Thirty-Third workshop on Geothermal Reservoir Engineering*, pages 1–10, Stanford, California.
- Picard, R. R. and Berk, K. R. (1990). Data Splitting. *The American Statistician*, Volume 44:140 – 147.
- Pruess, K., Bodvarsson, G. S., and Lippmann, M. J. (1986). Modeling of geothermal systems. *Journal of Petroleum Technology*, 38:1007–1021.
- Rao, A. V. (2009). A survey of numerical methods for optimal control. *AAS/AIAA Astrodynamics Specialist Conference*.
- Reykjavik Energy (2011). Prices and Rates. [Online; accessed Oktober-2011].
- Rybach, L. and Mongillo, M. (2006). Geothermal sustainability - a review with identified research needs. *GRC Transactions*, 30:1083–1090.
- Sager, S. (2006). *Numerical methods for mixed-integer optimal control problems*. PhD thesis, Universität Heidelberg.
- Sager, S. (2012). A benchmark library of mixed-integer optimal control problems. In Lee, J. and Leyffer, S., editors, *Mixed Integer Nonlinear Programming*, pages 631–670. Springer.
- Satman, A., Sarak, H., and Onur, M. (2005). Lumped-parameter models for low-temperature geothermal fields and their application. *Geothermics*, 34:728–755.
- Sigurdardottir, S. R., Valfells, A., Palsson, H., and Stefansson, H. (2012). Mixed integer optimization model for harvesting of geothermal reservoir. *Geothermics (in review)*, pages 1–21.
- Statistics Iceland (2012). Manufacturing and Energy. [Online; accessed January-2012].
- Stefansson, V. (2000). The renewability of geothermal energy. In *Proceedings of the World Geothermal Congress 2000*, Orkustofnun, Grensasvegur 9, Reykjavik, Iceland.
- Stubbs, R. A. and Mehrotra, S. (1999). A branch-and-cut method for 0-1 mixed convex programming. *Mathematical Programming*, 86(3):515–532.

- Varun, Prakash, R., and Bhat, I. K. (2009). Energy, economics and environmental impacts of renewable energy systems. *Renewable and Sustainable Energy Reviews*, 13:2716–2721.
- von Stryk, O. (1993). Numerical solution of optimal control problems by direct collocation. In Bulirsch, R., Miele, A., Stoer, J., and Well, K. H., editors, *Optimal Control - Calculus of Variations, Optimal Control Theory and Numerical Methods*, volume 111 of *International Series of Numerical Mathematics*, pages 129–143, Basel. Birkhäuser.
- Wilson, R. B. (1963). *A simplicial algorithm for concave programming*. PhD thesis, Harvard University.
- Xin, S., Liang, H., Hu, B., and Li, K. (2012). Electrical power generation from low temperature co-produced geothermal resources at huabei oilfield. In *Proceedings of the Thirty-Seventh Workshop on Geothermal Reservoir Engineering*, pages 1–6, Stanford University, Stanford, California.

Appendix A

Paper 1

Optimizing Revenue of a Geothermal System with respect to operation and expansion

Silja Ran Sigurðardóttir¹, Halldor Palsson², Agust Valfells¹ and Hlynur Stefansson¹

¹University of Reykjavik, Kringlan 1, Reykjavik, IS-103, Iceland

²University of Iceland, Saemundargata 1, Reykjavik, IS-101, Iceland

siljars@ru.is, halldorp@hi.is, av@ru.is, hlynurst@ru.is

Keywords: optimization, sustainability, geothermal utilization, reservoir modeling, discrete approximation

ABSTRACT

The goal of this work is to conduct a decision-making tool that optimizes present value of profit when utilizing low temperature geothermal resources. The profit is measured as the difference between operating cost and price of energy. The usual approach in these studies, regarding the behaviour of the resource, is the lumped parameter model (LPM) which models pressure change in a geothermal reservoir with respect to given production history and drawdown. Here, a mixed integer linear programming (MILP) approach on the LPM will be used. The constraints are sustainability, demand and price of energy. A methodology for a quantitative definition of sustainability is established and coupled into the model. Demand and price of energy is simulated stochastically to account for uncertainty in future propagation using historical data. Results will include model comparison along with profit and lifetime under various conditions for different wells and values of parameters.

1. INTRODUCTION

The vast geothermal resources in Iceland have been utilized to a considerable extent and are primarily used for space heating, various industries, swimming pools and snow melting. Electricity generation using geothermal energy has also increased significantly in recent years and now accounts for over 20% of the total electricity generation in Iceland (Eggertsson, 2008).

Geothermal energy has generally been classified as a renewable energy source since it is believed to recharge at a similar rate as a normal production rate from the resource. This classification has occasionally been challenged, saying that the thermal depletion of geothermal systems requires such a long recovery time that strictly speaking it is not renewable on a human timescale. It has been found (Stefansson, 2000) that renewability of geothermal systems is ultimately determined by the transportation process of heat within the crust. All porous and hydrous geothermal systems can therefore be classified as renewable, with some reservations, while hot dry rock systems can hardly be classified as such (Stefansson, 2000).

It is important to make a clear distinction between renewability and sustainability. Renewability is a property of a resource where energy is continuously replaced at a similar rate as the extraction of energy. Sustainability on the other hand refers to the exploitation of a resource where the production system applied is able to maintain production levels over long periods of time (Rybach & Mongillo, 2006). Although many geothermal energy systems are renewable, the regeneration time of a geothermal reservoir may be quite long and it is unclear how to plan the operation strategy of power plants to ensure profitable and sustainable power production. The size and dynamic characteristics of

geothermal reservoirs is often poorly understood when capital investments begin, since thorough exploration is quite costly. The economic horizon of large-scale investments such as power plants may be greater than the characteristic time for regeneration of the reservoir for a given system. Thus it is important to take into account the effects of long-term utilization of such fields, but they are generally not very well known. The demand for the geothermal resource may also vary, whether it is for pure generation of electricity or cogeneration of heat and power. A main concern of this work is to look at how to develop the resource in a sustainable manner in light of different constraints and uncertainty of production capacity, reservoir dynamics and market demand.

Several methods exist for reservoir assessment in geothermal systems. The most commonly used are volumetric methods involving conceptual modeling, detailed mathematical modeling and lumped parameter modeling. Volumetric methods are based on estimation of the total heat stored in a volume of rock but do not take into account the dynamic response of the system (Axelsson, 2008). Detailed mathematical and numerical modeling is the most powerful modeling method available for geothermal reservoirs (Lippmann, O'Sullivan & Pruess, 2001), which can simulate the structure, conditions and response of a geothermal system with reasonable accuracy. Numerical modeling can despite its advantages be very time consuming which makes it an unsuitable method in statistical analysis such as that which will be applied in this study.

In this work lumped parameter modeling (LPM) with a mixed integer linear programming (MILP) approach will be applied for resource assessment. It requires few and commonly available parameters for the physical modeling, but does not require much processing power and has an acceptable accuracy in modeling pressure change for isothermal low-temperature systems (Satman, Sarak & Onur, 2005). Those advantages do come at some cost since lumped parameter models usually do not take into account well spacing or well injection locations, nor do they consider fluid flow within the reservoir. They are also unable to match average enthalpy and the non-condensable gas content of the produced fluid and cannot simulate phase changes or thermal fronts (Pruess, Bodvarsson & Lippmann, 1986).

2. PREVIOUS WORK

Lumped parameter modeling has been successfully applied to geothermal fields around the world, including Iceland (Axelsson, 1989, Björnsson, Axelsson & Quijano, 2005, Axelsson, 1991, Axelsson, Hjartarson and Hauksdóttir, 2002), P.R. of China (Youshi, 2002), Turkey (Satman, Sarak & Onur, 2005), Central America (Björnsson, Axelsson and Quijano, 2005) and at various other locations. In order to successfully model a geothermal field using lumped parameter modeling some production history must be available. The accuracy of the final model depends on the

time span and resolution of available data, since the data is used to estimate model parameters.

Despite the inherent simplicity of lumped parameter modeling it has been shown to predict pressure changes in reservoirs with good accuracy, given sufficient data quality. The ultimate goal of such modeling is to predict the production capacity of the geothermal field. The model then serves as a useful tool in the decision making process with regards to exploitation rate, investment cost and sustainability considerations.

From an economical point of view, excessive production is beneficial, mainly due to the time value of money, where the annual revenue in the early years has the greatest effect upon the present value of the operation. It has been concluded (Lovekin, 2000) that a particular aggressive exploitation scenario resulted in a discounted return of investment and present worth almost three times more than a conservative use of the resource, despite higher costs of make-up wells at later stages in the operation. The main drawback of excessive production is that it can lead to resource deterioration or even depletion. In (Eugster, Ryback, 2000) it was for example shown that the time required for a thermal recovery in a heat pump-coupled well heat exchanger system was roughly equal to production time.

The increased use of geothermal resources has raised questions regarding their renewability and how the resource is harnessed in an optimal manner. It is currently unclear how to design optimal operation strategies of power plants that ensure profitable and sustainable power production. This is a complex problem which requires advanced modelling techniques to be combined with specific expertise in the problem domain. A model of the geothermal reservoir is required in a combination with a model of the operational and market environment including all constraints and objectives. To our knowledge integrated models of geothermal systems including market constraints for operation have not been implemented.

There is a dearth of research on the optimal utilisation of geothermal resources. Stefansson (2000) is one of few who have proposed this issue. Among other things he proposed a strategy where power plants are built in small phases (20-30 MW) and use the first wells to gain understanding of the geothermal system at the same time as generating heat and power. In that way companies can make some profit from geothermal resources at the same time as studying their characteristics and make better judged decisions about further investments (Stefansson, 2002). Prior to this work, wells had been drilled for experiments without using them also for generating heat and power.

Recently there has been an increasing interest and discussion on the sustainable harnessing of geothermal resources (Lovekin, 2000; Stefansson, 2000; Flovenz, Axelsson & Armannsson, 2001; Rybach, 2006). These studies conclude that despite geothermal resources being generally considered as renewable they can be harnessed in an excessive manner which can lead to depletion or even deterioration if the removal rate of energy is greater than the rate of regeneration. Lovekin (Lovekin, 2000) investigated a certain case where the price of electricity is fixed, demand is unlimited and the production capacity of the geothermal resource is known. He concludes that the optimal harnessing

strategy is to build as large a power plant as possible and exploit the resource in an excessive manner due to the time value of money, where the annual revenue in the early years has the greatest effect upon the net present value (NPV) of the operation. Gudni Axelsson, Valgardur Stefansson, Grimur Bjornsson and Jiurong Liu (Bjornsson, Axelsson, Stefansson & Liu, 2005) have studied sustainable harnessing which they define as the possible continuous harnessing of the resource over an extended period (100-300 years). Among others they study the Nesjavellir area and their research indicates that it is currently not being harnessed in a sustainable manner and it will not be possible to maintain current removal rate for an extended period. The production will need to be reduced and probably shutdown in an attempt to let the geothermal resource regenerate.

The primary objective of this work is to develop new methods for creating strategies for harnessing geothermal resources that can ensure sustainable long-term utilization. The research is focused on optimal utilization of geothermal resources such that social and economic development objectives are fulfilled, in an environmentally benign way. In the following we use an innovative mathematical programming model to optimize the harnessing of geothermal resources and show how rules and regulations can be implemented with constraints in a simple manner.

3. METHODS AND MATERIALS

3.1 Model of a geothermal reservoir

The behavior of the geothermal reservoir plays a major part in any analysis of future cost and operational optimization of the system at hand. Therefore it is necessary to use a sufficiently accurate model to simulate this behavior, but it is also beneficial that the model is simple and can be run efficiently on a computer. The modeling in this study is based on a lumped parameter description of a water dominated geothermal reservoir, which is discretized in time for convenience in an operational optimization procedure.

3.1.1 Lumped parameter model

The lumped parameter model is based on three storage tanks, which represent the near neighbourhood of a geothermal well, a volume in some distance from the well and finally a large volume which covers the area of influence from the well utilization. These storage tanks are connected together so that fluid can flow between them and fluid can also flow from the tank nearest to the well to the surface. The state of the tanks is represented by pressure and the pressure difference along with connection resistances controls the actual flow between tanks. Figure 1 shows the connection between storage tanks.

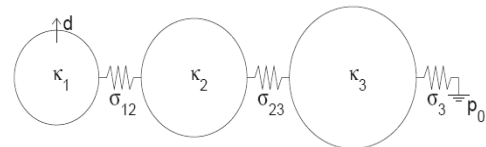


Figure 1: Storage tanks with connections.

In the description above, κ denotes the tank mass capacities, σ denotes resistance, p_0 is the external pressure of the environment and d is the flow through the well.

As mentioned before, the flow between the tanks is related to the actual pressure state in the tank. This relation can be written as three differential equations, one for each storage tank. This results in

$$\begin{aligned}\kappa_1 \frac{dp_1}{dt} &= \sigma_{12}(p_1 - p_2) + d \\ \kappa_2 \frac{dp_2}{dt} &= \sigma_{12}(p_1 - p_2) - \sigma_{23}(p_3 - p_2) \\ \kappa_3 \frac{dp_3}{dt} &= \sigma_{23}(p_2 - p_3) - \sigma_3(p_0 - p_3)\end{aligned}$$

which can be written in a more convenient matrix form (or state space form) as

$$K\dot{x} = Sx + u$$

where

$$K = \begin{bmatrix} \kappa_1 & 0 & 0 \\ 0 & \kappa_2 & 0 \\ 0 & 0 & \kappa_3 \end{bmatrix} \quad x = \begin{bmatrix} p_1 \\ p_2 \\ p_3 \end{bmatrix} \quad u = \begin{bmatrix} d \\ 0 \\ \sigma_3 p_0 \end{bmatrix}$$

$$S = \begin{bmatrix} -\sigma_{12} & \sigma_{12} & 0 \\ \sigma_{12} & -\sigma_{12} - \sigma_{23} & \sigma_{23} \\ 0 & \sigma_{23} & -\sigma_{23} - \sigma_3 \end{bmatrix}$$

There are various ways to solve the system above, either analytically with integration or with numerical methods, which is the topic of next section.

3.1.2 Discrete approximation of the lumped parameter model

One way of solving the differential equations for the lumped parameter model is to use numerical integration in time. Generally, such methods are classified into implicit methods and explicit methods, where the explicit ones are easier to implement but have stability issues and criteria.

A relatively simple and accurate method to integrate the lumped equations is to use central finite difference approximation of the time derivative. If x_k denotes the current state at time step k and x_{k+1} denotes a new update at a future time step, the numerical approximation of the update is

$$K \frac{x_{k+1} - x_k}{\Delta t} = S \frac{x_{k+1} + x_k}{2} + \frac{u_{k+1} + u_k}{2}$$

which can be solved for x_{k+1} , resulting in

$$x_{k+1} = \left(K - \frac{\Delta t}{2} S\right)^{-1} \left(\left(K + \frac{\Delta t}{2} S\right) x_k + \frac{\Delta t}{2} (u_{k+1} + u_k) \right)$$

Or *fully implicit* method where

$$K \frac{x_{k+1} - x_k}{\Delta t} = S \cdot x_{k+1} + u_{k+1}$$

so

$$x_{k+1} = (K - \Delta t S)^{-1} (K \cdot x_k + \Delta t \cdot u_{k+1})$$

where Δt is the length of the time step used. The implicit approach results in a very accurate and stable method, but requires some simple matrix operations in each time step.

Another approach is to use an explicit method where the update to a new time step is based on the current time step only. The resulting equation is

$$K \frac{x_{k+1} - x_k}{\Delta t} = Sx_k + u_k$$

and the solution for the state update is

$$x_{k+1} = x_k + K^{-1} \Delta t (Sx_k + u_k)$$

Note that A is a diagonal matrix and therefore easily invertible. The explicit method requires that the time step Δt is chosen sufficiently small in order to ensure stability, but it is assumed that the reservoir conditions change slowly, so a time step of one month should be sufficiently small.

3.2 Sustainability criteria

For each geothermal system, and for each mode of production, there exists a certain level of maximum energy production, E_0 , below which it will be possible to maintain a constant energy production for a very long time (100–300 years). If the production rate is greater than E_0 it cannot be maintained for this length of time. Geothermal energy production below or equal to E_0 , is termed sustainable production while production greater than E_0 is termed excessive production.

Sustainability can then be determined by the ratio between the power required to extract the water from the well and the specific exergy contained in the water times the demand:

$$St = \frac{E_s d}{P}$$

If c ($J \text{ kg}^{-1} \text{ K}^{-1}$) is the heat capacity of water (at 25°C), T_h (K) is the temperature of the heat source and T_0 (K) is the temperature of the heat sink the following approximation of the exergy per unit production can be made

$$E_s = c \left((T_h - T_0) - T_0 \ln \frac{T_h}{T_0} \right)$$

3.3 Operational optimisation model

To model the operation environment of the geothermal power plants mixed integer linear programming (MILP is a special type of mathematical programming techniques) as it is widely accepted that mathematical programming techniques offer appropriate methods to model and solve the complex constrained problems which arise in the planning and scheduling of complex production environments (Shah et al., 1999; Applequist et al., 1997; Engel et al., 2001). With the model we optimize the operation strategy of the geothermal power plant. Geothermal energy is classified as a renewable resource in the sense that water and heat flows into areas from which it has been removed. However, if water or heat is removed from the geothermal reservoir at greater rate than it is replenished, the time will come that plant operations are no longer profitable and the reservoir must be allowed to rest while the system heats up and / or fluid re-enters. The optimized operations strategy will determine initial investment, the rate of extraction and whether production should be continuous or intermittent.

To be able to provide decision support for creating sustainable harnessing strategies it is necessary to develop a model that mimics the feedback of the geothermal reservoir

to harnessing. Due to the extensive calculations needed for optimising the operation strategies it is important that the reservoir model is efficient but at the same time it needs to be accurate enough. The lumped parameter model contains differential equations that make it more difficult to solve the MILP model. To make the model easily solvable we use a implicit discrete time scale and replace the differential equations with discrete constraints that take care of mass balance in the tanks.

3. RESULTS

3.1 Parameter estimation

In order to estimate the accuracy of discrete lumped parameter models the model is fitted against data from Lauganes reservoir in SW-Iceland. Figure 3 shows the production history and the historical drawdown can be seen in figure 4. The model parameters are estimated by minimizing the squares of the difference between theoretical drawdown and empirical observation such as

$$\min_{h_0, K, S} \frac{1}{2} \|h_e - h(h_0, K, S)\|_2^2 = \frac{1}{2} \sum_j (h_{e,j} - p(h_0, K, S, t_j))^2$$

where $h_{e,j}$ is an empirical observation at time step j and $p(h_0, K, S, t_j)$ is the theoretical drawdown at the same time step. This returns the vectors of the values for the initial drawdown in each tank, h_0 the storage coefficients, K (from K) and the conductance values S (from S) which are the characteristic parameters for the particular geothermal system in question. This is solved by using `lsqnonlin` MATLAB function.

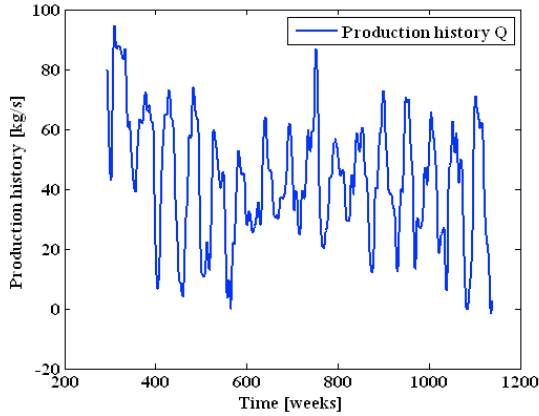


Figure 3: Production history in kg/s over 17 years.

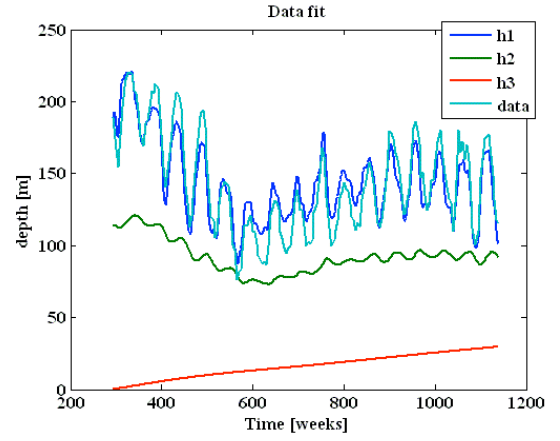


Figure 4: The drawdown data used to estimate model parameters versus the drawdown from the fitted model.

The discrete lumped parameter model follows the data quite accurately compared to the discrete approximation that has been done or root mean square (RMS) of 12.58 and standard deviation of 12.57. More accurate parameter estimation is obtained by solving the differential equation (see section 3.1.1) directly or RMS of 6.65 and standard deviation 6.74.

3.2 Behaviour of the discrete reservoir model

After the parameters have been estimated optimization is tested. We use CVX, a Matlab-based modeling system for convex optimization. CVX turns Matlab into a modeling language, allowing constraints and objectives to be specified using standard Matlab expression syntax (CVX, 2009).

We compare the behaviour of the discrete reservoir optimization model to data from Lauganes reservoir. We use one reservoir and assume decision variable Q can not exceed historical production. We run the optimization for 3 years (150 weeks).

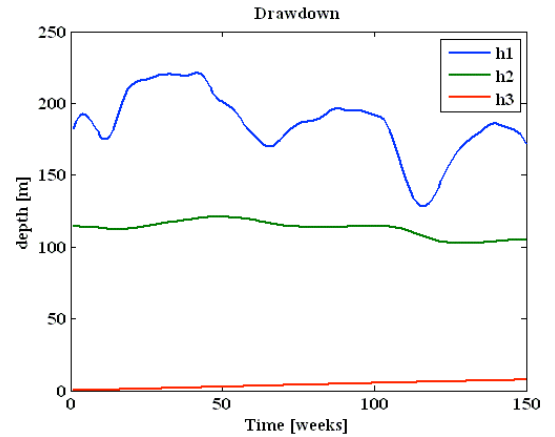


Figure 5: Results from optimization showing drawdown in tanks 1, 2 and 3.

From figure 5 we see that h_1 has the highest fluctuation of the 3 tanks and shows greatest response to variation in production rates; h_2 shows a slightly decreasing drawdown and h_3 slightly increasing drawdown. From figure 6 we see that the drawdown in tank one follows the data to some extent.

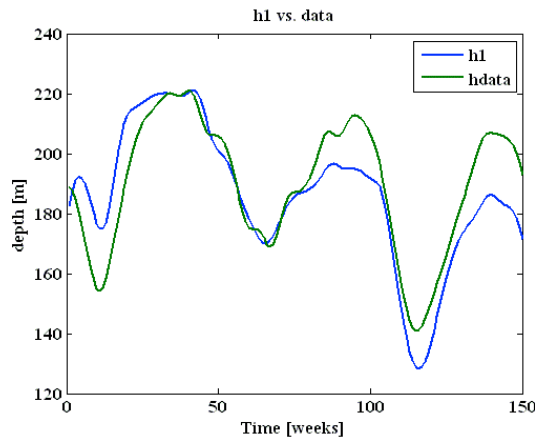


Figure 6: Historical drawdown compared with calculated drawdown from the simple model

We observe the relative error from this optimization. The relative error increases in year two and decreases again in year 3 where the optimized drawdown goes below historical drawdown.

Figure 7: Relative error from optimization

Let's now assume that Q can exceed historical production by 20% and not go lower than 80% of the historical production and drawdown can not exceed 200 m. We run the optimization for 1 year (50 weeks) and obtain the results shown in figures 8 and 9.

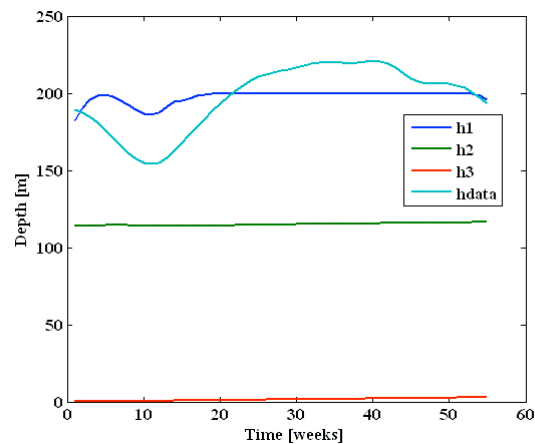


Figure 8: Result from optimization with more slack in production. Here the historical drawdown is compared with outcome of optimization model.

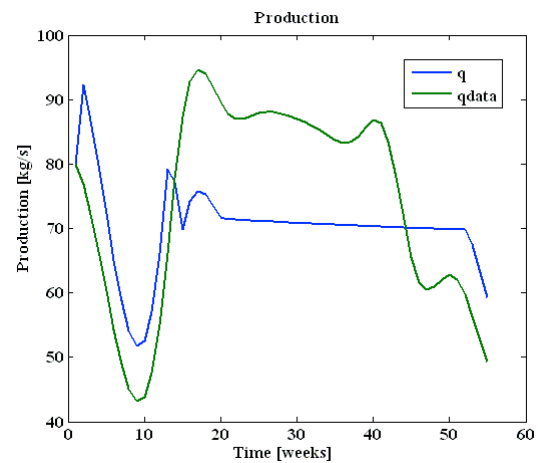


Figure 9: Result from optimization with increased slack in production. Here the historical production is compared with outcome of the optimization model.

The production is profitable with the data used for the Lauganes reservoir and we see that with increased slack in production the production increases to its maximum allowed limits and as a result the drawdown increases.

4. CONCLUSIONS AND FUTURE WORK

According to the parameter estimation implicit discrete approximation gives a relatively good estimate.

The optimization model indicates that such a model can be implied but relative error is still too large in our model.

Drawdown increases with more slack in the production constraint which is sensible since our revenue increases with more production. The interaction between the three tanks is also logical.

CVX in Matlab can only handle 3 years of optimization. With a stronger solver this could be applied for a longer period which would give better opportunities for validating the model behaviour and exploring the usability of the model.

Future work will focus on reducing the error of the model and solving it for extended time horizon and multiple reservoirs.

REFERENCES

- Applequist, G. et al. (1997). Issues in the use, design and evolution of process scheduling and planning systems. *ISA transactions*.
- Axelsson, G. (2008). Lecture notes. *Geothermal reservoir engineering (physics)*.
- Axelsson, G., Hjartarson A. & Hauksdóttir, S. (2002). Reassessment of the Thelamork low temperature geothermal system in N-Iceland following successful deepening of well lthn-10. *Proceedings Twenty-Seventh Workshop on Geothermal Reservoir Engineering*, Stanford University, Stanford, California.

- Axelsson, G. (1991). Reservoir engineering studies of small low-temperature hydrothermal systems in Iceland. *Proceedings Sixteenth Workshop on Geothermal Reservoir Engineering*, pages 143–149, Stanford University, Stanford, California.
- Axelsson, G. (1989). Simulation of pressure response data from geothermal reservoirs by lumped parameter models. *Proceedings Fourteenth Workshop on Geothermal Reservoir Engineering*, pages 257–263, Stanford University, Stanford, California.
- Bjornsson, G., Axelsson, G. & Quijano, J.E. (2005). Reliability of lumped parameter modeling of pressure changes in geothermal reservoirs. *Proceedings World Geothermal Congress 2005*, pages 1–8, Antalya, Turkey, Morgan Kaufmann Publishers Inc.
- Bjornsson, G., Axelsson, G., Stefansson, V. & Liu, J. (2005). Sustainable management of geothermal resources and utilization for 100–300 years. *Proceedings World Geothermal Congress 2005*, pages 1–8, Antalya, Turkey.
- CVX: Matlab Software for Disciplined Convex Programming. (2009). *Stanford University*. Retrieved October 9, 2009, from <http://www.stanford.edu/~boyd/cvx/>
- Eggertsson, H., Thorsteinsson, I. & Jonasson, T (eds.). (2008). Energy statistics in Iceland, *National Energy Authority and Ministries of Industry and Commerce*. Reykjavik.
- Engel, A. et al., 2001. Developing methodology for advanced systems testing - SYSTEST. *A research grant proposal for the European Commission*, the Research Proposal Office, GRD1-2001-40487.
- Eugster, W.J. & Rybach, L. (2000). Sustainable production from borehole heat exchanger systems. *Proceedings World Geothermal Congress 2000*, pages 825–830, Kyushu, Tohoku, Japan.
- Flovenz, O.G., Axelsson G. & Armannsson H. (2001). Sustainable production of geothermal energy: Suggested definition. *IGA-News*, 43:1–2.
- Lippmann, M J., O’Sullivan, M.J. & Pruess, K. (2001). State of the art of geothermal reservoir simulation. *Geothermics*, 30:395–429.
- Lovekin, J. (2000). The economics of sustainable geothermal development. *Proceedings World Geothermal Congress 2000*, pages 843–848, Kyushu - Tohoku, Japan.
- Pruess, K., Bodvarsson G.S. & Lippmann, M.J. (1986) Modeling of geothermal systems. *Journal of Petroleum Technology*, pages 1007–1021.
- Rybach, L. & Mongillo, M. (2006). Geothermal sustainability - a review with identified research needs. *GRC Transactions*, 30:1083–1090.
- Satman, A., Sarak, H. & Onur, M. (2005). Lumped-parameter models for low-temperature geothermal fields and their application. *Geothermics*, 34:728–755.
- Shah, N. et al. (1999). Modeling and optimization for pharmaceutical and fine chemical process development. *Proceedings of the Focapd99 Conference, Breckenridge CO, USA* (1999) Paper no. 105
- Stefansson, V. (2002). Investment cost for geothermal power plants. *Geothermics*, 31:263–272.
- Stefansson, V. (2000). The renewability of geothermal energy. *Proceedings World Geothermal Congress 2000*, pages 843–848, Kyushu - Tohoku, Japan.
- Youshi X. (2002). Assessment of geothermal resources in the Lishuiqiao area. *Technical Report 18*, The United Nations University, Beijing, China.
- Stefansson, V. (2000). *The renewability of geothermal energy*. Proceedings World Geothermal Congress 2000, pages 843–848, Kyushu - Tohoku, Japan.
- Youshi X. (2002). *Assessment of geothermal resources in the Lishuiqiao area*. Technical Report 18, The United Nations University, Beijing, China.

APPENDIX

A1 Nomenclature

A1.1 Indexes

t Index for time periods, $t \in [1, 2, \dots, T]$

w Index for wells, $w \in [1, 2, \dots, W]$

A1.2 Variables

Decision variables

$Q_{t,w}$ Extraction from tank 1, well w in time period t [kg/s]

$Y_{t,w}$ Binary variable. $Y_{t,w}=1$ if we buy well/pump w in time period t , otherwise $Y_{t,w}=0$

State variables

$h_{1,t,w}$ Height in tank 1 of well w in time period t

$h_{2,t,w}$ Height in tank 2 of well w in time period t

$h_{3,t,w}$ Height in tank 3 of well w in time period t

Parameters

$\sigma_{1,2}$ The conductivity between tanks 1 and 2

$\sigma_{2,3}$ The conductivity between tanks 2 and 3

σ_3 The conductivity between tanks 3 and the external environment of the system

$$S = \begin{bmatrix} -\sigma_{12} & \sigma_{12} & 0 \\ \sigma_{12} & -\sigma_{12} - \sigma_{23} & \sigma_{23} \\ 0 & \sigma_{23} & -\sigma_{23} - \sigma_3 \end{bmatrix}$$

H_0 The external drawdown

$h_{1,1,w}$ Drawdown in tank 1 of well w

$h_{2,1,w}$ Drawdown in tank 2 of well w

$h_{3,1,w}$ Drawdown in tank 3 of well w

H_1^{\max} Maximum drawdown of tank 1 for sustainability constraint

QW^{\max} Maximum production capacity for each well

κ_1 Storage coefficient of tank 1

κ_2 Storage coefficient of tank 2

κ_3 Storage coefficient of tank 3

$$K = \begin{bmatrix} \kappa_1 & 0 & 0 \\ 0 & \kappa_2 & 0 \\ 0 & 0 & \kappa_3 \end{bmatrix}$$

g Gravity

dt Length of each time period (in seconds)

ρ Density of water at 25°C.

C_{elect} Price of electricity [\$/kWh]

C_{water} Price of water [\$/m³]

C_{start} Pricing of adding a new well/pump[\$]

$$Q_{t,w} \geq D_{\min}$$

A1.4 Objective Function

$$\text{Total Revenue} = \sum_{t,w} \frac{dt \cdot Q_{t,w} \cdot C_{\text{water}}}{(1+r)}$$

$$\text{Production Cost} = \sum_{t,w} \frac{(h_{1,w} + Q_{t,w}/\rho g) \cdot dt \cdot C_{\text{elect}} \cdot \rho g}{(1+r)}$$

$$\text{Well Start Cost} = \sum_{t,w} \frac{C_{\text{water}} \cdot y_{w,t}}{(1+r)}$$

$$\text{Total Cost} = \text{Production Cost} + \text{Well Start Cost}$$

$$\text{Max (Total Revenue} - \text{Total Cost)}$$

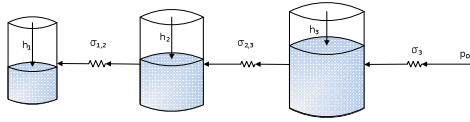


Figure 1: The three tank system.

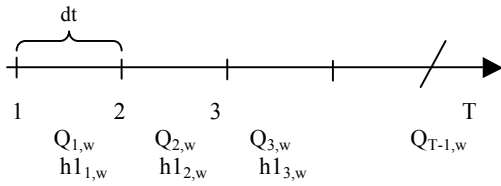


Figure 2: Explanation of the discrete time axis and examples of variables used in the model.

A1.3 Constraints

Mass balance equations on matrix form

$$h_{k+1,w} = (K - dtS)^{-1} \left(K h_{k,w} + \frac{dt Q_{k+1,w}}{\rho g} + dt \sigma_3 H_0 \right)$$

$$\forall w \in W, t \in T$$

Production capacity constraint for each well:

$$\sum_t Y_{t,w} = 1 \quad \forall w \in W$$

$$Q_{t,w} \leq \sum_0^t Y_{t,w} \cdot QW^{\max} \quad \forall w \in W, t \in T$$

Sustainability constraint:

$$h_{1,w} \leq H1^{\max} \quad \forall w \in W, t \in T$$

Setup-cost constraint

$$Q_{t,w} \leq y_w \cdot M \quad \forall w \in W, t \in T$$

Demand constraint:

$$Q_{t,w} \leq D_{\max}$$

Appendix B

Paper 2

Mixed Integer Optimization Model for Harvesting of Geothermal Reservoir

Silja R. Sigurdardottir^{a,*}, Agust Valfells^a, Halldor Palsson^b, Hlynur Stefansson^a

^a*Reykjavik University, 101 Reykjavik, Iceland*

^b*University of Iceland, 103 Reykjavik, Iceland*

Abstract

Low temperature geothermal resources provide hot water that is commonly used for space heating various or industrial activities. The geothermal resources are in most cases renewable and can be harvested by current and future generations if constraints regarding sustainability are respected. In this work we propose an innovative model to optimize the present value of profit from utilizing low temperature geothermal resources subject to operational and sustainability constraints. A fundamental part of the model is a sufficiently accurate and efficient reservoir model which simulates pressure changes (drawdown) in the reservoir with respect to harvesting levels. The approach proposed here seamlessly integrates a discretized lumped parameter model of the reservoir with a mixed integer linear program of the harvesting operations. The model is validated with real data from 26 years of harvesting of a geothermal reservoir in Iceland and results include different scenarios for illustrating the use of the model. The approach proposed in this paper has the potential to improve current decision-making in this area as it helps studying harvesting strategies in a thorough manner.

Keywords: OR in Energy, Linear Programming, Operational Optimization, Sustainability, Geothermal Utilization, Reservoir Modeling

*Corresponding author. Tel: +354 599 6200; fax: +354 599 6201
Email address: siljars@ru.is (Silja R. Sigurdardottir)

1. Introduction

Utilization of renewable and environmentally friendly energy has gained increased attention in recent years. Geothermal energy is a promising source for heat and power that may be harnessed in a sustainable manner by extracting the heat from the earth.

Geothermal systems can be classified according to their temperature and the presence of fluid. Hydrothermal systems are permeable and have geothermal fluid naturally present. This study examines low temperature hydrothermal systems, where geothermal fluid is naturally present and no phase change occurs.

Although many geothermal systems are considered renewable, the regeneration time of a geothermal reservoir may be quite long and it is unclear how to plan the operation strategy to ensure profitable and sustainable production. The size and dynamic characteristics of geothermal reservoirs are often poorly understood when capital investments begin, since thorough exploration is costly and will never completely eliminate uncertainty. Thus, it is important to make a clear distinction between renewability and sustainability. Renewability is a property of a resource where the energy is naturally replaced at a similar time scale as the extraction (Axelsson et al., 2001). Sustainability on the other hand refers to the exploitation of a resource where the production system applied is able to maintain production levels over long periods of time (Rybach and Mongillo, 2006).

Low temperature geothermal systems are most commonly used for space heating and provision of hot water and in some cases used for generation of electrical power. In particular, the vast geothermal resources in Iceland have been utilized to a considerable extent, mainly for space heating.

A low temperature geothermal field is harnessed by drilling a number of boreholes in the field and pumping geothermal fluid from them. This fluid is used as a heat source, and once heat has been extracted from the fluid it may or may not be re-injected into the field (without sufficient overpressure). The production from the field is determined simply by the flow rate and temperature of the fluid extracted. The production capacity of a geothermal field can thus be affected by a drop in the temperature of the fluid or by a decrease in the flow rate. Historical experience indicate that low temperature geothermal fields respond to production by declining pressure (here referred to as *drawdown*) and sometimes declining temperature (Axelsson, 1991; de Paly et al., 2012). This could imply that limiting production might

become a necessity after an extended period of operation.

From a financial point of view, due to the time value of money, excessive production is beneficial since the annual revenue in the early years has the greatest effect upon the present value of the operation. Lovekin (2000) concluded that a particular aggressive exploitation scenario resulted in a discounted return of investment and present worth almost three times higher than a conservative use of the resource, despite higher costs of make-up wells at later stages in the operation. However, the main drawback of excessive production is that it can lead to resource deterioration or even depletion. It was for example shown in (Eugster and Rybach, 2000) that the time required for thermal recovery in a specific geothermal system was roughly equal to production time. The increased use of geothermal resources has raised questions regarding their renewability and how the resource is harnessed in an optimal manner. Currently it is unclear how to design optimal operation strategies of power plants that ensure profitable and sustainable power production. It is then of considerable interest to be able to predict the dynamic response of the geothermal reservoir to production from it. By doing so it may be possible to manage production so as to maximize revenue, ensure long-term production capability and plan for capital investments such as purchasing and installing borehole pumps and drilling new boreholes. To do so it is necessary to construct a representative model of the underlying reservoir and how it responds to fluid being pumped from it.

Several methods exist for reservoir assessment in geothermal systems. Common ones are e.g. volumetric methods, detailed mathematical modeling and lumped parameter modeling (LPM). Volumetric methods involve conceptual modeling and are based on estimation of the total heat stored in a volume of rock but do not take into account the dynamic response of the system (Axelsson, 2008). Detailed numerical models include high resolution in three dimension and are eminently suitable for a number of tasks such as selecting borehole locations etc. The computational cost of these models can however become prohibitive when they are to be used for optimization applications. Also lack of historical data can make it difficult to support such a detailed modeling.

The lumped parameter modeling approach represents the dynamics of the system without information about detailed spatial variation and is thus useful in predicting the production capacity of geothermal fields. A representative lumped model could serve as a useful tool in the decision making process with regards to the exploitation rate, investment cost and sustainability con-

siderations.

A main concern of this work is to look at how to develop a resource in a sustainable manner in light of different constraints and uncertainty of production capacity, reservoir dynamics and market demand. In order to do this it is necessary to include both the dynamics of the reservoir and the markets. This sort of modeling was slightly tested in (Sigurdardottir et al., 2010), i.e. for 3 years of production, and synthetic sustainability constraint. The goal in this work is to optimize over 150 years with a validated parameter estimation and a sustainability constraint that can be estimated from the exergy and the temperature in the reservoir

Like in (Sigurdardottir et al., 2010), the focus is on low temperature geothermal fields with constant temperature. Historical production data (1985 till end of year 2010) from ten boreholes and drawdown data from one borehole from the Laugarnes geothermal system in South-West Iceland will be used here. The modeling approach will be carried out by first explaining the reservoir model (LPM) and then explaining the operational model, the optimization and the constraints. Results include parameter estimation and validation along with assessment of different operational scenarios.

2. Modeling approach

A lumped parameter modeling (LPM) combined with a mixed integer linear programming (MILP) approach is applied here. These two components are seamlessly integrated into a single mathematical model. The LPM is known for acceptable accuracy in modeling pressure change for isothermal low-temperature systems and requires relatively few commonly available parameters for the physical modeling (Satman et al., 2005). Those advantages do however come at some cost since lumped parameter models usually do not take into account well spacing or well injection locations. They are also unable to match average enthalpy and cannot simulate phase changes or thermal fronts in present state (Pruess et al., 1986).

Lumped parameter modelling has been successfully applied to geothermal fields around the world, including Iceland (Axelsson, 1989; Axelsson et al., 1989; Axelsson, 1991; Hjartarson et al., 2002), P.R. of China (Youshi, 2002), Turkey (Satman et al., 2005), Central America (Axelsson et al., 1989) and at various other locations. In order to successfully model a geothermal field using LPM, some production history must be available. The accuracy of the final model depends on the time span and resolution of available data, since

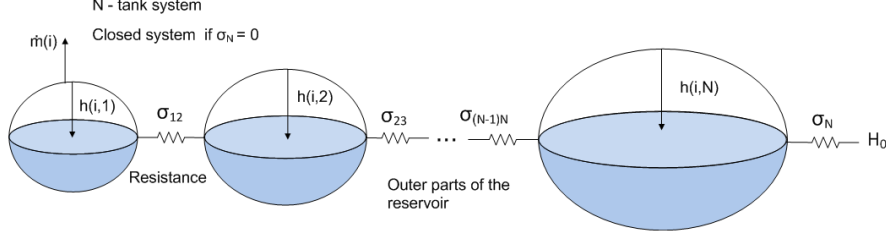
the data is used to estimate model parameters.

Historical data is used to fit the unknown parameters of the LPM model. The MILP model is used to find the optimal decisions regarding the future operation of the energy/water production facility and the lumped parameter component simultaneously simulates the behaviour of the geothermal system as an integrated part of the optimization. This is a decision making process in time, and in this case the time is divided into discrete steps or periods. During each period, an optimization variable decides the production from the well, which is then kept constant during that period. The objective is to maximise the profit of utilizing a single reservoir for a district heating system with the following in mind: Production can not exceed demand and installed capacity of the pumps must exceed the power needed to pump the fluid. A sustainability constraint is introduced, stating how much drawdown is allowed. The problem is inherently non-linear, so for a linear optimization a linear approximation needs to be performed. That includes finding suitable reference points for the approximation a threshold that prevents the linear solution of the objective function from jumping too far from the nonlinear solution, see equation 12 in chapter 2.2.

This chapter establishes the lumped parameter modeling, the discrete integration for the LPM and parameter fit, the objective function and the constraints of the model along with the linear approximation and the approach for finding suitable reference points to the approximation.

2.1. Lumped Parameter Reservoir Model (LPM)

The reservoir modeling in this study is based on a lumped parameter description of a liquid phase hydrothermal reservoir. Three storage tanks represent the neighbourhood of a geothermal well. These storage tanks are connected together so that fluid can flow between them and fluid can also flow from the smallest tank, representing the vicinity of the production wells to the surface. The state of these tanks is generally represented by pressure head and the pressure difference between tanks along with connection conductance that determine the actual flow between the tanks (see Figure 1). In this work, drawdown will be used to describe the states instead of pressure.



Descriptio 1: An N-tank system, a three-tank system will be considered in this work where $m_i := \dot{m}(i)$ $h_{i,j} := h(i, j) \forall j \in \{1, 2, 3\}$ (tank) and $t(i) = i \in \{1, \dots, n\}$ (time step)

The mass flow (production) from the actual reservoir is represented as $\dot{m}(i)$ and $h_1(i)$, $h_2(i)$ and $h_3(i)$ represent the drawdown in the three tanks at time step $t(i) = i$, see figure 1. The tank mass capacities are denoted by κ , σ denotes conductance and h_0 is the drawdown of the external environment which is assumed to be constant. As mentioned before, the flow between the tanks is related to the difference in drawdown in connected tanks. This relation can be written as three coupled differential equations, one for each storage tank. This results in

$$\kappa_1 \frac{dh_1}{dt} = \sigma_{12}(h_2 - h_1) + \dot{m}/\rho g \quad (1)$$

$$\kappa_2 \frac{dh_2}{dt} = \sigma_{12}(h_1 - h_2) + \sigma_{23}(h_3 - h_2) \quad (2)$$

$$\kappa_3 \frac{dh_3}{dt} = \sigma_{23}(h_2 - h_3) + \sigma_3(h_0 - h_3) \quad (3)$$

which can be written in a more convenient matrix form (or state space form) as

$$\mathbf{K} \frac{\partial}{\partial t} \mathbf{h} = \mathbf{S} \mathbf{h} + \mathbf{u} \quad (4)$$

where

$$\mathbf{K} = \begin{bmatrix} \kappa_1 & 0 & 0 \\ 0 & \kappa_2 & 0 \\ 0 & 0 & \kappa_3 \end{bmatrix} \quad \mathbf{h} = \begin{bmatrix} h_1 \\ h_2 \\ h_3 \end{bmatrix} \quad \mathbf{u} = \begin{bmatrix} \dot{m}/\rho g \\ 0 \\ \sigma_3 h_0 \end{bmatrix}$$

$$\mathbf{S} = \begin{bmatrix} -\sigma_{12} & \sigma_{12} & 0 \\ \sigma_{12} & -\sigma_{12} - \sigma_{23} & \sigma_{23} \\ 0 & \sigma_{23} & -\sigma_{23} - \sigma_3 \end{bmatrix}$$

There are various ways to integrate the system above, either analytically or with numerical methods, which is the topic of next section.

Integration of the Lumped Parameter Model

In the current study, the time step is partly based on availability of measured data, so an integration method that works without a limit on the time step is chosen. The Central Finite Difference Approximation or Modified Euler method is a stable and accurate computation scheme where the function is considered at both the beginning and end of the time step, taking the average of the two, consequently, (4) becomes.

$$\mathbf{K} \frac{\mathbf{h}(i+1) - \mathbf{h}(i)}{\Delta t} = \mathbf{S} \frac{\mathbf{h}(i+1) + \mathbf{h}(i)}{2} + \frac{\mathbf{u}(i+1) + \mathbf{u}(i)}{2} \quad (5)$$

Solving for $\mathbf{h}(i+1)$ gives

$$\mathbf{h}(i+1) = \left(\mathbf{K} - \frac{\Delta t}{2} \mathbf{S} \right)^{-1} \left(\left(\mathbf{K} + \frac{\Delta t}{2} \mathbf{S} \right) \mathbf{h}(i) + \frac{\Delta t}{2} (\mathbf{u}(i+1) + \mathbf{u}(i)) \right) \quad (6)$$

Parameter Fit

Now, the model parameters are estimated by minimising the sum squares of the difference between predicted drawdown and measured data:

$$\min \frac{1}{2} \|\mathbf{h}_e - \mathbf{h}(\mathbf{h}(i, 1), \mathbf{K}, \mathbf{S}, t)\|_2^2 = \min \frac{1}{2} \sum_i (h_e(i) - \mathbf{h}(\mathbf{h}(i, 1), \mathbf{K}, \mathbf{S}, t(i)))^2 \quad (7)$$

where $h_e(i)$ is a measured observation at time step i and $\mathbf{h}(\mathbf{h}(i, 1), \mathbf{K}, \mathbf{S}, t(i))$ is the predicted drawdown at the same time step. This returns the vectors of the values for the initial drawdown in each tank, \mathbf{h} the storage coefficients, κ (from \mathbf{K}) and the conductance values σ (from \mathbf{S}) which are the characteristic parameters for the particular geothermal system in question. This is solved by using a least squares minimiser that uses an interior-reflective Newton Method for large scale problems. See results in chapter 3.1.

2.2. Optimization Model

Objective Function

Water for district heating is assumed to be sold at a fixed price C_{Water} [\$/kg]. The electricity needed to pump the water from the well is assumed to be bought at fixed price C_{Electric} , [\$/J] and new pumps are added at a price

C_{Pump} . Profit is then calculated as the difference between the income from selling the water, production cost and cost by adding an additional pump.

The model has four state vectors, drawdown in the three tanks, $h(i, j), \forall j \in \{1, 2, 3\}$ and $i \in \{1, 2, \dots, n\}$ and two decision vectors, production, $\dot{m}(i), \forall i \in \{1, 2, \dots, n\}$, and an integer decision vector, that decides whether a pump should be added, $y(i), \forall i \in \{1, 2, \dots, n\}$. Here, Δt represents the time step and r the interest rate for calculating present value. The parameters ρ and g represent density of water and gravitational acceleration.

The present value of income is calculated as:

$$PV_{\text{Income}} = \sum_{i=1}^N \frac{\Delta t \cdot \dot{m}(i) \cdot C_{\text{Water}}}{\rho(1+r)^i} \quad (8)$$

The present value of the cost of adding an additional pump is calculated as

$$PV_{\text{Pump}} = \sum_{i=1}^N \frac{y(i) \cdot C_{\text{Pump}}}{(1+r)^i} \quad (9)$$

The present value of the production cost is calculated as:

$$PV_{\text{Production-nonlinear}} = \sum_{i=1}^N \frac{\Delta t \cdot C_{\text{Electric}} \cdot g \cdot \dot{m}(i) \cdot h(i, 1)}{(1+r)^i} \quad (10)$$

Equation (10) is a nonlinear equation since it holds a product of the variables $\dot{m}(i)$ and $h(i, 1)$. Therefore, a linear approximation is applied at this point. For any non-linear 2-dimensional function $f(x, y)$, $x, y \in \mathbb{R}$, the Taylor approximation is:

$$f(x, y) \approx f(x_0, y_0) + f_x(x_0, y_0)(x - x_0) + f_y(x_0, y_0)(y - y_0) \quad (11)$$

Linearization of (10) thus yields:

$$PV_{\text{Production-linear}} \approx \sum_{i=1}^N \frac{(h_z(i) \cdot \dot{m}_z(i) + h_z(i)(\dot{m}(i) - \dot{m}_z(i)) + \dot{m}_z(i)(h(i, 1) - h_z(i))) \Delta t \cdot C_{\text{Electric}} \cdot \rho \cdot g}{(1+r)^i} \quad (12)$$

Where $h_z(i)$ and $\dot{m}_z(i)$ represent the reference points for the linear approximation. Equation 12 is used in the objective function.

Updating Process

In order to obtain a good linear approximation an updating process with k iterations is necessary. The initial values for the reference points that relate to production ($m_z(i, k = 1)$) are chosen first and the reference points relating to drawdown ($h_z(i, k = 1)$) are calculated according to $m_z(i, 1)$ using equation 6, see also figure 2. The optimization is now updated until the error (in equation 13) between linear and nonlinear production is less than $\epsilon = 1\%$. The error is calculated by comparing the percentage difference between nonlinear and linear production from the optimal output from the objective function, ignoring present value ($r = 0$), see equations 10 and 12.

$$Err := \frac{100|\sum_{i=1}^N \text{NonPV}_{i,\text{Production-nonlinear}} - \sum_{i=1}^N \text{NonPV}_{i,\text{Production-linear}}|}{\sum_{i=1}^N \text{NonPV}_{i,\text{Production-nonlinear}}} \quad (13)$$

Constraints

The following constraints are applied in the optimization model.

Constraint 1: Mass balance equations on matrix form

Drawdown is a function of demand. Constraint 1 carries out this relationship with a discrete approximation of the Lumped Parameter Model. See also section 2.1.

$$\mathbf{h}(i+1) = (\mathbf{K} - \frac{\Delta t}{2}\mathbf{S})^{-1} ((\mathbf{K} + \frac{\Delta t}{2}\mathbf{S})\mathbf{h}(i) + \frac{\Delta t}{2}(\mathbf{u}(i+1) + \mathbf{u}(i))) \quad \forall i \in \{1, 2, \dots, n\} \quad (14)$$

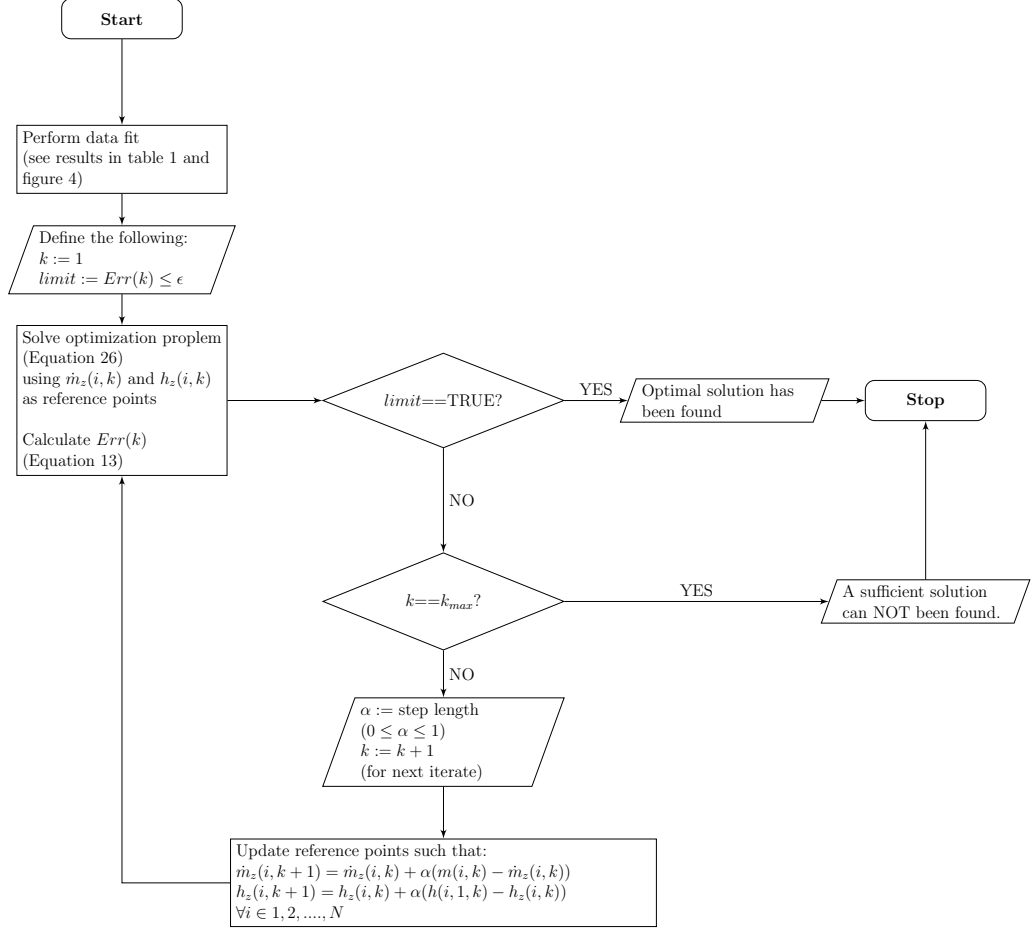
where

$$\mathbf{u}(i) = \begin{bmatrix} \dot{m}(i+1)/g\rho \\ 0 \\ \sigma_3 h_0 \end{bmatrix} \quad \forall i \in \{1, 2, \dots, n\} \quad (15)$$

Constraint 2: Demand

A demand constraint states that production $\dot{m}(i)$ can not exceed demand $\dot{m}_e(i)$. The optimization is carried out in periods according to the data, see chapter 3.2.

$$\dot{m}(i) \leq \dot{m}_e(i) \quad \forall i \in \{1, 2, \dots, n\} \quad (16)$$



Descriptio 2: The iteration algorithm to find suitable reference points for the linear approximation is represented as a flowchart. The initial values for the reference points are chosen as $\dot{m}_z(i, 1)$ and $h_z(i, 1)$, $\forall i \in 1, 2, \dots, n$ such that $\dot{m}_z(i, 1) := \beta \dot{m}_e(i)$ and since h is a function of \dot{m} (see equation 6), $h_z(i, 1)$ is calculated from $\dot{m}_z(i, 1)$. β is chosen $0 \leq \beta \leq 1$ such that $h_z(\dot{m}_z(i, 1)) \in F$ where F is the feasible region of the problem. $\dot{m}_z(i, 1)$ is in other words scaled down so that when $h_z(i, 1)$ is calculated, it never reaches the sustainability constraint, see equation 21.

Constraint 3: Sustainability

For each geothermal system, and for each mode of production, there is a certain power required to extract the water from the well, P_{Well} and a certain exergy contained in the water X_{Water}

$$P_{\text{Well}} = \dot{m}gh \quad (17)$$

$$X_{\text{Water}} = \dot{m}e_x \quad (18)$$

Exergy is a measure of how much work can be done by a system during a process that brings the system into equilibrium with its surroundings. For the geothermal liquid under consideration this is taken to be the work that could be done via Carnot cycle between the liquid and a heat sink at a given temperature as the liquid cools down. Thus the specific exergy of the fluid is approximated as:

$$e_x = c \left((T_h - T_0) - T_0 \ln \frac{T_h}{T_0} \right) \quad (19)$$

where c is the heat capacity of water in $\text{J} \cdot \text{kg}^{-1}\text{K}^{-1}$, T_h is the temperature of the fluid and T_0 is the temperature of the heat sink in Kelvin. The equation above is derived using the assumption that c is a constant in the temperature range T_0 to T_h , which is valid for a single phase fluid such as is being considered in this paper.

One possible sustainability criterion is to require that the energy needed to pump a given amount of water from the well must be less or equal to a given fraction of the exergy of that water:

$$P_{\text{Well}} \leq \delta X_{\text{Water}} \quad (20)$$

where δ is the exergy efficiency of a typical power production system at the well fluid temperature. For $\delta = 1$ the system is self-sustainable under Carnot condition. The efficiency of a space heating system such as the one in this work is of course considerably lower. The cost of the investment should also be taken into account for the sustainability limit. In this case efficiency is assumed to be 10% of the Carnot efficiency which means that there is at least 10 times more energy available in the geothermal fluid than can be utilized for power production under reversible condition.

Maximum drawdown can now be determined by the following equation:

$$h_1^{\text{max}} = \frac{e_x \delta}{g} \quad (21)$$

Thus the drawdown in the reservoir (tank 1, figure 1) is not allowed to exceed a certain maximum drawdown due to sustainability.

$$h(i, 1) \leq h_1^{\max} \quad \forall i \in \{1, 2, \dots, n\} \quad (22)$$

Constraint 4: Production Capacity

As described in the section above and by equation (17) there is a certain power required to extract the water from the well. The power needed for pumping at time i , $P_{\text{Power}}(i)$ is then calculated as:

$$P_{\text{Power}}(i) = g \cdot h(i, 1) \cdot \dot{m}(i) \leq P_{\text{Pump}} \cdot \sum_{l=1}^i y(l) \quad \forall i \in \{1, 2, \dots, n\} \quad \text{and} \quad l \leq i \leq n \quad (23)$$

Where P_{Pump} represents the power rating of one pump and $y(i)$ is an integer representing how many pumps need to be added at time i .

There are various options for choosing a pump for a reservoir and each case needs to be carefully considered, e.g. in regards of chemical properties of each reservoir, overpressure of the water, etc. In other words, each reservoir needs to be examined individually. Those considerations are outside the scope of this paper. It will be assumed that the power rating of the pumps is 250 kW.

Since $h(1, i)$ and $\dot{m}(i)$ from equation 23 are both unknown decision/state variables this is a nonlinear constraint and a linear approximation needs to be applied again. That is done in exactly the way it was done for the production part of the objective function (see equations 10 and 12). Now $y(i)$ represents the number of pumps added at time i , where y is a vector of non-negative integers. One pump needs to be present in the beginning so y at time $i = 1$ is always at least 1.

$$\begin{aligned} P_{\text{Power}}(i) &= g(h_z(i) \cdot \dot{m}_z(i) + h_z(i)(\dot{m}(i) - \dot{m}_z(i)) + \dot{m}_z(i)(h(i, 1) - h_z(i))) \quad (24) \\ &\leq 250 \cdot 10^3 \sum_{l=1}^i y(l) \end{aligned}$$

Constraint 5: Approximation

When production can not meet demand the optimization has a tendency to find solutions where $\dot{m}(i) \ll \dot{m}_z(i)$ and $h(1, i) \ll h_z(i)$ which leads to an unacceptable error in the linearisation of equation 12. To prevent this a constraint is put upon how far production and drawdown may deviate from the fixed points of the linearisation. This is described in the following equation

$$h_z(i) \cdot \dot{m}_z(i) + h_z(i)(\dot{m}(i) - \dot{m}_z(i)) + \dot{m}_z(i)(h(1, i) - h_z(i)) \geq \frac{h_z(i) \cdot \dot{m}_z(i)}{2} \quad (25)$$

The Optimization Model

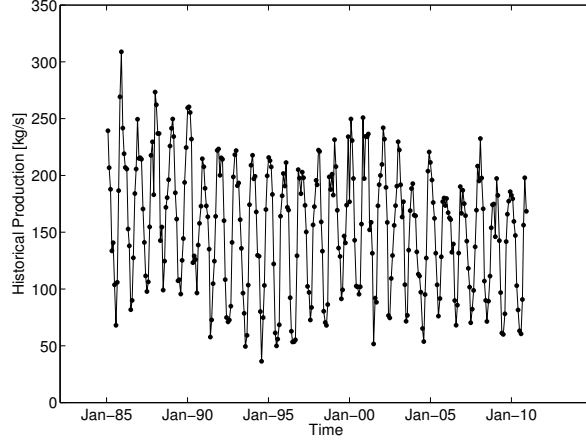
The optimization model now becomes:

$$\begin{aligned}
\text{Max}_{\mathbf{h}(i), \dot{m}(i), y(i)} \quad & \text{PV}_{\text{Profit}} = \text{PV}_{\text{Income}} - \text{PV}_{\text{Production}} - \text{PV}_{\text{Pump}} \\
\text{subject to} \quad & \\
h(j, i+1) = & \left(\mathbf{K} - \frac{\Delta t}{2} \mathbf{S} \right)^{-1} \left(\left(\mathbf{K} + \frac{\Delta t}{2} \mathbf{S} \right) h(j, i) + \frac{\Delta t}{2} (\mathbf{u}(i+1) + \mathbf{u}(i)) \right) \quad (26) \\
\dot{m}(i) \leq & \dot{m}_e(i) \\
h(1, i) \leq & h_1^{max} \\
\text{P}_{\text{Power}}(i) \leq & 250 \cdot 10^3 \sum_{l=n}^i y(n) \\
h_z(i) \cdot \dot{m}_z(i) + & h_z(i)(\dot{m}(i) - \dot{m}_z(i)) + \dot{m}_z(i)(h(i, 1) - h_z(i)) \geq \frac{h_z(i) \cdot \dot{m}_z(i)}{2}
\end{aligned}$$

3. Results

3.1. Measured field data, parameters and validation

Production data from 10 wells (see figure 3) in Laugarnes SW-Iceland have been combined and used to fit against drawdown of the system as reflected by the RV-34 well (also located in Laugarnes) a non-production well that is used to record changes in water level. The 10 production wells have all been in operation since 01.12.1982 (Ivarsson, 2011). Longer empirical records are available, but only for 8 of the production wells. In this work data from the period from 1982 until 2010 is used for estimating the parameters of the model.



Descriptio 3: Total production in Laugarnes, Reykjavik, Iceland during the years 1982 - 2010

Parameter Estimation and Validation

Although production from the 10 wells in Laugarnes field has been recorded since 1982 (at least), the water level in RV-34 has only been recorded since 1985. Parameter estimation is thus performed for 25.9 years (1985 till 2010) with a nonlinear iterative least square fit, according to equation 7. One way to carry out the modeling process is to start with a simplified version of the 3-tank open model described in section 2.1, i.e. 1-tank closed model. Fit the parameters, expand the model and use the output as input (guess) for the next step, 1-tank open model to 2-tank closed model etc. (Axelsson and Arason, 1992). This method is not perfect but helps finding a neighborhood for the solution. It is also possible to start with a 3-tank open model and apply randomized guessing until a sufficient solution is reached. That was not tested in this work.

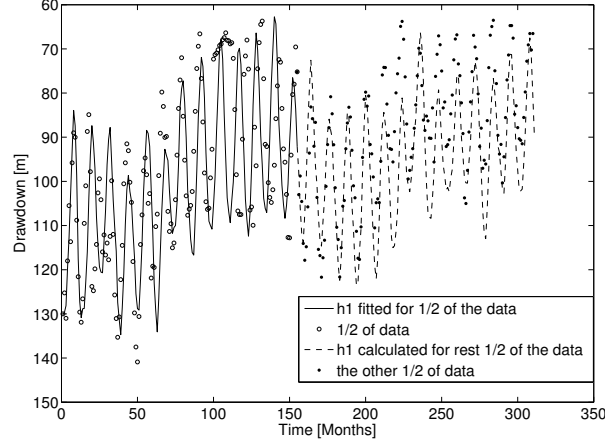
In this work the least-squares fit was implemented in Matlab (MATLAB, 2012). Finding the initial guess for the fit was quite tricky, thus the methodology described above, starting with a very simple model was used to construct a good initial guess for the parameters. That resulted in a rather good fit, presented in table 1 where $h(i = 1, j)$ represents the initial draw-down in all the tanks and h_0 is the environmental drawdown.

In order to validate the data fit, half of the data was fitted from the same initial guess as before. Those parameters were then used to calculate the re-

sponse for the second half of the data. See table 1 and graphically in figure 4. As said before, the discrete lumped parameter model follows the data quite accurately compared to the discrete approximation that has been done, with a root mean square (RMS) of 4.64 and maximum error of 20.76 m. In terms of the data validation the RMS goes slightly up but still remains sufficiently low. It is important to point out here that the third tank is very big so the solution is not sensitive to $h(3, i = 1)$ which is the drawdown in the third tank and h_0 which is the environmental drawdown. For this reason it does not affect the result of the fit that those value differ in comparison of fitting half of the data set and the whole data set. Results are shown in table 1 and figure 4.

Parameters	Parameter values (whole data set fitted)	Parameter values ($\frac{1}{2}$ of the data set fitted)	Other $\frac{1}{2}$ of the data set	Units
κ_1	50	50		ms ²
κ_2	1712	1698		ms ²
κ_3	10,426,317	11,515,673		ms ²
σ_{12}	0.093	0.089		ms
σ_{23}	0.00026	0.00028		ms
σ_3	0.0098	0.012		ms
$h(1, i = 1)$	131.99	128.10		m
$h(2, i = 1)$	130.63	127.05		m
$h(3, i = 1)$	39.57	130.63		m
h_0	6.35	45.30		m
RMS	4.64	5.05	5.40	
RMS _{misfit}	0.27	0.29	0.32	
R ²	92.51%	91.59%	89.80%	
Max Error	20.76	20.08	20.01	m
Mean Error	3.46	3.61	4.18	m

Tabula 1: Fitted parameters for the LPM model in Laugarnes for the period 01.12.1982 until 31.12.2010



Descriptio 4: Result for data validation, half of the data fitted, other half calculated from that fit

Other Parameters

Other parameters for the optimization model can be seen in table 2. The initial demand, $\dot{m}(i = 1)$ is the first significant value from the Laugarnes field data. The values for C_{Water} , and C_{Electric} , are taken from price listings from Reykjavik Energy (Reykjavik Energy, 2011).

The quoted retail price for electricity is used unchanged in the modeling since in the scenario of selling hot water for district heating, one would have to pay full retail price for electricity like any other customer. In selling the water however it is very likely that a district heating firm buys the water at relatively low (wholesale) price and sells it to the customer for a higher (retail) price.

Statistic Iceland (Statistics Iceland, 2012) holds numbers for retail price versus wholesale price for electricity from 1980 to 2004, for the following companies: Rarik (both wholesale price and retail price), Landsvirkjun (wholesale price) and Orkuveita Reykjavkur (retail price).

Assuming that the ratio between retail and wholesale price is somewhat similar for water, those numbers can be used to get an idea of what the correct water price might be. Those proportions range between 16% and 50% with an average around 40%. In addition, transportation and distribution of the water needs to be considered. Statistic Iceland (Statistics Iceland, 2012) also holds numbers (from 1983 - 2006) over production and primary energy

versus losses in transport and distribution. Assuming that something similar applies to transporting and distribution of water plus operational cost, it is assumed here that the wholesale water price is not more than 25% of the retail price (C_{Water}) see table 2.

The value for C_{Pump} is the cost for adding another pump. Those prices are of course dependent upon properties of the pumps, e.g, how much power they can handle and in what sort of condition they operate. Here, the price for one pump is assumed to be \$150,000.

The interest rate is taken from listing presented by the Central Bank of Iceland in November 2011. Interest rate here is considered to be a yearly based constant.

3.2. Behaviour of the Discrete Reservoir Model and Sensitivity Analysis

Two different operational scenarios A and B will be examined.

Scenario A

Demand for hot water is generated by repeating the period for historical production data, six times for a period longer than 155 year (see figure 5a). The initial values for the reference points are the demand (with damping factor $\beta = 1$), and the reference points for drawdown which are calculated from the demand with the LPM model. The optimization is then executed for 155.5 years.

The parameters used here can be viewed in table 2 and numerical results in table 3. For this scenario production was able to follow demand very accurately for the whole period, that resulted in a good linearisation in the first iteration so the updating algorithm (see figure 2) was not needed here.

Parameters	Scenario A: Values	Units
$\dot{m}(i = 1)$	239	kg/s
C_{Water}	$0.25 \cdot 0.8695$	\$/m ³
C_{Pump}	150,000	\$
C_{Elect}	0.0805/3600000	\$/J
r	5.5%	yearly rate
Efficiency δ	10%, (Maximum drawdown is 751 m)	
Exergy, e_x	73,612 ($T_0 = 288\text{K}$, $T_i = 400.7\text{K}$)	J/kg
Number of years, n	155.5 years or 1866 months	
Trend in production	0%	

Tabula 2: Parameters for Scenario A.

Figure 5a a) displays the demand, $\dot{m}_e(i)$, for the next 155.5 years versus optimized production $\dot{m}(i)$. For this scenario production follows demand exactly except in month two where production is 95% of the demand because of insufficient pumping capacity. A new pump is not added until in month 10. No more pumps are needed after that. This implies that production is in general not limited by financial or physical constraint for this scenario. The resolution of the data is on a monthly basis and for a better overview of the data, the demand and production are also represented as a *moving average* with a resolution in years, figure 5 a).

Results	Scenario A	Units
Profit , PV_{Profit}	19,373,936	\$
Income , PV_{Income}	21,683,752	\$
Production , $PV_{\text{Production-linear}}$	2,017,029	\$
Production , $PV_{\text{Production-nonlinear}}$	2,017,033	\$
Pump Cost , PV_{Pump}	292,787	\$
Number of pumps , y	2	
Pump added	In month 1 and 10	
Maxium Drawdown	135 m	
Iterations	1	
Error , Err	0.0000293%	%

Tabula 3: Results for Scenario A.

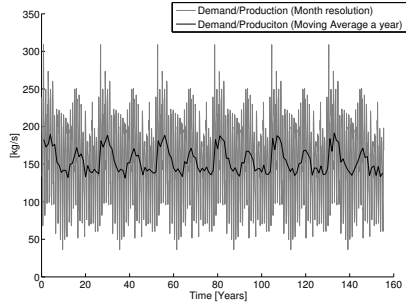
Figure 5 b) displays the development of drawdown in the tanks. Tank 1 and tank 2 fluctuate identically, and thus it is unnecessary to show tank 2 graphically. It is however necessary to model the reservoir in terms of three tanks to require optimal fit to the data.

By examining the drawdown it can be seen that after between 70 and 80 years the drawdown fluctuates between approximately 50 m drawdown and down to around 110 m drawdown and the trend in the drawdown is seemingly slightly upwards (less drawdown with time). For this period of data examined, there is a slight decline in the historical production data. That can be explained by the fact that after 1990 a new heat source, Nesjavellir, started production which resulted in reduced demand from Laugarnes area.

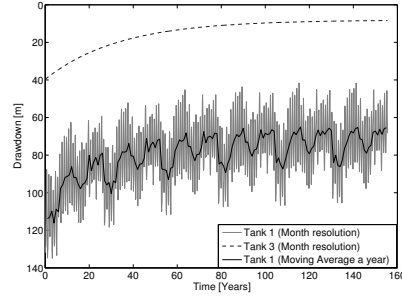
Adding other geothermal sources is however beyond the scope here. The main concerns are decisions regarding production and installation of pumps, and the timing of these decisions in the next 100 to 200 years for a profitable and sustainable production.

Assuming demand for the next 155 year (like in this scenario) the system will remain in equilibrium and operation remains profitable and sustainable. Two pumps need to be bought in the beginning, the maximum drawdown is

135 m, see table 3 and figure 5 b). Production plus pump cost are around 12% of the profit, see figure 6 a).



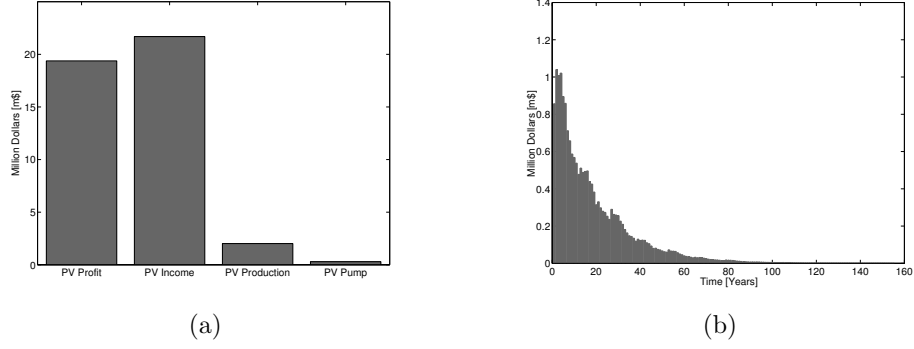
(a)



(b)

Descriptio 5: Scenario A. Production and drawdown. Figure a) displays production versus demand for the next 155.5 years. Demand is periodic and based on historical production data, repeated six times. Production can not exceed demand. In this scenario the production follows the demand exactly. Figure b) displays Development of drawdown in two of the three tanks (description of the LPM model in chapter 2.1). Tank 1 and tank 2 fluctuate identically which is why only tank 1 is represented graphically. There is a slight upwards trend in the drawdown due to the the reservoir having been in a depleted state initially.

The present value is substantially greater for the first 40 to 60 years (see figure 6 b)) where it then becomes almost zero in approximately 110 years. In terms of value of money from today it should be enough to look at 100 years at most.

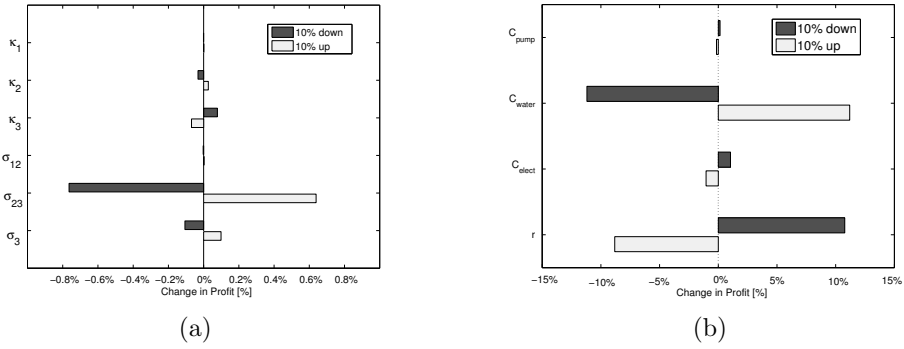


Descriptio 6: Scenario A. Figure a) displays graphical display of the cost components. Figure b) displays development of Present Value (PV) of profit for 155.5 years, resolution in years.

Sensitivity Analysis - Scenario A

It is of interest to see how much a small change in the parameters discussed in chapter 3.1 affect the profit.

Figure 7 a) and b) show the sensitivity of the profit with regards to variation of the Lumped Model Parameters κ , σ (see table 1) and the economical parameters from table 2. The values of the parameters are varied by 10% and the result from the optimization (the profit) compared.



Descriptio 7: Scenario A. Sensitivity analysis. Figure a) displays proportional change in profit considering 10 % increase/decrease in the parameters from the Lumped Parameter Model (LPM). Figure b) displays proportional change in Profit considering 10 % increase/decrease in the economical parameters. Please note different scales on the two figures above.

A 10% change in the Lumped Model Parameters affects the profit by less than 1%. That could suggest that the data fit does not need to be extremely accurate, or like according to Satman et al. (2005), a 3-tank open model might not be suitable since if the confidence interval range of the parameters is too high. The confidence interval of the parameters was not thoroughly tested here and there could still be parameters that have quite small confidence intervals that effect the pressure behavior significantly, even though they don't affect the profit for 155 years of production. Working with a different types of lumped parameter model, e.g. a model with only 2-tanks Satman et al. (2005) might however be helpful. Comparing different types of lumped parameter models is out of the scope here but will be considered in the future. The profit is most sensitive to the price received for water and interest rate. Those parameters are considered to be constants here, which they are of course not in reality. Those results indicates the need to model this problem with stochastic interest rate and price.

Scenario B

According to the National Energy Authority of Iceland, the annual increase in demand for low temperature geothermal fluid over the period 1990 to 2009 was 1.78% (National Energy Authority of Iceland, 2012). Looking more closely at the data, the trend seems to have increased more from 2000 till 2010, than from 1990 till 2000. Nevertheless, a scenario with a yearly trend of 2% will be executed. Parameters and change from Scenario A can be viewed in table 4 and numerical results in table 7.

Parameters	Scenario B: Values	Units	Change from Scenario A
$\dot{m}(i = 1)$	239	kg/s	
C_{Water}	$0.25 \cdot 0.8695$	$\$/\text{m}^3$	
C_{Pump}	150,000	\$	
C_{Elect}	0.0805/3600000	$\$/\text{J}$	
r	5.5%		yearly rate
Efficiency δ	10%, (Maximum drawdown is 738 m)		
Exergy, e_x	73,612 ($T_0 = 288\text{K}$, $T_i = 400.7\text{K}$)	J/kg	
Number of years, n	155.5 years or 1866 months		
Trend in production	2% a year		X

Tabula 4: Parameters for Scenario B.

For a production with 2% a trend the calculations from the LPM model show that the drawdown will reach the sustainability constraint of approximately 751 m in exactly 104 years. Since the initial values for the reference

points are set with regard to production data of six periods but with 2% trend a year, a large deviation in the linearisation is created. As a result, updating the optimization becomes necessary (see figure 2). The initial reference point guess is based on the assumed production data, \dot{m}_e , but \dot{m}_z is scaled down from year 104 with a scaling factor $\beta = 0.4$ so that the reference points for h_z , calculated from \dot{m}_z are in the feasible region ($h_z \leq 751$) and thus not too far from the an optimal solution.

By choosing the step length $\alpha = 0.4$, the algorithm converges with $Err < 1\%$ (equation 13) after 4 iterations. Smaller α requires more iterations, e.g. $\alpha = 0.2$ requires 6 iterations. A bigger α also gives a result after 4 iterations, $\alpha = 1$ does converge, but not to an error less than 1%. See results for iterations in table 5 for $\alpha = 0.4$ and table 6 for $\alpha = 0.2$.

Iteration	Err	Profit-linear	Profit-nonlinear	PV _{Profit-linear}	PV _{Profit-nonlinear}
1	19.4%	570,505,060\$	479,441,807\$	28,159,633\$	28,008,369\$
2	6.09%	514,983,732\$	491,786,817\$	28,059,936\$	28,016,446\$
3	1.75%	504,026,571\$	498,817,881\$	28,040,524\$	28,032,867\$
4	0.26%	502,141,486\$	501,269,858\$	28,036,628\$	28,035,019\$

Tabula 5: Results from the iteration algorithm see figure 2 for Scenario B. Step length: $\alpha = 0.4$

Iteration	Err	Profit-linear	Profit-nonlinear	PV _{Profit-linear}	PV _{Profit-nonlinear}
1	19.4%	570,505,060\$	479,441,807\$	28,159,633\$	28,008,369\$
2	12.07%	537,665,042\$	483,677,252\$	28,102,089\$	28,008,786\$
3	7.45%	518,612,637\$	487,785,677\$	28,067,111\$	28,010,909\$
4	3.24%	507,760,563\$	496,966,729\$	28,047,447\$	28,024,893\$
5	1.38%	503,905,723\$	499,551,034\$	28,040,986\$	28,033,649\$
6	0.47%	502,726,777\$	501,124,900\$	28,038,465\$	28,034,649\$

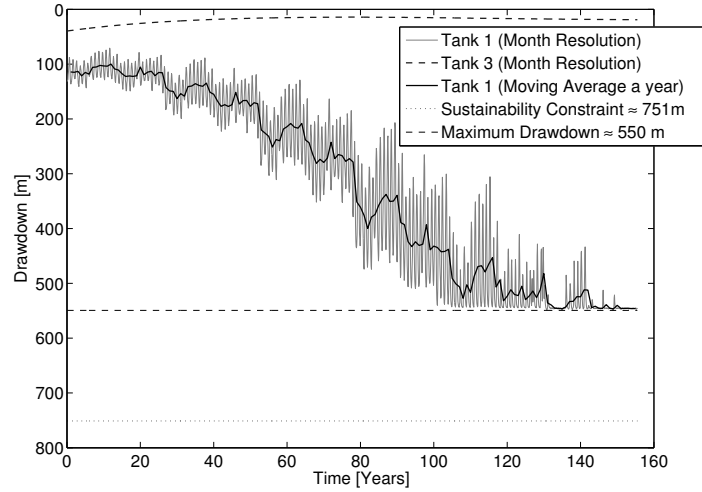
Tabula 6: Results from the iteration algorithm, see figure 2 for Scenario B. Step length: $\alpha = 0.2$

Results for $\alpha = 0.4$ will be used here. The profit has increased 44% from Scenario A and production and pump cost are 20% of the profit. The number of pumps needed is 27 and the maximum drawdown is only 550 m.

Results	Scenario B	Units
Profit , PV_{Profit}	28,036,628	\$
Income , PV_{Income}	33,552,366	\$
Production , $PV_{\text{Production-linear}}$	5,059,195	\$
Production , $PV_{\text{Production-nonlinear}}$	5,060,803	\$
Pump Cost , PV_{Pump}	456,543	\$
Number of pumps , y	27	
Pump added	In month 1 till year 100 (see figure 9)	
Maxium Drawdown	550 m	
Iterations	4	
Error , Err	0.26	%

Tabula 7: Results for Scenario B.

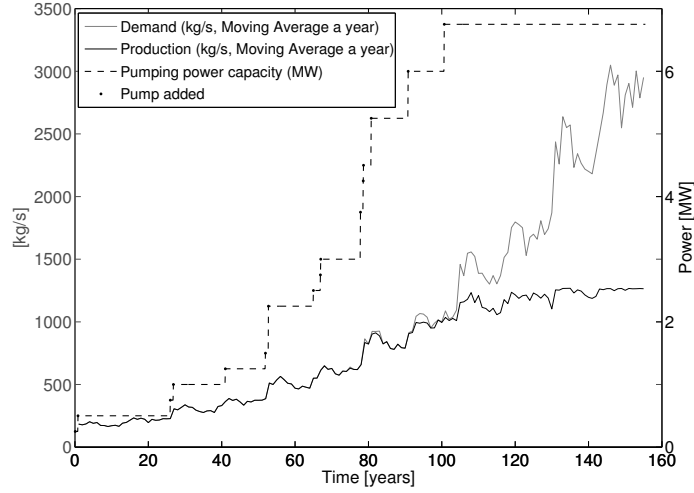
Figures 8 and 9 show results for production and drawdown. Production follows the demand quite accurately until in year 80, where it starts to decrease, but not substantially until after year 100.



Descriptio 8: Scenario B. Development of drawdown for two of the three tanks. Tank 1 and tank 2 fluctuate identically. The drawdown does not hit the sustainability constraint, it rather seems like an implicit sustainability constraint is at 550 m drawdown.

The drawdown here (figure 8) in tank 1 and tank 2 has a relatively high fluctuations in years 110 till 120. That is due to the fact that tank 1 and tank 2 are rather small (see table 1 and discussion on the lumped parameter model in chapter 2.1). The tanks recover quite quickly when production slows down. The time constant that describes recharging of tank 1 is $\frac{\kappa_1}{\sigma_{12}} \approx 9 \text{ minutes}$, and

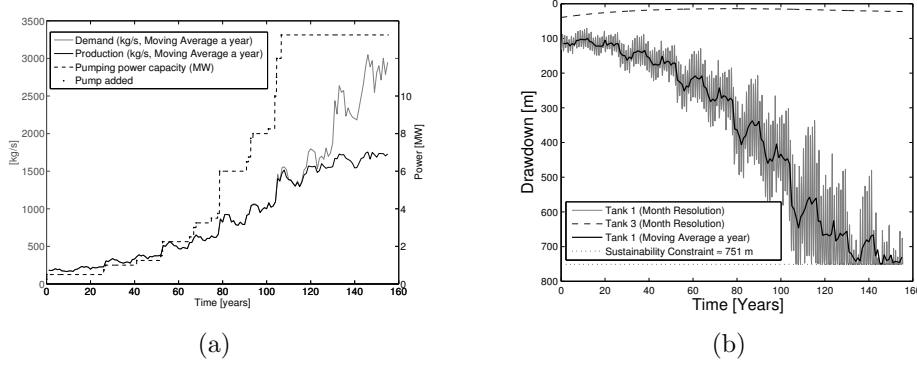
that of tank 2 is $\frac{\kappa_2}{\sigma_{23}} \approx 2.5$ months. The time step of the optimization is one month. This is also the reason why tank 1 and tank 2 seem to fluctuate identically, the time resolution is too big to see the difference. With a time resolution of one minute it would be easy to see how tank 1 is more dynamic than tank 2.



Descriptio 9: Scenario B. Installed pumping power in kW versus production and demand. The black dots represent when a new pump needs to be added. More than one pump can be added at a one time. For this case, 3 pumps were added in one month at the most. Looking at the production versus demand for the next 155.5 years, where the demand is based on historical production, production can not exceed demand. The production in this scenario follows the demand with 2% trend quite accurately until the year 100, where the difference between production and demand starts to increase substantially. The pumping capacity constraint and the price for the water are both slowing down the production. Note that the vertical axis on the right side represents pumping power (MW) and the vertical axis on the left side represents production/demand (kg/s)

It is immediately noticeable from figure 8 that the drawdown levels out before reaching the limit set by the sustainability constraint described in equation 22. The reason for this is simply that it is not optimal with regards to return on investment, to keep on producing hot water when the drawdown has reached this level, even though it is favorable from an energy standpoint. Three factors come into play here, the price of increasing installed pumping power, the price of hot water and the price of electricity. In this work there

are the least information about the price for hot water from the wells. It was assumed to be 25% of the retail price. By increasing the wholesale price to 37,5% of the retail price the sustainability limit is reached after approximately 118 years as can be seen in figure 10 b).



Descriptio 10: Production and drawdown with 50% price increase in C_{Water} . Production versus demand for the next 155.5 years. Demand is periodic and based on historical production data, repeated six times with a trend of 2% a year. Production can not exceed demand. Figure a) shows that the difference between production and demand starts to increase substantially after more than 120 years, or about 20 years later than before, see figure 9. Figure b) displays development of drawdown in two of the three tanks with an increase in water price C_{Water} . The drawdown first hits the sustainability at end of year 106 and from year 118 the sustainability constraint holds back the production.

Results	Scenario B	Units
Profit , PV_{Profit}	44, 870, 773	\$
Income , PV_{Income}	50, 607, 133	\$
Production , $PV_{\text{Production-linear}}$	5, 250, 471	\$
Production , $PV_{\text{Production-nonlinear}}$	5, 257, 079	\$
Pump Cost , PV_{Pump}	485, 889	\$
Number of pumps , y	53	
Pump added	In month 1 till year 106 (see figure 10a)	
Maxium Drawdown	751 m	
Iterations	4	
Error , Err	0.83	%

Tabula 8: Results for Scenario B with 50\$ increase in C_{Water} .

4. Conclusions and Future Work

The rigorous optimization of harvesting a geothermal reservoir in a sustainable manner where reservoir and operational optimization models are

connected directly is a relatively unexplored field. The optimization model is essentially seen as a Mixed Integer Nonlinear Programming (MINLP) with nonlinear and time dependent constraints. In order to solve this with an acceptable solution time the nonlinear parts of the model need to be linearized and for a robust linearization an iteration algorithm is proposed. A successful, relatively fast iteration algorithm for this case has been developed and the problem successfully solved. The benefit from optimizing where the production is a decision variable gives the opportunity to detect for example the economically implicit sustainability constraint that never would have appeared if the drawdown would have been calculated in terms of a given production.

An important next step is to see how this algorithm performs under various scenarios and how well it can be generalized, for example by applying it to another data set. It is of course possible to perform nonlinear optimization. However, for such a big data set that could take an enormous amount of time. The objective function could be written in a quadratic matrix form where Taylor approximation is still used for the single nonlinear constraint. Two dimensional piecewise functions have been considered as well, along with applying dynamic programming, although dynamic programming could be very hard due to the three dimensions in state variables. Future work includes not optimizing the profit but rather creating harvesting strategies from the consumers point of view and minimize deviation from demand. This deviation is not interest rate dependent and therefore does not value the next ten years more then say the last 10 years of 155 year period.

The model was most sensitive to change in interest rate and price for water. Price for electricity also plays a role, and in reality those parameters are not a constant scalar, but rather a time dependent variable that follows a certain trend and has a stochastic behavior. Such considerations could also be included in the modeling.

Nomenclature

Indices

$t(i)$	Discrete time, $t(1) \leq t(i) \leq t_n$, for all $i \in \{1, 2, \dots, n\}$, [s]
i	Discrete time index

Decision Variables

$\dot{m}(i)$	Extraction from tank 1 at time i , [kg/s]
$y(i)$	Number of pumps needed at time i

State Variables

$h(i, j)$	Drawdown at time i in tank j , for all $j \in \{1, 2, 3\}$ and $i \in \{1, 2, \dots, n\}$, [m]
-----------	-----------------------------------------------------------------------------------------------------

Parameters

σ_{12}	The conductivity between tanks 1 and 2, [m · s]
σ_{23}	The conductivity between tanks 2 and 3, [m · s]
σ_3	The conductivity between tanks 3 and the external environment of the system, [m · s]

S

h_0	The external drawdown, [m]
$h(1, j)$	Drawdown in tank j at time $i = 1$ for all $j \in \{1, 2, 3\}$, [m]
$h_1^{\max}(i)$	Maximum drawdown of tank 1, sustainability constraint, [m]
$h_e(i)$	Historical value of drawdown, at time i , [m]
$\dot{m}_e(i)$	Historical value of demand at time i , [kg/s]
$h_z(i)$	Appropriate zero point for Taylor approximation, [m]
$\dot{m}_z(i)$	Appropriate zero point for Taylor approximation, [kg/s]
κ_1	Storage coefficient of tank 1, [m · s ²]
κ_2	Storage coefficient of tank 2, [m · s ²]
κ_3	Storage coefficient of tank 3, [m · s ²]

K

g	Gravitational acceleration [m/s ²]
Δt	Timestep, $\Delta t = t(i + 1) - t(i)$, [s]
ρ	Density of water at 25°C, [kg/m ³]
C_{Elect}	Price of electricity, [\$/J]
C_{Water}	Price of water, [\$/m ³]
C_{Pump}	Price of adding another pump, [\$/]
$P_{\text{Power}}(i)$	Maximum pump power, [W]

Conspectus librorum

- Axelsson, G., 1989. Simulation of pressure response data from geothermal reservoirs by lumped parameter models., in: Proceedings of the Fourteenth Workshop on Geothermal Reservoir Engineering, Stanford University, Stanford, California. pp. 257–263.
- Axelsson, G., 1991. Reservoir engineering studies of small low-temperature hydrothermal systems in Iceland, in: Proceedings of the Sixteenth Workshop on Geothermal Reservoir Engineering, Stanford University, Stanford, California. pp. 143–149.
- Axelsson, G., 2008. Production capacity of geothermal systems, in: Proceedings of the Workshop for Decision Makers in the Direct Heating Use of Geothermal Resources in Asia, Tianjin, China.
- Axelsson, G., Arason, T., 1992. Lumpfit (Automated simulation of pressure change in hydrological reservoirs). National Energy Authority of Iceland (Orkustofnun) .
- Axelsson, G., Armannsson, H., Bjornsson, S., Flovenz, O.G., Gudmundsson, A., Palmason, G., Stefansson, V., Steingrimsson, B., Tulinius, H., 2001. Sustainable production of geothermal energy: suggested definition. IGA News Quarterly No. 43, 1–2.
- Axelsson, G., Bjornsson, G., Quijano, J., 1989. Reliability of lumped parameter modeling of pressure changes in geothermal reservoirs, in: Proceedings of the World Geothermal Congress 2005, Morgan Kaufmann Publishers Inc., Antalya, Turkey. pp. 1–8.
- Eugster, W., Rybach, L., 2000. Sustainable production from borehole heat exchanger systems, in: Proceedings of the World Geothermal Congress 2000, Kyushu, Tohoku, Japan. pp. 825–830.
- Hjartarson, A., Axelsson, G., Hauksdottir, S., 2002. Reassessment of the Thelamork low temperature geothermal system in N-Iceland following successful deepening of well LTHN-10, in: Proceedings of the Twenty-Seventh Workshop on Geothermal Reservoir Engineering, Stanford University, Stanford, California.

- Ivarsson, G., 2011. Heating Utility in Reykjavik (Hitaveita i Reykjavik). The Water Production 2010 (Vatnsvinnslan 2010) .
- Lovekin, J., 2000. The economics of sustainable geothermal development., in: Proceedings of the World Geothermal Congress 2000, Kyushu,Tohoku, Japan. pp. 843–848.
- MATLAB, 2012. Version 7.14.0 (R2012a). The MathWorks Inc., Natick, Massachusetts.
- National Energy Authority of Iceland, 2012. Geothermal use in Iceland. <http://www.nea.is>. Retrieved Jan 2012.
- de Paly, M., Heicht-Mendez, J., Beck, M., Blum, P., Zell, A., Bayer, P., 2012. Optimization of energy extraction for closed shallow geothermal systems using linear programming. *Geothermics* Volume 43, 57–65.
- Pruess, K., Bodvarsson, G., Lippmann, M., 1986. Modeling of geothermal systems. *Journal of Petroleum Technology* Volume 38, 1007–1021.
- Reykjavik Energy, 2011. Prices/Rates. <http://www.or.is>. Retrieved Okt 2011.
- Rybach, L., Mongillo, M., 2006. Geothermal sustainability - a review with identified research needs. *GRC Transactions* Volume 30, 1083–1090.
- Satman, A., Sarak, H., Onur, M., 2005. Lumped-parameter models for low-temperature geothermal fields and their application. *Geothermics* Volume 34, 728–755.
- Sigurdardottir, S.R., Valfells, A., Palsson, H., Stefansson, H., 2010. in: Proceedings World Geothermal Congress 2010 Bali, Indonesia, 25-29 April 2010, Bali, Indonesia.
- Statistics Iceland, 2012. Manufacturing and Energy. <http://www.statice.is>. Retrieved Jan 2012.
- Youshi, X., 2002. Assessment of geothermal resources in the Lishuiqiao area. The United Nations University Report 17.



School of Science and Engineering
Reykjavík University
Menntavegi 1
101 Reykjavík, Iceland
Tel. +354 599 6200
Fax +354 599 6201
www.reykjavikuniversity.is
ISBN 978-9935-9147-3-6